IL
NUOVO CIMENTO
ORGANO DELLA SOCIETÀ ITALIANA DI FISICA
SOTTO GLI AUSPICI DEL CONSIGLIO NAZIONALE DELLE RICERCHE

VOL. VI, N. 6 *Serie decima* 1° Dicembre 1957

Polarization Effects in Bremsstrahlung.

G. BÖBEL

Istituto di Fisica Teorica dell'Università - Genova
Istituto Nazionale di Fisica Nucleare - Sezione Aggregata di Genova

(ricevuto il 17 Marzo 1957)

Summary. — In pursuance of a method devised by LIPPS and TOLHOEK, the differential cross-section of bremsstrahlung is written as a sum of eight terms, each correlating the different polarizations of the electron in the initial and final states and of the emitted photon (Sect. **1**). The formulae of Bethe and Heitler and of May, Gluckstern and others are obtained as particular cases (Sect. **2**) and discussion is also carried on as to the emission of circularly polarized photons from electrons having longitudinal and transversal spin respectively (Sect. **3**).

Introduction.

In the past few years, with the development of the technique of detection, the polarization effects in beams of particles have assumed importance. This fact has induced many authors to develop methods for calculating and discussing the polarization effects, and TOLHOEK and LIPPS [1] have given a procedure for the case of photons and particles of spin $\frac{1}{2}$, which they have applied to the calculation of the differential cross-section for the Compton effect.

This method is essentially based on the description of polarization by the parameters which were introduced a century ago by Sir G. G. STOKES in the case of light beams [2] and have been more and more used in recent years as very significant tools for the description of polarization states [3].

(1) W. F. LIPPS and H. A. TOLHOEK: *Physica*, **20**, 83, 395 (1954).

(2) G. G. STOKES: *Mathematical and Physical Papers* (Cambridge, 1901), Vol. III, p. 233, see also *Trans. Camb. Phil. Soc.*, **9**, 399 (1852).

(3) See H. A. TOLHOEK: *Rev. Mod. Phys.*, **28**, 277 (1956).

In this paper, following TOLHOEK and LIPPS, we shall expose an application of the method to the calculation of the differential cross-section for bremsstrahlung.

We start from the formula which is deduced from the perturbation theory applied to quantum electrodynamics [4] and which is valid in the same approximation stated in [4].

The result, obtained by this method, contains, as particular cases, the Bethe and Heitler formula, which is valid when all the polarizations are averaged as well as the formula of May [5] and Gluckstern and others [6], which is valid when only the polarization of the photons is observed.

In Sect. **1** the cross-section is written as a sum of eight terms, each correlating the different polarizations. Each term is expressed as the trace of a product of several matrices.

1. – The formula from which we start, as already stated, is, in accordance with the perturbation theory:

$$(1)\qquad \mathrm{d}\Phi = \frac{Z^2e^4}{137\pi^2}\,\frac{pEE_0}{p_0q^4}\,\mathrm{d}\Omega\,\mathrm{d}\Omega_k k\,\mathrm{d}k\cdot \cdot\left|\sum\left[\frac{(u^*u')(u'^*\varrho_1(\boldsymbol{\sigma}\cdot\boldsymbol{e})u_0)}{E-E'}+\frac{(u^*\varrho_1(\boldsymbol{\sigma}\cdot\boldsymbol{e})u'')(u''^*u_0)}{E_0-E''}\right]\right|^2,$$

where

$$(2)\qquad E_0^2=p_0^2+\mu^2\,;\qquad E^2=p^2+\mu^2\,;\qquad E'^2=p'^2+\mu^2\,;\qquad E''^2=p''^2+\mu^2\,;$$

$$(3)\qquad \boldsymbol{p}'=\boldsymbol{p}_0-\boldsymbol{k}\,;\qquad \boldsymbol{p}''=\boldsymbol{p}+\boldsymbol{k}\,,$$

and $\boldsymbol{p}_0$, $\boldsymbol{p}$, E_0, E are the momentum and the total energy in the initial and final states of the electron; $\boldsymbol{k}$ is the momentum of the photon and $k=|\boldsymbol{k}|$ its energy; $\boldsymbol{e}$ is the vector along which it is polarized; $\boldsymbol{q}$ is the momentum transferred to the nucleus.

The conservation laws for the momentum and energy give the following relations

$$(4)\qquad E_0=E+k\,,$$

$$(5)\qquad \boldsymbol{q}=\boldsymbol{p}_0-\boldsymbol{p}-\boldsymbol{k}\,.$$

---

(4) W. HEITLER: *Quantum Theory of Radiation* (Oxford, 1954), p. 242.
(5) M. MAY: *Phys. Rev.*, **84**, 265 (1952).
(6) R. L. GLUCKSTERN, M. H. HULL and G. BREIT: *Phys. Rev.*, **90**, 1026 (1953).

The u are spinors, solution of Dirac equation ([1]):

$$-[\varrho_1(\boldsymbol{\sigma}\cdot\boldsymbol{p}) + \varrho_3\mu]u = Eu\,, \tag{6}$$

$\sum$ indicates the sum over the intermediate states.

This sum is carried out according to the well known methods, and by means of (2), (5) and (6) we obtain:

$$|\sum(1)|^2 = |(u^*Cu_0)|^2\,,$$

where

$$C = \frac{[2E - \varrho_1(\boldsymbol{\sigma}\cdot\boldsymbol{q})]\varrho_1(\boldsymbol{\sigma}\cdot\boldsymbol{e})}{E^2 - E'^2} + \frac{\varrho_1(\boldsymbol{\sigma}\cdot\boldsymbol{e})[2E_0 + \varrho_1(\boldsymbol{\sigma}\cdot\boldsymbol{q})]}{E_0^2 - E''^2}\,;$$

and then

$$|(u^*Cu_0)|^2 = \Big(\sum_{\mu\nu} u^*_\mu C_{\mu\nu} u_{0\nu}\Big)\Big(\sum_{\lambda\eta} u^*_\lambda C_{\lambda\eta} u_{0\eta}\Big)^* = \mathrm{Tr}\,[P(\boldsymbol{\zeta})CP(\boldsymbol{\zeta}_0)C^+]\,, \tag{7}$$

where C^+ is the hermitian conjugated of C.

The matrix $P(\boldsymbol{\zeta})$ is defined by

$$P_{\lambda\mu}(\boldsymbol{\zeta}) = u_\lambda u^*_\mu\,.$$

It may be regarded as the density matrix for the electron in the final state and it is a function of the polarization vector $\boldsymbol{\zeta}$ of the electron as well of its momentum $\boldsymbol{p}$ and its total energy E.

The $\boldsymbol{\zeta}$ components are the Stokes parameters for the electron and define the direction of the spin in the rest system ([7]).

The matrix $P(\boldsymbol{\zeta}_0)$ has the same meaning with respect to the electron in the initial state. $P(\boldsymbol{\zeta})$ has been calculated by Lipps and Tolhoek ([1]). Its expression is the following

$$P(\boldsymbol{\zeta}) = \tfrac{1}{4}[1 - \varrho_1(\boldsymbol{p}\cdot\boldsymbol{\sigma})/E - \varrho_3\mu/E + (\boldsymbol{R}\cdot\boldsymbol{\sigma}) - \\ - \varrho_1(\boldsymbol{p}\cdot\boldsymbol{\zeta})/E + \varrho_2(\boldsymbol{p}\wedge\boldsymbol{\zeta}\cdot\boldsymbol{\sigma})/E + \varrho_3(\boldsymbol{J}\cdot\boldsymbol{\sigma})]\,, \tag{8}$$

with

$$\boldsymbol{R} = (\mu/E)\boldsymbol{\zeta} + (\boldsymbol{p}\cdot\boldsymbol{\zeta})\boldsymbol{p}/E(E+\mu)\,; \qquad \boldsymbol{J} = -\boldsymbol{\zeta} + (\boldsymbol{p}\cdot\boldsymbol{\zeta})\boldsymbol{p}/E(E+\mu)\,.$$

([7]) H. A. Tolhoek and R. S. De Groot: *Physica*, **17**, 1 (1951).

As ϱ_1 commutes with the σ's and $\varrho_1^2 = 1$, introducing the following notation:

$$E^2 - E'^2 = -2[E_0 k - (\boldsymbol{p}_0 \cdot \boldsymbol{k})] = -2\Delta_0 ;$$

$$E_0^2 - E''^2 = 2[Ek - (\boldsymbol{p} \cdot \boldsymbol{k})] = 2\Delta ;$$

we obtain

$$C = \frac{[2E\varrho_1 - (\boldsymbol{\sigma} \cdot \boldsymbol{q})](\boldsymbol{\sigma} \cdot \boldsymbol{e})}{-2\Delta_0} + \frac{(\boldsymbol{\sigma} \cdot \boldsymbol{e})[2E_0\varrho_1 + (\boldsymbol{\sigma} \cdot \boldsymbol{q})]}{2\Delta} . \tag{9}$$

If we now introduce two unitary vectors $\boldsymbol{e}_1$ and $\boldsymbol{e}_2$ representing two opposite polarizations $[(\boldsymbol{e}_i \cdot \boldsymbol{e}_k^*) = \delta_{ik}]$ the vector $\boldsymbol{e}$ may be written as

$$\boldsymbol{e} = a_1 \boldsymbol{e}_1 + a_2 \boldsymbol{e}_2 ; \qquad a_1 a_1^* + a_2 a_2^* = 1 . \tag{10}$$

A photon being emitted, equation (9) may be written as follows:

$$C = a_1^* C_{e_1} + a_2^* C_{e_2} ,$$

where

$$C_{e_1} = C(1) + \varrho_1 C(\varrho_1)(\boldsymbol{\sigma} \cdot \boldsymbol{e}_1) ,$$

$$C_{e_2} = C(2) + \varrho_1 C(\varrho_1)(\sigma \cdot \boldsymbol{e}_2) ,$$

with

$$\left\{ \begin{array}{l} C(1) = (2\Delta\Delta_0)^{-1}[(\boldsymbol{\sigma} \cdot \boldsymbol{q})(\boldsymbol{\sigma} \cdot \boldsymbol{e}_1)\Delta + (\boldsymbol{\sigma} \cdot \boldsymbol{e}_1)(\boldsymbol{\sigma} \cdot \boldsymbol{q})\Delta_0] ; \\ C(2) = (2\Delta\Delta_0)^{-1}[(\boldsymbol{\sigma} \cdot \boldsymbol{q})(\boldsymbol{\sigma} \cdot \boldsymbol{e}_2)\Delta + (\boldsymbol{\sigma} \cdot \boldsymbol{e}_2)(\boldsymbol{\sigma} \cdot \boldsymbol{q})\Delta_0] ; \\ C(\varrho_1) = (\Delta\Delta_0)^{-1}(E_0\Delta_0 - E\Delta) . \end{array} \right. \tag{11}$$

Using these notations the trace (7) becomes:

$$\begin{aligned} \mathrm{Tr}\,[P(\zeta) C P(\zeta_0) C^+] = {} & \tfrac{1}{2}\,\mathrm{Tr}\,[P(\zeta) C_{e_1} P(\zeta_0) C_{e_1}^+ + P(\zeta) C_{e_2} P(\zeta_0) C_{e_2}^+] + \\ & + \tfrac{1}{2}\xi_1\,\mathrm{Tr}\,[P(\zeta) C_{e_1} P(\zeta_0) C_{e_1}^+ - P(\zeta) C_{e_2} P(\zeta_0) C_{e_2}^+] + \\ & + \tfrac{1}{2}\xi_2\,\mathrm{Tr}\,[P(\zeta) C_{e_1} P(\zeta_0) C_{e_2}^+ + P(\zeta) C_{e_2} P(\zeta_0) C_{e_1}^+] + \\ & + \tfrac{1}{2} i\xi_3\,\mathrm{Tr}\,[P(\zeta) C_{e_1} P(\zeta_0) C_{e_2}^+ - P(\zeta) C_{e_2} P(\zeta_0) C_{e_1}^+] . \end{aligned} \tag{12}$$

ξ_1, ξ_2 and ξ_3 are three quantities defined by:

$$\xi_1 = a_1 a_1^* - a_2 a_2^* ; \quad \xi_2 = a_1 a_2^* + a_2 a_1^* ; \quad \xi_3 = i(a_1 a_2^* - a_2 a_1^*) ,$$

and are the components of the polarization vector ξ which defines the filter (1ξ) by which the polarization of the photon is analyzed ([8]).

We now split the matric $P(\zeta)$ into two sets, one of which contains the vector ζ.

We therefore write:

$$P(\zeta) = P(\zeta)_{\text{no}} + P(\zeta)_{\text{yes}} ,$$

with

$$P(\zeta)_{\text{no}} = \tfrac{1}{4}[1 - \varrho_1(\boldsymbol{p}\cdot\boldsymbol{\sigma})/E - \varrho_3\mu/E] ,$$

$$P(\zeta)_{\text{yes}} = \tfrac{1}{4}[(\boldsymbol{R}\cdot\boldsymbol{\sigma}) - \varrho_1(\boldsymbol{p}\cdot\boldsymbol{\zeta})/E + \varrho_2(\boldsymbol{p}\wedge\boldsymbol{\zeta}\cdot\boldsymbol{\sigma})/E + \varrho_3(\boldsymbol{J}\cdot\boldsymbol{\sigma})] ,$$

and also:

$$P(\zeta_0) = P(\zeta_0)_{\text{no}} + P(\zeta_0)_{\text{yes}} .$$

The trace (7), then, may be written as a sum of eight terms

$$\Phi_0 + \Phi_\xi + \Phi_{\zeta_0} + \Phi_\zeta + \Phi_{\zeta_0,\xi} + \Phi_{\zeta,\xi} + \Phi_{\zeta_0,\zeta} + \Phi_{\zeta_0,\zeta,\xi} ,$$

each of them being a linear function of the polarization vectors, indicated as subscripts (Φ_0 is a term which does not depend on the polarization).

From equation (12) we obtain their expression as follows:

$$(13)\quad \begin{cases} \Phi_0 = \tfrac{1}{2}\,\mathrm{Tr}\,[P(\zeta)_{\text{no}}\, C_{e_1} P(\zeta_0)_{\text{no}}\, C^+_{e_1} + P(\zeta)_{\text{no}}\, C_{e_2} P(\zeta_0)_{\text{no}}\, C^+_{e_2}] ; \\ \Phi_\xi = \tfrac{1}{2}\xi_1\,\mathrm{Tr}\,[P(\zeta)_{\text{no}}\, C_{e_1} P(\zeta_0)_{\text{no}}\, C^+_{e_1} - P(\zeta)_{\text{no}}\, C_{e_2} P(\zeta_0)_{\text{no}}\, C^+_{e_2}] + \\ \quad + \tfrac{1}{2}\xi_2\,\mathrm{Tr}\,[P(\zeta)_{\text{no}}\, C_{e_1} P(\zeta_0)_{\text{no}}\, C^+_{e_2} + P(\zeta)_{\text{no}}\, C_{e_2} P(\zeta_0)_{\text{no}}\, C^+_{e_1}] + \\ \quad + \tfrac{1}{2} i\xi_3\,\mathrm{Tr}\,[P(\zeta)_{\text{no}}\, C_{e_1} P(\zeta_0)_{\text{no}}\, C^+_{e_2} - P(\zeta)_{\text{no}}\, C_{e_2} P(\zeta_0)_{\text{no}}\, C^+_{e_1}] ; \\ \Phi_{\zeta_0} = \tfrac{1}{2}\,\mathrm{Tr}\,[P(\zeta)_{\text{no}}\, C_{e_1} P(\zeta_0)_{\text{yes}} C^+_{e_1} + P(\zeta)_{\text{no}}\, C_{e_2} P(\zeta_0)_{\text{yes}} C^+_{e_2}] ; \\ \Phi_\zeta = \tfrac{1}{2}\,\mathrm{Tr}\,[P(\zeta)_{\text{yes}} C_{e_1} P(\zeta_0)_{\text{no}}\, C^+_{e_1} + P(\zeta)_{\text{yes}} C_{e_2} P(\zeta_0)_{\text{no}}\, C^+_{e_2}] ; \end{cases}$$

and so on.

The differential cross-section may be written in the form:

$$(14)\quad \mathrm{d}\Phi = \frac{Z^2e^4}{137\pi^2}\,\frac{pEE_0}{p_0q^4}\,\mathrm{d}\Omega\,\mathrm{d}\Omega_k k\,\mathrm{d}k[\Phi_0 + \Phi_\xi + \Phi_{\zeta_0} + \Phi_\zeta + \Phi_{\zeta_0,\xi} + \Phi_{\xi,\zeta} + \Phi_{\zeta_0,\zeta} + \Phi_{\zeta_0,\zeta,\xi}] .$$

([8]) W. H. McMaster: *Am. Journ. Phys.*, **22**, 351 (1954). We denote by ξ the vector $\boldsymbol{Q}$ of this paper.

We can deduce from this formula the cross-section of any experiment in which the polarizations of the particles are involved. However, in a feasible experiment, it is difficult to detect all the different polarizations simultaneously: so we have to average (14) over the initial polarization states, when unobserved, and to sum over the unobserved final ones. Since $-\xi$ and $-\zeta$ represent opposite states to ξ and ζ, we obtain as a result, the elimination from (14) of the terms involving the unobserved states of polarization.

2. – The differential cross-section for an experiment in which all the polarization effects are unobserved, is:

$$\mathrm{d}\Phi_0 = \frac{Z^2e^4}{137\pi^2}\,\frac{pEE_0}{p_0q^4}\,\mathrm{d}\Omega\,\mathrm{d}\Omega_k k\,\mathrm{d}k\cdot 4\,\Phi_0\,, \tag{15}$$

where

$$\Phi_0 = \frac{1}{16EE_0}\left[(4E^2-q^2)\,\frac{(\boldsymbol{p}_0\boldsymbol{e}_1)^2+(\boldsymbol{p}_0\boldsymbol{e}_2)^2}{\Delta_0^2} + (4E_0^2-q^2)\,\frac{(\boldsymbol{p}\cdot\boldsymbol{e}_1)^2+(\boldsymbol{p}\cdot\boldsymbol{e}_2)^2}{\Delta_2} - \right. \tag{16}$$

$$\left. - 2(4EE_0-q^2)\,\frac{(\boldsymbol{p}_0\boldsymbol{e}_1)(\boldsymbol{p}\boldsymbol{e}_1)+(\boldsymbol{p}_0\boldsymbol{e}_2)(\boldsymbol{p}\boldsymbol{e}_2)}{\Delta\Delta_0} + 2\left(\frac{q^2k^2}{\Delta\Delta_0}-\frac{\Delta}{\Delta_0}-\frac{\Delta_0}{\Delta}+2\right)\right].$$

This coincides, as it is easy to verify, with the Bethe and Heitler formula.

The formula of May and Gluckstern and others is obtained by taking an average on the initial polarization and a sum over the final polarization of the electron.

It is given by

$$\mathrm{d}\Phi_\xi = \frac{Z^2e^4}{137\pi^2}\,\frac{pEE_0}{p_0q^4}\,\mathrm{d}\Omega\,\mathrm{d}\Omega_k k\,\mathrm{d}k\cdot 2(\Phi_0+\Phi_\xi)\,, \tag{17}$$

Φ_ξ being expressed in the following form

$$\Phi_\xi = \frac{1}{16EE_0}\left[(4E^2-q^2)\,\frac{\xi_1[(\boldsymbol{p}_0\boldsymbol{e}_1)^2-(\boldsymbol{p}_0\boldsymbol{e}_2)^2]+2\xi_2(\boldsymbol{p}_0\boldsymbol{e}_1)(\boldsymbol{p}_0\boldsymbol{e}_2)}{\Delta_0^2} + \right. \tag{18}$$

$$+ (4E_0^2-q^2)\,\frac{\xi_1[(\boldsymbol{p}\boldsymbol{e}_1)^2-(\boldsymbol{p}\boldsymbol{e}_2)^2]+2\xi_2(\boldsymbol{p}\boldsymbol{e}_1)(\boldsymbol{p}\boldsymbol{e}_2)}{\Delta^2} -$$

$$\left. - 2(4EE_0-q^2)\,\frac{\xi_1[(\boldsymbol{p}_0\boldsymbol{e}_1)(\boldsymbol{p}\boldsymbol{e}_1)-(\boldsymbol{p}_0\boldsymbol{e}_2)(\boldsymbol{p}\boldsymbol{e}_2)]+\xi_2[(\boldsymbol{p}_0\boldsymbol{e}_1)(\boldsymbol{p}\boldsymbol{e}_2)+(\boldsymbol{p}_0\boldsymbol{e}_2)(\boldsymbol{p}\boldsymbol{e}_1)]}{\Delta\Delta_0}\right].$$

We have chosen the vectors $\boldsymbol{e}_1$ and $\boldsymbol{e}_2$ in (10) as characterizing the states of linear polarization, $\boldsymbol{e}_1$ in the emission plane and $\boldsymbol{e}_2$ perpendicular to this plane ($\boldsymbol{e}_2 = \boldsymbol{k}\wedge\boldsymbol{e}_1/k$).

In this manner, $[(\xi_1^{ph})^2+(\xi_2^{hp})^2]^{\frac{1}{2}}$ represents the degree of linear polarization and $|\xi_3^{hp}|$ the degree of circular polarization. $\boldsymbol{\xi}^{ph}$ is the polarization vector for the emitted photon.

From equation (17) we can derive (9) the expression of the Stokes parameters for the photon. In fact it may be written in the form

$$d\Phi_\zeta = \tfrac{1}{2}\, d\Phi_0[1 + (\boldsymbol{\xi}\cdot\boldsymbol{\xi}^{ph})]$$

and we obtain in our case

$$\xi_1^{ph} = \frac{1}{16\,EE_0}\,\Phi_0^{-1}\left[(4\,E^2 - q^2)\,\frac{(\boldsymbol{p}_0\boldsymbol{e}_1)^2 - (\boldsymbol{p}_0\boldsymbol{e}_2)^2}{\Delta_0^2} + (4\,E_0^2 - q^2)\,\frac{(\boldsymbol{p}\boldsymbol{e}_1)^2 - (\boldsymbol{p}\boldsymbol{e}_2)^2}{\Delta^2} - \right.$$

$$\left. - 2(4\,EE_0 - q^2)\,\frac{(\boldsymbol{p}_0\boldsymbol{e}_1)(\boldsymbol{p}\boldsymbol{e}_1) - (\boldsymbol{p}_0\boldsymbol{e}_2)(\boldsymbol{p}\boldsymbol{e}_2)}{\Delta\Delta_0}\right],$$

$$\xi_2^{ph} = \frac{1}{16\,EE_0}\,\Phi_0^{-1}\left[2(4\,E^2 - q^2)\,\frac{(\boldsymbol{p}_0\boldsymbol{e}_1)(\boldsymbol{p}_0\boldsymbol{e}_2)}{\Delta_0^2} + 2(4\,E_0^2 - q^2)\,\frac{(\boldsymbol{p}\boldsymbol{e}_1)(\boldsymbol{p}\boldsymbol{e}_2)}{\Delta^2} - \right.$$

$$\left. - 2(4\,EE_0 - q^2)\,\frac{(\boldsymbol{p}_0\boldsymbol{e}_1)(\boldsymbol{p}\boldsymbol{e}_2) + (\boldsymbol{p}_0\boldsymbol{e}_2)(\boldsymbol{p}\boldsymbol{e}_1)}{\Delta\Delta_0}\right],$$

$$\xi_3^{hp} = 0\,.$$

Let us introduce the quantities

$$F_{1+} = (2E + q)/\Delta_0\,; \qquad F_{2+} = (2E_0 + q)/\Delta\,;$$

$$F_{1-} = (2E - q)/\Delta_0\,; \qquad F_{2-} = (2E_0 - q)/\Delta\,; \qquad F = \frac{q^2k^2}{\Delta\Delta_0} - \frac{\Delta}{\Delta_0} - \frac{\Delta_0}{\Delta} + 2\,;$$

and putting

$$\Gamma_{1+} = F_{1+}(\boldsymbol{p}_0\cdot\boldsymbol{e}_1) - F_{2+}(\boldsymbol{p}\cdot\boldsymbol{e}_1)\,; \qquad \Gamma_{2+} = F_{1+}(\boldsymbol{p}_0\cdot\boldsymbol{e}_2) - F_{2+}(\boldsymbol{p}\cdot\boldsymbol{e}_2)\,;$$

$$\Gamma_{1-} = F_{1-}(\boldsymbol{p}_0\cdot\boldsymbol{e}_1) - F_{2-}(\boldsymbol{p}\cdot\boldsymbol{e}_1)\,; \qquad \Gamma_{2-} = F_{1-}(\boldsymbol{p}_0\cdot\boldsymbol{e}_2) - F_{2-}(\boldsymbol{p}\cdot\boldsymbol{e}_2)\,,$$

we easly obtain

$$\text{(19)} \qquad \begin{cases} \xi_1^{ph} = (1/16\,EE_0)\,\Phi_0^{-1}(\Gamma_{1-}\Gamma_{1+} - \Gamma_{2-}\Gamma_{2+}) \\ \xi_2^{ph} = (1/16\,EE_0)\,\Phi_0^{-1}(\Gamma_{1-}\Gamma_{2+} + \Gamma_{2-}\Gamma_{1+}) \\ \xi_3^{ph} = 0 \\ \Phi_0 = (1/16\,EE_0)(\Gamma_{1-}\Gamma_{2+} + \Gamma_{2-}\Gamma_{1+} + 2F)\,. \end{cases}$$

(9) U. FANO: *Journ. Opt. Soc. Am.*, **39**, 854 (1949). We have denoted by $\boldsymbol{\xi}^{ph}$ and $\boldsymbol{\xi}$ vectors $\boldsymbol{P}$ and $\boldsymbol{Q}$ of this paper.

$\xi^{\mathrm{ph}} = 0$ indicates the lack of circular polarization ([10]), while the degree of linear polarization is

$$p_{\mathrm{ph}} = \frac{[(\Gamma_{1-}^2 + \Gamma_{2-}^2)(\Gamma_{1+}^2 + \Gamma_{2+}^2)]^{\frac{1}{2}}}{\Gamma_{1-}\Gamma_{1+} + \Gamma_{2-}\Gamma_{2+} + 2F} . \tag{20}$$

The angle α formed by the electric vector with $\boldsymbol{e}_1$, is given by

$$\cos 2\alpha = \frac{\xi_1^{\mathrm{ph}}}{[(\xi_1^{\mathrm{ph}})^2 + (\xi_2^{\mathrm{ph}})^2]^{\frac{1}{2}}} = \cos(\gamma_- + \gamma_+) ,$$

where

$$\gamma_- = \operatorname{arctg}(\Gamma_{2-}/\Gamma_{1-}) ; \qquad \gamma_+ = \operatorname{arctg}(\Gamma_{2+}/\Gamma_{1+}) ;$$

therefore

$$\alpha = (\gamma_- + \gamma_+)/2 . \tag{21}$$

In the non-relativistic approximation, we may put $E_0 \simeq E \simeq \mu$, and p_0, p, $k \ll \mu$ and obtain

$$\Gamma_{1-} = \Gamma_{1+} = 2((\boldsymbol{p}_0 - \boldsymbol{p})\cdot\boldsymbol{e}_1)/k$$

$$\Gamma_{2-} = \Gamma_{2+} = 2((\boldsymbol{p}_0 - \boldsymbol{p})\cdot\boldsymbol{e}_2)/k$$

then

$$p_{\mathrm{ph}} \simeq 1 ; \qquad \gamma_+ = \gamma_- ; \qquad \alpha = \operatorname{arctg}\frac{((\boldsymbol{p}_0 - \boldsymbol{p})\cdot\boldsymbol{e}_2)}{((\boldsymbol{p}_0 - \boldsymbol{p})\cdot\boldsymbol{e}_1)} .$$

The emitted photon is completely polarized. The electric vector lies in a plane parallel to the vector $\boldsymbol{p}_0 - \boldsymbol{p}$ ([10]).

3. – We now wish to discuss the terms depending on the polarization of the electron.

The terms Φ_{ζ_0} and Φ_{ζ} are both zero,

$$\Phi_{\zeta_0} = 0 ; \qquad \Phi_{\zeta} = 0 .$$

That is, the cross-section of bremsstrahlung does not depend on the polarization of one of the electrons, if the other polarizations are averaged.

([10]) See reference ([6]).

This result is a consequence of the use of Born's first approximation in the calculation of the matrix elements for the Coulomb interaction.

The term $\Phi_{\zeta_0,\xi}$ contributes only to the circular polarization of the photon. It is of the form $\Phi_{\zeta_0,\xi} = \xi_3 \varphi_{\zeta_0}$.

The differential cross-section for the emission of circular-polarized photons from a beam of polarized electrons is

$$(22) \qquad \mathrm{d}\Phi_{\zeta_0,\xi} = \frac{Z^2 e^4}{137\pi^2} \frac{pEE_0}{p_0 q^4} \mathrm{d}\Omega \, \mathrm{d}\Omega_k k \, \mathrm{d}k \cdot 2(\Phi_0 + \Phi_{\zeta_0,\xi}) = \frac{1}{2} \mathrm{d}\varphi_0 (1 + \xi_3 \xi_3^{\mathrm{ph}}) \, ;$$

where

$$(23) \qquad \xi_3^{\mathrm{ph}} = \frac{\varphi_{\zeta_0}}{\Phi_0} = \frac{I_R - I_L}{I_R + I_L} \, ,$$

where I_R and I_L are the intensities for right and left circularly polarized radiation [11].

We have made the calculation of φ_{ζ_0} in two particular cases: that is, for the spin parallel to the direction of propagation of the incident electron (longitudinal spin) and for the spin perpendicular to this direction (transversal spin), and the following results have been obtained

i) longitudinal spin:

$$(24) \qquad \varphi_{\zeta_0} = \frac{1}{8EE_0} \frac{k}{p_0^2} (\boldsymbol{p}_0 \boldsymbol{\zeta}_0) \left\{ E_0 (p \cos\theta + p_0 \cos\theta_0) \left[\frac{p_0^2 \sin^2\theta_0}{\Delta_0^2} + \frac{p^2 \sin^2\theta}{\Delta^2} - \right. \right.$$

$$- \left. \frac{2pp_0 \sin\theta \sin\theta_0 \cos\varphi}{\Delta\Delta_0} \right] + (\mu^2 - E_0 k) \left[\frac{r_0^2 \sin^2\theta_0}{\Delta_0^2} - \frac{p^2 \sin^2\theta}{\Delta^2} + \frac{p^2 \sin^2\theta - p_0^2 \sin^2\theta_0}{\Delta\Delta_0} \right] +$$

$$\left. + \left(\frac{\mu^2}{\Delta^2} - \frac{\mu^2}{\Delta_0^2} \right) pp_0 \sin\theta \sin\theta_0 \cos\varphi + \frac{\mu^2 k^2}{\Delta_0^2 \Delta} (p^2 \sin^2\theta - p_0^2 \sin^2\theta_0) \right\} \, ;$$

ii) transversal spin:

$$(25) \qquad \varphi_{\zeta_0} = \frac{p}{16EE_0} (\boldsymbol{\zeta}_0 \boldsymbol{k}) \left\{ \frac{2(2E + k)(k - p_0 \cos\theta_0) + 2Ek + q^2}{\Delta_0^2} + \right.$$

$$+ \frac{2k(p_0 \cos\theta_0 - p \cos\theta) - 2(E + E_0) p \cos\theta - 2E_0 k + q^2}{\Delta^2} +$$

$$\left. + 2 \frac{2E_0 p_0 \cos\theta_0 + 2Ep \cos\theta - 2E_0 k + q^2}{\Delta\Delta_0} \right\} + \frac{\mu k^2}{8EE_0} (\boldsymbol{p} \cdot \boldsymbol{\zeta}_0) \frac{p_0^2 \sin^2\theta_0 - p^2 \sin^2\theta}{\Delta^2 \Delta_0} \, ;$$

---

[11] $\xi_3^{\mathrm{ph}} > 0$ means right-handed polarization: $\boldsymbol{e} = (\boldsymbol{e}_1 + i\boldsymbol{e}_2)/\sqrt{2}$,
$\xi_3^{\mathrm{ph}} < 0$ means left-handed polarization: $\boldsymbol{e} = (\boldsymbol{e}_1 - i\boldsymbol{e}_2)/\sqrt{2}$.

θ_0 and θ are the angles between $\boldsymbol{k}$ and $\boldsymbol{p}_0$ or $\boldsymbol{p}$, respectively, φ the angle between the planes $\boldsymbol{p}_0\boldsymbol{k}$ and $\boldsymbol{p}\boldsymbol{k}$.

In the particular case of forward emission, the degree of circular polarization is

i) longitudinal spin ([12]):

$$(26)\quad \xi_3^{\mathrm{ph}} = 2k\left[\frac{(E - p\cos\theta)(E_0 - p_0 + k) + \mu^2}{(4E_0^2 - q^2)(E_0 - p_0) + 2k^2(E - p\cos\theta)}\right]\frac{(\boldsymbol{\zeta}_0\boldsymbol{p}_0)}{p_0} = f_{\parallel}(k,\theta)\frac{(\boldsymbol{\zeta}_0\boldsymbol{p}_0)}{p_0}\,.$$

ii) transversal spin:

$$(27)\quad \xi_3^{\mathrm{pb}} = -\frac{2\mu k p\sin\theta}{(GE_0^2 - q^2)(E_0 - p_0) + 2k^2(E - p\cos\theta)}\cdot\frac{(\boldsymbol{p}\boldsymbol{\zeta}_0)}{p\sin\theta} = -f_{\perp}(k,\theta)\frac{(\boldsymbol{p}\boldsymbol{\zeta}_0)}{p\sin\theta}\,.$$

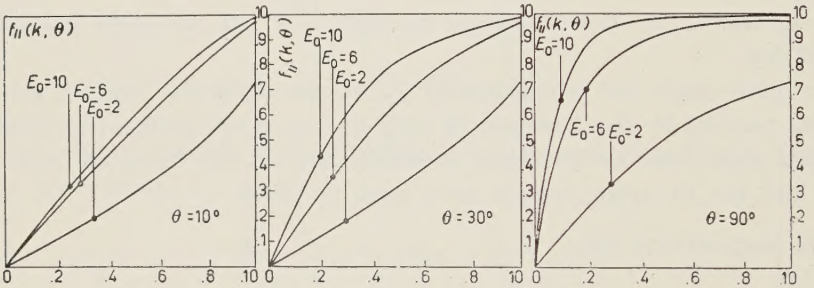

Fig. 1. – Function $f_{\parallel}(k,\theta)$, defined by (26), for three values of the energy of the incident electron $E_0 = 2, 6, 10$ (units mc^2) and three values of the scattering angle $\theta = 10°, 30°, 90°$.

In the Fig. 1 and 2 we have plotted the quantities $f_{\parallel}(k,\theta)$, $f_{\perp}(k,\theta)$ as functions of the energy k of the emitted photon.

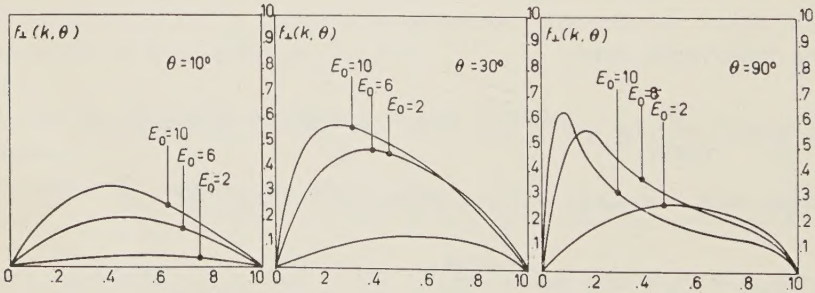

Fig. 2. – Function $f_{\perp}(k,\theta)$, defined by (27), for the same values of E_0 and θ.

([12]) Formula (26) agrees with a result recently obtained by K. M. McVoy: *Phys. Rev.*, **106**, 828 (1957). I am indebted to Professor S. De Benedetti who made available to me a preprint of this paper.

It is interesting to note that (24) and (25) are vanishing at the limit of the low energies, in agreement with the fact that at these energies the photon has a complete linear polarization.

In the extreme relativistic approximation (E_0, E, $k \gg \mu$) we find the following result for $f_\parallel$ and $f_\perp$:

1) Small values of θ ($\theta \cong \mu/E_0 \cos\theta \cong 1$)

$$f_\parallel = 1 - (E^2/E_0^2)(1 + kE/E_0^2) ; \qquad f_\perp = -(1 - E_0^2/kE)^{-1} .$$

These expressions are functions of the ratio k/E_0 only.

2) Large values of θ ($\sin\theta \cong 1 \cos\theta \cong 0$)

$$f_\parallel = 1 - \mu^2(E_0 + k)/(2k^2E_0) \cong 1 ; \qquad f_\perp = \mu/k .$$

$f_\perp$ reaches a maximum value of $\frac{2}{3}$ for $k \cong \mu$ that is for a strong Coulomb interaction.

In a similar way one can see that $\Phi_{\zeta\xi}$, correlating the polarizations of the photon and of the electron in the final state, contributes only to the circular polarization of the photon.

The terms $\Phi_{\zeta_0\zeta}$ and $\Phi_{\zeta_0\zeta\xi}$ are expressed as sums of many terms involving correlations between the various vectors $\boldsymbol{p}_0$, $\boldsymbol{p}$, $\boldsymbol{k}$, $\boldsymbol{\zeta}_0$, $\boldsymbol{\zeta}$.

* * *

The present writer wishes to thank Professor A. Borsellino for his encouragement and suggestions during the course of this work.

He also wishes to thank Dr. M. Carrassi and Dr. G. Passatore for some useful discussion.

RIASSUNTO (*)

Seguendo un metodo ideato da Lipps e Tolhoek si esprime la sezione d'urto differenziale della bremsstrahlung come la somma di otto termini, che mettono in correlazione le differenti polarizzazioni dell'elettrone negli stati iniziale e finale e del fotone emesso (Sez. **1**). Le formule di Bethe e Heitler e di May, Gluckstern e altri si ottengono come casi particolari (Sez. **2**) e si discute anche l'emissione di fotoni polarizzati circolarmente da elettroni con spin rispettivamente longitudinale e trasversale.

(*) *Traduzione a cura della Redazione.*

Dispersion Relations for Fermions.

RIAZUDDIN

Fitzwilliam House - Cambridge, England (*)

(ricevuto il 12 Aprile 1957)

Summary. — Generalized dispersion relations for scattering of 2 fermions are derived in a way similar to that used for fermion-boson scattering. The 2-nucleon problem is discussed in particular. The relations are written for functions which can be expressed in terms of the phase shifts.

1. – Introduction.

Recently several authors ([1-3]) have given dispersion relations for Boson-Fermion scattering. In this paper we shall study the dispersion relations for Fermion-Fermion scattering (with particular reference to the 2-nucleon problem) by a method similar to that used for the Boson-Fermion case. There are two main difficulties in using these dispersion relations; one is that the relations involve « mixing » of cross-sections for antiparticles which is inconvenient for the two-nucleon problem since the cross-sections for antinucleons are not yet experimentally known. The second difficulty, as we shall see later, is connected with the unphysical range which is very complex in this case. In this paper we shall also briefly discuss the electron-proton scattering.

(*) Present address: Department of Mathematics, Imperial College of Science and Technology, London.

([1]) M. L. GOLDBERGER: *Phys. Rev.*, **99**, 979 (1955); M. L. GOLDBERGER *et al.*: *Phys. Rev.*, **99**, 986 (1955); R. OEHME: *Phys. Rev.*, **100**, 1503 (1955); **102**, 1174 (1956).

([2]) A. SALAM: *Nuovo Cimento*, **3**, 424 (1956); A. SALAM and W. GILBERT: *Nuovo Cimento*, **3**, 607 (1956); G. TAKEDA and R. CAPPS: *Phys. Rev.*, **103**, 1877 (1956); M. L. GOLDBERGER: *Proc. of 6-th Rochester Conference* (1956).

([3]) N. BOGOLIUBOV: preprint.

2. – Scattering amplitude.

We shall denote the two fermions by a, b, and their antiparticles by $\bar{a}$, $\bar{b}$. We shall first take the two fermions as distinguishable. Let p, i, k, j be the initial momenta and spin states of the fermions a and b respectively and p^1, i^1, k^1, j^1 similar quantities for final states. Then we may write the 2-fermion S-matrix as

$$(1) \qquad S^{ab}(i^1p^1, ip, j^1k^1, jk) = \langle p^1i^1;\, k^1, j^1 \,|\, S \,|\, p, i;\, k, j\rangle =$$

$$= (\Psi_0,\, \chi^{out}(i^1p^1)\, \chi^{out}(j^1k^1)\, \bar{\chi}^{in}(j, k)\, \bar{\chi}^{in}(i, p)\Psi_0)\,.$$

Following a procedure similar to that of LEHMANN *et al.* [4] for Boson-Fermion scattering, we can write the transition matrix T ($S = i + iT$) as

$$T^{ab}(i^1p^1, ip;\, j^1k^1, jk) =$$

$$= -i\iint \mathrm{d}^4x\, \mathrm{d}^4y\, U^{j'}_b(k') \exp[+ik'x][D_x(p'i' \,|\, T(\psi_b(x)\bar{\psi}_b(y)) \,|\, pi)\, D_y] U^j_b(k) \exp[-iky],$$

where

$$(2) \qquad Dx = \gamma_\mu \frac{\partial}{\partial x_\mu} + m\,, \qquad \bar{D}_y = \gamma_\mu \frac{\partial}{\partial y_\mu} - m \qquad \text{and} \qquad U_b(k),\ U_b(k')\,,$$

are free particle Dirac spinors.

Let $D_x\psi(x) = K(x)$, $\bar{K}(x) = K^+(x)\gamma^4$. Then

$$(3) \qquad T^{ab} = -i\iint \mathrm{d}^4x\, \mathrm{d}^4y\, U^{i'}_b(k') \langle p'i' \,|\, T(K(x)K(y)) \,|\, pi\rangle U^j_b(k) \exp[+i(k'x - ky)].$$

We can also write

$$(4) \qquad S(i^1p^1, ip, j^1k^1, jk) =$$

$$= (\lim x_0,\, y_0 \to -\infty;\, x'_0,\, y'_0 \to \infty) \int \mathrm{d}^4x\, \mathrm{d}^4x'\, \mathrm{d}^4y\, \mathrm{d}^4y' \exp[-i(px - p'x' + ky - k'y'] \cdot$$

$$\cdot U^{j'}(k')\gamma^0_b U^{i'}(p')\gamma^0_a \langle T(\psi(x')\psi(y')\bar{\psi}(x)\bar{\psi}(y))\rangle \gamma^0_a U^i(p)\gamma^0_b U^j(k)\,,$$

$$(5) \qquad = \bar{U}^{i'}(p')\bar{U}^{j'}(k')\, \mathcal{S}(p', p;\, k', k)\, U^j(k)\, U^i(p)\,.$$

---

[4] H. LEHMANN, K. SYMANZIK and W. ZIMMERMANN: *Nuovo Cimento*, **1**, 205 (1955).

Invariance under charge conjugation and S.R. (*) leads to

$$(6)\qquad (p's_1';\ k's_2'|S|p, s_1;\ k, s_2) = s_1's_2's_1s_2(p'-s_1';\ k'-s_2'|S|p-s_1;\ k-s_2)\,,$$

where $s_1 = +$ or $-$ according as $i = 1$ or $i = 2$ and similarly for others.

From (4) it follows immediately that invariance under charge conjugation leads to

$$(7)\qquad \mathcal{S}(p', p;\ k', k) = C_a C_b \mathcal{S}^t(-p, -p';\ -k, -k')C_a^{-1}C_b^{-1}\,,$$

where $\gamma^\mu = -C\gamma_\mu^t C^{-1}$ etc., and t denotes the spinor transpose.

Invariance under S.R. leads to

$$(8)\qquad \mathcal{S}(p', p;\ k', k) = \gamma_a^5\gamma_b^5\mathcal{S}(-p', -p;\ -k', -k)\gamma_a^5\gamma_b^5\,.$$

Using translational invariance we obtain

$$T^{ab}(i^1p^1, ip;\ j^1k^1, jk) = (2\pi)^4\,\delta^4(p^1 + k^1 - p - k)\,T_R^{ab}(i^1p^1, ip;\ j^1k^1, jk)\,,$$

$$(9)\qquad T_R^{ab} = -i\int \mathrm{d}^4x\,\bar{U}^{j'}(k')(p'i'|\,T(K(0)\bar{K}(x))\,|pi)\,U^j(k)\exp[-ikx]\,.$$

Again using translational invariance we get

$$(10)\qquad T_R^{ab} = -(2\pi)^3\left[\sum_{\substack{n_0\\ n=p+k}} \frac{U^{j'}(k')\langle p'i'|K(0)|n\rangle\langle n|K(0)|pi\rangle U^j(k)}{n_0 - p_0 - k_0 - i\varepsilon} - \right.$$

$$\left. -\sum_{\substack{n_0\\ n=p'-k}} \frac{U^{j'}(k')\langle p'i'|K(0)|n\rangle\langle n|K(0)|pi\rangle U^j(k)}{n_0 - p_0' + k_0 - i\varepsilon}\right].$$

As is well known T is not a proper scattering amplitude for deriving dispersion relations. The proper scattering amplitude for derivation of dispersion relations is M which is obtained by replacing $T(K(0)\bar{K}(x))$ by the quantity $\theta(-x)\{K(0), \bar{K}(x)\}$, where $\{\ \}$ denotes the anticommutator. Thus

$$(11)\qquad M^{ab}(i^1p^1, ip, j^1k^1, jk) = (2\pi)^4\delta^4(p^1 + k^1 - p - k)M_R^{ab}(i^1p^1, ip;\ j^1k^1, jk)\,,$$

$$(12)\qquad M_R^{ab} = -i\int \mathrm{d}^4x\,U^{j'}(k')\theta(-x)\,(p'i'|\{K(0), K(x)\}|pi)\,U^j(k)\exp[-ikx] =$$

$$= -i\int \mathrm{d}^4x\,U^{j'}(k')\theta(-x)[D_z(p'i'|\{\psi(z), \bar{\psi}(x)\}|pi)D_x]_{z\to 0}U^j(k)\exp[-ikx] =$$

$$= \bar{U}^{j'}(k')\bar{U}^{i'}(p')\mathcal{M}^{ab}(p', p;\ k', k)U^i(p)U^j(k)\,.$$

(*) S. R. and W. R. have the same meanings as defined by Prof. Pauli in his article in *Niels Bohr and Development of Physics*.

From translational invariance we get

$$M_R^{ab} = -(2\pi)^3 \Big[\sum_{\substack{n \\ n_0 \\ p+k}} \frac{U^{j'}(k')\langle p'i'|K(0)|n\rangle\langle n|K(0)|pi\rangle U^j(k)}{n_0 - p_0 - k_0 - i\varepsilon} - \sum_{\substack{n_0 \\ n=p'-k}} \frac{\bar{U}^{j'}(k')\langle p'i'|\bar{K}(0)|n\rangle\langle n|K(0)|pi\rangle U^j(k)}{n_0 - p_0' + k_0 + i\varepsilon} \Big] . \tag{13}$$

It can be easily seen that $T = M$ for positive energies. The causality condition in this case is

$$\{K(x), \bar{K}(y)\} = 0 \qquad \text{when } (x-y)^2 < 0. \tag{14}$$

Thus the quantity $\theta(-x)\{K(0), \bar{K}(x)\}$ vanishes everywhere except in the backward light cone.

We now note certain properties of M_R^{ab}. From (6) it follows that

$$\begin{cases} M_R(11;11) = M_R(22;22) & M_R(11;12) = -M_R(22;21) \\ M_R(22;11) = M_R(11;22) & M_R(11;21) = -M_R(22;12) \\ M_R(12;12) = M_R(21;21) & M_R(12;11) = -M_R(21;22) \\ M_R(12;21) = M_R(21;12) & M_R(21;11) = -M_R(12;22) . \end{cases} \tag{15}$$

This shows that only 8 matrix elements are different. We shall see that only 6 matrix elements are independent. Equations (7) and (8) give

$$\mathcal{M}(p^1, p, k^1, k) = C_a C_b \mathcal{M}^t(-p, -p^1; -k, -k^1) C_a^{-1} C_b^{-1} , \tag{16}$$

$$\mathcal{M}(p^1, p, k^1, k) = \gamma_a^5 \gamma_b^5 \mathcal{M}(-p^1, -p; -k^1, -k) \gamma_b^5 \gamma_a^5 . \tag{17}$$

From invariance considerations the most general form of $\mathcal{M}$ is given by

$$\mathcal{M}^{ab} = \sum_{i=1}^{8} \Omega_i L_i , \tag{18}$$

where

$$\Omega_1 = I_a I_b , \qquad \Omega_2 = i\gamma_a^\mu k^\mu I_b , \qquad \Omega_3 = I_a i\gamma_b^\mu p^\mu ,$$
$$\Omega_4 = i\gamma_a^\mu k^\mu i\gamma_b^\mu p^\mu , \qquad \Omega_5 = \gamma_a^5 \gamma_b^5 , \qquad \Omega_6 = i\gamma_a^5 \gamma_a^\mu k_a^\mu \gamma_b^5 ,$$
$$\Omega_7 = \gamma_a^5 i\gamma_b^5 \gamma_b^\mu p^\mu , \qquad \Omega_8 = i\gamma_a^5 \gamma_a^\mu k^\mu i\gamma_b^5 \gamma_b^\mu p^\mu ,$$

On the energy shell we have

$$p^2 = p^{12} = M^2 , \qquad k^2 = k^{12} = m^2 , \qquad k \cdot (p - p^1) = p \cdot p^1 - M^2 .$$

Therefore out of the invariants, $k\cdot p$, $k\cdot p^1$, $p\cdot p^1$ only two are independent which we take as $k\cdot(p+p^1)$, $p\cdot p^1$. Thus L_i are functions of $k\cdot(p+p^1)$, $p\cdot p^1$.

Equation (16) imposes restrictions on form (18) of $\mathcal{M}$ and these are

$$L_6 = -mL_8\,, \qquad L_7 = -ML_8\,,$$

Hence

$$\mathcal{M}^{ab} = \sum_{i=1}^{8} \Omega_i L_i(k\cdot\overline{p+p'},\ p\cdot p')\,, \tag{19}$$

where

$$L_6 = -mL_8\,, \qquad L_7 = -ML_8\,.$$

(19) contains 6 indipendent functions. The other possible invariants which do not appear in (18) are expressible in terms of those which appear in (18).

It may be noted that (17) does not introduce any restriction on (19). It may also be noted that W.R. introduces the same restrictions as equation (16).

3. – Frames of references.

3·1. – First of all we consider the frame defined by $p+p'=0$, in which the dispersion relations take the simplest form. We choose

$$p = p_0(=\sqrt{P^2+M^2}),\ 0,\ 0,\ P; \qquad p^1 = p_0,\ 0,\ 0,\ -P\,,$$

$$k = k_0(=\sqrt{P^2+Q^2+m^2}),\ Q,\ 0,\ -P; \quad k^1 = k_0,\ Q,\ 0,\ P\,.$$

It follows that functions L's really depend on k_0 and P^2 only. We now show that without making any approximation M_R^{ab} can be written in the usual form i.e. in terms of σ's. For this purpose we note that

$$\omega(p) = -\sqrt{\frac{M}{r_0}}\,\frac{(M+p_0)+i\boldsymbol{\gamma}\cdot p}{[2p_0(p_0+M)]^{\frac{1}{2}}}\,U(p) = t(p)U(p)\,,$$

where

$$\omega^1(p) = \begin{pmatrix}\alpha(1)\\ 0\end{pmatrix}, \qquad \omega^2(p) = \begin{pmatrix}\beta(1)\\ 0\end{pmatrix}$$

and similarly for other spinors.

Making these substitutions we get

$$M_R^{ab}(i^1p^1,\ ip;\ j^1k^1,\ jk) = \bar{\omega}_b^{j'}\bar{\omega}_a^{i'}\,\overset{'}{\mathcal{M}}{}^{ab}\omega_a^i\omega_b^j\,, \tag{20}$$

where $\overset{'}{\mathcal{M}}{}^{ab} = t^+(k')t^+(p')\,\mathcal{M}^{ab}t^+(k)t^+(p)$.

Evaluating $\mathcal{M}'^{ab}$ we find that

$$\mathcal{M}'^{ab} = F_1^{ab} + i\boldsymbol{\sigma}_1 \cdot \boldsymbol{I} F_2^{ab} + i\boldsymbol{\sigma}_2 \cdot \boldsymbol{I} F_3^{ab} + \boldsymbol{\sigma}_1 \cdot \boldsymbol{I}\boldsymbol{\sigma}_2 \cdot \boldsymbol{I} F_4^{ab} + \tag{21}$$
$$+ \boldsymbol{\sigma}_1 \cdot \boldsymbol{m}\boldsymbol{\sigma}_2 \cdot \boldsymbol{m} F_5^{ab} + \boldsymbol{\sigma}_1 \cdot \boldsymbol{n}\boldsymbol{\sigma}_2 \cdot \boldsymbol{n} F_6^{ab} ,$$

where $\boldsymbol{I} = \boldsymbol{k}' \wedge \boldsymbol{k}$, $\boldsymbol{m} = \boldsymbol{k}' - \boldsymbol{k}$, $\boldsymbol{n} = \boldsymbol{k}' + \boldsymbol{k}$.

It is to be noted that in addition to equality of matrix elements given by (15), we have

$$M_R(11; 12) = M_R(22; 12) ; \qquad M_R(12; 11) = M_R(12; 22) .$$

It will be useful to write down the relationships between F's and L's. Such relations are

$$\left\{\begin{aligned}
F_1^{ab} &= \frac{1}{m + k_0}\left[\frac{p_0 a}{Mm} L_1 - \frac{k_0 a}{m} L_2 - \frac{p_0^2 b}{Mm} L_3 + \frac{p_0 k_0 b}{m} L_4\right], \\
F_2^{ab} &= \frac{1}{2(m + k_0)}\left[-\frac{a}{Mm} L_2 + \frac{p_0 b}{Mm} L_4\right], \\
F_3^{ab} &= \frac{1}{2(m + k_0)}\left[-\frac{p_0}{Mm} L_1 + \frac{k_0}{m} L_2 - \frac{p^2}{Mm} L_3 + \frac{k_0 r_0}{m} L_4\right], \\
F_4^{ab} &= \frac{1}{4(m + k_0)}\left[-\frac{1}{Mm} L_2 - \frac{p_0}{Mm} L_4\right], \\
F_5^{ab} &= \frac{1}{4}\left[-\frac{1}{mM} L_5 + L_8\right], \\
F_6^{ab} &= \frac{1}{4}\left[-\frac{p_0^2}{Mm} L_3\right],
\end{aligned}\right. \tag{22}$$

where $a = m(m+k_0) + P^2$, $b = m(m+k_0) + Q^2$.

3·2. *Center of mass frame.* – Center of mass quantities will be distinguished by the superscript « c »,

$$p_\mu^c = a_{\mu\nu} p_\nu ,$$

where

$$a_{11} = a_{44} = \cosh x , \qquad a_{14} = -a_{41} = i \sinh x , \qquad a_{22} = a_{33} = 1 ,$$

all others are zero; $\operatorname{tgh} x = Q/(p_0 + k_0)$ (²).

In this frame M_R^{ab} can be written as

$$M_R^{ab}(i^1 p^1, ip; j^1 k^1, jk) = \bar{\omega}_b^{j'} \bar{\omega}_a^{i'} \mathcal{M}'^{(ab)} \omega_a^i \omega_b^j , \tag{23}$$

$$(24)\qquad \overset{\prime c}{\mathcal{M}}{}^{(ab)} = H_1^{ab} + i\boldsymbol{\sigma}_1\cdot\hat{\boldsymbol{I}}^c H_2^{ab} + i\boldsymbol{\sigma}_2\cdot\hat{\boldsymbol{I}}^c H_3^{ab} + \boldsymbol{\sigma}_1\cdot\hat{\boldsymbol{I}}^c\boldsymbol{\sigma}_2\cdot\hat{\boldsymbol{I}}^c H_4^{ab} + \\ + \sigma_1\cdot\hat{\boldsymbol{m}}^c\boldsymbol{\sigma}_2\cdot\hat{\boldsymbol{m}}^c H_5^{ab} + \boldsymbol{\sigma}_1\cdot\hat{\boldsymbol{n}}^c\boldsymbol{\sigma}^2\cdot\hat{\boldsymbol{n}}^c H_6^{ab}\,,$$

where

$$\hat{\boldsymbol{I}}^c = \frac{\boldsymbol{k}'^c\wedge\boldsymbol{k}^c}{|\boldsymbol{k}'^c\wedge\boldsymbol{k}^c|}\,,\qquad \hat{\boldsymbol{m}}^c = \frac{\boldsymbol{k}'^c-\boldsymbol{k}^c}{|\boldsymbol{k}'^c-\boldsymbol{k}^c|}\,,\qquad \hat{\boldsymbol{n}}^c = \frac{\boldsymbol{k}'^c+\boldsymbol{k}^c}{|\boldsymbol{k}'^c+\boldsymbol{k}^c|}\,.$$

3-momentum k_c and angle θ_c in center of mass system are given by

$$(25)\qquad k_c^2(1-\cos\theta_c) = 2P^2\,,\qquad k_0p_0 + P^2 = k_0^cp_0^c + k_c^2\,.$$

In this frame also in addition to equality of matrix elements given by (15), we have

$$M_R^c(11;12)\qquad M_R^c(22;12)\,;\qquad M_R^c(12;11) = M_R^c(12;22)\,.$$

4. – Symmetry properties and derivation of dispersion relations.

To eliminate the integration with respect to negative energies in our later work, we have to consider the relationship between the scattering amplitude for negative energy and the charge conjugate amplitude for positive energy. This will, however, lead to « mixing » of cross-sections for antiparticles which in the case of the 2-nucleon problem is inconvenient as the cross-sections for antinucleons are not yet available. Anyhow we have to carry out this procedure. For this purpose we write the amplitude for scattering of « b » with $\bar{a}$:

$$(26)\qquad M_R^{\bar{a}b}(i'p', ip; j'k', jk) = \bar{U}^{j'}(k')\bar{U}^{i'}(p')\mathcal{M}^{\bar{a}b}(p', p, k', k)U^i(p)U^j(k) = \\ = -i\int \mathrm{d}^4x\;\bar{U}^j(k')\theta(-x)[D_z(p'i'|\{\psi'(z),\bar{\psi}'(x)\}|p_i)\overleftarrow{D}_x]_{z=0}U^j(k)\exp[-ikx]\,,$$

where $\psi'(x) = c\bar{\psi}^T(x)$, $\bar{\psi}'(x) = \psi^Tc^{-1}$.

It can be shown that

$$(27)\qquad \overset{+}{\mathcal{M}}{}^{\bar{a}b}(p', p; k', k) = \gamma_a^1\gamma_b^4c_b\overset{t_b}{\mathcal{M}}{}^{ab}(p, p'; -k', -k)c_b^{-1}\gamma_b^4\gamma_a^4\,,$$

where t_b denotes the spinor transpose w.r.t. fermion b only and $+$ denotes the Hermitian conjugate.

The most general form for $\mathcal{M}^{\bar{a}b}$ can be written as

$$(28)\qquad \mathcal{M}^{ab} = \sum_{i=1}^{8}\Omega_iM_i(k\cdot\overline{p+p'}^1,\ p\cdot p'^1)\,,$$

where $\Omega_i = \Omega_i$ except that p is replaced by p'; $M_6 = mM_8$, $M_7 = -MM_8$.

Then from (27) we get

$$L_i(-k\cdot\overline{p+p^1},\, p\cdot p^1) = \pm \overset{*}{M}_i(k\cdot\overline{p+p^1},\, p\cdot p^1)\,, \tag{29}$$

where $+$ or $-$ to be taken according as $i = 1, 4, 5,$ or $2, 3, 8.$

Write

$$Q_i = L_i + M_i\,; \qquad R_i = L_i - M_i\,. \tag{30}$$

Then

$$\begin{cases} Q_i^*(k\cdot\overline{p+p'},\, p\cdot p^1) = \pm Q_i(-k\cdot\overline{p+p'},\, p\cdot p^1) \\ R_i^*(k\cdot\overline{p+p'},\, p\cdot p^1) = \mp R_i(-k\cdot\overline{p+p'},\, p\cdot p^1)\,, \end{cases} \tag{31}$$

where upper or lower signs are to be taken according as $i = 1, 4, 5,$ or $2, 3.$

We shall now derive the dispersion relations non-rigorously

We can write

$$M_R^{ab} = \bar{U}^{j'}(k')\bar{U}^{i'}(p')\cdot \tag{32}$$

$$\cdot\left[\int \mathrm{d}^4x \exp\left[-ikx\right]\left(\sum_{i=1}^{14} \Gamma^i A_i(x\cdot p,\, x\cdot p',\, p\cdot p',\, x^2)\right)\right] U^i(p)U^j(k)\,,$$

where Γ^i are $1_a 1_b$, $i\gamma_a^\mu x^\mu I_b$, $I_a i\gamma_b^\mu p^\mu$, $I_a i\gamma_b^\mu x^\mu$,

$$i\gamma_a^\mu x^\mu i\gamma_b^\mu p^\mu\,, \quad i\gamma_a^\mu x^\mu i\gamma_b^\mu x^\mu\,, \quad i\gamma_a^\mu i\gamma_b^\mu\,, \quad \gamma_a^5\gamma_b^5\,,$$

$$i\gamma_a^5\gamma_a^\mu x^\mu\gamma_b^5\,, \quad \gamma_a^5 i\gamma_b^5\gamma_b^\mu p^\mu\,, \quad \gamma_a^5 i\gamma_b^5\gamma_b^\mu x^\mu\,,$$

$$i\gamma_a^5\gamma_a^\mu x^\mu i\gamma_b^5\gamma_b^\mu p^\mu\,, \quad i\gamma_a^5\gamma_a^\mu x^\mu i\gamma_b^5\gamma_b^\mu x^\mu\,, \quad i\gamma_a^5\gamma_a^\mu i\gamma_b^5\gamma_b^\mu\,.$$

Similarly

$$M_R^{\bar{a}b} = \bar{U}^{j'}(k')\bar{U}^{i'}(p')\cdot \tag{33}$$

$$\cdot\left[\int \mathrm{d}^4x \exp\left[-ikx\right]\left(\sum_{i=1}^{14} \Gamma'^i B_i(x\cdot p,\, x\cdot p',\, p\cdot p',\, x^2)\right)\right] U^i(p)U^j(k)\,,$$

where $\Gamma'^i = \Gamma^i$ except that p is replaced by p^1.

Using equation (27), we see that

$$A_i(x, p^1, p) = \pm B_i^*(x, p, p^1)\,, \tag{34}$$

where $+$ or $-$ to be taken according as $i = 1, 2, 8, 12, 13, 14$ or $i = 3, 4, 5$

6, 7, 9, 10, 11; $A_i(x, p^1, p)$, $B_i(x, p^1, p)$ vanish everywhere except in the backward light cone.

We shall now use the frame $\boldsymbol{p}+\boldsymbol{p}^1=0$ for the derivation of dispersion relations. To find dispersion relations, say, for L_1, we note that

$$L_1 = \frac{1}{16}\,\text{Trace}\,(\mathcal{M}_R^{ab}) = \int \mathrm{d}^4x \exp[-ikx]\, A_1(x, p, p^1)\,,$$

$$M_1 = \frac{1}{16}\,\text{Trace}\,(\mathcal{M}_R^{\bar{a}\bar{b}}) = \int \mathrm{d}^4x \exp[-ikx]\, B_1(x, p, p^1)\,,$$

$$Q_1(k\cdot\overline{p+p^1},\, p\cdot p^1) = L_1(k\cdot\overline{p+p^1},\, p\cdot p^1) + M_1(k\cdot\overline{p+p^1},\, p\cdot p^1) =$$

$$= L_1(k\cdot\overline{p+p^1},\, p\cdot p^1) + M_1(k^1\cdot\overline{p^1+p},\, p\cdot p^1) =$$

$$= \int \mathrm{d}^4x \exp[-ikx]\, A_1(x, p, p') + \int \mathrm{d}^4x \exp[-ik'x] B_1(x, p', p)\,.$$

On account of our choice of axes $\boldsymbol{p} = 0, 0, P$; $\boldsymbol{p}^1 = 0, 0, -P$, $A_1(x, p, p^1) = A_1(x\cdot p, x\cdot p^1, p\cdot p^1, x^2)$ and $B_1(x, p^1, p)$ are even functions of x_1. Hence

$$Q_1(k_0, P) = \int \mathrm{d}^4x\, [J_1 \cos Px_3 + J_2 \sin Px_3] \cos Qxt \exp[-ik_0x_0]\,,$$

where

$$J_1 = A_1(x, p, p^1) + B_1(x, p^1, p)\,,$$

$$J_2 = -iA_1(x, p, p^1) + iB_1(x, p^1, p)$$

are both real (see equation (33)).

Thus

$$Q_1(k_0, P) = \int \mathrm{d}^4x f(x, P) \cos Qx_1 \exp[-ik_0x_0]\,,$$

where $f(x, P)$ vanishes everywhere except in the backward light cone. Using the identity

$$\exp[-ik_0x_0] \cos Qx_1 = \frac{1}{i\pi}\int_{-\infty}^{\infty} \exp[-ik_0'x_0]\, \frac{\cos Q'x_1}{k_0' - k_0}\, \mathrm{d}k_0'\,,$$

and the causality condition to change order of x-integration and k_0'-integration, we get the dispersion relation

$$\text{Re}\, Q_1(k_0, P) = \frac{\text{P.v.}}{\pi}\int_{-\infty}^{\infty} \frac{\mathrm{d}k_0'}{k_0' - k_0}\, \text{Im}\, Q_1(k_0', P)\,. \tag{34}$$

The same criticism applies for the above derivation of dispersion relations as for the Boson-Fermion case (see reference [3]).

(34) contains integration over negative energies. To get rid of this we use

the symmetry properties (31) and get

$$\text{(35)} \qquad \operatorname{Re} Q_1(k_0, P) = \frac{\text{P.v.}}{\pi}\int_0^\infty \frac{k_0' \mathrm{d}k_0'}{k_0'^2 - k_0^2} \operatorname{Im} Q_1(k_0', P)\,.$$

Similarly for R_1, we get

$$\text{(36)} \qquad \operatorname{Re} R_1(k_0, P) = \frac{2k_0}{\pi}\,\text{P.v.}\int_0^\infty \frac{\mathrm{d}k_0'}{k_0'^2 - k_0^2} \operatorname{Im} R_1(k_0', P)\,.$$

By multiplying $\mathcal{M}^{ab}$ and $\mathcal{M}^{\bar{a}b}$ by suitable factors, and taking trace, we can find dispersion relations for other Q's and R's:

Q_i, R_j satisfy dispersion relations of type (35),

R_i, Q_j » » » » » (36),

where $i = 1, 4, 5$, and $j = 2, 3, 8$.

Our purpose, however, is to write dispersion relations for F functions as they can easily be interpreted physcially, for example in the 2-nucleon case they can be written in terms of phase shifts. But we see from equation (22) that except for F_5^{ab}, F_6^{ab}, the functions F_1^{ab}, F_2^{ab}, etc., do not satisfy conditions of eveness or oddness as $k_0 \to -k_0$. However, combinations of F's can be found for which such conditions hold. Such combinations are

$$\theta_1^{ab} \pm \theta_1^{\bar{a}b}\,, \qquad \theta_2^{ab} \pm \theta_2^{\bar{a}b}\,, \quad \text{etc.}$$

where

$$\theta_1^{ab} = \left[-\frac{P^2}{Mm} L_5 + P^2 L_8\right] = 4P^2 F_5^{ab}\,,$$

$$\theta_1^{\bar{a}b} = \left[-\frac{P^2}{Mm} M_5 - P^2 M_8\right],$$

$$\theta_2^{ab} = \left[\frac{p_0 Q^2}{Mm} L_5\right] = 4Q^2 F_6^{ab}\,,$$

$$\theta_3^{ab} = \left(\frac{1}{m} + \frac{1}{M}\right)(p_0 k_0 L_4) - \frac{p_0^2}{Mm} L_3 - \frac{P^2 + m^2}{Mm} L_2 =$$

$$= \frac{1}{m + k_0}\left[(F_1^{ab} + 4P^2 Q^2 F_4^{ab}) + 2a(F_2^{ab} + F_3^{ab})\right],$$

$$\theta_4^{ab} = \left(\frac{1}{m} - \frac{1}{M}\right)(p_0 k_0 L_1) - \frac{p_0^2}{Mm} L_3 + \frac{P^2 + m^2}{Mm} L_2 =$$

$$= \frac{1}{m + k_0}\left[(F_1^{ab} - 4P^2 Q^2 F_4^{ab}) + 2a(F_3^{ab} - F_2^{ab})\right],$$

$$\theta_5^{ab} = \frac{p_0}{mM} L_1 - \frac{k_0}{m}\left(1 + \frac{m}{M}\right) L_2 + \frac{p_0}{Mm}(Q^2 + m^2)L_4 =$$

$$= \frac{1}{m + k_0}[(F_1^{ab} - 4P^2Q^2F_4^{ab}) - 2b(F_3^{ab} - F_2^{ab})],$$

$$\theta_6^{ab} = \frac{p_0}{Mm} L_1 - \frac{k_0}{m}\left(1 - \frac{m}{M}\right) L_2 - \frac{p_0}{Mm}(Q^2 + m^2)L_4 =$$

$$= \frac{1}{k_0 + m}[(F_1^{ab} + 4P^2Q^2F_4^{ab}) - 2b(F_2^{ab} + F_3^{ab})].$$

Write

$$T_i(k_0, P) = \theta_i^{ab} + \theta_i^{\bar{a}\bar{b}}; \qquad S_i(k_0, P) = \theta_i^{ab} - \theta_i^{\bar{a}\bar{b}}.$$

Then

$$T_i^*(k_0, P) = \mp T_i(-k_0, P); \qquad S_i^*(k_0, P) = \pm S_i(-k_0, P),$$

where upper or lower sign is to be taken according as $i = 2, 3, 4$ or $1, 5, 6$. We are now in a position to write the dispersion relations for θ_i^{ab}.

They follows from our previous work and are

$$\text{(38)} \qquad \text{Re}\,\theta_i^{ab}(k_0, P) - \frac{1}{\pi}\,\text{P.v.}\int_0^\infty \frac{\text{Im}\,\theta_i^{ab}(k_0', P)}{k_0' - k_0}\,dk_0' - \frac{1}{\pi}\,\text{P.v.}\int_0^\infty \frac{\text{Im}\,\theta_i^{\bar{a}\bar{b}}(k_0', P)\,dk_0'}{k_0' + k_0},$$

for $i = 2, 3, 4$ and

$$\text{(39)} \qquad \text{Re}\,\theta_j^{ab}(k_0, P) = \frac{1}{\pi}\,\text{P.v.}\int_0^\infty \frac{\text{Im}\,\theta_j^{ab}(k_0', P)}{k_0' - k_0}\,dk_0' + \frac{\text{P.v.}}{\pi}\int_0^\infty \frac{\text{Im}\,\theta_j^{\bar{a}\bar{b}}(k_0', P)\,dk_0'}{k_0' + k_0},$$

for $j = 1, 5, 6$.

If the integrals on the R.H.S. are not convergent, then we have to supply extra powers of k_0' in the denominators. Right hand sides of the dispersion relations still contain the integrations over the unphysical range 0 to $(P^2 + M^2)^{\frac{1}{2}}$.

We now write θ_i^{ab} in the center of mass frame quantities. We get

$$\text{(40)} \qquad \begin{cases} \theta_1^{ab} = H_5^{ab}, \\ \theta_2^{ab} = H_6^{ab}, \\ \theta_3^{ab} = g_1[H_1^{ab} + H_4^{ab}] + \dfrac{g_2}{k_c^2}\dfrac{1}{\sin\theta_c}(H_2^{ab} + H_3^{ab}), \\ \theta_4^{ab} = g_1'[H_1^{ab} - H_4^{ab}] + \dfrac{g_c'}{k_c^2}\dfrac{1}{\sin\theta_c}(H_3^{ab} - H_2^{ab}), \\ \theta_5^{ab} = h_1[H_1^{ab} - H_4^{ab}] + \dfrac{h_2}{k_c^2}\dfrac{1}{\sin\theta_c}(H_3^{ab} - H_2^{ab}), \\ \theta_6^{ab} = h_1'[H_1^{ab} + H_4^{ab}] + \dfrac{h_2'}{k_c^2}\dfrac{1}{\sin\theta_c}(H_3^{ab} + H_2^{ab}), \end{cases}$$

where

$$g_1 = \frac{1}{p_0^c + k_0^c}\left[\frac{M}{k_0^c + m} + \frac{m}{p_0^c + M} + \frac{2P^2}{(p_0^c + M)(k_0^c + m)}\right],$$

$$g_2 = \frac{2}{p_0^c + k_0^c}\left[Mm + \frac{P^2 M}{k_0^c + m} + \frac{mP^2}{p_0^c + M} + P^2\frac{2P^2 - k_c^2}{(p_0^c + M)(k_0^c + m_0^c)}\right],$$

$$g_1' = \frac{1}{p_0^c + k_0^c}\left[\frac{M}{k_0^c + m} - \frac{m}{p_0^c + M}\right],$$

$$g_2' = \frac{2}{p_0^c + k_0^c}\left[Mm + \frac{mP^2}{p_0^c + M} + \frac{MP^2}{k_0^c + m} + \frac{P^2 k_c^2}{(k_0^c + m)(p_0^c + M)}\right],$$

$$h_1 = \frac{1}{p_0(p_0^c + k_0^c)}\left[\frac{mp_0^c + M(p_0^c + k_0^c)}{k_0^c + m} + \frac{k_0^c(p_0^c + k_0^c) - mk_0^c}{p_0^c + M}\right],$$

$$h_2 = -\frac{2}{p_0(p_0^c + k_0^c)}\left[p_0 k_0 M + \frac{P^2 p_0^c k_0^c}{p_0^c + M} - \frac{P^2 p_0^{c2}}{k_0^c + m}\right],$$

$$h_1' = \frac{1}{p_0(p_0^c + k_0^c)}\cdot$$

$$\cdot\left[2M + \frac{M(p_0^c - k_0^c) - mp_0^c}{k_0^c + m} + \frac{2P^2 - k_0^c(p_0^c + k_0^c) + mk_0^c}{p_0^c + M} + \frac{2p_0^c P}{(p_0^c + M)(k_0^c + m)}\right],$$

$$h_2' = \frac{2}{p_0(p_0^c + k_0^c)}\cdot$$

$$\cdot\left[-Mp_0 k_0 + \frac{P^2(2Mp_0^c - p_0^{c2})}{(k_0^c + m)} - \frac{P^2(2p_0 k_0 - p_0^c k_0^c)}{p_0^c + M} + \frac{2P^2 p_0^c}{(p_0^c + M)(k_0^c + m)}\right].$$

5. – Electron-proton scattering.

It is very difficult to use the general dispersion relations for electron-proton scattering. We shall consider this scattering in the lowest order for electro magnetic interaction and to all orders in meson-nucleon interaction. Then

$$M^{ab} = -M^{a\bar{b}},$$

where a denotes the proton, b the electron and $\bar{b}$ the positron. Now to this order of approximation, the most general form of M_R^{ab} can be written as

$$M_R^{ab} = \bar{U}_b^{j'}(k')\,\bar{U}_a^{i'}(p')[N_1 i\gamma_b^\mu p^\mu + N_2\gamma_a^\mu\gamma_b^\mu]U_a^i(p)\,U_b^j(k)\,.$$

It should, however, be noted that N_1 and N_2 are function of $p\cdot p^1$ only i.e. of momentum transfer only and they are independent of k_0. So to this order of approximation the dispersion relations do not serve a useful purpose. (*)

6. – Two nucleons case.

In this case $M = m$, $H_3 = H_2$ and we get the following expressions for θ_i^{ab} in the center of mass frame:

$$
(41)\quad
\begin{cases}
\theta_1^{ab} = H_5\,, \\
\theta_2^{ab} = H_6\,, \\
\theta_3^{ab} = \dfrac{Mp_0^c + p_c^2}{p_0^c(p_0^c + M_0^c)^2}[H_1 + H_4] + \\
\qquad + \dfrac{1}{p_0^c}\left[M^2 + \dfrac{2P^2M}{p_0^c + M} + P^2\dfrac{2P^2 - k_c^2}{(p_0^c + M)_0^c}\right]\dfrac{1}{k_c^2\sin\theta_c}\,H_2\,, \\
\theta_4^{ab} = 0\,, \\
\theta_5^{ab} = \dfrac{1}{p_0}[H_1 - H_4]\,, \\
\theta_6^{ab} = \dfrac{1}{p_0p_0^c}\left[M + \dfrac{P^2 - p_0^{c2}}{p_0^c + M} + \dfrac{p_0^cP^2}{(p_0^c + M)^2}\right](H_1 + H_4) + \\
\qquad + \dfrac{1}{p_0p_0^c}\left[-Mp_0k_0 + \dfrac{2P^2(Mp_0^c - p_0k_0)}{p_0^c + M} + \dfrac{2P^4p_0^c}{(p_0^c + M)^2}\right]\dfrac{H_2}{k_c^2\sin\theta_c}\,.
\end{cases}
$$

It is clear that for identical particles (p-p scattering) we need to antisymmetrize only the above five functions. Since the expressions for H_1, H_2, H_4, H_5, H_6 in terms of phase shifts for both n-p and p-p scattering are well known ([5]), we can easily write down θ_i^{ab} in terms of phase shifts for the two cases.

There are two main difficulties in using the dispersion relations for the two-nucleon problem. On of these, as already noted, is that dispersion relations involve imaginary parts of amplitudes for nucleon-antinucleon scattering. The second main difficulty is the calculation of contribution from unphysical range which is very complex in this case (see below).

(*) *Note added in proof*: It is, however, possible to write dispersion type relations for N_1 and N_2 when momentum transfer is varied.

([5]) C. Wright: *Phys. Rev.*, **99**, 996 (1955); H. P. Stapp, T. J. Ypsilantis and N. Metropolis: *Phys. Rev.*, **105**, 302 (1957).

7. – The unphysical range for the two nucleon-case.

In our dispersion relations, $k_0 \geqslant (P^2+M^2)^{\frac{1}{2}}$ is the physical range; the region 0 to $(P^2+M^2)^{\frac{1}{2}}$ is unphysical. For the energy interval 0 to $(P^2+M^2)^{\frac{1}{2}}$, we shall use the expression (13) for M_R^{ab}. We can write it as

$$M_R^{ab} = -(2\pi)^3 \Big[\sum_{\substack{n_0 \\ \boldsymbol{n}-\boldsymbol{p}+\boldsymbol{k}=\boldsymbol{p}_n}} \frac{U^{j'}(k')U^{i'}(p')E^{(n)}_{ab}(p_n^\mu, p^\mu, p'^\mu)U^i(p)U^j(k)}{n_0 - p_0 - k_0 - i\varepsilon} - \sum_{\substack{n_0 \\ \boldsymbol{n}=\boldsymbol{p}'-\boldsymbol{k}=\boldsymbol{p}_n}} \frac{U^{j'}(k')U^{i'}(p')K^{(n)}_{ab}(p_n^\mu, p^\mu, p'^\mu)U^i(p)U^j(k)}{n_0 - p_0' + k_0 + i\varepsilon} \Big] .$$

Here

$$\overline{U}^{i'}(p')\, E^{(n)}_{ab}(p_n^\mu, p^\mu, p'^\mu)U^i(p) = \langle p'|K(0)|n_0, \boldsymbol{p}_n = \boldsymbol{p}+\boldsymbol{k}\rangle\langle n_0, \boldsymbol{p}_n|\overline{K}(0)|p\rangle ,$$

$$\overline{U}^{i'}(p')K^{(n)}_{ab}(p_n^\mu, p^\mu, p'^\mu)U^i(p) = \langle p'|\overline{K}(0)|n_0, \boldsymbol{p}_n = \boldsymbol{p}'-\boldsymbol{k}\rangle\langle n_0, \boldsymbol{p}_n|K(0)|p\rangle .$$

Similarly

$$M_R^{\bar{a}\bar{b}} = -(2\pi)^3 \Big[\sum_{\substack{n_0 \\ \boldsymbol{p}_n=\boldsymbol{n}=\boldsymbol{p}+\boldsymbol{k}}} \frac{U^{j'}(k')\overline{U}^{i'}(p')E^{(n)}_{\bar{a}\bar{b}}(p_n^\mu, p^\mu\ p'^\mu)U^i(p)U^j(k)}{n_0 - p_0 - k_0 - i\varepsilon} - \sum_{\substack{n_0 \\ \boldsymbol{p}_n=\boldsymbol{p}'-\boldsymbol{k}=\boldsymbol{n}}} \frac{\overline{U}^{j'}(k')\overline{U}^{i'}(p')K^{(n)}_{\bar{a}\bar{b}}(p_n^\mu, p^\mu, p'^\mu)U^i(p)U^j(k)}{n_0 - p_0' + k_0 + i\varepsilon} \Big] ,$$

It can be shown that the numerators in above equations are real. Then

$$\operatorname{Im} M_R^{ab} = (2\pi)^4 \overline{U}^{j'}(k')\overline{U}^{i'}(p')\Big[\sum_{\substack{r_n^0 - n_0 \\ \boldsymbol{p}_n=\boldsymbol{p}+\boldsymbol{k}}} E^{(n)}_{ab}(p_n^\mu, p^\mu, p'^\mu)\delta(p_n^0 - p_0 - k_0) - \sum_{\substack{p_{n0}=n_0 \\ \boldsymbol{p}_n=\boldsymbol{p}'-\boldsymbol{k}}} K^{(n)}_{ab}(p_n^\mu, p^\mu, p'^\mu)\delta(p_n^0 - p_0' + k_0)\Big]U^i(p)U^j(k) .$$

Similar expression for $\operatorname{Im} M_R^{\bar{a}\bar{b}}$ can be written out. Let us consider the forward scattering:

$$P = 0 , \qquad p' = p , \qquad k' = k$$

and unphysical range is from 0 to M. Both terms of $\operatorname{Im} M_R^{ab}$ contribute to the absorption integrals. In the first term of $\operatorname{Im} M_R^{ab}$, $p_n = p+k$ and so $k_0 = ((p_n^2 = M_n^2)/2M) - M$ and the possible state which can contribute is deu-

teron (*) of energy, say, E_D. In the second term of Im M_R^{ab}, $p_n = p' - k$ and so $k_0 = M - ((p_n^2 = M_n^2)/2M)$ and possible states which can contribute are 1 pion state, two and more mesons states of energies, say, E_1, E_2, ... respectively. Write

$$k_D = E_D - M \quad \text{and} \quad k_n = E_n - M\,,$$

$$E_1 = \frac{\mu^2}{2M}\,, \qquad E_n = \frac{(\mu_n)^2}{2M} \quad \text{and} \quad E_D = 2M - 2B + \frac{B^2}{2M},\ B = \text{Binding energy}\,.$$

Then we can write (for example)

$$\text{Im}\, L_1(k_0) = (2\pi)^4[E^d_{1(ab)}\delta(k_0 - k_D) - K^{(1)}_{1(ab)}\delta(k_0 + k_1) - \\ - \text{contribution from 2 and more mesons states}].$$

Here $E_1^{(d)}(ab) = \text{Trace}\,(E^{(d)}_{ab})$ and $K^{(1)}_{1(ab)} = \text{Trace}\,(K^{(1)}_{(ab)})$.

Consider now Im M_R^{ab}. The contributing states are those which have nucleon number. zero. There is no term corresponding to $\delta(k_0 - k_1)$ in this case.

If we now consider

$$\frac{k_0^2 - k_D^2}{k_D^2 - a_D^2}\,\frac{k_0^2 - k_1^2}{k_D^2 - a_1^2}\,,$$

instead of $Q_1(k_0)$ and in the end take limits $a_D \to k_D$, $a_1 \to -k_1$, we get the following dispersion relation for $L_1(k_0)$

$$\text{Re}\, L_1(k_0) = \frac{1}{\pi} P\int_M^\infty \mathrm{d}k_0' \frac{\text{Im}\, L_1(k_0')}{k_0' - k_0} + \frac{1}{\pi} P\int_M^\infty \mathrm{d}k_0' \frac{\text{Im}\, M_1(k_0')}{k_0' + k_0} + \\ + \frac{1}{\pi} P\int_0^{M-(2\mu^2/M)} \mathrm{d}k_0' \frac{\text{Im}\, L_1(k_0')}{k_0' - k_0} + \frac{1}{\pi} P\int_0^M \frac{\text{Im}\, M_1(k_0')}{k_0' + k_0}\,\mathrm{d}k_0' + \\ + \frac{\text{Residue Re}\, L_1(k_0)_{k_0 = k_D}}{k_0 - k_D} + \frac{\text{Residue Re}\, L_1(k_0)_{k_0 = -k_1}}{k_0 + k_1}\,.$$

Similarly we can write the dispersion relations for other functions. It is not very difficult to calculate the contribution of the one meson state.

It may be noted from (41) that for forward scattering H_1 and H_4 also decouple but $H_2/\sin\theta_c$ does not.

(*) This contribution is for the $n - p$ case only.

* * *

The author is deeply indebted to Professor A. Salam for guidance and encouragement. A scholarship awarded by the Ministry of Education, Government of Pakistan, is gratefully acknowledged.

Note added in proof.

The author has recently seen a preprint by M. L. Goldberger, Y. Nambu and R. Oehme giving similar relations. Their results agree with ours. They have discussed the relations in detail.

RIASSUNTO (*)

In modo simile a quello usato per lo scattering fermione-bosone si derivano relazioni di dispersione generalizzate per lo scattering di due fermioni. Si discute in particolare il problema dei due nucleoni. Le relazioni si scrivono per funzioni esprimibili in termini degli spostamenti di fase.

(*) *Traduzione a cura della Redazione.*

Neutron Polarization from Electron Disintegration.

M. Suffczyński

Institute of Theoretical Physics - Warsaw, Poland

(ricevuto il 30 Maggio 1957)

Summary. — The polarization of neutrons from disintegration of the deuteron by fast electrons is calculated in dipole approximation.

The nuclear disintegrations caused by electrons have not been investigated very exhaustively. The deuteron disintegration cross-section has been calculated in a well known paper by Bethe and Peierls [1] and Peters and Richman [2]. More general approaches to electrodisintegration have been given by Amaldi, Fidecaro, Mariani [3], Ter-Martirosyan [4], Thie, Mullin, Guth [5] and by others authors [6,7].

Recently Czyż and Sawicki [8,9] have given the method for calculation of the polarization of photonucleons. The procedure can be applied to the case of disintegration caused by electrons. Here it seemed hopeless to find out experimentally the polarization because the cross-section for electron disintegration is generally 137 times smaller than the photo cross-section. Theoretically, however, the problem is interesting. It differs from the photodisintegration mainly because here we have an outgoing electron besides the outgoing neutron in contradistinction to the case of photoeffect. Moreover the interaction between the electron and the proton is assumed in the form of a Møller interaction and the Møller potentials are not transverse only.

[1] H. A. Bethe and R. Peierls: *Proc. Roy. Soc.*, A **148**, 146 (1935).
[2] B. Peters and C. Richman: *Phys. Rev.*, **59**, 804 (1941).
[3] E. Amaldi, G. Fidecaro and F. Mariani: *Nuovo Cimento*, **7**, 757 (1950).
[4] K. Ter-Martirosyan: *Journ. Exp. Theor. Phys.*, **20**, 925, 937 (1950).
[5] J. A. Thie, C. J. Mullin and E. Guth: *Phys. Rev.*, **87**, 962 (1952).
[6] I. N. Sneddon and B. F. Touscheck: *Proc. Roy. Soc.*, A **193**, 344 (1948).
[7] V. Z. Jankus: *Phys. Rev.*, **102**, 1586 (1956).
[8] W. Czyż and J. Sawicki: *Nuovo Cimento*, **3**, 864 (1956).
[9] W. Czyż and J. Sawicki: *Nuovo Cimento*, **5**, 45 (1957).

The energy and momentum of the incoming electron in units of electron mass will be denoted by E, $\boldsymbol{p}$, those of the outgoing electron by E', $\boldsymbol{p}'$. The energy momentum transfer during the collision is $\omega = E - E'$, $\boldsymbol{q} = \boldsymbol{p} - \boldsymbol{p}'$. The electron plane waves have the amplitudes u and u' respectively. The Dirac matrices are $\boldsymbol{\alpha}$, the electron rest energy is mc^2.

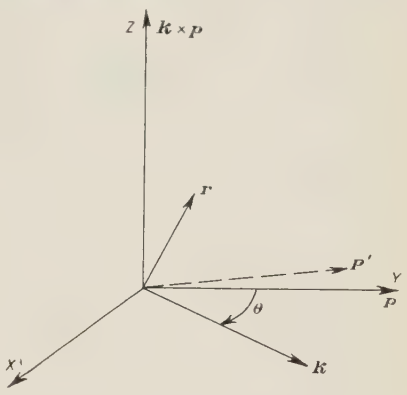

Fig. 1.

The radius vector from the neutron to the proton is $\boldsymbol{r}$, the nucleon mass is M, the neutron and proton magnetic momenta are μ_n and μ_p in nuclear magnetons, the spin operators are $\boldsymbol{\sigma}_n$ and $\boldsymbol{\sigma}_p$ respectively.

Fig. 1 helps to orientate in the reference system used. The direction of momentum $\boldsymbol{k}$ of the outgoing neutron makes the angle θ with the direction of the incoming electron. The quantization axis is chosen in the direction of $\boldsymbol{k}\times\boldsymbol{p}$.

The interaction between the electron and the neutron-proton system will be considered here only in the dipole approximation. In this approximation the hamiltonian is proportional to

$$u'^{*}\left[\omega\boldsymbol{\alpha}\boldsymbol{r} - \boldsymbol{q}\boldsymbol{r} + \frac{\hbar}{2Mc}(\mu_n - \mu_p)(\boldsymbol{\sigma}_n - \boldsymbol{\sigma}_p)\boldsymbol{q}\times\boldsymbol{\alpha}\right] u(q^2 - \omega^2)^{-1}\,. \tag{1}$$

The calculation of the reaction amplitude $f\chi$ follows the method of Czyż and Sawicki ([9]). Now besides averaging and summing over the deuteron states we average over the initial and sum over the final electron spins and integrate over the angles of the outgoing electron. The neutron polarization thus obtained has only the z component different from zero

$$P = \frac{\langle f\chi\,|\,\sigma_{nz}\,|f\chi\rangle_{av}}{\langle f\chi\,|f\chi\rangle_{av}} = \frac{a\sin 2\theta + b\sin\theta}{g + h\cos 2\theta}\,. \tag{2}$$

Assuming for the deuteron the simple theory of Rarita and Schwinger ([10]) the coefficients in (2) can be written

$$\begin{cases} a &= a\,a_l\,, \\ a &= \dfrac{1}{4p}\left[3E\omega - 7E^2 - 5 + \dfrac{2E^2(2E^2+\omega^2-2E\omega)+\omega^2-8E\omega-4E^2}{pp'}\ln\right], \\ a_l &= \tfrac{1}{3}I_0I_2\sin(\eta_0-\eta_2) + \tfrac{1}{2}I_1I_2\sin(\eta_1-\eta_2)\,, \\ b &= \left[E + E' - \dfrac{E(p^2+p'^2)}{pp'}\ln\right]\dfrac{\hbar}{Mc}(\mu_n-\mu_p)I_sI_1\sin(\delta_s-\eta_1)\,, \end{cases} \tag{3}$$

([10]) W. Rarita and J. Schwinger: *Phys. Rev.*, **59**, 436, 556 (1941).

$$
(4)\quad
\begin{cases}
g = g' + g'' + g''', \\
g' = \dfrac{1}{2p}\left[E\omega + 1 - 5E^2 + \dfrac{2E^2(2E^2+\omega^2-2E\omega)-\omega^2-4E^2}{pp'}\ln\right]\cdot \\
\qquad \cdot\left[\dfrac{1}{9}I_0^2 + \dfrac{5}{16}I_1^2 + \dfrac{73}{144}I_2^2 - \dfrac{1}{18}I_0I_2\cos(\eta_0-\eta_2) - \dfrac{1}{8}I_1I_2\cos(\eta_1-\eta_2)\right], \\
g'' = \dfrac{1}{2p}\left[3 + E^2 - E\omega + \dfrac{\omega(4E-\omega)}{pp'}\ln\right]\cdot \\
\qquad \cdot\left[\dfrac{1}{9}I_0^2 + \dfrac{3}{8}I_1^2 + \dfrac{47}{72}I_2^2 + \dfrac{1}{9}I_0I_2\cos(\eta_0-\eta_2) + \dfrac{1}{4}I_1I_2\cos(\eta_1-\eta_2)\right], \\
g''' = \left[\dfrac{p^2+p'^2}{p'}\ln\right]\left[\dfrac{\hbar}{Mc}(\mu_n-\mu_t)I_s\right]^2, \\
h = -a\,h_1, \\
h_1 = \dfrac{1}{8}I_1^2 + \dfrac{7}{24}I_2^2 + \dfrac{1}{3}I_0I_2\cos(\eta_0-\eta_2) + \dfrac{3}{4}I_1I_2\cos(\eta_1-\eta_2), \\
\ln \equiv \ln\dfrac{EE'+pp'-1}{E-E'}.
\end{cases}
$$

Here the I_J ($J = 0, 1, 2$) and I_S are the radial integrals for ^3P_J and $^1S_0$-states and η_J, δ_S are the appropriate phase shifts (9). To compute numerical examples the values of the radial integrals and phase shifts have been taken from the work of CZYŻ and SAWICKI (9) for the energy transfer $E - E' = \omega = 17.6$ MeV. Maximum polarizations are given in Table I.

TABLE I.

Electron total energy	Deuteron theory		
	Symmetrical	Charged	Neutral
$E = 18.11$ MeV	$P(18°) = 10\%$	$P(155°) = 10\%$	$P(145°) = -5\%$
$E = 22.91$ MeV	$P(20°) = 9\%$	$P(154°) = 10\%$	$P(144°) = -5\%$

Obviously, fixing the energy transfer in electron disintegration is not a satisfactory procedure. We should rather, for comparison with a feasible experiment, calculate the polarization by taking the sum over all outgoing electrons, that means with the fixed direction of observation of the outgoing neutron over all energies of the outgoing electron. This however can be done in a simple way only by making the crude approximation of the central zero range forces for the deuteron. Following this approximation one can effectively integrate over the final electron energies. The polarization comes now exclu-

sively from the interference between electric and magnetic dipole terms ([11]) thus it will be appreciable for lower energies where the electric and magnetic dipole cross-sections are small but of comparable magnitude. The electric transition is to the P-portion of plane wave. The magnetic transition is to the singlet $^1S_0$-state, the radial function of which is assumed in the form $\sin(kr+\delta)/r$ where $\operatorname{ctg}\delta = (\gamma/(E-E'-\varepsilon))^{\frac{1}{2}}$. The absolute value of the deuteron binding energy in units of electron mass will be denoted by ε, so the limits of integration over electron energy will be from 1 to $E-\varepsilon$. The resulting expression for polarization can be cast into the form

$$P = \frac{b \sin\theta}{c + d \sin^2\theta}, \tag{5}$$

$$b = (\mu_n - \mu_p)\left(\frac{m}{M}\right)^{\frac{1}{2}} (\gamma^{\frac{1}{2}} + \varepsilon^{\frac{1}{2}}) \cdot \int \left[p'(E+E') - \frac{E}{p}(p^2 + p'^2)\ln\right] \frac{(E-E'-\varepsilon)^{\frac{3}{2}}\,\mathrm{d}E'}{(E-E')^3(E-E'-\varepsilon+\gamma)}, \tag{6}$$

$$\left\{\begin{aligned} c &= 3\int\left[\frac{p'}{p}(3+EE') + \frac{3E^2-2EE'-E'^2}{p^2}\ln\right]\frac{(E-E'-\varepsilon)^{\frac{3}{2}}\,\mathrm{d}E'}{(E-E')^4} + \\ &\quad + \frac{1}{2}\frac{m}{M}(\mu_n-\mu_p)^2(\gamma^{\frac{1}{2}}+\varepsilon^{\frac{1}{2}})^2\int\left[(p^2+p'^2)\ln\right]\frac{(E-E'-\varepsilon)^{\frac{1}{2}}\,\mathrm{d}E'}{(E-E')^2(E-E'-\varepsilon+\gamma)}, \\ d &= \frac{3}{2}\int\left[-\frac{p'}{p}(5+4E^2+3EE') + \frac{2E^2(E^2+E'^2)+E'^2+6EE'-11E^2}{p^2}\ln\right]\cdot \\ &\quad \cdot\frac{(E-E'-\varepsilon)^{\frac{3}{2}}}{(E-E')^4}\,\mathrm{d}E'. \end{aligned}\right. \tag{7}$$

Adopting the numerical values of PETERS and RICHMAN ([2]) we get the following maximum polarization of the neutron irrespective of outgoing electron energy: for the incoming total electron energy $E = 5.18$ MeV, i.e. 2.5 MeV kinetic energy above the threshold $\max P(42°) = 28\,\%$ and for energy $E = 8.3$ MeV, $\max P(32°) = 26\,\%$. These values are considerable. In spite of the difficulties caused by small values of the total cross-section the modern intense electron beams may render the polarization experiment possible.

The calculated values of polarization depend much on the theory assumed for the neutron-proton system. All shortcomings of the present treatment are obvious, such as for instance the complete omission of the question of exchange meson current in the deuteron.

([11]) L. N. ROSENZWEIG: *Physica*, **22**, 1182 (1956).

* * *

I am greatly indebted to Dr. J. SAWICKI for suggesting this problem to me, and to him and Dr. W. CZYŻ for giving me their detailed calculations on photoeffect. I thank Professor L. ROSENFELD for an interesting discussion.

RIASSUNTO (*)

In approssimazione di dipolo si calcola la polarizzazione dei neutroni derivanti dalla disintegrazione del deutone da parte di elettroni veloci.

(*) *Traduzione a cura della Redazione.*

IL NUOVO CIMENTO Vol. VI, N. 6 1° Dicembre 1957

Dispersion Relations for Heavy Meson-Nucleon Interaction in a Fixed Source Theory.

II. – Effective Range Relations.

D. Amati

Istituto di Fisica Teorica dell'Università - Napoli
Istituto Nazionale di Fisica Nucleare - Sezione di Roma

B. Vitale

Istituto di Fisica dell'Università - Catania
Centro Siciliano di Fisica Nucleare - Catania

(ricevuto il 6 Giugno 1957)

Summary. — The dispersion relations for heavy meson-nucleon interaction in fixed source theory, derived in a previous paper (I), are used here in order to obtain effective range type relations. Both scalar and pseudoscalar K-mesons are considered. In the first section of this paper we carry out the desired inversion of the scattering amplitudes satisfying dispersion relations. In the third one the obtained effective range relations are discussed together with the possibility of obtaining approximate solutions for the scattering amplitudes starting directly from the dispersion relations.

It is our aim in this paper to analyze the dispersion relations for heavy meson-nucleon interaction obtained in a preceding paper [1], in order to discuss the possibilities of deriving effective range relations and of solving them in an approximate way for the scattering amplitudes.

Our problem will therefore be to obtain equations satisfyed by the reciprocals of the scattering amplitudes. The real part of these reciprocals, when the phase shifts are real, will give us a quantity directly related to the $k \cot \delta$

[1] D. Amati and B. Vitale: *Nuovo Cimento* **6**, 1027 (1957), referred to as I in the following.

which appears in the usual effective range relations; when the phase shifts are complex, we shall obtain an expression where a combination of the real and imaginary parts of a phase shift is equated to a sum of terms containing the renormalized coupling constant and integrals over the cross-sections. We shall in general call effective range relations all those in which the inverse of a scattering amplitude is involved.

In the first two sections of this paper we shall deal with the formal problem of the inversion of scattering amplitudes, following consistently a method used by KLEIN [2] for pion nucleon interaction. In the third section the obtained effective range relations are discussed together with the possibility of obtaining approximate solutions for the scattering amplitudes.

1. – It is worthwhile to note that it is not possible to carry out in a straightforward fashion the inversion of $f_i(\omega)$ or $\bar{f}_i(\omega)$ satisfying the dispersion relation derived in I, because of the possible zeros of the scattering amplitudes. In order to be able to carry out the inversion, we shall introduce the following functions of the complex variable z:

$$D_i(z,\omega) = 1 - \frac{z}{\omega}\frac{k^2v^2(\omega)}{\pi b_i(\omega)}\int_\mu^\infty \frac{d\omega'}{v^2(\omega')k'^2}\left[\frac{\operatorname{Im} f_i(\omega')}{\omega'-z} + \frac{\operatorname{Im}\bar{f}_i(\omega')}{\omega'+z}\right], \tag{1a}$$

$$\bar{D}_i(z,\omega) = 1 - \frac{z}{\omega}\frac{k^2v^2(\omega)}{\pi \bar{b}_i(\omega)}\int_\mu^\infty \frac{d\omega'}{v^2(\omega')k'^2}\left[\frac{\operatorname{Im}\bar{f}_i(\omega')}{\omega'-z} + \frac{\operatorname{Im} f_i(\omega')}{\omega'+z}\right], \tag{1b}$$

where

$$b_i(\omega) = C_i^\Lambda(\omega) + C_i^\Sigma(\omega) + \frac{1}{2v^2(m_K)}\left(1+\frac{\omega}{m_K}\right)\operatorname{Re} f_i(m_K) + \frac{1}{2v^2(m_K)}\left(1-\frac{\omega}{m_K}\right)\operatorname{Re}\bar{f}_i(m_K), \tag{2a}$$

$$\bar{b}_i(\omega) = \bar{C}_i^\Lambda(\omega) + \bar{C}_i^\Sigma(\omega) + \frac{1}{2v^2(m_K)}\left(1+\frac{\omega}{m_K}\right)\operatorname{Re}\bar{f}_i(m_K) + \frac{1}{2v^2(m_K)}\left(1-\frac{\omega}{m_K}\right)\operatorname{Re} f_i(m_K), \tag{2b}$$

the $C_i^H(\omega)$ and $\bar{C}_i^H(\omega)$ being defined by (18) of I. We note that

$$b_i(-\omega) = \bar{b}_i(\omega). \tag{3}$$

It is readily seen that $D_i(z,\omega)b_i(\omega)$ and $D_i(z,\omega)\bar{b}_i(\omega)$ satisfy the dispersion relations (17) of I when $z=\omega+i\varepsilon$, where ε is a vanishing small positive

[2] A. KLEIN: *Phys. Rev.*, **104**, 1136 (1956).

number. This means that the D are defined in such a way that

$$\lim_{z\to\omega+i0} D_i(z,\omega) = \frac{f_i(\omega)}{b_i(\omega)}, \qquad \lim_{z\to\omega+i0} \bar{D}_i(z,\omega) = \frac{\bar{f}_i(\omega)}{b_i(\omega)}. \tag{4}$$

Putting $z = x + iy$ the functions defined by (1) have the following properties:

a) they are analytic in the cut z plane with branch lines on the real axis going from $-\mu$ to $-\infty$ and from m_K to ∞ for $D(z,\omega)$, and from $-m_K$ to $-\infty$ and from μ to ∞ for $\bar{D}(z,\omega)$.

b) $D_i(0,\omega) = \bar{D}_i(0,\omega) = 1$.

c) $D_i^{-1}(z,\omega)$ and $\bar{D}_i^{-1}(z,\omega)$ are bounded for $z\to\infty$.

d) Using (3) we see that they present the following crossing property:

$$D_i(-z,-\omega) = D_i(z,\omega).$$

e) They are real functions, in the sense that $D(z^*,\omega) = D^*(z,\omega)$; $\bar{D}(z^*,\omega) = \bar{D}^*(z,\omega)$.

f) Crossing the real axis from negative to positive values of y their imaginary parts are subject to discontinuities expressed by:

$$\lim_{y\to+0}[D_i(z,\omega) - D_i^*(z,\omega)] = \begin{cases} 2i\dfrac{k^2v^2(\omega)}{\omega b_i(\omega)}\dfrac{x\,\mathrm{Im}\,f_i(x)}{v^2(x)k_x^2}, & x > m_K, \\ 0, & -\mu < x < m_K, \\ -2i\dfrac{k^2v^2(\omega)}{\omega b_i(\omega)}\dfrac{x\,\mathrm{Im}\,\bar{f}_i(x)}{v^2(x)k_x^2}, & x < -\mu, \end{cases}$$

$$\lim_{y\to+0}[\bar{D}_i(z,\omega) - \bar{D}_i^*(z,\omega)] = \begin{cases} 2i\dfrac{k^2v^2(\omega)}{\omega b_i(\omega)}\dfrac{x\,\mathrm{Im}\,f_i(x)}{v^2(x)k_x^2}, & x > \mu, \\ 0, & -m_K < x < \mu, \\ -2i\dfrac{k^2v^2(\omega)}{\omega b_i(\omega)}\dfrac{x\,\mathrm{Im}\,f_i(x)}{v^2(x)k_x^2}, & x < -m_K. \end{cases}$$

g) They have no zeros for complex values of z. We shall assume that D_i and $\bar{D}_i$ have no zeros on the real axis; this assumption imposes a restriction on the behaviour of the individual cross-sections for K and $\bar{\text{K}}$ mesons. How the following arguments have to be modified if zeros are indeed present on the real axis is indicated in the appendix of KLEIN's paper [2].

[3] G. F. CHEW and F. E. LOW: *Phys. Rev.*, **101**, 1570 (1956).

We consider now the integral of the function:

$$R_i(z') = [D_i(z', \omega)\, z'(z' - z)]^{-1}, \tag{5}$$

over the contour in the z-plane given in Fig. 1. Applying Cauchy's theorem and using properties *d*) and *g*) listed above we obtain after taking the real part of the equation:

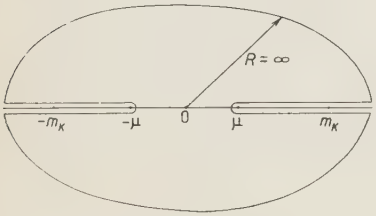

Fig. 1.

$$\text{Re}\,\frac{1}{D_i(\omega, \omega)} = 1 - \frac{k^2 v^2(\omega)}{\pi b_i(\omega)} \int_{\mu}^{\infty} \frac{\mathrm{d}\omega'}{v^2(\omega') k'^2} \cdot \left[\frac{\text{Im}\, f_i(\omega')}{(\omega' - \omega)\, |D_i(\omega', \omega)|^2} + \frac{\text{Im}\, \bar{f}_i(\omega')}{(\omega' + \omega)\, |\bar{D}_i(\omega', -\omega)|^2} \right]. \tag{6a}$$

In an analogous way we find for the reciprocal of $D_i(\omega, \omega)$:

$$\text{Re}\,\frac{1}{D_i(\omega, \omega)} = 1 - \frac{k^2 v^2(\omega)}{\pi \bar{b}_i(\omega)} \cdot \int_{\mu}^{\infty} \frac{\mathrm{d}\omega'}{v^2(\omega') k'^2} \left[\frac{\text{Im}\, \bar{f}_i(\omega')}{(\omega' - \omega)\, |D_i(\omega', \omega)|^2} + \frac{\text{Im}\, f_i(\omega')}{(\omega' + \omega)\, |D_i(\omega', -\omega)|^2} \right]. \tag{6b}$$

From (6*a*) we get for the $i = \frac{1}{2}$ case corresponding to K^+-p interaction (pure $T = 1$ state) whose phase shift is real:

$$k \cot \delta_{\frac{1}{2}}(\omega) = \frac{1}{b_{\frac{1}{2}}(\omega)} - \frac{k^2 v^2(\omega)}{\pi b_{\frac{1}{2}}^2(\omega)} \int_{\mu}^{\infty} \frac{\mathrm{d}\omega'}{v^2(\omega') k'^2} \left[\frac{\text{Im}\, f_{\frac{1}{2}}(\omega')}{(\omega' - \omega)\, |D_{\frac{1}{2}}(\omega', \omega)|^2} + \frac{\text{Im}\, \bar{f}_{\frac{1}{2}}(\omega')}{(\omega' + \omega)\, |\bar{D}_{\frac{1}{2}}(\omega', -\omega)|^2} \right], \tag{7}$$

Eq. (6) and in particular (7) are the desired « effective range » relations.

It would be tempting to derive effective range relations similar to (6) for pure isobaric spin states in order to obtain an expression like (7) also for $k \cot \delta^{\alpha}$. But, as can be easily seen from (22) of I, the functions $D^{\alpha}(z, \omega)$ and $D^{\alpha}(z, \omega)$ defined in analogy with the D and $\bar{D}$ given in (1), do not have crossing properties corresponding to *d*) and there is also the possibility of failure of property *g*) due to negative signs of elements of the first row and column of the crossing matrix A (see (23) of I).

In the particular case of Hamiltonians considered in Sect. 2 of I, we obtain immediately the effective range relations in terms of the two renormalized

coupling constants G_Λ and G_Σ (for the « scalar » case) of F_Λ and F_Σ (for the « pseudoscalar » case) just by substituting the values of $C_i^{\mathrm{II}}(\omega)$ and $\bar{C}_i^{\mathrm{II}}(\omega)$ given in Sect. 2 of I into (2).

2. – With a method similar in all to that used in the preceding section, we can find the relations involving the reciprocals of the scattering amplitudes satisfying the dispersion relations (40) and (43) of I obtained by the Chew and Low method. Defining again functions $D(z, \omega)$ and $\bar{D}(z, \omega)$ in a way analogous to that of Sect. **1**, i.e. so that

$$\lim_{z\to\omega+i0} D_i(z, \omega) = \frac{f_i(\omega)}{I_i(\omega)}, \qquad \lim_{z\to\omega+i0} \bar{D}_i(z, \omega) = \frac{f_i(\omega)}{\bar{I}_i(\omega)}, \tag{8}$$

where $I_i(\omega)$ and $\bar{I}_i(\omega)$ are given by (38) of I for « scalar » heavy mesons, and by (44) of I for « pseudoscalar » ones; the desired dispersion relations can be straightforwardly obtained. For simplicity we write down only those for K^+-p interaction (pure $T=1$ state), i.e.

$$k \cot \delta_{\frac{1}{2}}(\omega) = \frac{1}{I_{\frac{1}{2}}(\omega)} - \frac{f^2(\omega)}{4\pi^2 I_{\frac{1}{2}}^2(\omega)} \int_\mu^\infty \frac{k'\, \mathrm{d}\omega'}{v^2(\omega)} \left[\frac{\sigma_{\frac{1}{2}}(\omega')}{(\omega' - \omega)\, |D_{\frac{1}{2}}(\omega', \omega)|^2} + \frac{\bar{\sigma}_{\frac{1}{2}}(\omega')}{(\omega' + \omega)\, |\bar{D}_{\frac{1}{2}}(\omega', -\omega)|^2} \right], \tag{9}$$

for « scalar » heavy mesons, and

$$k \cot \delta_{\frac{1}{2}}(\omega) = \frac{1}{\bar{I}_{\frac{1}{2}}(\omega)} - \frac{v^2(\omega)}{4\pi_{p.s.}^2 I_{\frac{1}{2}}^2(\omega)} \int_\mu^\infty \frac{\mathrm{d}\omega'}{k' v^2(\omega')} \left[\frac{\sigma_{\frac{1}{2}}(\omega')}{(\omega' - \omega)\, |D_{\frac{1}{2}}(\omega', \omega)|^2} + \frac{\bar{\sigma}_{\frac{1}{2}}(\omega')}{(\omega' - \omega)\, |D_{\frac{1}{2}}(\omega', -\omega)|^2} \right], \tag{10}$$

for « pseudoscalar » heavy mesons.

3. – We want to discuss now in some detail, the effective range relations derived in the previous sections, and the possibility of using them to investigate the behaviour of the scattering amplitudes with energy. First of all we compare the effective range relations obtained in the first section (derived from Klein type dispersion relations) with those derived in the second section (from Chew-Low type dispersion relations). We shall examine particularly among the effective range relations the K^+-p interaction ($T=1$) for the scalar case; namely eq. (7) and (9).

In order to obtain from them effective range relations more similar to those we are used to in the theory of scattering by short range potentials, we should have to disregard the ω dependence of the integrals over the cross-sections in (7) and (9). When ω is of the order of m_K the D functions are slowly varying functions of ω: but in both cases the important part of the integrals seems to come from the low energy region. This is due to the k'^{-1} present in the denominator of the integrand in (7) and the k' that is also implicitly present in the denominator of the integrand in (9), because of the k^{-2} dependence of $\sigma(\omega)$. It is however clear that, while the very low energy region of the integral in (9) can be disregarded because there the cross-sections are nearly constant, this cannot be done in (7). It seems then that even if effective range relations with an effective range very slowly depending on the energy cannot be derived in a completely reliable way from dispersion relations, the best approximation to such effective range relations can be obtained from the Chew-Low dispersion relations.

Let us now compare (9) (scalar case) with (10) (pseudoscalar case). It is easy to see that also in this case eq. (9) presents the advantage of containing an integral over the cross-sections whose lowest energy contribution can be considered small; this means that in the pseudoscalar case standard type effective range relations are less reliable than in the scalar case. On the other hand, we note that (7) and (10) present the advantage over (9) of being much more convergent for large values of ω', which means that they can be used even if the integral present in (9) actually does not converge.

We want here to emphasize why our result for the pseudoscalar case is quite different from that found by CHEW and LOW ([3]) and by KLEIN ([2]) for pseudoscalar pions. This is closely connected with the different ω dependence of the terms containing the coupling constants, which gives in our case a vanishing $\omega f_i(\omega)$, when ω goes to 0. It is easy to see that this difference depends on the different energy spectrum of the Hamiltonian used here compared to the energy spectrum of the π-N Hamiltonian that presents a state for $\omega = 0$ (physical nucleon).

Approximate methods have already been applied in order to study the heavy meson-nucleon interaction; in particular models analogous to the Lee model have been applied both to K-N and $\overline{\text{K}}$-N scattering ([4]). We want here to discuss the limit of validity of these calculations by an analysis of the corresponding dispersion relations.

We start again from the dispersion relations for the physical states. A very straightforward iteration procedure can be applied at once to (40a) of I, calculating Re $f_i(\omega)$ at zero order as given only by the term containing the renormalized coupling constant, namely $I_i(\omega)$. If we limit our analysis to

([4]) D. AMATI and B. VITALE: *Nuovo Cimento*, **5**, 1533, (1957); **6**, 261, (1957).

the $i = \frac{1}{2}$ physical system (real phase shift) and to the scalar case,

$$\text{Re}\, f_{\frac{1}{2}}^{(0)}(\omega) = \frac{1}{2k} \sin 2\delta_{\frac{1}{2}}^{(0)}(\omega) = I_{\frac{1}{2}}(\omega)\,, \tag{11}$$

from which, being:

$$\sigma_{\frac{1}{2}}^{(0)}(\omega) = \frac{2\pi}{k^2}\left[1 - \sqrt{1 - 4k^2 I_{\frac{1}{2}}^2(\omega)}\right], \tag{12}$$

It is easy to find out the first order approximation for $\text{Re}\, f_{\frac{1}{2}}(\omega)$:

$$\text{Re}\, f_{\frac{1}{2}}^{(1)}(\omega) = I_{\frac{1}{2}}(\omega) + \frac{v^2(\omega)}{4\pi^2} \int_{\mu}^{\infty} \frac{k'\, \mathrm{d}\omega'}{v'(\omega')} \frac{\sigma_{\frac{1}{2}}^{(0)}(\omega')}{\omega' - \omega}\,. \tag{13}$$

In order to get (13) we have disregarded the contribution to the integrand coming from the $\bar{\sigma}(\omega')$. This part of the approximation cannot be justified « a priori ». In order to obtain the order of magnitude of the error involved in this approximation (which is equivalent to an expansion in powers of the renormalized coupling constant) we have compared the first order result (13) with the experiment. The following choice for the coupling constant

$$\frac{G_\Lambda^2}{4\pi} = \frac{G_\Sigma^2}{4\pi} = 0.3\,,$$

gives at $E_K^{\text{lab}} = 100$ MeV, a cross-section of about 7 mb to be compared with the 15 mb given by the experiment ([5]). We note that with the previous choice of the coupling constants, the contribution of the integral to the first order approximation is relatively small and that the contribution coming from the disregarded part of the integral involving the cross-section $\bar{\sigma}$ is positive definite, justifying so the sense of the discrepancy observed. The previous result is however rather sensitive to the numerical values of the coupling constants and cannot be considered therefore as a conclusive evidence about the possibility of disregarding without too great disagreement the contribution coming from $\overline{\text{K}}$ in K-N interaction.

We note besides, that our choice for the coupling constants, $G_\Lambda^2 = G_\Sigma^2$ give a negligible $T = 0$ interaction (as it is easy to see from (42*a*) of I), which is in good agreement with experiment, at least at low energy.

An inspection of eq. (13) reveals that, at least at low energy, $\sin 2\delta_{\frac{1}{2}}$ is positive; the addition of the disregarded term containing $\bar{\sigma}$, which is positive

([5]) See for instance G. Cocconi, G. Puppi, G. Quareni and A. Stanghellini: *Nuovo Cimento*, **5**, 172 (1957).

definite, cannot change this result. It seems rather improbable that the next step in the iteration procedure could reverse the sign of $\sin 2\delta_{\frac{1}{2}}$, at least for small values of the coupling constants.

A similar iteration procedure is of course not possible for the $\overline{\text{K}}$-N interaction because of the impossibility of expressing $\bar{\sigma}$ in terms of $\bar{f}$, due to absorption processes.

A less crude approximation can be archived starting again from the dispersion relations, or even better from those for isobaric spin states given in (41) of I. If in those for K-N interaction we disregard the contribution of $\bar{\sigma}$ and the presence of inelastic processes (at all energies ω') in the cross-section that appears under the integration, we get:

$$f^{\alpha}(\omega) = I^{\alpha}(\omega) + \frac{v^2(\omega)}{\pi} \int_{\mu}^{\infty} \frac{\mathrm{d}\omega'}{v^2(\omega')} \frac{|f^{\alpha}(\omega')|^2}{\omega' - (\omega + i\varepsilon)}, \tag{14}$$

where α is an isobaric spin index (0 or 1) and the I^{α} are given by (42a) of I. A similar approximation could be employed also for $\bar{f}^{\alpha}(\omega)$.

Eq. (14) and the corresponding one for $\bar{f}^{\alpha}(\omega)$ are closely connected with the integral equation representation of [4]; it indeed coincides with the analogous equation that can be derived from the Hamiltonian given in [4] going through the construction of the Low equation and the corresponding dispersion relations by the Chew and Low model. As for the corresponding equation for $\bar{f}^{\alpha}(\omega)$, there is a significant difference with the equation derived with the Lee model for K-N interaction, i.e. that the integral goes from μ up to ∞ and no more from m_{K} to ∞. This is clearly due to the contribution of the pion field which allows absorption processes that were excluded from the beginning in [4]. Besides, in the present derivation the effects of virtual pions and heavy mesons (of both type) are implicitely contained in the definition of the coupling constants.

Finally we want to stress the fact that the phase shifts for K-N interaction will always be complex owing to the competing absorption processes $\text{K}+\text{N} \to \text{H}+\pi$. Considering for simplicity only the scalar case, we write for isobaric spin states

$$\delta^{\alpha}(\omega) = \bar{\xi}^{\alpha}(\omega) + i\bar{\eta}^{\alpha}(\omega), \tag{15}$$

where $\bar{\xi}^{\alpha}$ and $\bar{\eta}^{\alpha}$ are real. Then

$$\bar{\sigma}^{\alpha}(\omega) = \frac{2\pi}{k^2} (1 - \exp[-2\bar{\eta}^{\alpha}(\omega)] \cos 2\bar{\xi}^{\alpha}(\omega)), \tag{16}$$

$$\operatorname{Re} \bar{f}^{\alpha}(\omega) = \frac{\exp[-2\bar{\eta}^{\alpha}(\omega)] \sin 2\bar{\xi}^{\alpha}(\omega)}{2k}, \tag{17}$$

so that

$$\text{tg}\, 2\bar{\xi}^{\alpha}(\omega) = \frac{2k\ \text{Re}\ \bar{f}^{\alpha}(\omega)}{1 - (k^2/2\pi)\bar{\sigma}^{\alpha}(\omega)}, \tag{18}$$

$$\exp\left[-4\bar{\eta}^{\alpha}(\omega)\right] = 4k^2(\text{Re}\ \bar{f}^{\alpha}(\omega))^2 + \left(1 - \frac{k^2}{2\pi}\,\bar{\sigma}^{\alpha}(\omega)\right)^2. \tag{19}$$

We then see that with the only knowledge of the total cross-sections it is possible, by means of dispersion relations, to express separately the real and imaginary parts of the phase shifts as function only of the coupling constants and then to have a theoretical insight on the relations between the scattering and absorption of $\overline{\text{K}}$ on nucleons.

* * *

We are deeply indebted to Prof. M. Cini for many criticisms and discussions which originated the main part of the content of this paper.

RIASSUNTO

Si usano le relazioni di dispersione derivate in un lavoro precedente (I) per l'interazione di mesoni pesanti con i nucleoni in teoria di sorgente fissa, per ottenere da esse delle relazioni del tipo « effective range ». Sono considerati mesoni pesanti « scalari » e « pseudoscalari ». Nei primi due paragrafi di questo lavoro si effettua l'inversione delle ampiezze di diffusione che soddisfano le relazioni di dispersione. Nel terzo paragrafo le relazioni di « effective range » sono discusse e confrontate tra loro, e si analizza anche il problema di ottenere soluzioni approssimate per le ampiezze di diffusione direttamente dalle relazioni di dispersione.

IL NUOVO CIMENTO Vol. VI, N. 6 1° Dicembre 1957

Analysis of Processes Involving Baryons, Pions and Heavy Mesons.

D. Amati

Istituto di Fisica Teorica dell'Università - Napoli
Istituto Nazionale di Fisica Nucleare - Sezione di Roma

B. Vitale (*)

Istituto di Fisica dell'Università - Catania
Centro Siciliano di Fisica Nucleare - Catania

(ricevuto il 1° Luglio 1957)

Summary. — The role played by the fields present in any strong interaction is analyzed by means of dispersion relation techniques. This helps to clarify the effects of virtual states in physical processes where only a few of the many interacting fields are present in the initial and final states as real particles, and the way the renormalized coupling constants appear in the integral relations for the amplitudes corresponding to scattering, production and absorption processes.

Introduction.

Some attempts have been made recently in order to study the behaviour of scattering amplitudes when many strongly interacting fields are present. These attempts have been limited to the analysis of the role played in intermediate states by the fields which are not present as real particles in the initial and final states. The physical processes analysed were the π-N [1] and the K-N and $\overline{\text{K}}$-N [2] scattering. Both analyses were done by means of dispersion relation techniques.

(*) Now at Istituto di Fisica Teorica - Università di Napoli.

[1] A. Agodi, M. Cini and B. Vitale: Communication to the Seventh Rochester Conference (1957); *Phys. Rev.*, **107**, 630 (1967).

[2] D. Amati and B. Vitale: *Nuovo Cimento*, **5**, 1533 (1957), **6**, 1013 (1957); and *Nuovo Cimento*, in press.

We want here to generalize the previous attempts, including in our analysis also production and absorption processes, in order to discuss together all the processes involving baryons, pions and heavy mesons and physically realizable in our laboratories at the present time. As it will become clear in the following such a generalization is necessary if we desire a clear picture of the effects of virtual states in physical processes. The amplitudes for these processes will turn out to be connected one to another in a well defined way through the integral relations satisfied by each of them.

The effects of intermediate states will be apparent in those integral relations, where they give raise to unphysical regions of integration and to residues containing the renormalized coupling constants. They will also contribute in a well defined although not exactly calculable way to the renormalization of the coupling constants which appear in the interaction Hamiltonian; as far as only the renormalized coupling constants can be measured these contributions will not be of any importance for practical purposes.

We shall indicate in the following how the « crossing » relations among amplitudes corresponding to different physical processes come out directly from Low's equations. We shall see however that, in order to connect in an integral relation such « crossed » amplitudes, dispersion relation techniques are necessary.

Another important point that will be clear from the following analysis is the fact that the renormalization of the coupling constants can be done in a unique way, this meaning that only *one* renormalizing matrix element will appear for each of the coupling constants also in the case that many interacting fields are considered.

As we have already said, we shall take into account only strongly interacting fields, this meaning as usual that the interaction Hamiltonian conserves strangeness. We shall therefore disregard both weak interactions and radiative absorption and photoproduction processes. Hyperon states will therefore be considered in the following as « stable » states. How radiative corrections at the lowest order could modify dispersion relations has been already studied in the particular case of π-N scattering ([1-3]). Corrections seem to be of a non-essential nature and would not modify our results in a qualitative way.

We shall also disregard in the following the possibility of a direct K-π coupling, as proposed for instance by SCHWINGER ([4]).

We shall work for simplicity in the static case with fixed extended sources, and we shall use the dispersion relation techniques due to A. KLEIN ([5]).

([3]) A. AGODI and M. CINI: *Nuovo Cimento*, **6**, 686 (1957).
([4]) J. SCHWINGER: *Phys. Rev.*, **104**, 1164 (1956).
([5]) A. KLEIN: *Phys. Rev.*, **104**, 1131 (1956).

1. – Physical processes and notation.

We shall study scattering, production and absorption processes involving baryons (nucleons, Λ^0-particles and Σ-particles), π-mesons and heavy mesons (K and $\overline{\text{K}}$-mesons). In the following H^I will denote the interaction Hamiltonian. We shall use throughout the symbols $p(\omega_p)$ for the momentum (the energy) of π-mesons, and $q(\omega_q)$ for the corresponding quantities for K-mesons (*). E_Λ and E_Σ will denote the differences in mass between Λ^0 particle and nucleon, and between Σ-particle and nucleon, respectively.

We define:

$$V_p = [H^I, a_p^-]\,; \qquad U_q = [H^I, b_q^+]\,; \qquad \overline{U}_q = [H^I, c_q^+]\,, \tag{1}$$

where a^+, b^+ and c^+ are creation operators of π, K and $\overline{\text{K}}$ respectively.

The following important properties are clear from the general structure of H^I:

$$\begin{cases} V_p^+ = V_{-p} \\ U_q^+ = \overline{U}_{-q} \end{cases} \tag{2}$$

(we note here that, in the particular case that the H^I is the fixed source version of Salam's Hamiltonian (see [2])) relation (2) give: $V_p^- = -V_p$ and $U_q^+ = \pm \overline{U}_q$, where the $+$ sign holds for « scalar » K-mesons, and the $-$ sign for « pseudoscalar » K-mesons).

We define now the amplitudes that we want to study in the following; they are:

$$\begin{cases} \text{initial state} \quad \pi + \text{N} & T_p = \langle \Psi_n^{(-)} | V_p | \boldsymbol{N} \rangle \\ a) \quad \pi + \text{N} \to \pi + \text{N} & \Pi_p = \langle \boldsymbol{N\pi} | V_p | \boldsymbol{N} \\ b) \qquad\qquad \to \text{K} + \text{H} & P_p^{\text{H}} = \langle \boldsymbol{HK} | V_p | \boldsymbol{N} \rangle \\ \text{initial state} \quad \text{K} + \text{N} & S_q = \langle \Psi_n^{(-)} | U_q | \boldsymbol{N} \rangle \\ c) \quad \text{K} + \text{N} \to \text{K} + \text{N} & K_q = \langle \boldsymbol{NK} | U_q | \boldsymbol{N} \rangle \\ \text{initial state} \quad \overline{\text{K}} + \text{N} & \overline{S}_q = \langle \Psi_n^{(-)} | \overline{U}_q | \boldsymbol{N} \rangle \\ d) \quad \overline{\text{K}} + \text{N} \to \overline{\text{K}} + \text{N} & \overline{K}_q = \langle \boldsymbol{N\overline{K}} | \overline{U}_q | \boldsymbol{N} \rangle \\ e) \qquad\qquad \to \pi + \text{H} & A_q^{\text{H}} = \langle \boldsymbol{H\pi} | \overline{U}_q | \boldsymbol{N} \rangle \end{cases} \tag{3}$$

where of course H can be a Λ^0 or a Σ-particle.

(*) p and q will generally include also spin and isobaric spin indexes. For their behaviour under « crossing » see Sect. **2** *a*) and (2).

It will be necessary in the following to consider also amplitudes that do not correspond to processes that can be realized in a laboratory at the present time; they are:

$$(4)\qquad \begin{cases} \text{initial state:} \quad \pi + \mathrm{H} & M_p^{\mathrm{H}} = \langle \Psi_n^{(-)} | \, V_p \, | \boldsymbol{H} \rangle \\ \qquad\qquad\quad \mathrm{K} + \mathrm{H} & N_q^{\mathrm{H}} = \langle \Psi_n^{(-)} | \, U_q \, | \boldsymbol{H} \rangle \\ \qquad\qquad\quad \overline{\mathrm{K}} + \mathrm{H} & \bar{N}_q^{\mathrm{H}} = \langle \Psi_n^{(-)} | \, \overline{U}_q \, | \boldsymbol{H} \rangle \end{cases}$$

It will turn out however that these amplitudes do not appear in any of the « crossing » relations among amplitudes corresponding to physically realizable processes; they are present merely as possible intermediate states and disappear in the final dispersion relations for physical processes.

We shall also need in the following the quantities:

$$(5)\qquad \begin{cases} D(p, p) = \langle \boldsymbol{N} | [a_p, V_p] | \boldsymbol{N} \rangle \\ E(q, q) = \langle \boldsymbol{N} | [b_q, U_q] | \boldsymbol{N} \rangle \\ \overline{E}(q, q) = \langle \boldsymbol{N} | [c_q, \overline{U}_q] | \boldsymbol{N} \rangle . \end{cases}$$

2. – Low's equations and dispersion relations.

We shall now analyse in some details the amplitudes defined by (3), using the following scheme: for each amplitude we shall write down the corresponding Low's equation; discuss the singularities of the amplitude and the cuts in the energy axis; derive its crossing properties and the dispersion relation satisfied by it. We shall then discuss this dispersion relation, with particular attention to unphysical regions, residues and presence of renormalized coupling constants.

2·1. – $\pi + \mathrm{N} \to \pi + \mathrm{N}$.

$$(3a)\qquad \Pi_{p,m} = \langle \boldsymbol{N}\pi \, | \, V_{p,m} \, | \boldsymbol{N} \rangle ,$$

where m is the mesonic charge index, now explicitely indicated. Low's equation is now:

$$(6)\qquad \Pi(\omega_p) = D(p, p) - \sum_n \left[\frac{T^+_{-p} T_{-p}}{E_n + (\omega_p + i\eta)} + \frac{T^-_p T_p}{E_n - (\omega_p + i\eta)} \right] .$$

There is a pole at $\omega_p = 0$; the residue of $z\,\Pi(z)$ at $z = 0$ is:

$$(7)\qquad \mathrm{R}(z\Pi(z))_0 = -\omega_p [| \langle \boldsymbol{N} | \, V_p \, | \boldsymbol{N} \rangle |^2 + | \langle \boldsymbol{N} | \, V^+_p \, | \boldsymbol{N} \rangle |^2] ,$$

$g_{\pi N}$ will be therefore renormalized by:

$$g_{\pi N}\langle \boldsymbol{N}|0|\boldsymbol{N}\rangle = G_{\pi N}\langle N|0|N\rangle \tag{8}$$

as usual. There are branch lines on the ω_p axis going from m_π to ∞ and from $-m_\pi$ to $-\infty$. The « crossing » is here represented by:

$$\Pi_{p,m}(-\omega_p) = -\Pi^{+}_{-p,-m}(\omega_p)\,. \tag{9}$$

We introduce now $f = -(\omega/2\pi)\Pi$; the dispersion relation for f_m now reads:

$$\begin{aligned}\frac{\operatorname{Re} f_m(\omega_p)}{v^2(\omega_p)} - \frac{1}{2}\left(1 + m\frac{\omega_p}{m_\pi}\right) f_m(m_\pi) - \frac{1}{2}\left(1 - m\frac{\omega_p}{m_\pi}\right) f_{-m}(m_\pi) = \\ = \frac{q^2}{4\pi^2}\int_{m_\pi}^{\infty}\frac{\mathrm{d}\omega'}{q' v^2(\omega')}\left[\frac{\sigma_m(\omega')}{\omega' - \omega_p} + \frac{\sigma_{-m}(\omega')}{\omega' + \omega_p}\right] + m\,\frac{G^2_{\pi N}}{2\pi m_\pi^2 \omega_p}\,,\end{aligned} \tag{10}$$

where $v(\omega_p)$ is the usual source function for baryon-pion interaction.

There are no unphysical regions and the contributions coming from hyperons and heavy meson virtual states are all contained in the renormalization of $g_{\pi N}$. This result was already noticed in [1].

2·2. – $\pi + \mathrm{N} \to \mathrm{K} + \mathrm{H}$.

$$P^{\mathrm{H}}_{pq} = \langle \boldsymbol{HK}|V_{pq}|\boldsymbol{N}\rangle \tag{3b}$$

Low's equation is now:

$$P^{\mathrm{H}}_{pq} = -\sum_n \left[\frac{M^{\mathrm{H}+}_{-p}\bar{S}_{-q}}{E_n + (\omega_q + i\eta)} + \frac{N^{\mathrm{H}+}_q T_p}{E_n - E_{\mathrm{H}} - (\omega_q + i\eta)}\right]. \tag{11}$$

Let us introduce:

$$P^{\mathrm{H}}_{pq}(z) = -\sum_n \left[\frac{M^{\mathrm{H}+}_{-p}(\omega_p)\,\bar{S}_{-q}(\omega_q)}{E_n + z} + \frac{N^{\mathrm{H}+}_q(\omega_q)\,T_p(\omega_p)}{E_n - E_{\mathrm{H}} - z}\right], \tag{12}$$

where z is a complex variable. $P(z)$ has poles at $-E_\Lambda$ and $-E_\Sigma$; the residues of $P(z)$ there are:

$$\begin{cases} \mathrm{R}(P^{\Lambda}(z))_{-E_\Lambda} = \quad \langle \boldsymbol{\Lambda}|U^{+}_q|\boldsymbol{N}\rangle\langle \boldsymbol{N}|V_p|\boldsymbol{N}\rangle \\ \mathrm{R}(P^{\Sigma}(z))_{-E_\Lambda} = -[\langle \boldsymbol{\Sigma}|V_p|\boldsymbol{\Lambda}\rangle\langle \boldsymbol{\Lambda}|U^{+}_q|\boldsymbol{N}\rangle - \langle \boldsymbol{\Sigma}|U^{+}_q|\boldsymbol{N}\rangle\langle \boldsymbol{N}|V_p|\boldsymbol{N}\rangle] \\ \mathrm{R}(P^{\mathrm{H}}(z))_{-E_\Sigma} = -\langle \mathbf{H}|V_p|\boldsymbol{\Sigma}\rangle\langle \boldsymbol{\Sigma}|U^{+}_q|\boldsymbol{N}\rangle\,. \end{cases} \tag{13}$$

Therefore we shall make use of the following renormalizations:

$$(14)\qquad \begin{cases} g_{\pi\Lambda\Sigma}\langle \boldsymbol{\Lambda}\,|\,0\,|\,\boldsymbol{\Sigma}\rangle = G_{\pi\Lambda\Sigma}\langle \Lambda\,|\,0\,|\,\Sigma\rangle \\ g_{\mathrm{KNH}}\langle \boldsymbol{H}\,|\,0\,|\,\boldsymbol{N}\rangle = G_{\mathrm{KNH}}\langle \mathrm{H}\,|\,0\,|\,\mathrm{N}\rangle \\ g_{\pi\mathrm{N}}\ \langle \boldsymbol{N}\,|\,0\,|\,\boldsymbol{N}\rangle = G_{\pi\mathrm{N}}\ \langle \mathrm{N}\,|\,0\,|\,\mathrm{N}\rangle \\ g_{\pi\Sigma}\ \langle \boldsymbol{\Sigma}\,|\,0\,|\,\boldsymbol{\Sigma}\rangle = G_{\pi\Sigma}\ \langle \Sigma\,|\,0\,|\,\Sigma\rangle \end{cases}$$

The branch line on the ω_q axis will run from $m_\pi - E_{\mathrm{H}}$ to ∞ and from $-(E_\Lambda + m_\pi)$ to $-\infty$.

The following « crossing » property is present:

$$(15)\qquad P^{\mathrm{H}}_{p,q}(-z) = A^{\mathrm{H}}_{-p,-q}(z)$$

as it can be easily seen from (12) and (27).

The dispersion relations for the P^{H}'s read now:

$$(16)\qquad \frac{P^{\Pi}_{qp}(\omega_q)}{v(\omega_q)w(\omega_q)} - \frac{1}{2}\left(1+\frac{m_{\mathrm{K}}}{\omega_q}\right)\frac{P^{\mathrm{H}}_{q\mathfrak{P}}(m_{\mathrm{K}})}{v(m_{\mathrm{K}})w(m_{\mathrm{K}})} - \frac{1}{2}\left(1-\frac{m_{\mathrm{K}}}{\omega_q}\right)\frac{A^{\mathrm{H}}_{-q,\ p}(m_{\mathrm{K}})}{v(m_{\mathrm{K}})w(m_{\mathrm{K}})} +$$

$$+\frac{q^2}{2}\left(\frac{1}{m_{\mathrm{K}}}-\frac{1}{\omega_q}\right)C(A^{\mathrm{H}}_{-q,-p}) + \frac{q^2}{2}\left(\frac{1}{m_{\mathrm{K}}}+\frac{1}{\omega_q}\right)C(P^{\mathrm{H}}_{q,p}) =$$

$$= -\frac{i}{\pi}\frac{q^2}{\omega_q}\cdot\left\{\int_0^\infty \frac{P^{\mathrm{H}}_{p'q'}(\omega'_q)\omega_{q'}\,\mathrm{d}\omega_{q'}}{v(\omega_{q'})w(\omega_{q'})q'^2(\omega_{q'}-\omega_q)} + \left(\int_0^{E_{\mathrm{H}}-m_\pi} + \int_{E_\Lambda+m_\pi}^\infty\right)\frac{A^{\mathrm{H}}_{-q',-p'}(\omega_{q'})\omega_{q'}\,\mathrm{d}\omega_{q'}}{v(\omega_{q'})w(\omega_{q'})q'^2(\omega_{q'}+\omega_q)}\right\},$$

where

$$C(X^{\mathrm{H}}_{qp}) = \left[\frac{E_\Lambda R(X^{\mathrm{H}}_{pq})_{\,E_\Lambda}}{v(E_\Lambda)w(E_\Lambda)(E_\Lambda \pm m_{\mathrm{K}})(E_\Lambda^2-\omega_q^2)} + \frac{E_\Sigma R(X^{\mathrm{H}}_{pq})_{\,E_\Sigma}}{v(E_\Sigma)w(E_\Sigma)(E_\Sigma \pm m_{\mathrm{K}})(E_\Sigma^2-\omega_q^2)}\right],$$

and $w(\omega_q)$ is the source function for baryon-K meson interactions.

(X stands for P and A, and the upper sign holds for P, the lower sign for A).

Production of K-mesons and absorption of K-mesons are therefore strongly correlated by (16); in (16) there are many unphysical regions, the integrations over $A(\omega_q)$ finding the physical region at $\omega_q = m_\pi + \mathrm{E}_{\mathrm{H}}$ and that over $P(\omega_q)$ at $\omega_q = m_{\mathrm{K}}$.

2·3. – $\mathrm{K}+\mathrm{N}\to\mathrm{K}+\mathrm{N}$.

$$(3c)\qquad K_q = \langle \boldsymbol{NK}\,|\,U_q\,|\,\boldsymbol{N}\rangle$$

This process has been already extensively studied by us [2]. We quote here just the results in order to compare them with those here obtained for the other amplitudes.

Low's equation for K_q is:

$$K_q(\omega_q) = E(q, q) - \sum_n \left[\frac{S_q^+ S_q}{E_n - (\omega_q + i\eta)} + \frac{\bar{S}_{-q}^+ \bar{S}_{-q}}{E_n + (\omega_q + i\eta)} \right]. \tag{17}$$

Let us introduce:

$$K_q(z) = E(q, q) - \sum_n \left[\frac{S_q^+(\omega_q) S_q(\omega_q)}{E_n - z} + \frac{\bar{S}_{-q}^+(\omega_q) \bar{S}_{-q}(\omega_q)}{E_n + z} \right], \tag{18}$$

$K_q(z)$ will have poles at $-E_\Lambda$ and $-E_\Sigma$; the residues there of the function $zK_q(z)$ will be:

$$\mathrm{R}(zK_q(z))_{-E_H} = \omega_q |\langle \boldsymbol{H} | \bar{U}_{-q} | \boldsymbol{N} \rangle|^2 . \tag{19}$$

The coupling constants g_{KNH} have therefore to be renormalized by:

$$g_{KNH} \langle \boldsymbol{H} | 0 | \boldsymbol{N} \rangle = G_{KNH} \langle H | 0 | N \rangle . \tag{20}$$

$K(z)$ presents branch lines on the ω_q axis going from m_K to ∞ and from $-(E_\Lambda + m_\pi)$ to $-\infty$.

The following « crossing » relation holds:

$$K_q(-\omega_q) = -\bar{K}_{-q}^+(\omega_q) \tag{21}$$

as it can be easily derived from (17) and (24).

We introduce now (see [2]) the function:

$$g(\omega_q) = -\frac{\omega_l}{2\pi} K_q(\omega_q) . \tag{22}$$

The dispersion relation for $g(\omega_q)$ reads:

$$\frac{\mathrm{Re}\, g(\omega_q)}{w^2(\omega_q)} - C(g(\omega_q)) - \frac{1}{2w^2(m_K)} \left(1 + \frac{\omega_q}{m_K}\right) \mathrm{Re}\, g(m_K) - \tag{23}$$

$$- \frac{1}{2w^2(m_K)} \left(1 - \frac{\omega_q}{m_K}\right) \mathrm{Re}\, g(m_K) = \frac{q^2}{\pi} P \int_{E_\Lambda + m_K}^{\infty} \frac{\mathrm{d}\omega_{q'}}{w^2(\omega_{q'}) q'^2} \left[\frac{\mathrm{Im}\, g(\omega_{q'})}{\omega_{q'} - \omega_q} + \frac{\mathrm{Im}\, \bar{g}(\omega_{q'})}{\omega_{q'} + \omega_q} \right],$$

where

$$C = C^\Lambda + C^\Sigma , \quad \text{and} \quad C^H = + E_H \frac{q^2}{2\pi} \frac{|\langle \boldsymbol{H} | U^+(E_H) | \boldsymbol{N} \rangle|^2}{(\omega_q + E)(m_K^2 - E_H^2)} ,$$

where $w(\omega_q)$ is the usual baryon-heavy meson source function.

The unphysical region is here in the integration over the $\sigma_{\bar{K}N}$, from $\omega_q = E_\Lambda + m_\pi$ to $\omega_q = m_K$, and it is clearly due to the virtual presence of pions and hyperons.

2·4. – $\overline{K} + N \to \overline{K} + N$.

(3*d*) $$\bar{K}_q = = \langle \boldsymbol{N}\bar{\boldsymbol{K}} | \, \bar{U}_q | \boldsymbol{N} \rangle \, .$$

This process also was already discussed in (2). Low's equation for $\bar{K}_q$ is:

(24) $$\bar{K}_q(\omega_q) = \bar{E}(q, q) - \sum_n \left[\frac{\bar{S}_q^+ \bar{S}_q}{E_n - (\omega_q + i\eta)} + \frac{S_{-q}^+ S_{-q}}{E_n + (\omega_q + i\eta)} \right] .$$

A $\bar{K}(z)$ function can be introduced in analogy with (18); $\bar{K}(z)$ will have poles at E_Λ and E_Σ; residues there of the function $z\bar{K}_q(z)$ will be:

(25) $$R(z\bar{K}_q(z))_{E_H} = - |\langle \boldsymbol{H} | \, \bar{U}_{-q} | \boldsymbol{N} \rangle|^2 \, .$$

The coupling constants g_{KNH} have therefore to be renormalized again according to (20).

$\bar{K}(z)$ presents branch lines on the ω_q axis going from $E_\Lambda + m_\pi$ to ∞ and from $-m_K$ to $-\infty$.

Introducing a function $\bar{g}$ analogous to (22) and using again (21) the dispersion relation for $\bar{g}(\omega_q)$ reads:

(26) $$\frac{\operatorname{Re} \bar{g}(\omega_q)}{w^2(\omega_q)} - \bar{C}(\bar{g}(\omega_q)) - \frac{1}{2w^2(m_K)} \left(1 + \frac{\omega_q}{m_K}\right) \operatorname{Re} \bar{g}(m_K) -$$

$$- \frac{1}{2w^2(m_K)} \left(1 - \frac{\omega_q}{m_K}\right) \operatorname{Re} g(m_K) = \frac{q^2}{\pi} P \int_{E_\Lambda + m_\pi}^{\infty} \frac{\mathrm{d}\omega_{q'}}{w^2(\omega_{q'}) q'^2} \left[\frac{\operatorname{Im} \bar{g}(\omega_{q'})}{\omega_{q'} - \omega_q} + \frac{\operatorname{Im} g(\omega_{q'})}{\omega_{q'} + \omega_q} \right] ,$$

where

$$\bar{C} = \bar{C}_\Lambda + \bar{C}_\Sigma \, , \quad \text{and} \quad \bar{C}_H = E_H \frac{q^2}{2\pi} \frac{|\langle \boldsymbol{H} | \, U^+(E_H) | \boldsymbol{N} \rangle|^2}{(\omega_q - E_H)(m_K^2 - E_H^2)} \, .$$

The unphysical region is here the same that in case 2*c*).

2·5. – $\overline{K} + N \to \pi + H$.

(3*e*) $$A_{q\mathfrak{p}}^H = \langle \boldsymbol{H}\pi | \, \bar{U}_q | \boldsymbol{N} \rangle \, .$$

Low's equation for the A_q^{H} is:

$$A_{qp}^{\mathrm{H}}(\omega_q) = -\sum_n \left[\frac{N_{-q}^{\mathrm{H}+} T_{-p}}{E_n - E_{\mathrm{H}} + (\omega_q + i\eta)} + \frac{M_p^{\mathrm{H}+} \bar{S}_q}{E_n - (\omega_q + i\eta)} \right]. \tag{27}$$

Let us introduce $A_{qp}^{\mathrm{H}}(z)$ in analogy with (12). $A^{\mathrm{H}}(z)$ has poles at E_Λ and E_Σ; the residues of $A^{\mathrm{H}}(z)$ there are:

$$\begin{cases} \mathrm{R}(A^{\Lambda}(z))_{E_\Lambda} = -[\langle \boldsymbol{\Lambda} | \bar{U}_q | \boldsymbol{N} \rangle \langle \boldsymbol{N} | V_p^+ | \boldsymbol{N} \rangle] \\ \mathrm{R}(A^{\Lambda}(z))_{E_\Sigma} = -[\langle \boldsymbol{\Lambda} | V_p^+ | \boldsymbol{\Sigma} \rangle \langle \boldsymbol{\Sigma} | \bar{U}_q | \boldsymbol{N} \rangle] \\ \mathrm{R}(A^{\Sigma}(z))_{E_\Lambda} = \langle \boldsymbol{\Sigma} | V_p^+ | \boldsymbol{\Lambda} \rangle \langle \boldsymbol{\Lambda} | \bar{U}_q | \boldsymbol{N} \rangle \\ \mathrm{R}(A^{\Sigma}(z))_{E_\Sigma} = \langle \boldsymbol{\Sigma} | V_p^+ | \boldsymbol{\Sigma} \rangle \langle \boldsymbol{\Sigma} | \bar{U}_q | \boldsymbol{N} \rangle - \langle \boldsymbol{\Sigma} | \bar{U}_q | \boldsymbol{N} \rangle \langle \boldsymbol{N} | V_p^+ | \boldsymbol{N} \rangle . \end{cases} \tag{28}$$

Renormalization will therefore be defined in the same way as in 2*b*), see (14). The branch lines on the ω_q axis run from $E_\Lambda + m_\pi$ to ∞ and from $E_{\mathrm{H}} - m_\pi$ to $-\infty$. The crossing is of course given again by (15). The dispersion relations for the A^{H}'s now read:

$$\begin{aligned} &\frac{A_{q,p}^{\mathrm{H}}(\omega_q)}{v(\omega_q) w(\omega_q)} - \frac{1}{2}\left(1 + \frac{m_{\mathrm{K}}}{\omega_q}\right) \frac{A_{q,p}^{\mathrm{H}}(m_{\mathrm{K}})}{v(m_{\mathrm{K}}) w(m_{\mathrm{K}})} - \frac{1}{2}\left(1 - \frac{m_{\mathrm{K}}}{\omega_q}\right) \frac{P_{-q,-p}^{\mathrm{H}}(m_{\mathrm{K}})}{v(m_{\mathrm{K}}) w(m_{\mathrm{K}})} + \\ &+ \frac{q^2}{2}\left(\frac{1}{m_{\mathrm{K}}} - \frac{1}{\omega_q}\right) C(P_{-q,-p}^{\mathrm{H}}) + \frac{q^2}{2}\left(\frac{1}{m_{\mathrm{K}}} + \frac{1}{\omega_q}\right) C(A_{q,p}^{\mathrm{H}}) = \\ &= -\frac{i}{\pi}\frac{q^2}{\omega_q}\left\{\left(\int_0^{E_\Lambda - m_\pi} + \int_{E_\Lambda + m_\pi}^{\infty}\right) \frac{A_{p',q'}^{\mathrm{H}}(\omega_{q'}) \omega_{q'} \mathrm{d}\omega_{q'}}{v(\omega_{q'}) w(\omega_{q'}) q'^2(\omega_{q'} - \omega_q)} + \int_0^{\infty} \frac{P_{-q',-p'}^{\mathrm{H}}(\omega_{q'}) \omega_{q'} \mathrm{d}\omega_{q'}}{v(\omega_{q'}) w(\omega_{q'}) q'^2(\omega_{q'} + \omega_q)}\right\}. \end{aligned} \tag{29}$$

As we already noticed in 2*b*), absorption of K is correlated with production of $\bar{\mathrm{K}}$ on nucleons by the dispersion relations (29). For the discussion of the unphysical regions we refer to what was already said in 2*b*).

3. – Conclusions.

We shall here briefly summarize the main points resulting from the analysis made in Sect. 2. They are:

a) All of the strongly interacting fields are of importance in determining the behaviour of scattering, absorption and production amplitudes. Fields which are not present in the initial and final states as real particles introduce unphysical regions in the integral relations satisfied by the amplitudes an contribute to the location and the residues of the poles and to the renormalization of the coupling constants.

b) There are very general « crossing » properties among the amplitudes, connecting them in such a way that negative regions in the integrals over the energy axis can be substituted by positive region integrations over « crossed » amplitudes. It is of some interest to notice that it is possible to find crossings mixing only the amplitudes defined in (3), without making use of those defined in (4). This means that it is possible to have dispersion relations for physically measurable amplitudes without physical unmeasurable amplitudes appearing in them.

c) There is a unique way of defining the renormalization of the coupling constants involved in strong interactions. This result would not be altered by taking into account also the physically unmeasurable processes (4), and deriving for them also Low's equations and calculating the corresponding residues of the amplitudes at their poles.

We think that our previous results could be also of some interest and utility for searching for approximate methods for obtaining equations satsified by the scattering production and absorption amplitudes and more easily solvable than the dispersion relations previously derived.

The qualitative aspect of the present analysis would not be altered by considering the general features of the relativistic interaction Hamiltonian, as opposed to the non-relativistic, fixed extended source Hamiltonian used here.

* * *

One of us (B.V.) is grateful to Prof. E. Caianiello for the kind hospitality found in the Istituto di Fisica Teorica dell'Università di Napoli.

RIASSUNTO

Mediante la tecnica delle relazioni di dispersione si analizza il ruolo dei diversi campi presenti in interazioni forti (barioni, pioni e mesoni K). L'analisi qui effettuata rende più chiari gli effetti degli stati virtuali in processi fisici durante i quali alcuni dei campi interagenti non sono presenti nello stato iniziale e finale come particelle reali. È anche discussa l'unicità delle procedure di rinormalizzazione per le costanti di accoppiamento che sono presenti nella Hamiltoniana di interazione per interazioni forti.

The Formation of ^{22}Na From Atmospheric Argon by Cosmic Rays (*).

L. Marquez, N. L. Costa and I. G. Almeida

Centro Brasileiro de Pesquisas Físicas - Rio de Janeiro, Brasil

(ricevuto il 9 Luglio 1957)

Summary. — It was found that ^{22}Na is formed as a spallation product of atmospheric argon by cosmic rays. It was isolated from the fresh rain water of Rio de Janeiro, and its average activity is 0.017 dpm/l.

1. – Introduction.

It has been established recently that several radio-isotopes are formed as spallation products of argon by cosmis rays. They have all been found in the rain water. The formation of ^{32}P was measured (1). Winsberg (2) found the ^{39}Cl; Goel (3) found the ^{35}S; and Lal et al. (4) verified the result of ^{32}P and established the formation of ^{33}P.

We have in this work isolated the 2.6 yr ^{22}Na. This isotope is the longest-lived found so far from the spallation of argon.

2. – Experimental method.

The rain water from a large roof was collected and stored in tanks of 1000 liters. The water was allowed to stand until it was clear and the dust settled. The water was passed throungh an ion-exchange column of 50 cm² area and

(*) This work was done under the auspices of the Conselho Nacional de Pesquísas of Brazil.

(1) L. Marquez and N. L. Costa: *Nuovo Cimento*, **2**, 1038 (1955).

(2) L. Winsberg: *Geochim. et Cosmochim. Acta*, **9**, 183 (1956).

(3) P. S. Goel: *Nature*, **178**, 1458 (1956).

(4) D. Lal, N. Narasappaya and P. K. Zutshi: *Nucl. Phys.*, **3**, 69 (1957).

50 cm height, loaded with Amberlite IR-120 resin. The flow rate was about 30 l/hr. After passing three to four thousand liters of rain water through the column, it was regenerated with 4N HCl, until it would not give more test for metals. About 20 liters of 4N HCl were required.

The 4N HCl containing the metals was evaporated to near dryness. The hydroxides were precipitated with NH_4OH and filtered. The filtrate was treated with $(NH_4)_2CO_3$ until all Ca, Mg, and the like were precipitated, allowed to stand and filtered. The filtrate was taken to dryness and then treated with a mixture of one part concentrated HCl and four parts concentrated HNO_3, boiled until all the ammonium salts were destroyed, and then taken to dryness again.

The dry residue contained only the alkaline metals. It was dissolved in water and passed through an ion-exchange column of 20 cm^2 area and 100 cm height and washed with a very dilute HCl solution to separate the anions. Then the column was eluted with 0.1N HCl and the Na was collected; the K came out afterwards and it was rejected, and then the column was washed with 4N HCl to determine the ^{137}Cs which comes with the rain water too.

The solution containing the Na was evaporated to a small volume and taken to dryness in a beaker having the same diameter as the crystal detector. The amount of NaCl from each sample varied from 15 to 60 g and this is in agreement with the amount expected from the known amount of Na in rain water.

The solution containing the Cs was evaporated to a volnme of 1 m and transfered to a test tube.

The samples were counted with a scintillation spectrometer Model 516 built by Baird-Atomic, Inc., Cambridge, Mass., U.S.A.; we used a well crystal having 1 $\frac{3}{4}$ in. diameter and 2 in. height; the size of the well was $\frac{5}{8}$ in. diameter and 1$\frac{1}{2}$ in. height.

The ^{137}Cs was counted in the well, but the Na had to be placed outside because, in the volume of the well, one could only use a small fraction of the amount of NaCl that we had at the end.

The ^{22}Na was measured by the annihilation of the positrons that it emits. The ^{137}Cs was measured by the 662 keV γ-ray of its daughter ^{137}Ba. The energy scale of the spectrometer was calibrated using positrons from an artificial source of ^{22}Na. The counting efficiency was determined by counting a sample of artificial ^{22}Na whose absolute activity had been determined previously by two methods already described ([5]).

The energy of the γ-rays from the natural ^{22}Na agreed with the energy of the annihilation radiation from the artificial ^{22}Na within 20 keV. The ^{137}Cs

([5]) L. Marquez: *Phys. Rev.*, **86**, 405 (1952).

had a greater activity and its γ-ray energy agreed with the tabulated energy within 5 keV.

3. – Results.

The channel width of the spectrometer was adjusted to maximize the product of the figure of merit for detection S^2/B and the resolution. In this condition, the efficiency for the ^{22}Na placed outside the crystal was 3.5% in the photoelectric peak. It would have been 7.3% if we could have counted it inside the well. The resolution of the spectrometer was 8%, measured as full width at half the maximum.

The background was counted with NaCl reagent, treated and mounted in the same way as the NaCl from the rain water. Its counting rate in the photoelectric peak was 20 cpm.

The results of three experiments are shown in Table I. The spread in the values found for the activities is common in this kind of experiments. The average activity of ^{22}Na in the rain water of Rio de Janeiro is then 0.017 dpm/l. This is compatible with other activities found already and with spallation data.

TABLE I. – *The activity of* ^{22}Na *in rain water of Rio de Janeiro.*

Date 1957	Amount of water l	Observed activity cpm	Absolute activity dpm/l
January	2.500	0.0 ± 0.5	0.000
March	4.000	1.7 ± 0.4	0.012
June	3.000	4.0 ± 1.0	0.038

The average activity of the ^{137}Cs was 1.2 dpm/l ([6]). It is 70 times greater than the average activity of the natural ^{22}Na. Since it is likely that in any nuclear weapon test the amount of ^{137}Cs formed would be hundreds of times greater than the amount of ^{22}Na formed, we conclude that the ^{22}Na observed has a natural origin and that it is formed as a spallation product of argon by cosmic rays.

We would not attempt to calculate the formation rate of ^{22}Na in this work, since this envolves the times of mixing of the atmosphere. The use of these

([6]) L. MARQUEZ, N. L. COSTA and I. G. ALMEIDA: *An. Acad. Bras. Ciencias* (to be published).

radio-isotopes to study atmospheric process is a new line of research and there has been made one work of this nature by BENIOFF (7) with the data on ^{7}Be. Perhaps using the data of all the radio-isotopes produced in the atmosphere by cosmic rays, one could get a more complete picture.

(7) P. A. BENIOFF: *Phys. Rev.*, **104**, 1122 (1956).

RIASSUNTO (*)

Si è trovato che ^{22}Na è un prodotto di degradazione dell'argon atmosferico da parte dei raggi cosmici. È stato isolato dall'acqua piovana di Rio de Janeiro recentemente caduta e la sua attività media è di 0.017 dpm/l.

(*) *Traduzione a cura della Redazione.*

About Damping and Antidamping Betatron Oscillations, Taking into Account Non-Adiabatic Properties of the Radiation.

A. N. Matveev

State University - Moscow

(ricevuto il 10 Luglio 1957)

Summary. — Radiation effects on operation of high energy electron synchrotrons are discussed. It is shown that there exist neither a damping nor an antidamping of betatron oscillations due to radiation. Accelerating cavities are taken into account with the aid of difference equations. The equation for betatron oscillations is presented taking account of the radiation and all kinds of accelerating fields. The life time of adiabatic invariants is calculated.

1. – Introduction.

The question about radiation effects on the operation of high energy electron synchrotrons is very important. Betatron and phase oscillations induced by quantum fluctuations of the radiation have been considered in papers [1-3]. Various aspects of this problem have been discussed in [4-8].

---

[1] A. A. Sokolov and I. M. Ternov: *Dokl. Akad. Nauk SSSR*, **92**, 537 (1953); *Žu. Ėkper. Teor. Fiz.*, **25**, 698 (1953).

[2] A. A. Sokolov and I. M. Ternov: *Dokl. Akad. Nauk SSSR*, **97**, 823 (1954); *Žu. Ėksper. Teor. Fiz.*, **28**, 432 (1955).

[3] M. Sands: *Phys. Rev.*, **97**, 470 (1955).

[4] A. A. Kolomenskij: *Žu. Ėksper. Teor. Fiz.*, **30**, 207 (1956).

[5] A. N. Matveev: *Dokl. Akad. Nauk SSSR*, **107**, 671 (1956).

[6] A. N. Matveev: *Dokl. Akad. Nauk SSSR*, **108**, 432 (1956).

[7] A. N. Matveev: *Dokl. Akad. Nauk SSSR*, **109**, 495 (1956).

[8] A. N. Matveev: *Nuovo Cimento*, **5**, 1782 (1957).

Here we shall consider damping and antidamping effects which were discussed in LIVINGSTON's and KOLOMENSKIJ's reports at the CERN Symposium [9] and in the paper [10] (*). It will be shown that the consideration of these effects taking account of non-adiabatic properties of the radiation, essentially changes the conclusions reported in [9,10]. We shall also discuss some other aspects of the problem in consideration.

2. – Damping and antidamping of betatron oscillations if it were possible to consider radiation as an adiabatic process.

In order to take into account radiation effects on the electron motion in synchrotrons, we must use the Dirac equation for a point electron:

$$m_0 \frac{\mathrm{d}^2 \xi_\mu}{\mathrm{d}\zeta^2} = \frac{e}{c} F_{\mu\nu} \frac{\mathrm{d}\xi_\nu}{\mathrm{d}\zeta} + \frac{2}{3} \frac{e^2}{c^2} \left(\frac{\mathrm{d}^3 \xi_\mu}{\mathrm{d}\zeta^3} - \frac{1}{c^2} W_4^2 \frac{\mathrm{d}\xi_\mu}{\mathrm{d}\zeta} \right) . \tag{1}$$

Here m_0 is the rest mass of the electron, $F_{\mu\nu}$ is the tensor of electromagnetic field, τ is the proper time of an electron,

$$W_4^2 = \frac{\mathrm{d}\xi^2_\nu}{\mathrm{d}\zeta^2} \frac{\mathrm{d}\xi^2_\nu}{\mathrm{d}\zeta^2} .$$

First of all it is necessary to notice that for the problem in consideration we cannot represent the accelerating field as being smoothly distributed around a circumference. This assertion is a consequence of the properties of the phenomenon under consideration. Indeed, we can represent the accelerating field as being smoothly distributed around a circumference only when we are interested in the mean increase of the energy of a particle due to the accelerating field. In this case we can neglect all higher harmonics in the Fourier representation of the accelerating field, because the total increase of energy due to these higher harmonics is equal to zero. But for the problem in consideration we cannot neglect these higher harmonics and, consequently, cannot represent the accelerating field as smoothly distributed because an antidamping effect is due to the correlation between the phase of a betatron

---

(9) *CERN Symposium*, Vol. **1**, (Geneva, 1956), p. 439, 447.

(10) A. A. KOLOMENSKIJ and A. N. LEBEDEV: *Žu. Èksper. Teor. Fiz.*, **30**, 1161 (1956).

(*) *Note added in proof*: See also I. G. HENRY: *Phys. Rev.*, **106**, 1057 (1957).

oscillation and the radiation intensity. Therefore the accelerating field will be represented with the aid of difference equations (see Sect. 4).

Now we shall neglect the effect of the induced electric field. This effect will be taken into account in Sect. 5 of this paper. Therefore we can consider the electromagnetic field outside the accelerating cavities to be purely the magnetic field $\boldsymbol{H} = (0, 0, H_z = H)$. Let r be the distance of a particle from the center of the synchrotron. The equation of motion, taking into account the radiation, may be written in the following form:

$$m\ddot{r} + \dot{m}\dot{r} = m\omega^2 r - \frac{e}{c}\omega r H - \frac{W_t}{c^2}\dot{r}\,, \tag{2}$$

with $\omega = v_q/r$; W_t is the energy radiated per unit time. We have omitted very small terms proportional to $\ddot{r}$ and $\dddot{r}$ which are not essential. The term $-(W_t/c^2)\dot{r}$ in Eq. (2) represents radiation effects on the motion of an electron.

Putting

$$\varphi = \int^t \omega\,\mathrm{d}t\,, \qquad r' = \frac{\mathrm{d}r}{\mathrm{d}\varphi}\,, \quad \text{etc.},$$

we can represent the Eq. (2) in the following form:

$$mr'' + m\left(\frac{m'}{m} + \frac{\omega'}{\omega}\right)r' = mr - \frac{e}{c}\frac{r}{\omega}H - \frac{W_q}{c^2}r'\,, \tag{3}$$

where W_q is the energy radiated per unit azimuthal angle. Let r_i be the radius of the instantaneous equilibrium orbit determined by the equation $\beta E = eH_i r_i$ ($\beta \approx 1$) an let x be the difference $x = r - r_i$. Then instead of the Eq. (3) we can write the equation:

$$x'' + \left(\frac{m'}{m} + \frac{\omega'}{\omega}\right)x' + (1-n)x = -r_i'' - \left(\frac{m'}{m} + \frac{\omega'}{\omega}\right)r_i' - \frac{W_q}{E}x' - \frac{W_q}{E}r_i'\,, \tag{4}$$

Here n is the magnetic field index.

That is the equation for betatron oscillations taking account of the radiation.

If radiatine were an adiabatic process we would use the following equation

$$\frac{\delta r_i}{\delta\varphi} = \frac{r_i}{(1-n)E}\frac{\delta E}{\delta\varphi} = -\frac{r_i}{(1-n)E}W_\varphi\,, \tag{5}$$

which is valid only in the case of adiabatic processes. It is obvious that

$$W_\varphi = W_i\left[1 + (1-2n)\frac{x}{r_i}\right], \qquad W_i = \frac{2}{3}\frac{e^2}{r_i}\left(\frac{E}{m_0c^2}\right)^4$$

and from the Eq. (5) follows the equation

$$r_i'' = -\frac{1-2n}{1-n}\frac{W_i}{E}x' .$$

Consequently

$$-r_i'' - \frac{W_\varphi}{E}x' = -\frac{n}{1-n}\frac{W_i}{E}x' \tag{6}$$

and if radiating were an adiabatic process the equation for betatron oscillations would have the form:

$$x'' + \left(\frac{m'}{m} + \frac{\omega'}{\omega} + \frac{n}{1-n}\frac{W_i}{E}\right)x' + (1-n)x = 0 . \tag{7}$$

Here we have considered that $x = 0$ is the solution of the Eq. (4) and did not write some small inessential terms, proportional to x. The term $[n/(1-n)](W_i/E)x'$ represents the damping and the antidamping of betatron oscillations reported in [9,10]. Our calculations show that this effect would take place only if radiating were an adiabatic process.

3. – Damping and antidamping of betatron oscillations taking account of non-adiabatic properties of the radiating.

Really radiating is not an adiabatic process because it consists of the emission of single photons, each photon being emitted non-adiabatically. Therefore the Eq. (5) is not valid for this process. In this case we have $W_\varphi = \sum \varepsilon_i \delta(\varphi - \varphi_i)$ and consequently $W_\varphi = 0$ when $\varphi \neq \varphi_i$. Therefore the right side of the Eq. (4) is equal to zero when $\varphi \neq \varphi_i$. Thus we are interested only in the points $\varphi = \varphi_i$ $(i = 1, 2, ...)$.

Let ϱ be the curvature radius of the electron orbit. It can be shown that

$$\varrho = r_i + nx = r_i(1-n) + nr . \tag{8}$$

We also have the equation

$$\beta E = eH(r)\varrho \qquad (\beta \approx 1). \tag{9}$$

In the points $\varphi = \varphi_i$ we have to take into account only singular terms because the amount of the points φ_i is countable. Taking into account that in consequence of the emission of any photon the radius r is constant and E and ϱ vary, we have from Eq's (8) and (9) the following equations

$$\frac{\delta E}{\delta \varphi} = eH(r)\frac{\delta \varrho}{\delta \varphi}, \qquad \frac{\delta \varrho}{\delta \varphi} = (1-n)\frac{\delta r_i}{\delta \varphi}.$$

Hence we have

$$\frac{\delta r_i}{\delta \varphi} = \frac{\varrho}{(1-n)E}\frac{\delta E}{\delta \varphi} = -\frac{\varrho}{(1-n)E}W_\varphi, \tag{10}$$

instead of Eq. (5). In contrast to Eq. (5) this, Eq. (10) is valid for non-adiabatic radiation. From the Eq. (10) we have

$$-r_i'' - \frac{W_\varphi}{E}x' = 0, \tag{11}$$

instead of the Eq. (6). Therefore the equation for betatron oscillations, taking account of the non-adiabatic properties of the radiation, may be written in the following form:

$$x'' + \left(\frac{m'}{m} + \frac{\omega'}{\omega}\right)x' + (1-n)x = 0. \tag{12}$$

This means that in reality, when the non-adiabatic properties of the radiating are taken into account, there are neither damping nor antidamping effects.

The radiation damping time of betatron oscillations may be estimated in the following simple manner. We shall consider z-oscillations. A conservation law for the energy-momentum product of an electron, when a photon with energy ε is emitted, has the form:

$$\delta(m\dot{z}) = -(\varepsilon/c)\sin\alpha, \quad \delta m = -\varepsilon/c^2, \quad \sin\alpha = \dot{z}/v.$$

Hence we have

$$\delta\dot{z} = -\frac{1}{2}\frac{\varepsilon}{E}\left(\frac{m_0 \cdot c^2}{E}\right)^2 \dot{z},$$

and consequently the radiation damping time of betatron oscillations is equal to

$$\tau \sim \frac{E}{W}\left(\frac{E}{m_0c^2}\right)^2, \qquad W = \frac{2}{3}\frac{ce^2}{r^2}\left(\frac{E}{m_0c^2}\right)^4.$$

Thus the radiation damping of betatron oscillations is not essential for energies of electrons up to hundreds of GeV.

4. – Effect of accelerating cavities.

The effect of accelerating cavities may be studied with the aid of difference equations. This method was elaborated in collaboration with Prof. A. A. SOKOLOV.

For simplicity we shall consider a weak focusing synchrotron without straight sections when there is only one accelerating cavity. Let $x_m(t)$ be the quantity x after the m-th passage through the accelerating cavity. From the Eq. (12) we have

$$(13) \qquad x_m(t) = \sqrt{\frac{r_{im}(t)}{E_m(t)}} \left\{ A_m \sin \sqrt{1-n} \int_0^t \frac{v}{r_i}\,\mathrm{d}t + B_m \cos \sqrt{1-n} \int_0^t \frac{v}{r_i}\,\mathrm{d}t \right\}. \quad 0 \leqslant t \leqslant T .$$

Taking account of the impulse conservation law

$$E_m(T)\,\dot{x}_m(T) = E_{m+1}(0)\,\dot{x}_{m+1}(0)$$

and of the continuity condition for the electron trajectory

$$x_m(T) + \Delta r_m = x_{m+1}(0) ,$$

we can write the following recurrence equations:

$$(14) \qquad \frac{q_{m+2}}{q_{m+1}} A_{m+2} - b\left(q_{m+1} + \frac{1}{q_{m+1}}\right) A_{m+1} + A_m = -\,a\,\frac{\Delta r_m}{\gamma_m(T)} ,$$

$$(15) \qquad \frac{q_{m+1}}{q_{m+2}} B_{m+2} - b\left(q_{m+1} + \frac{1}{q_{m+1}}\right) B_{m+1} + B_m = -\,b\,\frac{\Delta r_m}{\gamma_m(T)} + q_{m+1}\frac{\Delta r_{m+1}}{\gamma_{m+1}(T)} ,$$

with

$$a = \sin \sqrt{1-n} \int_0^T \frac{v}{r_i}\,\mathrm{d}t , \qquad b = \cos \sqrt{1-n} \int_0^T \frac{v}{r_i}\,\mathrm{d}t ,$$

$$\gamma_m(t) = [r_{im}(t)/E_m(t)]^{\frac{1}{2}} , \qquad q_{m+1} = \gamma_m(T)/\gamma_{m+1}(0) .$$

Let us consider a stationary process. In this case we have

$$\Delta r_m = \Delta r = \text{const} , \qquad \gamma_m(T) = \gamma = \text{const} , \qquad q_m = q = \text{const}$$

and the recurrence relations (14), (15) may be represented in the following form

$$A_{m+2} - 2\cos\varphi A_{m+1} + A_m = -a\frac{\Delta r}{\gamma}, \tag{14a}$$

$$B_{m+2} - 2\cos\varphi B_{m+1} + B_m = -b\frac{\Delta r}{\gamma} + q\frac{\Delta r}{\gamma}. \tag{15a}$$

It follows from (14*a*), (15*a*) that accelerating cavities do not give any damping of betatron oscillations in addition to the damping determined by the Eq. (12). It means that the adiabatic invariant $\sqrt{E}\omega\lambda$ is conserved also in the presence of the radiation.

5. – The equation for betatron oscillations taking into account all kinds of accelerating fields and the radiation.

Now we shall deduce the equation for betatron oscillations taking account of all kinds of accelerating fields and of the radiation.

It is well known that a betatron oscillation is the relative motion of two particles which have the same energy. Therefore it is convenient to consider this motion in a coordinate system which is moving with one of the two particles. This system is not inertial. In this method of consideration there exist no distinction between adiabatic and non-adiabatic cases.

Covariant equations of the motion of an electron in a non-inertial coordinate system may be written in the following form:

$$\begin{cases} m_0(\ddot{x}^i + \Gamma^i_{,\alpha\beta}\dot{x}^\alpha\dot{x}^\beta) = \dfrac{e}{c}F^i{}_\alpha\dot{x}^\alpha + \dfrac{2}{3}\dfrac{e^2}{c^3}\left(K^i - \dfrac{1}{c^2}W_4^2\dot{x}^i\right), \\ K^i = \dddot{x}^i + 3\Gamma^i_{,\alpha\beta}\ddot{x}^\alpha\dot{x}^\beta + \left(\Gamma^i_{,\varepsilon\gamma}\Gamma^\varepsilon_{,\alpha\beta} + \dfrac{\partial\Gamma^i_{,\alpha\beta}}{\partial x^\gamma}\right)\dot{x}^\alpha\dot{x}^\beta\dot{x}^\gamma. \end{cases} \tag{16}$$

W_4^2 is the square of the acceleration four-vector, $F^i{}_\alpha$ is the tensor of the electromagnetic field; $\Gamma^i_{,\alpha\beta}$ are the Christoffel symbols of the second kind which are connected with the metric tensor $g_{\mu\nu}$ through the relations

$$\Gamma^i_{,\mu\nu} = g^{i\alpha}\Gamma_{\alpha,\mu\nu};\ \Gamma_{\alpha,\mu\nu} = \frac{1}{2}\left(\frac{\partial g_{\alpha\mu}}{\partial x^\nu} + \frac{\partial g_{\alpha\nu}}{\partial x^\mu} - \frac{\partial g_{\mu\nu}}{\partial x^\alpha}\right); \tag{17}$$

Let $\boldsymbol{r}_1$, $\boldsymbol{r}_2$, $\boldsymbol{r}_3$ be unit vectors of the coordinate trihedron moving with one of the two particles. The unit vector $\boldsymbol{r}_1$ is the tangential vector to the trajectory of the electron, the unit vector $-\boldsymbol{r}_3$ is directed along the principal normal, and $\boldsymbol{r}_2 = -[\boldsymbol{r}_1, \boldsymbol{r}_3]$. For simplicity we shall suppose the trajectory of the first electron to be flat. The coordinates of the second electron in this coordinate

system are x^n $(n=1, 2, 3)$, $x^4 = ic\tau$, where τ is a proper time of the first electron. In the coordinate system in consideration a metric tensor may be represented in the following form:

$$(18)\qquad \begin{cases} g_{\alpha\beta} = \delta_{\alpha\beta} + (q_\alpha \delta_{4\beta} + q_\beta \delta_{4\alpha}) + q^2 \delta_{4\alpha}\delta_{4\beta}\,, \\ \boldsymbol{q} = \dfrac{1}{ic}\dfrac{u}{\varrho}\{\boldsymbol{r}_1 \varrho + [\boldsymbol{r}_2, \boldsymbol{r}_n x^n]\}\,, \quad q'_\alpha = (\boldsymbol{q}, \boldsymbol{r}_\alpha), \quad q_4 = 0\,. \end{cases}$$

Here u is the spatial part of the velocity four-vector of the first electron, ϱ is the radius of the curvature of the trajectory of the first electron. The tensor $F^i{}_\alpha$ gives the same elastic forces which are well known in the theory of betatron oscillations without radiation.

Let us consider betatron oscillations in z-direction $(z = x^2)$. It follows from (18) and (17) that $\Gamma^2_{,\alpha\beta} = \Gamma^4_{,\varepsilon\gamma} \equiv 0$. It can be verified that the third and the first of equations (16) do not contain the variable $x^2 = z$. Therefore the equations for z-oscillations are

$$(19)\qquad \begin{cases} \ddot{z} + n\Omega^2 z = \dfrac{2}{3}\dfrac{r_0}{c}\left(\dddot{z} - \dfrac{1}{c^2} W_4^2 \dot{z}\right), \\ \ddot{\tau} = P(x^\alpha, \dot{x}^\alpha) + \dfrac{2}{3}\dfrac{r_0}{c}\left(\dddot{\tau} - \dfrac{1}{c^2} W_4^2 \dot{\tau}\right), \end{cases}$$

where $\Omega = u/\varrho$, $r_0 = e^2/m_0 c^2$. The quantity $P(x^\alpha, \dot{x}^\alpha)$ is easily shown to be of the first order with respect to $(x^\alpha, \dot{x}^\alpha)$. Indeed, when $x^n = 0$ the equations (19) become the equations of the motion in the coordinate rest system of the electron. In this case, as it is well known, we have $\dot{\tau} = 1$, $\ddot{\tau} = 0, \dddot{\tau} = (1/c^2) W_4^2$. Consequently, from the second equation (19) we have $P(0, 0) = 0$. It means that the quantity $P(x^\alpha, \dot{x}^\alpha)$ is at least of first order with respect to $(x^\alpha, \dot{x}^\alpha)$.

It is convenient, instead of derivatives with respect to proper time, to use in the Eq. (19) derivatives with respect to the coordinate time τ. We have

$$(20)\qquad \dot{z} = \frac{\mathrm{d}z}{\mathrm{d}\tau}\dot{\tau}\,, \quad \ddot{z} = \frac{\mathrm{d}^2 z}{\mathrm{d}\tau^2}\dot{\tau}^2 + \frac{\mathrm{d}z}{\mathrm{d}\tau}\ddot{\tau}\,, \quad \dddot{z} = \frac{\mathrm{d}^3 z}{\mathrm{d}\tau^3}\dot{\tau}^3 + 3\frac{\mathrm{d}^2 z}{\mathrm{d}\tau^2}\ddot{\tau}\dot{\tau} + \frac{\mathrm{d}z}{\mathrm{d}\tau}\dddot{\tau}\,,$$

and therefore, instead of the first Eq. (19), the following equation can be written:

$$(21)\qquad \frac{\mathrm{d}^2 z}{\mathrm{d}\tau^2}\dot{\tau}^2 + \boxed{\frac{\mathrm{d}z}{\mathrm{d}\tau}\ddot{\tau}} + n\Omega^2 z = \frac{2}{3}\frac{r_0}{c}\left(\frac{\mathrm{d}^3 z}{\mathrm{d}\tau^3}\dot{\tau}^3 + 3\frac{\mathrm{d}^2 z}{\mathrm{d}\tau^2}\ddot{\tau}\dot{\tau}\right) + \boxed{\frac{2}{3}\frac{r_0}{c}\left(\dddot{\tau} - \frac{1}{c^2} W_4^2 \dot{\tau}\right)\frac{\mathrm{d}z}{\mathrm{d}\tau}}\,.$$

In this equation the terms in $\square$, in view of the second equation (19), are equal to the quantity $P(x^\alpha, \dot{x}^\alpha)\,(\mathrm{d}z/\mathrm{d}\tau)$, which is a second order quantity with respect to $(x^\alpha, \dot{x}^\alpha)$ and may therefore be omitted. Taking into account that in the case of betatron oscillations we have $\langle\dot{\tau}\rangle = 1$, $\langle\ddot{\tau}\rangle = 0$ we can represent the equation for betatron oscillations, taking account of the radiation and of all kinds of accelerating fields, in the following form:

$$\frac{\mathrm{d}^2 z}{\mathrm{d}\tau^2} + n\Omega^2 z = \frac{2}{3}\frac{r_0}{c}\frac{\mathrm{d}^3 z}{\mathrm{d}\tau^3}\,. \tag{22}$$

The left part of this equation is the Kerst-Serber expression, and the right part of this equation represents a radiation effect proportional to the third derivative. From the Eq. (22) we have

$$z \sim \frac{1}{\sqrt{m\omega}} \exp\left[-\frac{n}{3}\frac{r_0 c}{r_i^2}\int^t \frac{E}{m_0 c^2}\,\mathrm{d}t\right] \sin\int^t n\omega\,\mathrm{d}t\,. \tag{23}$$

It means that the life time of the adiabatic invariant $\sqrt{m\omega}A$ is equal to $t \sim (r_i^2/r_0 c)(m_0 c^2/E) \sim 10^7 (m_0 c^2/E)$ s. In comparison with the acceleration times used in practice, the life time of adiabatic invariants is practically equal to infinity for energies up to hundreds of GeV.

* * *

The author wishes to express his gratitude for helpful discussions to Prof. A. A. Sokolov.

RIASSUNTO (*)

Si discutono gli effetti della radiazione sul funzionamento dei sincrotroni a elettroni di alta energia. Si dimostra che non c'è ne smorzamento ne antismorzamento delle oscillazioni di betatrone dovuto alla radiazione. Si tien conto delle cavità acceleratrici con l'ausilio di equazioni alle differenze finite. Si scrive l'equazione per le oscillazioni di betatrone tenendo conto della radiazione e di tutte le specie di campo acceleratore. Si calcola la vita media degli invarianti adiabatici.

(*) *Traduzione a cura della Redazione.*

IL NUOVO CIMENTO Vol. VI, N. 6 1° Dicembre 1957

Electron Motion in Synchrotrons in the Presence of Radiation.

A. N. Matveev

State University - Moscow

(ricevuto il 10 Luglio 1957)

Summary. — The effect of radiation fluctuations on electron motion in synchrotrons is discussed. A stochastic theory of betatron and phase oscillations, induced by radiation fluctuations, is presented.

1. – Introduction.

Special features of high energy electron synchrotrons are conditioned by the presence of a very intensive radiation. Radiation losses are compensated by means of an increasing number of accelerating cavities. This compensation of radiation losses is not a principal difficulty. More essential and principal difficulties arise from quantum properties of the radiation.

Considering the electron motion in uniform and axially symmetric magnetic fields Sokolov and Ternov ([1,2]) pointed out a « widening » of the electron path due to the radiation. Sands ([3]) considered phase oscillations induced by radiation fluctuations in weak focusing synchrotrons and emphasized the importance of these oscillations for the operation of high energy electron synchrotrons. Various aspects of the same problem were considered in the papers ([4-8]).

([1]) A. A. Sokolov and I. M. Ternov: *Dokl. Akad. Nauk SSSR*, **92**, 537 (1953); *Žu. Éksper. Teor. Fiz.*, **25**, 698 (1953).

([2]) A. A. Sokolov and I. M. Ternov: *Dokl. Akad. Nauk SSSR*, **97**, 823 (1954); *Žu. Éksper. Teor. Fiz.*, **28**, 432 (1955).

([3]) M. Sands: *Phys. Rev.*, **97**, 470 (1955).

([4]) A. A. Kolomenskij: *Žu. Eksper. Teor. Fiz.*, **30**, 207 (1956).

([5]) A. N. Matveev: *Dokl. Akad. Nauk SSSR*, **107**, 671 (1956).

([6]) A. N. Matveev: *Dokl. Akad. Nauk SSSR*, **108**, 432 (1956).

([7]) A. N. Matveev: *Dokl. Akad. Nauk SSSR*, **109**, 495 (1956).

([8]) A. N. Matveev: *Nuovo Cimento*, **5**, 1782 (1957).

A very important question for the operation of high energy electron synchrotrons is that about damping and antidamping of betatron oscillations discussed in LIVINGSTON's and KOLOMENSKIJ's reports at CERN Symposium ([9]) and in the paper ([10]). This question was considered in detail in our paper ([11]).

In the paper presented here we consider a stochastic theory of electron motion in synchrotrons. Stochastic features of the electron motion in the presence of radiation are conditioned by quantum properties of the radiation.

2. - Electron motion in the presence of radiation as a stochastic process.

In order to emphasize more distinctly the stochastic features of the phenomenon in consideration we consider, first of all, the electron motion in a constant uniform magnetic field in the presence of radiation, taking into account quantum properties of the radiation. In the constant uniform magnetic field H in the absence of radiation the trajectory of an electron is a circumference with radius of curvature equal to,

$$R = \beta E/eH\,, \tag{1}$$

where E, e, βc are respectively the energy, the charge and the velocity of an electron. The equation (1) describes the electron trajectory between successive photon emissions. We are interested in relativistic electron velocities. Therefore we can suppose the direction of the photon velocity to coincide with the direction of the electron velocity and the change of the electron velocity to be negligible ($\beta \approx 1$). It follows from the Eq. (1) that a change of R due to the emission of a photon with the energy ε is equal to

$$\Delta R = -\varepsilon R/E\,. \tag{2}$$

Thus the center of curvature of the electron trajectory moves step by step, each step being only stochastically determined. The radius-vector ρ of the center of curvature of the electron trajectory is determined by the equation:

$$\rho = -\sum_i \boldsymbol{n}_i R_i(\varepsilon_i/E_i)\,. \tag{3}$$

([9]) *CERN Symposium*, Vol. **1** (Geneva, 1956), S. 439, 447.

([10]) A. A. KOLOMENSKIJ and A. N. LEBEDEV: *Žu. Éksper. Teor. Fiz.*, **30**, 1161 (1956).

([11]) A. N. MATVEEV: *Nuovo Cimento*, 6, 1296 (1957).

Here $\boldsymbol{n}_i$ is an unit vector directed normally to the electron trajectory. The probability for any photon to be emitted and consequently the probability for any step in the Eq. (3) to be made are well known in the theory of radiation of an electron moving in the magnetic field. Thus we have the classical stochastic problem about a rambling. We can determine the probability for the center of curvature of the electron trajectory to be in a prescribed region. But the distance between the final center of curvature and the initial one is the amplitude of the betatron oscillation. Consequently we can determine the probability for any betatron oscillation amplitude to be induced by quantum radiation fluctuations. From the Eq. (3) we obtain for a mean square $\langle x^2 \rangle$ of betatron oscillations the following formula:

$$\langle x^2 \rangle = \frac{55}{48\sqrt{3}} \frac{hc^2 r_0}{ER} \int_0^t \left(\frac{E}{mc^2} \right)^6 \mathrm{d}t \, ; \qquad r_0 = e^2/mc^2. \tag{4}$$

This formula agrees with the Sokolov's and Ternov's formula ([1]) obtained by quantum mechanical methods. The method presented above more distinctly demonstrates the stochastic properties of the phenomenon in consideration.

The method in consideration may be generalized. Let us consider the weak focusing synchrotron without straight sections. It is well known that the set of possible trajectories in absence of the radiation in this case depends on three parameters. The general equation for any trajectory of the set has the following form:

$$L(r, a, b, \varphi) = r + a \sin \sqrt{1-n}\, \varphi + b \cos \sqrt{1-n}\, \varphi \, . \tag{5}$$

Here n is the magnetic field index, φ is the azimuthal angle, r, a, b are the parameters which determine the concrete trajectory of the set. When any photon is emitted, an electron makes a transition from one trajectory of the set to another. The rules for these transitions can be easily found. We denote by $\hat{\varepsilon}_i(\varphi_j)$ the operator representing the emission of a photon with the energy ε_i, when the azimuthal angle of the electron is φ_j. The following rule can be established for the operetor $\hat{\varepsilon}_j(\varphi_j)$:

$$\hat{\varepsilon}_i(\varphi_j) L(r, a, b, \varphi) = \tag{6}$$
$$= L(r + \Delta r_i,\ a - \Delta r_i \sin \sqrt{1-n}\, \varphi_j,\ b - \Delta r_i \cos \sqrt{1-n}\, \varphi_j, \varphi) \, ,$$

where $\Delta r_i = \Delta \varrho_i/(1-n)$ and $\Delta \varrho_i$ is the change in the radius of curvature due to the photon emission.

An operator corresponding to accelerating cavities can be determined analogously. But accelerating cavities being correlated with the phase of the be-

tatron oscillation, create only a systematic drift which is not essential for a stochastic process. Therefore we are not interested in an operator of accelerating cavities. Let $\langle x^2 \rangle$ be the mean square for betatron oscillations induced by quantum radiation fluctuations. According to the definition of betatron oscillations we have:

$$\langle x^2 \rangle = \langle \left| [\prod_{i,j} \hat{\varepsilon}_i(\varphi_j)] L(r, a, b,) - \langle [\prod_{i,j} \hat{\varepsilon}_i(\varphi_j)] L(r, a, b, \varphi)_j \rangle \right|^2 \rangle_{i,j,\varphi} \,. \tag{7}$$

Here the symbol $\langle \rangle_{a,b,\ldots}$ denotes an average over the quantities $a, b, \ldots$. By carrying out the calculations of the Eq. (7) we obtain the following expression for the mean square $\langle x^2 \rangle$ of betatron oscillations:

$$\langle x^2 \rangle = \frac{55}{48\sqrt{3}} \frac{hc^2}{(1-n)^2} \frac{r_0}{ER} \int_0^t \left(\frac{E}{mc^2} \right)^6 \mathrm{d}t \,. \tag{8}$$

A generalization of this method can be performed also for other kinds of cyclic accelerators. But it is more convenient to formulate the problem under consideration by means of differential equations as the problem of betatron and phase oscillations induced by quantum radiation fluctuations.

3. – Stochastic equations.

We shall consider radial betatron oscillations and phase oscillations. Amplitudes of vertical betatron oscillations induced by radiation fluctuations are smaller, in comparison to amplitudes of radial betatron oscillations, by the factor (mc^2/E). Therefore vertical betatron oscillations induced by radiation fluctuations are not essential.

As it is shown in the paper ([11]) there exist neither damping nor antidamping effects. Therefore we can use the Kerst-Serber equation ([12]) which can be represented in the following form:

$$\ddot{x} + \frac{\dot{E}}{E} \dot{x} + (1-n) \frac{v^2}{R^2} x = \frac{R}{E} \frac{v^2}{R^2} \delta E \,. \tag{9}$$

Here x is the radial distance of a particle from the equilibrium orbit corresponding to the energy difference δE, n is the magnetic field index.

([12]) D. W. Kerst and R. Serber: *Phys. Rev.*, **60**, 53 (1941).

Obviously we have

$$\delta E = E - E_s = \sum eV_0(\cos\varphi - \cos\varphi_s) + \int_0^t \mu W_s \,\mathrm{d}t - \sum_i \varepsilon_i \,. \tag{10}$$

where E is the energy of an electron, eV_0 is the amplitude of the rf-field, φ is the phase of the rf-field; E_s and φ_s are equilibrium values of E and φ; W_s is the equilibrium value of the radiation energy per unit time; μ is zero on the straight sections of a synchrotron where there is no radiation and is equal to unity otherwise; ε_i is the energy of the photon. Substituting the relation (10) into the Eq. (9) we obtain the following stochastic equation for radial oscillations:

$$\ddot{x} + \frac{\dot{E}}{E}\dot{x} + (1-n)\frac{v^2}{R^2}x = \mu\frac{R}{E}\frac{v^2}{R^2}\cdot \left\{\sum eV_0(\cos\varphi - \cos\varphi) - \left[\sum_i \varepsilon_i - \int_0^t \mu W_s \,\mathrm{d}t\right]\right\}. \tag{11}$$

It is to notice that the quantity x contains both betatron and synchrotron parts of the radial oscillation.

Let $\zeta = \int^t (v/R)\,\mathrm{d}t$ be a new independent variable. Then, instead of the Eq. (11), we can write the following equation:

$$(x\sqrt{E})'' + q(\zeta)x\sqrt{E_s} = \frac{R}{\sqrt{E_s}}\mu(\zeta)\left\{\sum_c \mu(\zeta,\zeta_c)eV_0(\cos\varphi - \cos\varphi_s) - \left[\sum_i \mu(\zeta,\zeta_i)\varepsilon_i - \int_0^{\zeta} \mu(\zeta')W_{s\zeta}\,\mathrm{d}\zeta'\right]\right\}. \tag{12}$$

Here $\mu(\zeta,\zeta') = 1$ when $\zeta > \zeta'$, and $\mu(\zeta,\zeta') = 0$ when $\zeta < \zeta'$. In the following exposition we shall denote the quantity ζ as ζ_j when this quantity corresponds to the radiating parts of the electron trajectory, and as ζ_0, when this quantity corresponds to straight sections of the synchrotron. We have $\mu(\zeta_0) = 0$, $\mu(\zeta_j) = 1$, $q(\zeta) = 1 - n(\zeta)$, $q(\zeta_0) = 0$.

Let $x_i(\zeta)$ $(i = 1, 2)$ be two independent solutions of the equation

$$x_i'' + qx_i = 0 \tag{13}$$

and $W = x_1'x_2 - x_2'x_1$. Let $Y_i(\zeta)$ be the function

$$Y_i(\zeta) = \int^{\zeta} \mu(\zeta)x_i(\zeta)\,\mathrm{d}\zeta, \tag{14}$$

where the constant is determined by the condition $\langle Y_i \rangle_{\zeta_w} = 0$. A solution of the equation

$$x'' + qx = \mu(\zeta)\mu(\zeta, \zeta')\,\delta E/E \tag{15}$$

can be represented in the following form:

$$x = [\alpha(\zeta, \zeta) - \alpha(\zeta, \zeta')]\,\delta E/E\,, \tag{16}$$

$$\alpha(\zeta, \zeta') = [x_1(\zeta)\,Y_2(\zeta') - x_2(\zeta)\,Y_1(\zeta')]/W\,. \tag{16a}$$

Let S be the length of the electron trajectory. It follows form the Eq. (16) that

$$\mathrm{d}S = 2\pi\alpha R\,\delta E/E\,, \qquad \alpha = \langle \alpha(\zeta, \zeta') \rangle_{\zeta_w}\,. \tag{17}$$

We have

$$\frac{\delta E}{E} = \frac{\lambda}{k\omega\alpha}\,\dot{\Psi}\,. \tag{18}$$

Here ω is the frequency of an electron revolution in the synchrotron; $\lambda = 1 + l/2\pi R$, where l is the total length of straight sections of the synchrotron; $\Psi = \varphi - \varphi_s$; k is the order of the harmonic of the rf-field.

We shall denote by I the energy emitted per period of revolution and by δI the difference $\delta I = I - I_s$. The formula

$$\Delta P_i = (2e^4/3m^2c^5) \int (F_{\mu\nu} U_\nu)^2\,\mathrm{d}x_i\,, \tag{19}$$

where ΔP_i is the radiated four-impulse is well known. Hence we have:

$$\delta I = \sigma_0 I_s\,\delta E/E\,, \tag{20}$$

$$\sigma_0 = 2 - \frac{1}{2\pi} \int_{\zeta_w} \alpha(\zeta, \zeta)\,\mathrm{d}\zeta + \frac{1}{\pi} \int q(\zeta)\,\alpha(\zeta, \zeta)\,\mathrm{d}\zeta. \tag{20a}$$

The solutions x_i are the Floquett solutions. Therefore it can be shown that

$$\sigma_0 = 4 - \alpha\,.$$

From the Eq. (10) and the Eq. (18) we obtain:

$$\frac{\lambda E_s}{k\omega\alpha}\,\dot{\Psi} = \int^t \frac{\omega}{2\pi}\,eV_0(\cos\varphi - \cos\varphi_s)\,\mathrm{d}t - \int^t \frac{\omega}{2\pi}\,(4 - \alpha)\,\frac{\lambda E_s}{k\omega\alpha}\,I_s\dot{\Psi}\,\mathrm{d}t + \tag{21}$$

$$+ \left[\int^t \frac{\omega}{2\pi}\,I\,\mathrm{d}t - \sum_i \int^t \varepsilon_i\,\delta(\tau - t_i)\,\mathrm{d}\tau \right].$$

It follows from the Eq. (21) that the non-linear stochastic equation for phase oscillations induced by radiation fluctuations has the following form

$$(22)\quad \begin{cases} \ddot{\Psi} + \gamma\dot{\Psi} + f^2[\cos\varphi_s - \cos(\varphi_s + \Psi)] = \dfrac{k\omega\alpha}{\lambda E_s}[W_s - \sum_i \varepsilon_i \delta(t - t_i)], \\ \gamma = (4 - \alpha)\dfrac{2\omega r_0}{3R}\left(\dfrac{E_s}{mc^2}\right)^3, \quad r_0 = e^2/mc^2, \quad \omega = c/R\lambda, \\ f^2 = \dfrac{k\omega^2\alpha}{2\pi\lambda}\dfrac{eV_0}{E_s}, \qquad W_s = \dfrac{2}{3}\dfrac{ce^2}{R^2}\left(\dfrac{E_s}{mc^2}\right)^4. \end{cases}$$

When the phase difference Ψ is a small quantity the non-linear equation (22) can be linearized and we obtain the following linear stochastic equation

$$(23)\quad \ddot{\Psi} + \gamma\dot{\Psi} + \Omega^2\Psi = \frac{k\omega\alpha}{\lambda E_s}[W_s - \sum_i \varepsilon_i \delta(t - t_i)],$$

where

$$\Omega^2 = f^2 \sin\varphi_s .$$

The equations (11), (12), (22), (23) describe the radial betatron and phase oscillations induced by quantum radiation fluctuations.

4. – Stochastic theory of betatron oscillations for weak focusing synchrotrons.

In the case of weak focusing synchrotrons without straight sections the problem in consideration can be exactly solved. First of all we notice that correlation between electron losses due to betatron oscillations and electron losses due to phase oscillations is practically negligible. Consequently we can consider betatron oscillations and phase oscillations independently also from the stochastic viewpoint.

The term

$$\sum eV_0(\cos\varphi - \cos\varphi_s)$$

on the right hand of the equations (11), (12) represents the effect of accelerating cavities on betatron oscillations. This effect was considered in the paper [13]. Now we can omit this term and can represent the stochastic equation for betatron oscillations in the case of weak focusing synchrotrons in the following

---

[13] A. N. Matveev: *Žu. Éksper. Teor. Fiz.*, **30**, 804 (1956).

form:

$$(24)\qquad \begin{cases} x'' + \dfrac{E'}{E}\,x' + x = \dfrac{R}{E\,(1-n)}\left[\int\limits_0^{\zeta} W_{s\zeta}\,\mathrm{d}\zeta - \sum\limits_i \mu(\zeta,\zeta_i)\varepsilon_i\right], \\ \zeta = \int\limits^{t} (1-n)(v/R)\,\mathrm{d}t\,, \qquad v = c\,, \qquad \mathrm{d}x/\mathrm{d}\zeta \simeq x'\,, \quad \text{etc.} \end{cases}$$

Let $W(x, x', \zeta)$ be the distribution function in the phase space (x, x'). Using the standard technique we obtain the following equation for the function W:

$$(25)\qquad \begin{cases} \dfrac{\partial W}{\partial \zeta} + x'\dfrac{\partial W}{\partial x} - x\dfrac{\partial W}{\partial x'} = \dfrac{\beta}{2}\left(x\dfrac{\partial W}{\partial x} + x'\dfrac{\partial W}{\partial x'}\right) + \beta W + \sigma\left(\dfrac{\partial^2 W}{\partial x^2} + \dfrac{\partial^2 W}{\partial x'^2}\right), \\ \sigma = \dfrac{R^2}{4E_s^2(1-n)^2}\langle\varepsilon^2\rangle_\zeta\,, \qquad \beta = \dfrac{E'}{E}\,, \\ \langle\varepsilon^2\rangle_\zeta = \dfrac{R}{(1-n)v}\langle\varepsilon^2\rangle_t\,, \qquad \langle\varepsilon^2\rangle_t = \dfrac{55}{24\sqrt{3}}\,\dfrac{\hbar c^2 e^2}{\lambda R^3}\left(\dfrac{E}{mc^2}\right)^7. \end{cases}$$

The damping and the exciting of betatron oscillations are negligibly small during one revolution in the phase space. Therefore W depends only on $r = \sqrt{x^2 + x'^2}$ and ζ. Thus we have to solve the following equation:

$$(26)\qquad \begin{cases} \dfrac{\partial W(r,\zeta)}{\partial \zeta} = \dfrac{\beta}{2}\,r\dfrac{\partial W}{\partial r} + \beta W + \sigma\left(\dfrac{\partial^2 W}{\partial r^2} + \dfrac{1}{r}\dfrac{\partial W}{\partial r}\right), \\ W(r,0) = W_0(r)\,, \quad W(a_0, r) = 0\,. \end{cases}$$

Here $2a_0$ is the radial width of the vacuum chamber. This equation can be solved exactly only when there is no damping of betatron oscillations, i.e. when $\beta = 0$. In order to solve this equation taking into account the damping of betatron oscillations we may use the method of limiting solutions.

We are interested in the number $N(\zeta)$ of electrons which did not collide with the walls of the vacuum chamber during the time interval $(0, \zeta)$. This number $N(\zeta)$ is determined by the relations

$$(27)\qquad \begin{cases} N(\zeta) = N(0)\,F(\zeta)\,, \qquad F(\zeta) = \int\limits_0^{a_0} W(r,\zeta)\,r\,\mathrm{d}r\,, \\ \int\limits_0^{a_0} W_0(r)\,r\,\mathrm{d}r = 1\,. \end{cases}$$

Putting

$$\xi = r \exp\left[\frac{1}{2}\int_0^\zeta \beta \, \mathrm{d}\zeta\right], \qquad \mathcal{P} = W \exp\left[-\int_0^\zeta \beta \, \mathrm{d}\zeta\right],$$

we obtain

$$\text{(28)} \qquad \begin{cases} \dfrac{\partial \mathcal{P}(\xi, \zeta)}{\partial \zeta} = \varphi(\zeta)\left(\dfrac{\partial^2 \mathcal{P}}{\partial \xi^2} + \dfrac{1}{\xi}\dfrac{\partial \mathcal{P}}{\partial \xi}\right), \\ \mathcal{P}(\xi, 0) = W_0(\xi), \qquad \mathcal{P}(a(\zeta), \zeta) = 0, \end{cases}$$

$$\text{(28}a\text{)} \qquad \begin{cases} \varphi(\zeta) = \sigma \exp\left[\displaystyle\int_0^\zeta \beta \, \mathrm{d}\zeta\right], \qquad a(\zeta) = a_0 \exp\left[\frac{1}{2}\int_0^\zeta \beta \, \mathrm{d}\zeta\right], \\ F(\zeta) = \displaystyle\int_0^{a_0} W(r, \zeta) r \, \mathrm{d}r = \int_0^{a(\zeta)} \mathcal{P}(\xi, \zeta) \xi \, \mathrm{d}\xi . \end{cases}$$

Let $\mathcal{P}_1(\xi, \zeta)$ and $\mathcal{P}_2(\xi, \zeta)$ be two solutions of the Eq. (28) with the identical initial conditions

$$\mathcal{P}_1(\xi, 0) = \mathcal{P}_2(\xi, 0) = \mathcal{P}(\xi, 0) = W_0(\xi)$$

but with the different limiting conditions

$$\mathcal{P}_1(\alpha_1(\zeta), \zeta) = \mathcal{P}_2(a_2(\zeta), \zeta) = \mathcal{P}(a(\zeta), \zeta) = 0$$

$$\text{(29)} \qquad a_1(\zeta) \leqslant a(\zeta) \leqslant a_2(\zeta) .$$

Then it can be shown that the following relations take place:

$$\text{(30)} \qquad F_1(\zeta) \leqslant F(\zeta) \leqslant F_2(\zeta), \qquad F_i(\zeta) = \int_0^{a_i(\zeta)} \mathcal{P}_i \xi \, \mathrm{d}\xi .$$

The validity of the relations (30) can be grounded by the following method. Let $P(a_i(\zeta), \xi_0, \zeta) = P_i$ be the probability for an electron not to collide with the wall $\xi = a_i(\zeta)$ during the time interval $(0, \zeta)$ if initially $(\zeta = 0)$ an electron has been placed at $\xi = \xi_0$. Obviously we have

$$\text{(31)} \qquad P_1 \leqslant P \leqslant P_2 ,$$

for all ξ_0. Indeed, an electron can collide with the wall $a_1(\zeta)$ without having

collided with the wall $a(\zeta)$ but an electron cannot collide with the wall $a(\zeta)$ without having collided with the wall $a_1(\zeta)$. Analogous considerations are valid concerning the walls $a(\zeta)$ and $a_2(\zeta)$. These considerations prove the validity of the relations (31). But the relations (31) are another expression for the relations (30). Thus the relations (30) are proved.

Dividing the interval $(0, \zeta)$ by the points ζ_n $(n = 1, 0, \ldots)$ and putting

$$a_n^{(+)} = a(\zeta_{n+1}), \qquad a_n^{(-)} = a(\zeta_n),$$

we have

$$a_n^{(-)} \leqslant a(\zeta) \leqslant a_n^{(+)}, \qquad \zeta_n \leqslant \zeta \leqslant \zeta_{n+1}. \tag{32}$$

Let the functions $\mathcal{P}^{(\mp)}_{n,n+1}(\xi, \zeta)$, $(n = 0, 1, \ldots)$ be solutions of the Eq. (28) with homogeneous limiting conditions on the broken lines $a_n^{(\pm)}$, i.e. the functions $\mathcal{P}^{(\pm)}_{n,n+1}(\xi, \zeta)$ are determined for the following values of ξ and ζ:

$$0 \leqslant \xi \leqslant a_n^{(\pm)}, \qquad \zeta_n \leqslant \zeta \leqslant \zeta_{n+1}, \qquad (n = 0, 1, \ldots).$$

We have

$$\mathcal{P}^{(\pm)}_{n,n+1}(\xi, \zeta) = \frac{2}{(a_n^{(\mp)})^2} \sum_i \frac{J_0(\lambda^{(\pm)}_{n,i}\xi)}{J_1^2(\lambda_i)}\, b^{(+)}_{n,i} \exp\left[-(\lambda^{(+)}_{n,i})^2 \int_{\zeta_n}^{\zeta} \varphi(\zeta)\,\mathrm{d}\zeta\right], \tag{33}$$

$$b^{(\pm)}_{n,i} = \int_0^{a_{n-1}^{(\pm)}} \mathcal{P}^{(\pm)}_{n-1,n}(\xi, \zeta_n) J_0(\lambda^{(\pm)}_{n,i}\xi)\,\xi\,\mathrm{d}\xi. \tag{33a}$$

Here J's are the Bessel-functions of the first kind, $\lambda^{(\mp)}_{n,i} = \lambda_i / a_n^{(\mp)}$ and λ_i are determined by the equation

$$J_0(\lambda_i) = 0.$$

Substituting the Eq. (33) into the Eq. (33a) we obtain the following recurrence relations for $b^{(\mp)}_{n,i}$:

$$b^{(\mp)}_{n,i} = \frac{2J_0(\lambda^{(\pm)}_{n,i} a_{n-1}^{(\pm)})}{a_{n-1}^{(\pm)}} \sum_j \frac{b^{(\pm)}_{n-1,j} \exp\left[-(\lambda^{(\pm)}_{n-1,j})^2 \int_{\zeta_{n-1}}^{\zeta_n} \varphi(\zeta)\,\mathrm{d}\zeta\right]}{J_0'(\lambda_j)} \frac{\lambda^{(\mp)}_{n-1,j}}{(\lambda^{(\pm)}_{n,i})^2 - (\lambda^{(\pm)}_{n-1,j})^2}. \tag{34}$$

It follows from the Eq. (33) and the Eq. (28a) that

$$F^{(\pm)}_{n,n+1}(\zeta) = \int_0^{a_n^{(\pm)}} \mathcal{P}^{(\pm)}_{n,n+1}(\xi, \zeta)\,\xi\,\mathrm{d}\xi = 2 \sum_i \frac{b^{(\pm)}_{n,i} \exp\left[-(\lambda^{(\pm)}_{n,i})^2 \int_{\zeta_n}^{\zeta} \varphi(\zeta)\,\mathrm{d}\zeta\right]}{\lambda_i J_1(\lambda_i)}. \tag{35}$$

Taking into account the Eq.'s (32), (29), (30) we can write the following relations

$$F^{(-)}_{n,n+1}(\zeta) \leqslant F(\zeta) \leqslant F^{(+)}_{n,n+1}(\zeta)\,, \qquad \zeta_n \leqslant \zeta \leqslant \zeta_{n+1}\,. \tag{36}$$

Thus we have obtained solutions $F^{(+)}_{n,n+1}$ and $F^{(-)}_{n,n+1}$ which limit an exact solution $F(\zeta)$ from above and from below. Choosing suitable solutions $F^{(+)}$ and $F^{(-)}$ we can obtain the unknown exact solution $F(\zeta)$ with the prescribed accuracy. It can be verified that the method in consideration is very efficient.

5. – A note about the stochastic theory of betatron oscillations for AC-synchrotrons.

In this case the problem under consideration is more complicated. We can only estimate the order of magnitude of electron losses.

It is well known that if we have a sum S_n of independent stochastic quantities x_i

$$S_n = \sum_{i=1}^{n} x_i \tag{37}$$

then the probability $P(S, B)$ for the sum S_n to be less then S (i.e. $S_n < S$) satisfies the differential equation

$$\frac{\partial P}{\partial B} = \frac{1}{2}\,\frac{\partial^2 P}{\partial S^2}\,, \qquad B = \sum_{i=1}^{n} \langle x_i^2 \rangle\,. \tag{38}$$

This theorem is valid when very general assumptions are fulfilled.

From the Eq. (12) we have

$$x = -\frac{R}{\sqrt{E_s}} \sum_i \int_{\zeta_i}^{\zeta} \frac{\partial \alpha(\zeta, \tau)}{\partial \tau}\,\frac{\mu(\tau)}{\sqrt{E_s}}\,\varepsilon_i\,\mathrm{d}\tau + \frac{R}{\sqrt{E_s}} \int_0^{\zeta} \frac{\partial \alpha(\zeta, \tau)}{\partial \tau}\,\frac{\mu(\tau)}{\sqrt{E_s}}\,\mathrm{d}\tau \int_0^{\zeta} \mu(\tau') W_s\,\mathrm{d}\tau'\,, \tag{39}$$

where we have omitted non-essential terms containing the quantities $eV_0(\cos\varphi - \cos\varphi_s)$. We can apply the above mentioned theorem expressed by the Eq.'s (37), (38) to the sum (39), if the quantity ζ in this sum is supposed to be a constant and x is supposed to be a function of quantities ζ_i. Thus for a free space we can obtain an exact distribution function. But in the presence of vacuum chamber walls we have to formulate limiting conditions.

Putting

$$a = \frac{l_{\text{lf}}}{2R}, \qquad l_{\text{lf}} = 2a_0 \frac{\sqrt{\langle |\overline{\alpha(\zeta, \zeta')|^2}\rangle_{\zeta,\zeta'}}}{\langle |\alpha(\zeta, \zeta')|_{\max}\rangle_{\zeta'}},$$

we can obtain for the function $F(\zeta) = \mathcal{D}(t)$ the formula (7) of paper [7]. In the case of weak focusing synchrotrons $l_{\text{lf}} = l\sqrt{2}$ and it can be verified that this formula agrees with the exact solution expressed by the formulae (35), (36) with good accuracy. But the in general case of AC-synchrotrons it is very difficult to estimate the accuracy of this formula. It is hoped that this formula gives a correct order of magnitude of electron losses in the general case of AC-synchrotrons.

6. – Stochastic theory of phase oscillations.

We shall consider a stochastic theory outgoing from the linear stochastic Eq. (23). The effect of non-linearity will be taken into account by means of limiting conditions on the basis of paper [8].

Putting

$$\zeta = \int^t \Omega \, \mathrm{d}t,$$

we obtain instead of the Eq. (23) the following equation

$$\text{(40)} \qquad \begin{cases} \Psi'' + \beta\Psi' + \Psi = \dfrac{k\omega\alpha}{\lambda E \Omega}\left[W_{s\zeta} - \sum_i \varepsilon_i \delta(\zeta - \zeta_i)\right], \\ \beta = \dfrac{\gamma}{\Omega} + \dfrac{\Omega'}{\Omega}, \qquad \Psi' = \mathrm{d}\Psi/\mathrm{d}\zeta, \quad \text{etc.} \end{cases}$$

Further calculations proceed in complete analogy to the calculations contained in Sect. 4 of this paper. For instance, instead of the Eq. (25) we have the same equation with

$$\text{(41)} \qquad \begin{cases} x \to \Psi, \quad x' \to \Psi', \quad \beta = \dfrac{\gamma}{\Omega} + \dfrac{\Omega'}{\Omega}, \qquad \zeta = \int^t \Omega \, \mathrm{d}t, \\ \sigma = \left(\dfrac{k\omega\alpha}{2\lambda E \Omega}\right)^2 \Omega^{-1} \cdot \varepsilon^2\rangle_t, \quad \text{etc.} \end{cases}$$

The only question we have to discuss is the question about limiting conditions. In a linear theory oscillations are symmetric with respect to the zero-point. But this is not the case in a non-linear theory. This obstacle makes

it impossible to exactly formulate limiting conditions in a linear theory. We shall formulate limiting conditions in such a way which enables us to take into account the effect of non-linearity.

It follows from the results of paper ([8]) that the main cause for the non-linear theory to give a larger magnitude of electron losses in comparison with the linear theory is the smaller depth of the potential wall in the non-linear theory. In order to take into account the effect of non-linearity we must take the depth of the potential well from the non-linear theory and determine the maximum possible amplitude of oscillations in the linear theory in conformity with this depth of the potential well taken from the non-linear theory. Thus from the Eq.'s (22) and (23) we obtain the following expression for the maximum possible amplitude $a_0(\zeta)$ of oscillations in linear theory

$$a_0(\zeta) = 2(1 - \varphi_s \operatorname{ctg} \varphi_s)^{\frac{1}{2}} . \tag{42}$$

Consequently we have to solve the equation (25) (with substitutions (41)) with the following limiting condition

$$W(a_0(\zeta), \zeta) = 0 \qquad \text{(see the Eq. (26))}. \tag{43}$$

In this case we cannot solve the problem exactly even if the damping of oscillations is absent. But the method of limiting solutions presented in Sect. 4 can be applied also to this case without any alteration. There is no necessity to write out corresponding formulas which are quite analogous to the formulae obtained in Sect. 4 of this paper.

7. – Conclusions.

We shell not illustrate applications of the formulas obtained in this paper to any accidental example. Because of the efficiency of the method considered in the paper all calculations needed in concrete cases cause not too much trouble. We shall only emphasize once more the importance of the phenomenon in consideration for high energy (~ 1 GeV) electron synchrotrons. It is also to notice that for electron energies of few GeV the utilization of the AC-principle is inevitable.

RIASSUNTO (*)

Si discute l'effetto delle fluttuazioni della radiazione sul moto degli elettroni nei sincrotroni. Si presenta una teoria stocastica delle oscillazioni di betatrone e di fase indotte dalle fluttuazioni della radiazione.

(*) *Traduzione a cura della Redazione.*

K-Meson Photoproduction in a Many Field Interaction.

D. Amati

Istituto di Fisica Teorica dell'Università - Napoli
Istituto Nazionale di Fisica Nucleare - Sezione di Roma

B. Vitale (*)

Istituto di Fisica dell'Università - Catania
Istituto Siciliano di Fisica Nucleare - Catania

(ricevuto il 12 Luglio 1957)

Summary. — K-meson photoproduction is analysed by means of dispersion relation techniques, in order to clarify the role played by pion and $\overline{K}$ virtual states, the « crossing » relation between K photoproduction on nucleons and radiative absorption of K by nucleons, and the way charge and magnetic moments appear in the relation satisfied by the amplitude corresponding to the photoproduction process.

Introduction.

In a previous paper (1) the technique of dispersion relations for fixed source theories was applied to strong interaction processes involving barions, pions and heavy mesons in order to analyse the role played by the various fields in any physical process. It was shown also that the renormalization of the coupling constants for strong interactions is uniquely defined.

We want here to extend our previous analysis to phenomena which include also electromagnetic interactions, at least at the first order. We thought this to be of some interest mainly for two reasons: first, because of the growing interest towards photoproduction of K-mesons, now experimentally realizable;

(*) Now at the: Istituto di Fisica Teorica, Università di Napoli.
(1) D. Amati and B. Vitale: *Nuovo Cimento*, 6, 1282 (1957).

second, because some attempts of perturbation calculations have been made quite recently on K photoproduction ([2,3]), where the influence of the virtual pions and $\bar{K}$'s was taken into account only by using a phenomenological anomalous magnetic moment interaction. We felt that this way of dealing with pion and K virtual state effects was rather inconsistent with the perturbative approach, and that the actual role played by the pions and the $\overline{K}$ in the photoproduction of K-mesons on nucleons was left quite obscure by these attempts.

It is besides clear that perturbation theory will work rather poorly for processes involving strong interacting fields. We were therefore willing to see how much it could be derived by a dispersion relation approach not only on the effects of virtual pion and K states, but also on the connections among K photoproduction and other physical processes involving baryons, heavy mesons and electromagnetic fields, and on the way charge and magnetic moments appear in the relations satisfied by the amplitude corresponding to the physical processes.

We shall restrict ourselves also here to the fixed source theory, although recoil effects can be of some importance because of the large mass of the heavy mesons. Many of the qualitative results reached here however would not be altered by a fully relativistic approach, as it will be briefly discussed at the end of this paper.

We shall treat the electromagnetic field in a perturbative way at its first order, disregarding therefore radiative corrections. We shall also disregard the possibility of a direct K-pion interaction, as proposed for instance by SCHWINGER ([4]).

1. – Low's equations for photoproduction and radiative absorption.

We shall study together the K-meson photoproduction on nucleons ($\gamma + \mathrm{N} \to \mathrm{K} + \mathrm{H}$) and the radiative absorption of $\overline{\mathrm{K}}$-mesons by nucleons ($\overline{\mathrm{K}} + \mathrm{N} \to \gamma + \mathrm{H}$). It will become apparent from what follows that these processes are connected to each other and that we shall need both of them in order to find out dispersion-like relations.

We shall use in the following the symbols:

$$C_k = -\int \boldsymbol{j} \cdot \boldsymbol{A}_k \, \mathrm{d}\boldsymbol{x} \,, \tag{1}$$

where $\boldsymbol{j}$ is the total current and $\boldsymbol{A}_k$ is the vector potential associated with a

([2]) M. KAWAGUKI and M. J. MORAVCSIK: *Phys. Rev.* **107**, 563 (1957).
([3]) A. FUJII and R. E. MARSHAK: *Phys. Rev.* **107**, 570 (1957).
([4]) J. SCHWINGER: *Phys. Rev.* **104**, 1164 (1956).

photon of momentum k; the following property holds:

$$C_k^+ = C_{-k}\,; \tag{2}$$

$$\begin{cases} U_q = [H^I, b_q^+]\,, \\ \overline{U}_q = [H^I, c_q^+]\,, \end{cases} \tag{3}$$

where H^I is the total interaction Hamiltonian, b_q^+ and c_q^+ are the creation operators for a K or a $\overline{\mathrm{K}}$ meson of momentum q, respectively; the following property is clear from the general structure of H^I:

$$U_q^+ = \overline{U}_{-q}\,, \tag{4}$$

(which gives (see [1])) $U_q^+ = +\overline{U}_q$ for « scalar » K-mesons, and $U_q^+ = -\overline{U}_q$ for « pseudoscalar » K-mesons);

$$T_{kq}^H(\omega_q) = \langle \boldsymbol{N}\boldsymbol{K}_q | C_k | \boldsymbol{N}\rangle\,, \tag{5}$$

which represents the amplitude for K photoproduction on nucleons, by a γ of momentum k, with production of a K-meson of momentum q and a hyperon H (H stands here for a Σ or for a Λ^0);

$$S_{kq}^H(\omega_q) = \langle \mathrm{H}\gamma_k | U_q | \mathrm{N}\rangle\,, \tag{6}$$

which represents the amplitude for $\overline{\mathrm{K}}$-meson radiative absorption by nucleons.

Low's equations for $T(\omega_q)$ and $S(\omega_q)$ are readily derived; they are:

$$T_{kq}^H(\omega_q) = \langle \boldsymbol{H}|[b_q, C_k]|\boldsymbol{N}\rangle - \sum_n \left[\frac{\langle \boldsymbol{H}|C_k|\Psi_n^{(-)}\rangle\langle\Psi_n^{(-)}|U_q^+|\boldsymbol{N}\rangle}{E_n + (\omega_q + i\varepsilon)} + \frac{\langle \boldsymbol{H}|U_q^+|\Psi_n^{(-)}\rangle\langle\Psi_n^{(-)}|C_k|\boldsymbol{N}\rangle}{E_n - E_H - (\omega_q + i\varepsilon)} \right], \tag{7}$$

$$S_{kq}^H(\omega_q) = \langle \boldsymbol{H}|[b_{-q}, C_{-k}]|\boldsymbol{N}\rangle - \sum_n \left[\frac{\langle \boldsymbol{H}|U_q|\Psi_n^{(-)}\rangle\langle\Psi_n^{(-)}|C_k^+|\boldsymbol{N}\rangle}{E_n - E_H + (\omega_q + i\varepsilon)} + \frac{\langle \boldsymbol{H}|C_k^+|\Psi_n^{(-)}\rangle\langle\Psi_n^{(-)}|U_q|\boldsymbol{N}\rangle}{E_n - (\omega_q + i\varepsilon)} \right], \tag{8}$$

where E_H represents the difference in mass between the hyperon H and the nucleon (the self-energy of the nucleon is here put as usual equal zero). In writing down (8) we have used the obvious relation

$$[C_k^+, c_q^+] = [b_{-q}, C_{-k}]\,. \tag{9}$$

We shall now separate the $\omega_q + i\varepsilon$ dependence on the denominators of the R.H.S. of (7) and (8) from the ω_q dependence of the commutators $[b, c]$ and of the numerators, by introducing a complex variable $z = \omega_q + i\varepsilon$. In terms of z (7) and (8) read now

$$(10) \qquad T^H_{kq}(z) = \langle \boldsymbol{H} | b_q, C_k] | \boldsymbol{N} \rangle - \\ - \sum_n \left[\frac{\langle \boldsymbol{H} | C_k | \Psi_n^{(-)} \rangle \langle \Psi_n^{(-)} | U_q^+ | \boldsymbol{N} \rangle}{E_n + z} + \frac{\langle \boldsymbol{H} | U_q^+ | \Psi_n^{(-)} \rangle \langle \Psi_n^{(-)} | C_k | \boldsymbol{N} \rangle}{E_n - E_H - z} \right],$$

$$(11) \qquad S^H_{kq}(z) = \langle \boldsymbol{H} | [b_q, C_k] | \boldsymbol{N} \rangle - \\ - \sum_n \left[\frac{\langle \boldsymbol{H} | \bar{U}_q | \Psi_n^{(-)} \rangle \langle \Psi_n^{(-)} | C_k^+ | \boldsymbol{N} \rangle}{E_n - E_H + z} + \frac{\langle \boldsymbol{H} | C_k^+ | \Psi_n^{(-)} \rangle \langle \Psi_n^{(-)} | \bar{U}_q | \boldsymbol{N} \rangle}{E_n - z} \right],$$

where the commutators and the numerators at R.H.S. depend still, of course, on ω_q).

It is now clear that the following « crossing » property exists:

$$(12) \qquad T^H_{kq}(-z) = S^H_{-k,-q}(z) .$$

No hermitean conjugation is present in the crossing relation (12); this has the important consequence that no Chew-Low dispersion relation approach can be used in this case, at least in so far as we want to use the crossing between the T and the S amplitude. It would be possible indeed to extend also to this case the Chew-Low method, but only by introducing an analytic continuation of the S amplitude over all the negative energy region; or by using a « crossing » between the T amplitude and that corresponding to the process $\mathrm{K} + \mathrm{H} \to \gamma + \mathrm{N}$, which is clearly not realizable at present in any way.

We have therefore to use the Klein approach to dispersion relations. It is surely more general than the Chew-Low method, and applies to interaction Hamiltonians for which the Chew-Low method does not work; but on the other hand it compels us to introduce more free parameters into the dispersion relations, and it hides the direct dependence of the dispersion relations on some of the physical constants involved. In this case, for instance, the commutator $[b, C]$ which is proportional to the charge of the boson fields will not give any explicit contribution. It was just the same with the constants λ and λ^0, in the case of the S and P wave pion-nucleon interaction Hamiltonian. We remind besides that an explicit dependence on the charge e is present in the relativistic dispersion relations for pion photoproduction [5]; this makes even clearer the limits of the dispersion relations here analyzed.

---

[5] G. F Chew, M. L. Goldgerger, F. E. Jow and Y. Nambu: *Phys. Rev.* **106**, 1345 (1957).

2. – Discussion of Low's equations and of the dispersion relation for T.

It is clear from (10) that the function T^H_{kq} is analytic in the upper half plane; has two poles of the first order at $z = -E_\Lambda$ and $z = -E_\Sigma$; presents branch lines going from $-(E_H - m_\pi)$ to $+\infty$ and from $-(E_\Lambda + m_\pi)$ to $-\infty$. By using Klein's method the dispersion relation satisfied by T can be easily derived, using (12) in order to avoid the negative energy region. We shall however not write down this dispersion relation in details, first because experiment is still too far from giving us the amplitudes necessary in order to test it; second because of the objections moved at the end of the previous paragraph on the validity of a Klein approach, which does not reproduce in this case all of the features of the relativistic approach. What we shall in the following briefly indicate will be enough for our purposes of discussing the role of the virtual pion and K states and the way charge and magnetic moment appear.

We shall write down the dispersion relation satisfied by $T(\omega_q)$ in the following symbolic form:

$$(13) \qquad T^H_{kq}(\omega_j) = P^H(\omega_j) + f_1(\omega_j)\, T^H_{kq}(m_K) + f_2(\omega_j)\, S^H_{-k,-q}(m_K) + \\ + \int_0^\infty f_3(\omega_q, \omega')\, T^H_{kq}(\omega')\, d\omega' + \left[\int_0^{E_H - m_\pi} + \int_{E_\Lambda + m_\pi}^\infty\right] f_4(\omega_j, \omega')\, S^H_{-k,-q}(\omega')\, d\omega' ,$$

where $f_1(m_K) = 1$ and $f_2(m_K) =$ in order (13) to be an identity for $\omega_1 = m_K$; $P^H(\omega_q)$ represents the contribution coming from the two poles at $-E_\Lambda$ and $-E_\Sigma$.

We shall now discuss in some details (13) separately for the different problems we had in mind in beginning this analysis. They are:

a) *Contributions of pion virtual states.* – They are apparent from the presence of unphysical regions in the integrals over $T(\omega')$ and $S(\omega')$. The integration finds the physical regions at $\omega' = m_K$ in both cases; the unphysical region is in particular of great importance in the integral over $S(\omega')$, where it goes from 0 to $E_H - m_\pi$ and from $E_\Lambda + m_\pi$ to m_K, because the radiative absorption process is an exoergic one and presents therefore high cross-sections at the lowest energies,.

b) *Contributions of* $\bar{K}$ *mesons.* – The contributions of $\bar{K}$ virtual states are not apparent from (13), because the cut on the energy axis begins before the energy of the first state conserving strangeness and containing a $\bar{K}$ can be reached. $\bar{K}$-mesons are however very important, through the presence of the $\bar{K}$ radiative capture amplitude S in (13), and clearly cannot be disregarded in any study concerning the photoproduction of K-mesons.

c) *Charge and magnetic moments.* – As we have already seen, the charge of the bosons does not appear explicitely in (13) because of the method used here in deriving the dispersion relation. The term $P^{II}(\omega_q)$ contains instead matrix elements of the type:

(14) $$\langle \boldsymbol{N} | C_k | \boldsymbol{N} \rangle ,$$

(15) $$\langle \boldsymbol{K} | C_k | \boldsymbol{K} \rangle$$

(besides other matrix elements clearly connected with the renormalization of the coupling constants; see (1)); matrix elements of type (14) are clearly proportional to the magnetic moments of the nucleons; matrix elements of type (15) to the magnetic moments of the hyperons. In our static theory, the anomalous magnetic moments only will be involved here.

d) *Radiative decay of* Σ^0 *into* Λ^0. – The term $P^{II}(\omega_q)$ contains also another type of matrix element:

(16) $$\langle \Sigma | C_k | \Lambda^0 \rangle .$$

Expressions of the type (16) are clearly connected with the amplitude for radiative decay of a Σ^0 into a Λ^0. It is evident from (13) that this process cannot be disregarded, as it has been made, for instance, in (2), because the Σ - Λ - γ interaction appears there on the same basis as the Σ - Σ - γ and the Λ - Λ - γ interactions.

The content of the present paper represents only a first attempt of application of dispersion relation analysis to the K photoproduction problem; has we have made clear in Sect. **1**, this non relativistic, fixed source approach can give only a rough insight into this problem, and can help to clarify the role of pions and $\bar{\mathrm{K}}$-mesons. A fully relativistic approach is now in progress (*); among our first results is that the « crossing » relation (12) is confirmed, when the variable z is given by a suitable combination of the momenta of the photon and of the heavy meson.

RIASSUNTO

Si analizza la foto-produzione dei mesoni K su nucleoni, mediante la tecnica delle relazioni di dispersione, per rendere più chiaro il ruolo degli stati virtuali dei mesoni π e dei K: per ottenere relazioni di « crossing » tra l'ampiezza per fotoproduzione e quella di assorbimento radiativo di $\bar{\mathrm{K}}$ da parte di nucleoni; per studiare infine il modo con cui la carica dei campi bosonici e i momenti magnetici dei barioni sono presenti nelle relazioni soddisfatte dalle ampiezze di fotoproduzione.

(*) *Note added in proof*: We have recently received a paper on this subject by C. Okubo.

IL NUOVO CIMENTO Vol. VI, N. 6 1° Dicembre 1957

A General Treatment of Expanding Systems (*).

I. Formulation.

Y. Takahashi and H. Umezawa (+)

Department of Physics, State University of Iowa - Iowa City, Iowa

(ricevuto il 12 Luglio 1957)

Summary. — A general method of handling an expanding system will be proposed from the field theoretical view point. It is shown that the canonical variables of a system $S[V]$ enclosed in a volume V are connected by a unitary transformation with the canonical variables of a system $S[V']$ in a larger volume V'. The unitary transformation connecting these two systems is generated by the difference of the respective Hamiltonians.

1. – Introduction.

One of the interesting problems in statistical mechanics is to describe the behavior of a large number of particles in an external (or internal) disturbance. The usual approach to this problem is based on calculating the probability per unit time of a particle making a transition from one given state to another, and obtaining from this the rate of change of the number of particles in any given state. The calculation is usually carried out by the Bloch or Boltzmann equation.

We shall present in this paper a method of treating this kind of non-stationary phenomena in quantized field theoretical fashion (1).

(*) This work is supported partly by the National Science Foundation.

(+) Present address: Department of Physics, University of Tokyo, Tokyo, Japan.

(1) The quantum field theoretical treatment of equilibrium states is discussed by many authors. A. E. Scheidegger and C. D. McKay: *Phys. Rev.*, **83**, 125 (1951); H. Ezawa, Y. Tomozawa and H. Umezawa: *Nuovo Cimento*, **5**, 810 (1957).

Let a particle system be enclosed in a volume V at time $t = -\infty$. (This system will be denoted by $S[V]$ in what follows.) If the walls of $S[V]$ are taken off, the particles will emerge into free space or into a larger finite volume V'. The expansion of the system $S[V]$ to the $S[V']$ will occur due to the facts that the wave packet enclosed in the volume V at time $t = -\infty$ will be spread out because of the uncertainty principle and the particles in the system interact with each other.

As will be seen in Sect. 2, one can show the existence of a unitary transformation $u(t)$ (time dependent) which associates the $S[V]$ with the $S[V']$. The unitary transformation is generated by the difference of the Hamiltonians for the systems $S[V']$ and $S[V]$ (*).

We shall first illustrate our method, in Sect. 2, by taking a simple model, a quantized free boson field enclosed in a volume V at time $t = -\infty$ expands into a larger finite volume V', This simple case will then be generalized. In the last section, statistical ideas will be introduced into the discussion of section 2 based on a purely fieldtheoretical point of view.

One of the features of our method is that it gives the narrow angular distribution of mesons produced by a high-energy nucleon-nucleon collision, which has been explained only by Landau's hydrodynamical analogy. The detailed account of the multiple meson production will appear in a following paper.

2. – General treatment of expanding systems (+).

a) In order to make our discussion concrete, we shall take a model in which a quantized free boson system enclosed in a box V expands into a larger finite box V'. The general case will be discussed later on.

The whole system is characterized by the Lagrangian

$$\mathcal{L}[V'] = \int_{V'} \mathrm{d}^3 z \mathcal{L}(z) \,, \tag{2.1}$$

where

$$\mathcal{L}(z) \equiv -\frac{1}{2}\left\{\frac{\partial \varphi_{V'}(z)}{\partial z_\mu}\,\frac{\partial \varphi_{V'}(z)}{\partial z_\mu} + \varkappa^2 \varphi_{V'}(z)\varphi_{V'}(z)\right\}, \tag{2.2}$$

(*) The existence of the unitary transformation between $S[V]$ and $S[V']$ has been proved by Jauch, in connection with the « scale transformation », for the finite volume V and V'. J. M. Jauch: *Proc. Theor. Seminar* (State University of Iowa, 1956), unpublished. We shall here take the unitarity of the transformation for granted.

(+) For the sake of simplicity, natural units will be employed throughout, i.e., $c = \hbar = 1$.

and

$$-\frac{L_i'}{2} \leqslant z_i \leqslant \frac{L_i'}{2} . \qquad (i = 1, 2, 3). \tag{2.3}$$

If one introduces a scale parameter λ defined by

$$L_i' \equiv \lambda_i L_i \qquad (i = 1, 2, 3) \tag{2.4}$$

and a new field variable

$$\varphi^\lambda(x) \equiv \sqrt{\lambda_0}\,\varphi_{V'}(z) , \tag{2.5}$$

where

$$\left\{ \begin{array}{l} \lambda_0 \equiv \lambda_1\lambda_2\lambda_3 , \\ z \equiv x^\lambda \equiv (\lambda_1 x_1, \lambda_2 x_2, \lambda_3 x_3, it) , \\ -\dfrac{L_i}{2} \leqslant x_i \leqslant \dfrac{L_i}{2} , \end{array} \right. \qquad (i = 1, 2, 3). \tag{2.6}$$

then the Lagrangian (201) becomes

$$\mathcal{L}[V'] = -\frac{1}{2}\int_{V'} \mathrm{d}^3x \left\{ \frac{\partial\varphi^\lambda(x)}{\partial x_\mu^\lambda} \frac{\partial\varphi^\lambda(x)}{\partial x_\mu^\lambda} + \varkappa^2\varphi^\lambda(x)\varphi^\lambda(x) \right\} , \tag{2.7}$$

and

$$\delta\mathcal{L}[V'] = -\int_V \mathrm{d}^3x \left\{ -\frac{\partial}{\partial x_i^\lambda} \frac{\partial\varphi^\lambda(x)}{\partial x_i^\lambda} + \varkappa^2\varphi^\lambda(x) \right\} \delta\varphi^\lambda(x) + \int_V \mathrm{d}^3x \, \frac{\partial\varphi^\lambda(x)}{\partial t} \cdot \delta\dot{\varphi}^\lambda(x) . \tag{2.8}$$

One obtains therefore

$$\frac{\delta\mathcal{L}[V']}{\delta\varphi^\lambda(x)} = \frac{\partial}{\partial x_i^\lambda} \frac{\partial\varphi^\lambda(x)}{\partial x_i^\lambda} - \varkappa^2\varphi^\lambda(x) , \tag{2.9}$$

$$\frac{\delta\mathcal{L}[V']}{\delta\dot{\varphi}^\lambda(x)} = \frac{\delta\varphi^\lambda(x)}{\partial t} \equiv \pi^\lambda(x) . \tag{2.10}$$

The equation of motion is consequently

$$\left(\frac{\partial}{\partial x_\mu^\lambda} \frac{\partial}{\partial x_\mu^\lambda} - \varkappa^2 \right) \varphi^\lambda(x) = 0 , \tag{2.11}$$

or

$$(\Box - \varkappa^2)\varphi^\lambda(x) = -\sum_{i=1}^{3} \left(\frac{1}{\lambda_i^2} - 1 \right) \frac{\partial^2}{\partial x_i^2} \varphi^\lambda(x) \equiv J(x) . \tag{2.12}$$

We shall here make use of a general quantization procedure proposed by the present authors (2). The more rigorous formulation can be seen in the original paper. We shall here only roughly sketch the method.

The solution of the equation (2·12) which coincides with $\varphi_V(x)$ (field variable defined in a box V) at $t=-\infty$ is, from (2.12),

$$\varphi^{\lambda}(x) = \varphi_V(x) + \int_{-\infty}^{t} \Delta(x-x')J(x')\,(\mathrm{d}x')\,, \tag{2.13}$$

from which one can derive a new variable by

$$\varphi^{\lambda}(x,\sigma) \equiv \varphi_V(x) + \int_{-\infty}^{\sigma} \Delta(x-x')J(x')(\mathrm{d}x')\,, \tag{2.14}$$

and

$$\varphi^{\lambda}(x) = \varphi^{\lambda}(x/\sigma) \qquad (x \in \sigma).$$

Since the $\varphi^{\lambda}(x,\sigma)$ satisfies

$$(\Box - \varkappa^2)\varphi^{\lambda}(x,\sigma) = 0 \qquad (x \notin \sigma), \tag{2.15}$$

it can also be determined in such a way that the commutation relation becomes

$$[\varphi^{\lambda}(x,\sigma), \varphi^{\lambda}(x',\sigma)] = i\Delta(x-x') \tag{2.16}$$

(for the same σ). Let us suppose, therefore,

$$\varphi^{\lambda}(x,\sigma) \equiv u^{-1}(\sigma)\varphi_V(x)u(\sigma) \tag{2.17}$$

and

$$i\frac{\delta U(\sigma)}{\delta\sigma(x)} = \varkappa(x)U(\sigma) = U(\sigma)\varkappa(x/\sigma)\ (*)\,, \tag{2.18}$$

we have, then, from (2.14), (2.17) and (2.18)

$$i\frac{\delta\varphi^{\lambda}(x,\sigma)}{\delta\sigma(x')} = [\varphi^{\lambda}(x,\sigma), \varkappa(x'/\sigma)] = i\Delta(x-x')J(x')\,. \tag{2.19}$$

---

(2) Y. Takahashi and H. Umezawa: *Progr. Theor. Phys.*, **9**, 14 (1953).

(*) $\varkappa(x)$ is a function of $\varphi_V(x)$, while $\varkappa(x/\sigma)$ is a function of $\varphi^{\lambda}(x/\sigma)$. See the original paper.

From equations (2.19) and (2.16), $\varkappa(x)$ is determined to be

$$\varkappa(x) = \frac{1}{2}\sum_{i=1}^{3}\left(\frac{1}{\lambda_i^2}-1\right)\frac{\partial\varphi_V(x)}{\partial x_i}\frac{\partial\varphi_V(x)}{\partial x_i}\,. \tag{2.20}$$

We have now found a unitary transformation which connects $\varphi_V(x)$ with $\varphi^\lambda(x)$ (or $\varphi_V(x^\lambda)$).

Let us investigate the physical meaning of the quantity $\varkappa(x)$.

The total Hamiltonian is from the (2.7)

$$H[V'] = \frac{1}{2}\int_V \mathrm{d}^3z\left\{\pi_{V'}(z)\pi_{V'}(z) + \frac{\partial\varphi_{V'}(z)}{\partial z_i}\frac{\partial\varphi_{V'}(z)}{\partial z_i} + \varkappa^2\varphi_{V'}(z)\varphi_{V'}(z)\right\} = \tag{2.21}$$

$$= \frac{1}{2}\int_V \mathrm{d}^3x\left\{\pi^\lambda(x)\pi^\lambda(x) + \frac{\partial\varphi^\lambda(x)}{\partial x_i^\lambda}\frac{\partial\varphi^\lambda(x)}{\partial x_i^\lambda} + \varkappa^2\varphi^\lambda(x)\varphi^\lambda(x)\right\}.$$

Substituting

$$\left\{\begin{aligned}\varphi^\lambda(x) &= u^{-1}(\sigma)\varphi_V(x)\,u(\sigma)\,,\\ \pi^\lambda(x) &= u^{-1}(\sigma)\pi_V(x)\,u(\sigma)\,,\end{aligned}\right. \qquad (x\in\sigma)\,, \tag{2.22}$$

we have

$$H[V'] = U^{-1}(\sigma)\frac{1}{2}\int_V \mathrm{d}^3x\left\{\pi_V(x)\pi_V(x) + \frac{\partial\varphi_V(x)}{\partial x_i^\lambda}\frac{\partial\varphi_V(x)}{\partial x_i^\lambda} + \varkappa^2\varphi_V(x)\varphi_V(x)\right\}U(\sigma)\,. \tag{2.23}$$

In the interaction picture, the $H[V']$ is

$$H_0[V'] \equiv U(\sigma)H[V']U^{-1}(\sigma) = \tag{2.24}$$

$$= \frac{1}{2}\int_V \mathrm{d}^3x\left\{\pi_V(x)\pi_V(x) + \frac{\partial\varphi_V(x)}{\partial x_i^\lambda}\frac{\partial\varphi_V(x)}{\partial x_i^\lambda} + \varkappa^2\varphi_V(x)\varphi_V(x)\right\},$$

and we have

$$H_0[V'] - H[V] = \frac{1}{2}\sum_{i=1}^{3}\left(\frac{1}{\lambda_i^2}-1\right)\int_V \mathrm{d}^3x\,\frac{\partial\varphi_V(x)}{\partial x_i}\frac{\partial\varphi_V(x)}{\partial x_i} = \int_V \mathrm{d}^3x\,\varkappa(x) = \varkappa(t)\,, \tag{2.25}$$

which means that the expansion of the variables from $\varphi_V(x)$ to $\varphi^\lambda(x)$ occurs due to the difference of the Hamiltonians for the $S[V']$ and the $S[V]$.

b) The relation (2.25) between the Hamiltonian and $\varkappa(t)$ holds even in more general cases. This can be seen as follows.

The Hamiltonians of the systems $S[V']$ and $S[V]$ are, respectively,

$$\left\{\begin{array}{l} H[V'] = \int_{V'} \mathrm{d}^3z\, H\left(\varphi_{V'}(z),\, \pi_{V'}(z),\, \dfrac{\partial \varphi_{V'}(z)}{\partial z_i}\right), \\ H[V] = \int_{V} \mathrm{d}^3x\, H\left(\varphi_{V}(x),\, \pi_{V}(x),\, \dfrac{\partial \varphi_{V}(x)}{\partial x_i}\right). \end{array}\right. \tag{2.26}$$

Introducing new variables

$$\left\{\begin{array}{l} \varphi^\lambda(x) \equiv \sqrt{\lambda_0}\,\varphi_{V'}(x^\lambda) \\ \pi^\lambda(x) \equiv \sqrt{\lambda_0}\,\pi_{V'}(x^\lambda) \\ x^\lambda \equiv z \equiv (\lambda_1 x_1,\, \lambda_2 x_2,\, \lambda_3 x_3,\, it)\,, \end{array}\right. \tag{2.27}$$

one can easily verify that $\varphi^\lambda(x)$ and $\pi^\lambda(x)$ satisfy the same commutation relation as $\varphi_V(x)$ and $\pi_V(x)$, i.e.,

$$\left\{\begin{array}{l} [\varphi^\lambda(x)\,\pi^\lambda(x')] = i\lambda_0[\varphi_{V'}(x^\lambda),\, \pi_{V'}(x^{\lambda'})] \\ \qquad\qquad = i\lambda_0\,\delta(x^\lambda - x^{\lambda'}) \\ \qquad\qquad = i\,\delta(x - x')\,, \qquad\qquad (t = t')\,. \end{array}\right. \tag{2.28}$$

There exists therefore a unitary transformation which associates $\varphi^\lambda(x)$ and $\pi^\lambda(x)$ with $\varphi_V(x)$ and $\pi_V(x)$. We shall denote this unitary transformation by $u(t)$, namely,

$$\left\{\begin{array}{l} \varphi^\lambda(x) = U^{-1}\varphi_V(x)U(t)\,, \\ \pi^\lambda(x) = U^{-1}(t)\pi_V(x)U(t)\,. \end{array}\right. \tag{2.29}$$

Suppose the $U(t)$ to be determined by an equation

$$i\,\frac{\partial U(t)}{\partial t} = \varkappa(t)U(t)\,, \tag{2.30}$$

and let us find the relation between the $\varkappa(t)$ and the Hamiltonians (2.26).

From (2.29) and 2.30), we have

$$\left\{\begin{array}{l} i\,\dfrac{\partial \varphi^\lambda(x)}{\partial t} = [\varphi^\lambda(x),\, U^{-1}(t)\varkappa(t)U(t)] + [\varphi^\lambda(x),\, U^{-1}(t)H[V]U(t)]\,, \\ \text{and} \\ i\,\dfrac{\partial \pi^\lambda(x)}{\partial t} = [\pi^\lambda(x),\, U^{-1}(t)\varkappa(t)U(t)] + [\pi^\lambda(x),\, U^{-1}(t)H[V]U(t)]\,, \end{array}\right. \tag{2.31}$$

where use had been made of the equations

$$(2.32)\qquad \begin{cases} i\dfrac{\partial\varphi_r(x)}{\partial t} = [\varphi_r(x), H[V]]\,, \\ i\dfrac{\partial\pi_r(x)}{\partial t} = [\pi_r(x), H[V]]\,. \end{cases}$$

Since the variables $\varphi^\lambda(x)$ and $\pi^\lambda(x)$ satisfy

$$(2.33)\qquad \begin{cases} i\dfrac{\partial\varphi^\lambda(x)}{\partial t} = [\varphi^\lambda(x), H[V']]\,, \\ i\dfrac{\partial\pi^\lambda(x)}{\partial t} = [\pi^\lambda(x), H[V']]\,, \end{cases}$$

we have, comparing (2.33) and (2.31),

$$H[V'] = U^{-1}(t)\varkappa(t)U(t) + U^{-1}(t)H[V]U(t)$$

or

$$(2.34)\qquad \begin{aligned} \varkappa(t) &= U(t)H[V']U^{-1}(t) - H[V]\,, \\ &= H_0[V'] - H[V]\,, \\ &= \int_\Gamma \mathrm{d}^3x\lambda_0\, H\Big(\frac{1}{\sqrt{\lambda_0}}\varphi_r(x), \frac{1}{\sqrt{\lambda_0}}\pi_r(x), \frac{1}{\lambda_i\sqrt{\lambda_0}}\frac{\partial\varphi_r(x)}{\partial x_i}\Big) - \\ &\quad - \int_V \mathrm{d}^3x\, H\Big(\varphi_r(x), \pi_r(x), \frac{\partial\varphi_r(x)}{\partial x_i}\Big)\,, \end{aligned}$$

$$(2.34')\qquad \varkappa(t) = -\lambda_0\int_\Gamma \mathrm{d}^3x\, \mathcal{L}\Big(\frac{1}{\sqrt{\lambda_0}}\varphi_r(x), \frac{1}{\lambda_i\sqrt{\lambda_0}}\frac{\partial\varphi_r(x)}{\partial x_i}, \frac{1}{\sqrt{\lambda_0}}\dot\varphi_r(x)\Big) + \\ + \int_V \mathrm{d}^3x\, \mathcal{L}\Big(\varphi_r(x), \frac{\partial\varphi_r(x)}{\partial x_i}, \dot\varphi_r(x)\Big)\,.$$

This shows an intimate connection between $\varkappa(t)$ and the difference of the Hamiltonians for $S[V]$ and $S[V']$. If a meson field interacts with a nucleon field via non-derivative coupling, for instance, we have

$$(2.35)\qquad \mathcal{L}_r = -\bar\psi_r(x)\Big(\gamma_\mu\frac{\partial}{\partial x_\mu} + m\Big)\psi_r(x) - \frac{1}{2}\Big\{\frac{\partial\varphi_r(x)}{\partial x_\mu}\frac{\partial\varphi_r(x)}{\partial x_\mu} + \varkappa^2\varphi_r(x)\varphi_r(x)\Big\} - \\ - if\bar\psi_r(x)O\psi_r(x)\varphi_r(x)\,,$$

and therefore

$$(2.36)\quad \varkappa(t) = \int_V \mathrm{d}^3x \left\{ \frac{1}{2} \sum_{i=1}^{3} \left(\frac{1}{\lambda_i^2} - 1 \right) \frac{\partial \varphi_V(x)}{\partial x_i} \frac{\partial \varphi_V(x)}{\partial x_i} \right\} + \\ + \sum_{i=1}^{3} \left(\frac{1}{\lambda_i} - 1 \right) \overline{\psi}_V(x) \gamma_i \frac{\partial}{\partial x_i} \psi_V(x) + i\hbar \left(\frac{1}{\lambda_0} - 1 \right) \overline{\psi}_V(x) O \psi_V(x) \varphi_V(x) .$$

c) It would be appropriate to add here some discussion on the relation between the fields $\varphi_V(z)$ and $\varphi^\lambda(x)$.

Both fields are written in terms of annihilation and creation operators as follows,

$$(2.37)\quad \varphi_V(z) = \frac{1}{\sqrt{V}} \sum_n \frac{1}{\sqrt{2\omega_k}} \{ a(\boldsymbol{k}, t) \exp[i\boldsymbol{kz}] + a^*(\boldsymbol{k}, t) \exp[-i\boldsymbol{kz}] \},$$

$$(2.38)\quad \varphi^\lambda(x) = \frac{1}{\sqrt{V}} \sum_n \frac{1}{\sqrt{2\omega_p}} \{ a^\lambda(\boldsymbol{p}, t) \exp[i\boldsymbol{px}] + a^{\lambda *}(\boldsymbol{p}, t) \exp[-i\boldsymbol{px}] \},$$

$$= \frac{1}{\sqrt{V}} \sum_n \frac{1}{\sqrt{2\omega_p}} \{ U^{-1}(t) a(\boldsymbol{p}, t) U(t) \exp[i\boldsymbol{px}] + U^{-1}(t) a^*(\boldsymbol{p}, t) U(t) \exp[-i\boldsymbol{px}] \},$$

where

$$(2.39)\quad \begin{cases} [a(\boldsymbol{k}, t), a^*(\boldsymbol{k}', t)] = \delta_{\boldsymbol{k},\boldsymbol{k}'} , \\ [a(\boldsymbol{p}, t), a^*(\boldsymbol{p}', t)] = \delta_{\boldsymbol{p},\boldsymbol{p}'} , \\ k_i = \dfrac{2\pi}{L_i'} n_i = \dfrac{2\pi}{\lambda_i L_i} n_i , \\ p_i = \dfrac{2\pi}{L_i} n_i . \qquad (i = 1, 2, 3). \end{cases}$$

Due to the relation (2.27) ,we have

$$(2.40)\quad \frac{1}{\sqrt{V}} \sum_n \frac{1}{\sqrt{2\omega_p}} \{ a^\lambda(\boldsymbol{p}, t) \exp[i\boldsymbol{px}] + a^{\lambda *}(\boldsymbol{p}, t) \exp[-i\boldsymbol{px}] \} =$$

$$= \frac{1}{\sqrt{V}} \sum_n \frac{1}{\sqrt{2\omega_k}} \{ a(\boldsymbol{k}, t) \exp[i\boldsymbol{kx}^\lambda] + a^*(\boldsymbol{k}, t) \exp[-i\boldsymbol{kx}^\lambda] \} =$$

$$= \frac{1}{\sqrt{V}} \sum_{\boldsymbol{n}} \frac{1}{\sqrt{2\omega_k}} \{ a(\boldsymbol{k}, t) \exp[i\boldsymbol{k}^\lambda \boldsymbol{x}] + a^*(\boldsymbol{k}, t) \exp[-i\boldsymbol{k}^\lambda \boldsymbol{x}] \} =$$

$$= \frac{1}{\sqrt{V}} \sum_n \frac{1}{\sqrt{2\omega_{p_\lambda}}} \{ a(\boldsymbol{p}_\lambda, t) \exp[i\boldsymbol{px}] + a^*(\boldsymbol{p}_\lambda, t) \exp[-i\boldsymbol{px}] \} =$$

$$\left(\boldsymbol{p}_\lambda = \left(\frac{1}{\lambda_1} p_1, \frac{1}{\lambda_2} p_2, \frac{1}{\lambda_3} p_3 \right) \right),$$

which gives

$$a^{\lambda}(\boldsymbol{p}, t) = c_{\lambda}(p)a(\boldsymbol{p}_{\lambda}, t) + S_{\lambda}(p)a^{*}(-\boldsymbol{p}_{\lambda}, t)\,, \tag{2.41}$$

where

$$\begin{cases} c_{\lambda}(p) = \dfrac{1}{2}\left\{\dfrac{\sqrt{\omega}_{p}}{\sqrt{\omega}_{p\lambda}} + \dfrac{\sqrt{\omega}_{p\lambda}}{\sqrt{\omega}_{p}}\right\}, \\ S_{\lambda}(p) = \dfrac{1}{2}\left\{\dfrac{\sqrt{\omega}_{p}}{\sqrt{\omega}_{p\lambda}} - \dfrac{\sqrt{\omega}_{p\lambda}}{\sqrt{\omega}_{p}}\right\}. \end{cases} \tag{2.42}$$

The relation (2.41) is convenient for actual calculation of physical quantities.

3. – Introduction of statistical ideas.

So far our discussion proceeded from a purely field-theoretical point of view. We now wish to consider the statistical aspects of our theory.

The application of statistical mechanics to field theory has been tried first by SCHEIDEGGER and MCKAY [1]. They discussed a field in « thermal equilibrium », which was characterized by the density matrix

$$\varrho = \exp\left[-\beta H\right], \tag{3.1}$$

where H is the second-quantized Hamiltonian of the field and $\beta = (kT)^{-1}$. If the system in thermal equilibrium is disturbed by an external field, a non-equilibrium state will be naturally reached. The effect of the external field will be taken into account in the following way.

In doing so, it is often advantageous to consider Gibbs' ensemble. Let us denote the ν-th system in the ensemble by $S^{(\nu)}[V']$. The discussion in the previous section holds true for any of the $S^{(\nu)}[V']$. One first defines a statistical operator by

$$\sigma(t) \equiv \lim_{N\to\infty} \frac{1}{N} \sum_{\nu=1}^{N} \Psi^{(\nu)}(t)\rangle\langle\Psi^{(\nu)}(t)\,, \tag{3.2}$$

where N is the number of systems in the ensemble and the $\Psi^{(\nu)}(t)$ is the Schrödinger wave function for the $S^{(\nu)}[V']$, i.e.,

$$i\frac{\partial\Psi^{(\nu)}(t)}{\partial t} = T(t)U(t)H[V']U^{-1}(t)T^{-1}(t)\Psi^{(\nu)}(t)\,. \tag{3.3}$$

As was shown in the previous section, $\Psi^{(\nu)}(t)$ is written as

$$\Psi^{(\nu)}(t) = T(t)u(t)\Phi_{V}^{(\nu)}\,. \tag{3.4}$$

Substituting (3.4) into (3.2), we have

$$\sigma(t) = \lim_{N\to\infty} \frac{1}{N} \sum_{\nu=1}^{N} T(t)U(t)\Phi_V^{(\nu)}\rangle\langle\Phi_V^{(\nu)}U^{-1}(t)T^{-1}(t)\,. \tag{3.5}$$

The statistical operator for thermal equilibrium state is given, as is well-known, by

$$\sigma_0 \equiv \lim_{N\to\infty} \frac{1}{N} \sum_{\nu=1}^{N} \Phi_V^{(\nu)}\rangle\langle\Phi_V^{(\nu)} = \exp\left[\beta(F - H[V]\right), \tag{3.6}$$

where F is the Gibbs free energy. We have then

$$\sigma(t) = T(t)u(t)\sigma_0 u^{-1}(t)T^{-1}(t)\,. \tag{3.7}$$

The statistical average of any physical quantity X (in Schrödinger picture) is therefore

$$\left\{\begin{aligned} \overline{X} &= \lim_{N\to\infty} \frac{1}{N} \sum_{\nu=1}^{N} \langle\Psi^{(\nu)}(t),\, X\Psi^{(\nu)}(t)\rangle = \mathrm{Tr}\left[U^{-1}(t)T^{-1}(t)XT(t)U(t)\sigma_0\right] = \\ &= \exp\left[\beta F\right]\mathrm{Tr}\left[X(t)\varrho_0\right] = \mathrm{Tr}\left[X(t)\varrho_0\right]/\mathrm{Tr}\left[\varrho_0\right], \end{aligned}\right. \tag{3.8}$$

where use has been made of the relations

$$\left\{\begin{aligned} &\sigma_0 = \exp\left[\beta F\right]\varrho_0\,, \\ &\varrho_0 \equiv \exp\left[-\beta H[V]\right], \\ &\exp\left[-\beta F\right] = \mathrm{Tr}\left[\varrho_0\right], \end{aligned}\right. \tag{3.9}$$

and the $X(t)$ is a corresponding physical quantity in Heisenberg representation. The equation (3.8) gives the statistical average of a physical quantity X when the system is initially in thermal equilibrium.

As an illustration, the number operator is

$$\left\{\begin{aligned} N &= T(t)\,U(t)\sum_n a^*(\boldsymbol{k},\,t)\,U^{-1}(t)\,T^{-1}(t) = \\ &= T(t)\,U(t)\sum_n \left\{c^{\lambda}(\boldsymbol{k})a^{\lambda *}(\boldsymbol{k}^{\lambda},\,t) - S^{\lambda}(\boldsymbol{k})a^{\lambda}(-\boldsymbol{k}^{\lambda},\,t)\right\}\cdot \\ &\quad\cdot\left\{c^{\lambda}(\boldsymbol{k})a^{\lambda}(\boldsymbol{k}^{\lambda},\,t) - S^{\lambda}(\boldsymbol{k})a^{\lambda *}(-\boldsymbol{k}^{\lambda},\,t)\right\}U^{-1}(t)\,T^{-1}(t) = \\ &= \sum_n \left\{\left(c_{\lambda}(\boldsymbol{p})^2\right)a^*(\boldsymbol{p})a(\boldsymbol{p}) + \left(S_{\lambda}(\boldsymbol{p})\right)^2 a(\boldsymbol{p})a^*(\boldsymbol{p}) - \right. \\ &\quad \left. - S_{\lambda}(\boldsymbol{p})c_{\lambda}(\boldsymbol{p})a^*(\boldsymbol{p})a^*(-\boldsymbol{p}) - S_{\lambda}(\boldsymbol{p})c_{\lambda}(\boldsymbol{p})a(\boldsymbol{p})a(-\boldsymbol{p})\right\}, \end{aligned}\right. \tag{3.10}$$

where the following relation has been used

$$a(\boldsymbol{k}, t) = c_\lambda(\boldsymbol{k}^\lambda) a^\lambda(\boldsymbol{k}^\lambda, t) - S_\lambda(\boldsymbol{k}^\lambda) a^{\lambda *}(-\boldsymbol{k}^\lambda, t) \tag{3.11}$$

with

$$\left\{ \begin{array}{l} c^\lambda(\boldsymbol{k}) = c_\lambda(\boldsymbol{k}^\lambda) = \dfrac{1}{2}\left\{ \dfrac{\sqrt{\omega_k^\lambda}}{\sqrt{\omega_k}} + \dfrac{\sqrt{\omega_k}}{\sqrt{\omega_k^\lambda}} \right\}, \\ S^\lambda(\boldsymbol{k}) = S_\lambda(\boldsymbol{k}^\lambda) = \dfrac{1}{2}\left\{ \dfrac{\sqrt{\omega_k^\lambda}}{\sqrt{\omega_k}} - \dfrac{\sqrt{\omega_k}}{\sqrt{\omega_k^\lambda}} \right\}. \end{array} \right. \tag{312}$$

* * *

In conclusion, we should like to express our thanks to the members of the theoretical physics group in the Department of Physics, State University of Iowa, for their stimulating discussions and encouragement. This work was done while one of the authors (H. U) was staying at the State University of Iowa. He is very grateful to Professor J. M. JAUCH for his kind hospitality.

RIASSUNTO (*)

Si propone dal punto di vista della teoria dei campi un metodo generale per la trattazione di un sistema in espansione. Si dimostra che le variabili canoniche di un sistema $S[V]$ racchiuso in un volume V sono connesse per mezzo di una trasformazione unitaria colle variabili canoniche di un sistema $S[V']$ racchiuso in un volume maggiore V'. La trasformazione unitaria che connette questi due sistemi è generata dalla differenza delle rispettive hamiltoniane.

(*) *Traduzione a cura della Redazione.*

IL NUOVO CIMENTO Vol. VI, N. 6 1° Dicembre 1957

Remarks on the Possible Existence of a Neutral Muon (*).

R. E. Marshak and E. C. G. Sudarshan

University of Rochester - Rochester, New York

(ricevuto il 16 Luglio 1957)

Summary. — The arguments for and against the existence of a neutral muon are discussed. The weak interactions in which a neutral muon might replace the neutrino are enumerated. It is concluded that the most favorable experimental circumstances, for the detection of the neutral muon would obtain if one searches for the reaction $K^+ \to \mu^+ + \mu^0$.

With the exception of the charged muon, all the charged fermions which have been observed in nature appear to have neutral counterparts with masses differing only by several electron masses. This is certainly true of the proton and the $\Sigma^{\pm}$ hyperon and the indirect evidence is strong for the existence of a neutral counterpart to the Ξ^- hyperon. The above statement also holds for the electron if the neutrino is regarded as the neutral conterpart of the electron although it is possible that the neutrino occupies a privileged position (cf. below). On the other hand, no evidence of any sort has been found for a neutral counterpart of the charged muon, namely a neutral particle with spin $\frac{1}{2}$, mass close to 207 m_e and extremely weak interaction with matter (i.e. cross-sections comparable to those for the neutrino). Such a hypothetical neutral muon should not possess a measurable anomalous magnetic moment and consequently should possess a mass slightly less than that of the charged muon [1].

We wish to discuss briefly the conditions under which the existence of a neutral muon might be established. Since, in many ways, a neutral muon would have the properties of a heavy neutrino, a good starting point is to

(*) This work was assisted in part by the Atomic Energy Commission.

(1) Cfr. R. Feynman and G. Speisman: *Phys. Rev.*, **94**, 500 (1954).

consider the reactions which involve neutrinos, namely:

$$(1a) \qquad \pi^+ \to \mu^+ + \nu$$

$$(1b) \qquad n \to p + e^- + \bar{\nu}$$

$$(1c) \qquad \mu^+ \to e^+ + \nu + \bar{\nu}$$

$$(1d) \qquad \mu^- + p \to n + \nu$$

$$(1e) \qquad K^+ \to \mu^+ + \nu$$

$$(1f) \qquad K^+ \to e^+ + \nu + \pi^0$$

$$(1g) \qquad K^+ \to \mu^+ + \nu + \pi^0 .$$

From a phenomenological point of view, it is plausible to allow all reactions in which the replacement of a neutral muon for a neutrino is consistent with energy conservation. Hence the allowed neutral muon reactions would be:

$$(1c') \qquad \mu^+ \to e^+ + \mu^0 + \bar{\nu}$$

$$(1d') \qquad \mu^- + p \to n + \mu^0$$

$$(1e') \qquad K^+ \to \mu^+ + \mu^0$$

$$(1f') \qquad K^+ \to e^+ + \mu^0 + \pi^0$$

$$(1g') \qquad K^+ \to \mu^+ + \mu^0 + \pi^0 .$$

If we estimate the mass difference between the charged and neutral muons by the method of Feynman and Speisman [1], we obtain $m(\mu^+) - m(\mu^0) \cong 0.13\ m_e$ and reaction $(1c')$ would be forbidden. Reaction $(1d')$ would be extremely difficult to detect because it would have to be distinguished from reaction $(1d)$ which already leaves the residual nucleus in a state of low excitation energy [2].

The three K-meson reactions $(1e')$–$(1g')$, are all possible candidates but the most promising is certainly reaction $(1e')$. The observable difference between reaction $(1e')$ and $(1e)$ is that the charged muon in reaction $(1e')$ should have a kinetic energy 142 MeV [3] as compared to 152 MeV in reaction $(1e)$. Reactions $(1f')$ and $(1g')$ would yield different energy spectra for the charged particles which are observed in reactions $(1f)$ and $(1g)$ respectively but, apart from the fact that the latter two reactions occur less frequently than reaction $(1e)$, the differences in energy spectra would be much more difficult to detect.

---

[2] Cfr. R. E. MARSHAK: *Meson Physics* (New York, 1952), chap. V.

[3] Assuming that $m(\mu^0) \cong 207\ m_e$.

If we assume that the neutral muon really behaves like a heavy neutrino, i.e. that it has the same coupling strength as the neutrino, reactions (1e′) and (1e) should be equally probable. Therefore, it should be possible to decide experimentally whether reaction (1e′) takes place. Surprisingly enough, the available experimental data do not rule out this reaction because the measurements of the kinetic energy of the charged muon from the $K_{\mu 2}$ decay have not been sufficiently accurate until now (4). It would be most desirable to perform a careful measurement of the energy spectrum of the charged muons from K-meson decays to ascertain whether there is any evidente for a discrete line at 142 MeV.

One may next inquire whether there are any theoretical arguments against the existence of the neutral muon. We have already remarked that the neutrino may be in a privileged position; if the mass of the neutrino is identically zero (5), the electron as well as the charged muon may be charged fermions without their neutral counterparts (in contrast to the charged baryons). It is difficult to assess this argument at the present time. Another argument against the existence of the neutral muon may be taken from the failure to observe the reactions $\pi^+ \to e^+ + \nu$ and $K^+ \to e^+ + \nu$. From our phenomenological point of view the absence of the last two reactions implies the absence of the corresponding reactions involving neutral muons, namely: $\pi^+ \to e^+ + \mu^0$ and $K^+ \to e^+ + \mu^0$. However, if one argues that the extremely small probability for the electron decay modes of the pion and of the kaon is due to the axial vector part of the weak four-fermion interactions (np; eν) and (Λp; eν) superimposed on the strong boson-fermion interactions (π; pn) and (K; pΛ) respectively (6), then one is in trouble with the neutral muon. That is to say, the axial vector interaction no longer suppresses the electron decay modes of the pion and of the kaon when the neutral muon replaces the neutrino. This follows simply from the fact that the axial vector interaction leads to a transition probability w proportional to $(m_\Lambda + m_B)^2$, where m_Λ and m_B are the masses of the two final decay particles. Hence, one would predict that $w(\pi^+ \to e^+ + \mu^0) \cong w(\pi^+ \to \mu^+ + \nu)$ and similarly for the electron decay of the kaon. These predictions are unaltered by allowing for parity break-down in the four-fermion interaction and are definitely contrary to experiment.

It would therefore appear that there are theoretical arguments against the existence of the neutral muon. However, it must be borne in mind that the axial vector explanation for the suppression of the electron decay modes of

(4) We are indebted to Professor M. F. Kaplon for checking over the experimental material on this point.

(5) Cfr. A. Salam: *Nuovo Cimento*, **5**, 299 (1957); also T. D. Lee and C. N. Yang: *Phys. Rev.*, **105**, 1671 (1957); L. Landau: *Žurn. Éxp. Theor. Fiz.*, **32**, 405 (1957).

(6) We are assuming here that the kaon behaves as a pseudoscalar particle in strong interactions.

the pion and kaon compared to the muon modes is not well established. Indeed, a recent analysis of all the weak particle decays (including all the parity breakdown experiments) indicates that it is difficult to explain *all* weak decays on the basis of a superposition of a universal weak four-fermion interaction on the strong boson-fermion interaction (7). In particular, while there is evidence for axial vector coupling of the ($\mu\nu$) fermion pair to the (np) and (Λp) fermion pairs, there is evidence against such coupling of the (eν) fermion pair. This discrepancy in the behaviour of the ($\mu\nu$) and (eν) fermion pairs opens up the possibility of a difference in the behaviour of the hypothesized ($\mu\mu^0$) and (eμ^0) fermion pairs and therefore leaves open the theoretical question as to whether the neutral muon exists or not.

It hardly pays to speculate further concerning the properties of the neutral muon without some positive evidence for its existence. Reaction (1e') is suggested as the most favorable for experimental investigation.

(7) E. C. G. SUDARSHAN and R. E. MARSHAK: *Proceedings of the Padua-Venice, Conference* (1957).

RIASSUNTO (*)

Si discutono gli argomenti pro e contro l'esistenza di un muone neutro. Si enumerano le interazioni deboli in cui un muone neutro potrebbe sostituire il neutrino. Si conclude che le più favorevoli condizioni sperimentali per la rivelazione del muone neutro si otterrebbero ricercando la reazione $K^+ \to \mu^+ + \mu^0$.

(*) *Traduzione a cura della Redazione.*

IL NUOVO CIMENTO Vol. VI, N. 6 1° Dicembre 1957

On the Correction of the Intensity of Cosmic Rays at Sea Level by Means of Atmospheric Data.

U. Fasoli and J. Pohl-Rüling

Istituto di Fisica dell'Università - Padova
Istituto Nazionale di Fisica Nucleare - Sezione di Padova

(ricevuto il 20 Luglio 1957)

Summary. — Various correlations have been investigated between the total intensity of Cosmic Rays and the meteorological factors of the atmosphere. These measurements have been carried out at Padua using three different sets of apparatus. An analysis is made of the atmospheric data, and the effect of the seasonal variation on the correlation coefficients is discussed.

1. – Introduction.

For an accurate measurement of Cosmic Rays at sea level it is necessary to take into account the influence of atmospheric factors. Early workers limited themselves to correcting the registered data for the mass of the atmosphere as indicated by the pressure at sea level. This method has not yielded satisfactory results and it has become apparent that other factors must be taken into account. After various attempts had been made (e.g. correlation with the temperature at sea level) Duperier [1] obtained better results by introducing the height of the 100 mb layer as a second correction factor. It is now generally admitted that the majority of the μ-mesons are produced near this strata, whose variations in height influence the probability that a meson decays before reaching the observation point.

It seems that corrections by means of these two factors (the pressure at sea level and the height of the 100 mb layer) are not completely satisfactory,

[1] A. Duperier: *Proc. Phys. Soc.*, A **61**, 34 (1948); A **62**, 684 (1949).

since the physical state of the atmosphere cannot be fully described by means of only two parameters. In fact various authors (2) note that after having applied the correction for the pressure at sea level, there remains a seasonal variation showing a maximum in the winter months relative to the point of observation. This clearly shows that other meteorological influences remain. ELLIOT (3) later applied the 100 mb layer correction and found that the seasonal variation remained with amplitude unchanged and with the maximum shifted by about six months. Furthermore the correction coefficients vary from author to author, and some even find that the coefficients themselves show a seasonal variation.

The purpose of the present paper is to study the influence of the meteorological factors on the intensity of the μ-mesons at sea level.

2. – Apparatus and measurements.

The measurements have been carried out at Padua at 25 m above sea level (longitude 11°53 E, latitude 45°24.5 N) in a thermally controlled space and under a roof whose thickness was negligible.

The apparatus is such that three measurements of the total intensity of the μ-mesons can be obtained contemporally. The greatest counting rate was given by a system of two equal telescopes each consisting of three trays of six counters, with a zenithal angle of 92° NS and 42° EW and with a cut-off of 10 cm of lead. The total number of counts was about 700 000 per day. In what follows this will be called set « *A* ».

Set « *B* » consists of two identical Geiger counter telescopes each of three trays of four counters with a zenithal aperture of 70° NS and 22° EW. These telescopes are those used for measurement of the positive excess of μ-mesons (4-6) and registered both the positive excess and the total intensity by means of a suitable electronic circuit. The cut-off of this set « *B* » is given by the 50 cm of iron making up the magnet and by the field of 13 000 gauss, which together give a lower limit for the energy of 0.7 GeV. The counting rate is about 190 000 per day.

---

(2) See e.g.: S. E. FORBUSH: *Rev. Mod. Phys.*, **11**, 168 (1939); A. R. HOGG: *Proc. Roy. Soc.*, A **192**, 128 (1947).

(3) H. ELLIOT: *Progress Cosmic Ray Physics*, p. 464 (1952).

(4) I. FILOSOFO, E. POHL and J. POHL-RÜLING: *Nuovo Cimento*, **12**, 809 (1954).

(5) I. FILOSOFO, I. MODENA, E. POHL and J. POHL-RÜLING: *Nuovo Cimento*, **3**, 112 (1956).

(6) U. FASOLI, C. MARONI, I. MODENA, E. POHL and J. POHL-RÜLING: *Nuovo Cimento*, **5**, 473 (1957).

The third measurement, which will be called set « B_1 » though this is not strictly correct, is given by the sum $(\mu^+ + \mu^-)$ of the mesons selected by set « B ». This measurement concerns only those particles lying in an energy band between 0.7 and 1.3 GeV with a counting rate of about 10 000 per day; it will serve for a usefull check on the other measurements.

The measurements have been carried out during the period which goes from April 1955 to October 1956, with 404, 402 and 462 effective working days for the repsective sets. These are divided into 14, 13 and 8 periods consisting of 29, 31 and 58 mean effective days respectively. The 14 periods of set « A », on which our work is mainly based, are given together with their effective days in Table I.

3. – Considerations about the atmosphere.

For a complete description of the state of the atmosphere one should know the pressure and temperature at all levels. These parameters are not however independent, since they are related by an ipsometric formula which becomes increasingly accurate as the thickness of the layer considered is reduced. Thus only one parameter is necessary, for example the altitude of each isobaric layer, which is given directly by the meteorological bulletins. The distance between two isobaric surfaces is proportional to the mean temperature of the layer lying between them. As is well known, the following formula is applicable:

$$(1) \quad (h_i - h_{i+1}) / \ln \frac{x_i}{x_{i+1}} = RT_l = H_l \,. \quad (*)$$

The mean density of a layer is:

$$(2) \qquad \varrho_l = \frac{x_l}{H_l} \,.$$

We have taken the altitude of the single isobaric layers from the « Täglicher Wetterbericht » of the « Deutscher Wetterdienst » (+) which provides the most

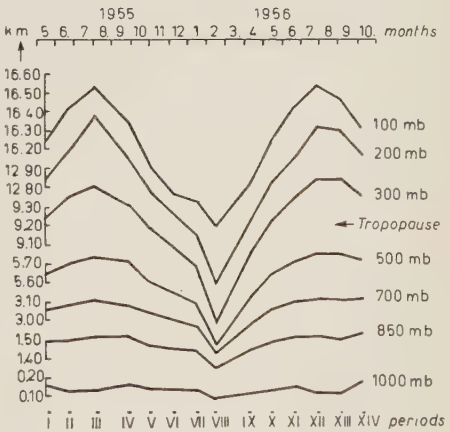

Fig. 1. – Height of the various isobaric layers. (The points in « Roman » numerals are the centres of the various periods).

(*) Where h_i is the height of the i-th isobar of pressure x_i (g/cm²), T_l is the mean temperature of the layer of air lying between the i-th and the $(i+1)$-th surface, and R is the characteristic constant of the gas.

(+) Zentralstelle *Bad Kissingen*, Postfach 50 (Germany).

Period	I	II	III	IV	V	V
from	25-4-55	3-6-55	13-7-55	7- 9-55	11-10-55	21-1
to	28-5-55	9-7-55	17-8-55	11-10-55	21-11-55	31-1
eff. days	23	24	22	29	40	3

complete data for Europe (*). This contains the absolute topographies for the isobars at 100, 200, 300, 500, 700 and 850 mb, and the relative topography for 500/1000 mb.

In order to find the relationship between the seasonal variation of the Cosmic Radiation and the meteorological factors, we must demonstrate the seasonal variation of the latter. For this purpose we give in Fig. 1 the mean of the heights of the single isobars relative to every period of observation of set « A », in Fig. 2 on the other hand, we have given the means of the thicknesses of the various layers. It will be noted in Fig. 1 that there is a net seasonal variation which is more marked at the greater heights, and having a maximum in July-August with a minimum in February. We have made a harmonic analysis in Fourier series of the seasonal variation for the 100 mb layer. Already with the first term the seasonal variation can be fully interpreted (Fig. 4). Fig. 2 shows clearly the well known fact of the different behaviour of the temperature above and below the tropopause (at our latitude about 300 mb). To correct the registrated data it will be con-

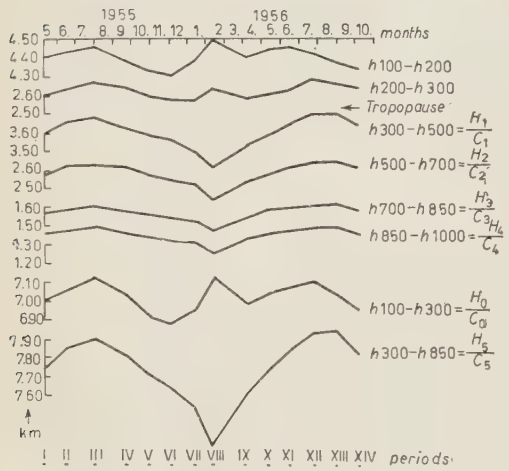

Fig. 2. – Thicknesses of the various layers lying between two isobars.

(*) For the altitude it is an advantage to make use of a meteorological bulletin rather than isolated data from only one station since the registrations from a single balloon are more subject to errors, whereas these are equalized on the maps. The heights are given for 03.00^h MET at which time the measurements are not influenced by the radiation of the sun.

VII	VIII	IX	X	XI	XII	XIII	XIV
12-55	31-1-56	22-3-56	20-4-56	1-6-56	10-7-56	10-8-56	18 -9-56
1-56	23-2-56	20-4-56	31-5-56	10-7-56	10-8-56	18-9-56	19-10-56
26	20	30	30	35	28	30	30

venient to refer to those meteorological data which have major importance, remembering that the tropopause divides the atmosphere into two parts having different behaviour, and that the production of mesons occurs to a greater degree above the tropopause.

4. – Experimental correction coefficient for multiple correction between the intensity of the mesons and the various meteorological factors.

When making multiple correlations we must limit ourselves to two or at most three parameters to avoid extremely laborious calculations.

We have applied the corrections to the day-to-day mean value of the meson intensity during each of the different measurement periods (see above). As pressures we took the mean values of eight observations made at different hours of the day and supplied by the « Servizio meteorologico dell'Aeronautica Militare » of Padua.

4.1. *Correlation of the intensity of the mesons with the pressure at sea-level and with the height of the* 100 mb *layer.* – The regression coefficients α and γ have been found by means of the method of least mean squares using the well

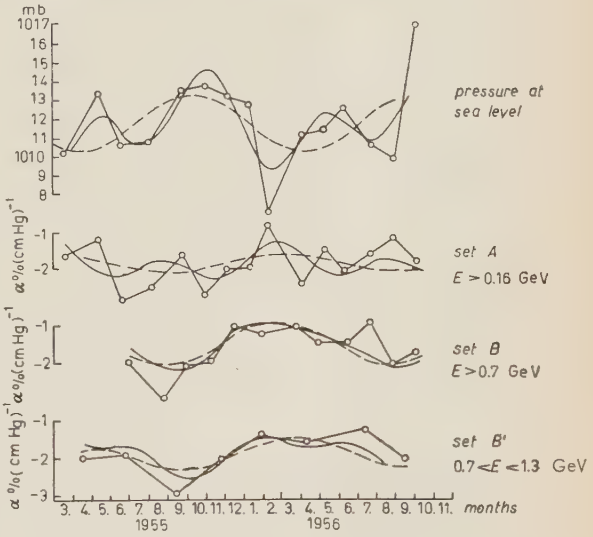

Fig. 3. – Pressure at sea level (in mb for set « A »). Coefficients α for set « A », set « B » and set « B_1 ». ——— Expansion in Fourier series (first term only); – – – – Expansion in Fourier series (first and second terms only).

known regression formula:

$$\frac{\Delta n}{n} = \alpha \Delta p + \gamma \Delta h_{100} \quad (*).$$

The seasonal variation of these coefficients for set « A », set « B » and set « B_1 » are given in Fig. 3 and 4. The coefficient γ present a similar seasonal variation for all three measurements. An harmonic analysis has been made in Fourier series as far as the second term. The results are also given in Fig. 3 and 4, while the amplitude of the various harmonics are expressed as percentages of the mean and given in Table II. The form is already well interpreted by the first term, however a slight improvement is found when one also takes into account the second term. A similar analysis for the coefficient α gives less satisfactory results, in particular for set « A ».

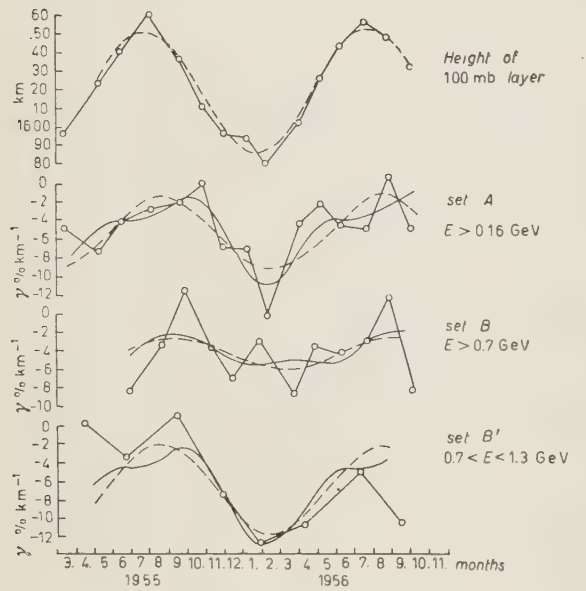

Fig. 4. – Height of the 100 mb layer (in km for the periods of set « A ») and coefficients γ for set « A », set « B » and set « B_1 ». ——— Expansion in Fourier series (first term only); – – – – Expansion in Fourier series (first and second terms only).

The cause of the seasonal variation of the coefficients is to be found in the similar seasonal variation of the meteoreological factors (see Fig. 3 and 4). In fact if one takes into account that the daily fluctuations of these parameters occur about mean values which in their turn have a seasonal variation with a much more pronounced amplitude, one concludes that, owing to the actual way in which the calculations are carried out, the seasonal variation of the coefficients cannot be avoided.

In order to obtain correct regression coefficients, the superimposed seasonal variation has to be considered and the mean has to be taken over one whole period. This might possibly be the reason why different authors find different values for the coefficients.

(*) Where n = hourly intensity of the meson, p = pressure at sea-level, and h_{100} = height of the 100 mb layer.

TABLE II. – *Amplitudes of the various harmonics.*

$y = A_0 + A_1 \sin \omega t + B_1 \cos \omega t + A_2 \sin 2\omega t + B_2 \cos 2\omega t.$

y	A_0	A_1	B_1	A_2	B_2
p mb	1011.7	+ 0.046	− 0.14	+ 0.072	+ 0.15
α% (cm Hg)$^{-1}$ set « A »	−1.88	−11.7	+ 5.3	− 8.0	−17.0
α% (cm Hg)$^{-1}$ set « B »	−1.51	−36.7	+ 7.7	+10.0	− 1.4
α% (cm Hg)$^{-1}$ set « B_1 »	−1.91	−17.2	+14.5	+12.3	− 5.2
h_{100} km	16.18	+ 1.73	+ 0.99	—	—
γ% km^{-1} set « A »	−5.58	+66.9	−11.7	−11.5	+29.4
γ% km^{-1} set « B »	−4.35	+35.2	+11.5	+ 7.4	−15.4
γ% km^{-1} set « B_1 »	−6.90	+63.9	−22.5	+ 3.9	+23.9

The A_0 are given in the same units as the y. The A_1, B_1, A_2, B_2 are given as percentages of A_0.

TABLE III.

Energy GeV	α % (cm Hg)$^{-1}$	γ % km^{-1}
> 0.70 set « B »	-1.51 ± 0.05	-4.35 ± 0.25
> 0.16 set « A »	-1.88 ± 0.04	-5.58 ± 0.15
$0.70 \div 1.30$ set « B_1 »	-1.91 ± 0.13	-6.90 ± 0.50

The mean values for the different sets found under these conditions are given in Table III.

From Fig. 4 one sees that the values of sets « A » and « B_1 » show a marked peak in February 1956, whereas those of set « B » do not. This might be caused by the activity of the Sun which in this month was very strong. As we have seen in one of our earlier works ([5]) the extra particles from the Sun are mainly of low energy. Though the cut-off of set « B » is the same as that of set « B_1 » it registers the integral energy spectrum whereas on the other hand set « B_1 » registers only a small energy band.

4.2. *Triple correlation of the intensity of the mesons with the pressure at sea-level, with the height of the* 100 mb *layers and the thickness of the layer between* 300 mb *and* 850 mb. – As the overall variation of the atmosphere is only partly taken into account by the two data p and h_{100} we have tried to represent its influence upon the intensity of the μ-mesons by three data. First of all we have taken the difference of height of the 300 mb and 850 mb layer as the parameter. This difference is connected with the mean temperature and the mean density of this layer by means of equations (1) and (2) respectively. The regression coefficient β' is found from the following regression equation:

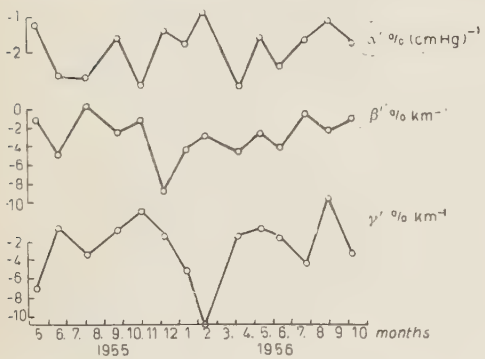

Fig. 5. – Regression coefficients as given by: $\Delta n/n = \alpha' \Delta p + \beta' \Delta(h_{300} - h_{850}) + \gamma' \Delta h_{100}$.

$$\frac{\Delta n}{n} = \alpha' \Delta p + \beta' \Delta(h_{300} - h_{8\,0}) + \gamma' \Delta h_{100},$$

which was solved by the method of least mean squares. This coefficient also gives an indication of the influence of the mean temperature and mean density of the troposphere upon the meson intensity.

The day-to-day values of the coefficients for the different periods of set « A » are given in Fig. 5. α' and β' show the same seasonal variations as α and γ; β' on the other hand only indicates an insignificant seasonal variation. The mean values over a whole period are given in Table IV.

4.3. *Triple correlation between the intensity of the mesons and the pressure at sea-level, the thickness of the layer between* 300 mb *and* 850 mb, *and the thickness of the layer between* 100 mb *and* 300 mb. – In order to make possible a comparison with the theoretically determined correction coefficients (see Sect. 5), we have also determined the regression coefficients from the day-to-day mean

TABLE IV. – *Correction coefficients for set « A ».*

	% (cm Hg)$^{-1}$		% km^{-1}	% °C^{-1}		% km^{-1}	% °C^{-1}
α	-1.88 ± 0.04				γ	-5.58 ± 0.15	
α'	-1.92 ± 0.04	β'	-3.45 ± 0.15	-0.099 ± 0.005	γ'	-3.38 ± 0.12	
α''	-2.15 ± 0.04	β''	-6.00 ± 0.15	-0.172 ± 0.005	γ''	-2.10 ± 0.12	-0.060 ± 0.004
δ_4	-1.08	δ_5	-6.29	-1.80	δ_0	-2.27	-0.065

values of set « *A* », by means of the following equation:

$$\frac{\Delta n}{n} = \alpha'' \Delta p + \beta'' \Delta (h_{300} - h_{850}) + \gamma'' \Delta (h_{100} - h_{300}) .$$

The mean values of these regression coefficients are given in Table IV and Fig. 6. α'' shows the same variation as α' and α; β'' and γ'' show a seasonal variation similar to that of γ and γ'. The experimental mean values of β'' and γ'' are in good agreement with the corresponding theoretical ones (see below).

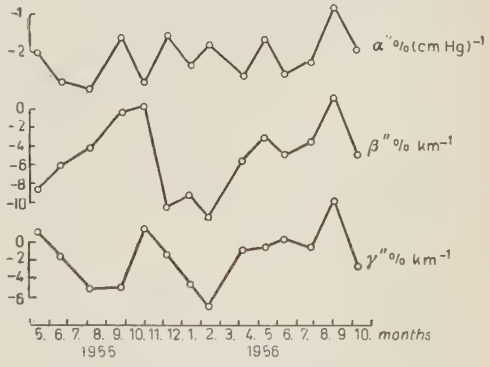

Fig. 6. – Regression coefficients as given by: $\Delta n/n = \alpha'' \Delta p + \beta'' \Delta (h_{300} - h_{850}) + \gamma'' \Delta (h_{100} - h_{300})$.

5. – Tentative interpretation of the results.

As is well known, the production of mesons is already notable in the upper layers of the atmosphere and one can consider that the greater part of the mesons registered at sea level have been produced above the 300 mb layer. With the meteorological data at our disposal it is only possible to study the behaviour throughout the atmosphere of that part of mesons which are produced below the 100 mb layer, since this is the highest layer for which data are available.

Even with this strong limitation one obtains results which represent sufficiently well the behaviour of the greater part of the mesons, as will be seen later.

If we put $G(R)$ as representing the production function, where R is the residual range in g cm^{-2}, and we indicate with x' the depth of the point of production in g cm^{-2}, we obtain for the mesons produced at this depth x'

$$\mu(R, x') = G(R + x_a - x') \exp\left[-\frac{x'}{L}\right] \mathrm{d}x' , \tag{3}$$

where x_a expresses the depth of sea level and the exponential factor takes account of the absorption of the primary in the atmosphere ($L = 125$ g cm^{-2}). The probability that a meson produced at a depth x_1 arrive at x_2 is given by the relation

$$w = \exp\left[-\frac{1}{\tau c}\int_{x_1}^{x_2}\frac{\mu c}{P}\frac{\mathrm{d}x'}{\varrho(x')}\right] , \tag{4}$$

where P is the momentum of the meson, μ and τ are the mass and the mean lifetime respectively and $\varrho(x')$ is the density of the air of the point x'.

Since it is convenient to express all these factors in terms of the range by means of Olbert's expression ([7]):

$$\frac{\mu c}{P(R)} = \frac{B}{b + R + x_a - x'} - K ,$$

where $B = 53.5$ g cm^{-2}, $b = 56$ g cm^{-2}, $k = 2.07 \cdot 10^{-3}$ we obtain

$$w = \exp\left[-\frac{1}{\tau c}\int_{x_1}^{x_2}\left(\frac{B}{R' - x'} - K\right)\frac{\mathrm{d}x'}{\varrho(x')}\right] , \tag{4'}$$

with $R' = b + R + x_a$. Thus the number of mesons produced between x_1 and x_2 which arrive at x_2 will be

$$\mu(R, x_2) = \int_{x_1}^{x_2} G(R + x_a - x') \exp\left[-\frac{x'}{L}\right] w \, \mathrm{d}x' . \tag{5}$$

In our case the number of mesons produced between 100 and 300 mb which effectively arrive at 300 mb is

$$\mu(R, x_{300}) = \int_{x_{100}}^{x_{300}} G(R + x_a - x') \exp\left[-\frac{x'}{L}\right] w \, \mathrm{d}x' . \tag{5'}$$

([7]) S. OLBERT: *Phys. Rev.*, **92**, 454 (1953).

In order to simplify the calculations we assume that the production of mesons finishes at 300 mb. In order to take account of the decays between 300 mb and sea level, we subdivide the troposphere into 4 layers taken between successive surfaces given by the meteorological maps. If we call the survival probability throughout the various layers w_1, w_2, w_3 and w_4, the spectrum in range of the mesons at sea level must be

$$\mu(R) = w_1 w_2 w_3 w_4 \int_{x_{100}}^{x_{300}} G(R + x_a - x') \exp\left[-\frac{x}{L}\right] w \, \mathrm{d}x' \,. \tag{6}$$

due to relations (1) and (2) the survival probability then becomes

$$w = \exp\left[-\frac{1}{\tau c} H_0 \int_{x'}^{x_{300}} \left(\frac{B}{R' - x'} - K\right) \frac{\mathrm{d}x'}{x'}\right], \tag{4''}$$

$$w_l = \exp\left[-\frac{1}{\tau c} H_l \int_{x_i}^{x_{i+1}} \left(\frac{B}{R' - x'} - K\right) \frac{\mathrm{d}x'}{x'}\right]. \quad (*) \tag{4'''}$$

Carrying out the integrals in (4'') and (4''') one obtains

$$\left(\frac{B}{R'} - K\right) \ln \frac{x_{300}}{x'} - \frac{B}{R'} \ln \frac{R' - x_{300}}{R' - x'} = B_{x'}(R) \,,$$

$$\left(\frac{B}{R'} - K\right) \ln \frac{x_{i+1}}{x_i} - \frac{B}{R'} \ln \frac{R' - x_{i+1}}{R' - x_i} = A_l(R) \,.$$

Finally the spectrum in range at sea level becomes

$$\mu(R) = \exp\left[-\frac{1}{c\tau} \sum_l H_l A_l(R)\right] \int_{x_{100}}^{x_{300}} \frac{7.31 \cdot 10^4}{(520 + x_a + R - x')^{3.58}} \cdot \exp\left[-\frac{x'}{L} - \frac{H_0}{\tau c} B_{x'}(R)\right] \mathrm{d}x' \,, \tag{6'}$$

where

$$G(R + x_a - x') = \frac{7.31 \cdot 10^4}{(520 + x_a + R - x')^{3.58}}$$

(*) $l = 1, 2, 3$ and 4; $i = 300$, 500, 700 and 850, $i+1 = 500$, 700, 850 and x_a.

represents the empirical range spectrum for the production of mesons given by OLBERT (7). The spectrum obtained by us under these conditions can be made to coincide with the experimental spectrum by applying a factor of 2.2 as is shown in Fig. 7. This signifies that the group of mesons considered by us represents sufficiently well the general behaviour of the mesons.

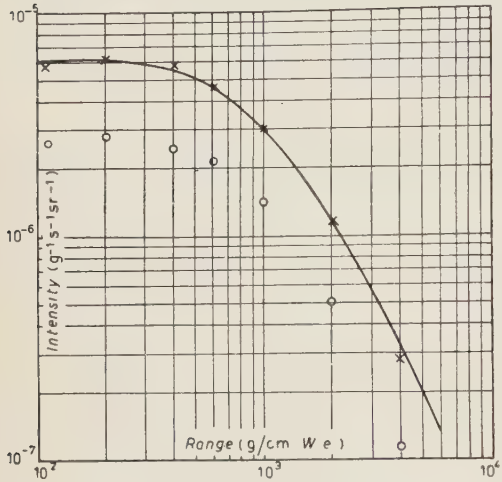

Fig. 7. – Comparison between experimental and calculated range-intensity spectrum. The full line represents the experimental curve as given by G. PUPPI (10); the points have been calculated with equation (7); the crosses are the calculated values multiplied by 2.2.

The integral spectrum at sea level evidently becomes

$$(7)\quad \mu = \int_{R_0}^{\infty} \mathrm{d}R \left\{ \exp\left[-\frac{1}{\tau c} \sum_l H_l A_l(R) \right] \cdot \int_{x_{100}}^{x_{300}} \frac{7.31 \cdot 10^4}{(520 + x_x + R - x')^{3.58}} \cdot \exp\left[-\frac{x'}{L} - \frac{H_0}{\tau c} B_{x'}(R) \right] \mathrm{d}x' \right\} .$$

with R_0 as the cut-off of the apparatus.

With this formula we have calculated the μ-mesons for the various periods of set « A » and have obtained a seasonal effect. In Fig. 8 the relative variations of the intensity of the μ-mesons are compared with those obtained experimentally with set « A ».

The correction coefficients for the thicknesses of the various layers may be obtained from

$$(7')\quad \delta_l = \frac{1}{\mu} \frac{\partial \mu}{\partial H_l} \frac{\partial H_l}{\partial \Delta h_l} = -\frac{1}{\mu} \frac{\partial \mu}{\partial H_l} \frac{1}{\ln (x_i / x_{i+1})} \cdot \quad (*)$$

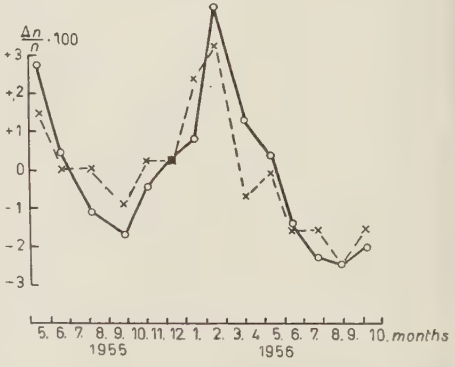

Fig. 8. – Relative seasional variations found experimentally for the μ-mesons;
O——O experimental,
×·····× calculated with equation (7).

(*) Δh_l = thickness of the l-th layer.

Putting $C(R)$ for the term under the second integral of expression (7) one has for δ_l:

$$(8) \qquad \delta_l = \frac{1}{\mu} \frac{1}{\ln (x_l/x_{l-1})} \cdot \frac{1}{\tau c} \int_{R_0}^{\infty} \mathrm{d}R \left\{ A_l(R) \exp \left[-\frac{1}{\tau c} \sum_l H_l A_l(R) \right] \int_{x_{100}}^{x_{300}} C(R)\, \mathrm{d}x' \right\}.$$

and δ_0 becomes:

$$(9) \qquad \delta_0 = \frac{1}{\mu} \frac{1}{\ln (x_{100}/x_{300})} \frac{1}{\tau c} \int_{R_0}^{\infty} \mathrm{d}R \left\{ \exp \left[-\frac{1}{\tau c} \sum_l H_l A_l(R) \right] \int_{x_{100}}^{x_{300}} C(R) B_{x'}(R)\, \mathrm{d}x' \right\}.$$

By means of (8) and (9) we first calculated the correction coefficients for the various layers and for the various periods of set « A ». The mean values of these are given in Table V.

TABLE V. – *Correction coefficients calculated by means of* (8) *and* (9).

	% km^{-1}	% °C^{-1}	% (cm Hg)$^{-1}$
$\frac{\delta_0}{h_{100} - h_{300}}$	— 2.27	— 0.065	
$\frac{\delta_1}{h_{300} - h_{500}}$	— 5.40	— 0.155	
$\frac{\delta_2}{h_{500} - h_{700}}$	— 6.68	— 0.192	
$\frac{\delta_3}{h_{700} - h_{850}}$	— 8.07	— 0.232	
$\frac{\delta_4}{h_{850} - p}$	— 9.72	— 0.279	— 1.08
$\frac{\delta_5}{h_{300} - h_{850}}$	— 6.29	— 0.180	

The mean values for the individual periods do not show seasonal effects. δ_0 and δ_5 are in good agreement with the experimental data (see Table IV). We have also calculated the mean temperature coefficients for the various

layers by means of

$$\frac{\partial \mu}{\partial T_l} = \frac{\partial \mu}{\partial H_l} \frac{H_l}{T_l} = \frac{\partial \mu}{\partial H_l} \cdot Z \quad (*) \tag{10}$$

and the results are given in Table V.

We have expressed δ_4 as a function of the pressure at sea level by means of

$$\frac{\partial \mu}{\partial p} = \frac{\partial \mu}{\partial H_l} \frac{H_l}{\ln (x_{850}/p)} \cdot \frac{1}{p} . \tag{11}$$

obtaining a value of about one half of the experimental. One must bear in mind however that the coefficient calculated by means of (11) only expresses the contribution of the pressure at sea level to the decay of the μ, since one takes into account the variations of H_4 (reduced height relative to the lowest layer of the atmosphere) as a function of the pressure. It must be observed, however, that—in the model we have chosen for describing the atmosphere—an increase in the pressure corresponds also to an increase in the mass of the lower layer (+), and an increase in the mass of the last layer corresponds to an increase in the cut-off of the apparatus. If we take account of this fact and add to the coefficient calculated by us, the partial coefficient of pressure due to the cut-off, already calculated by TREFALL (8) (which is of the order of 1 % per cm Hg) we obtain a good agreement with the mean experimental value.

As has already been pointed out (see Sect. 5), we have also tried to find correlations by dividing the troposphere into two layers: one between 300 and 850 mb and the other between 850 and the pressure at ground level, so as to obtain a comparison with the coefficients α'', β'' and γ'' found experimentally. (see δ_0, δ_4 and δ_5 in Table IV).

6. – Correction of the seasonal effect of the intensity of the mesons of the various coefficients.

In order to test the effectiveness of the various coefficients we have corrected the seasonal variation of the meson intensity registered by set « A ». The correction has been applied to the monthly mean values. Where the data were available, the mean values have been taken for the corresponding month of the two years. In Fig. 9 we have given a complete period which is partly repeated in order to give a better idea of the period.

(*) $Z = 2.87 \cdot 10^{-2}$ km/°C.

(+) In fact the mass of the upper layers are fixed and defined by the various isobars, and can only expand or vary their height.

(8) H. TREFALL: *Proc. Phys. Soc.*, A **68**, 953 (1955).

From the three experimentally found correction coefficients, the group α'', β'' and γ'' seems to be the most effective. A still more complete correction can be obtained using the theoretical coefficients.

On the whole all the corrections lead to the same results, namely to a diminution of the amplitude from 2% to 1% and a displacement of the maximum by three months. This seems to be in contradiction with the results of ELLIOT (3) who did not find any change in the amplitude after correction with both the pressure at sea level and the height of the 100 mb layer, and who also found a displacement of the maximum of nearly half a year. Furthermore it seems to be in contradiction with the results of the Cosmic Ray Group of Rome, who corrected almost completely the seasonal effect by means of various corrections (9). If we take into consideration that the three measurements have been made in years when the activity of the Sun was very different (ELLIOT, 1949: strong; BACHELET, 1954-55: very weak, and the Authors in 1955-56 when the activity was medium) one might think that there might be a connection between this and the meson intensity, and our results could be considered as a link between the two others.

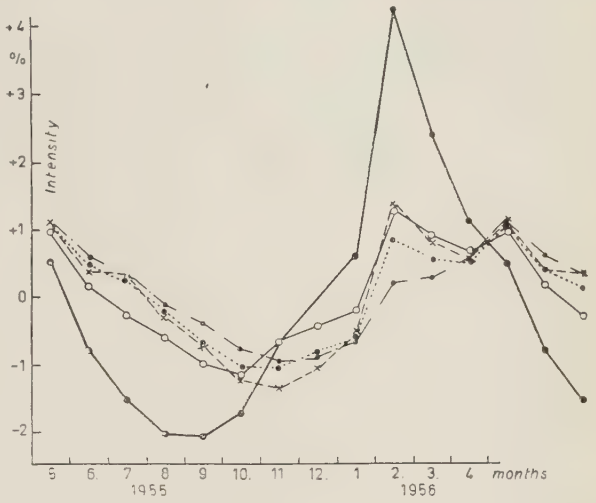

Fig. 9. - Seasonal variations of the total cosmic ray intensity as given by set « *A* ». ——— uncorrected data; – – – – corrected with α and γ; ——— corrected with α', β' γ' experimental; ····· corrected with α'', β'' and γ'' experimental; –·–·– corrected with the coefficients calculated theoretically.

A further confirmation comes from the fact that the marked peak in February 1956 could not be eliminated by any correction, as can be seen from Fig. 9. The peak may also be due to particles comming from the Sun which was very active at that time

It is remarkable that the intensity of set « *B* » which has a cut-off at 0.7 GeV does not show this peak, which agrees with the assumption that the additional particles coming from the Sun are only of low energy (10).

(9) F. BACHELET and A. M. CONFORTO: *Nuovo Cimento*, **4**, 1479 (1956).
(10) G. PUPPI: *Progress in Cosmic Rays*, p. 348 (1956).

7. – Mean daily variation.

All the data from set « A » have been corrected by means of the coefficients α and γ. We have calculated the mean daily variation. The results are given in Fig. 10. The curve shows a maximum at 13 h, local time and a minimum between 23 h and 24 h. The amplitude of the variation is $\pm 0.2\,\%$. Our results are not substantially different from those of other authors.

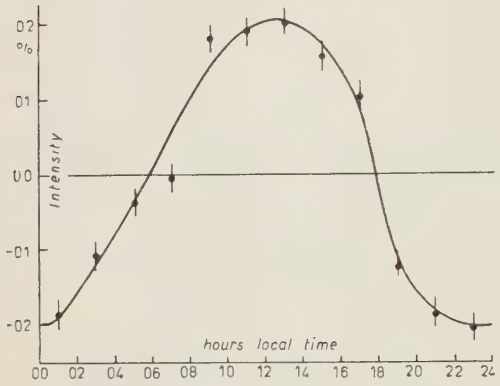

Fig. 10. – Mean diurnal variations computed from set « A » after correcting with α and λ.

As is known, one should expect a minimum in the Cosmic Ray intensity at 15 h owing to an upwards displacement of the layers of air due to solar heating, and this should be important in the phenomenon of decay. The contribution from the particles coming from the Sun enters into competition with a maximum between 9 h and 10 h local time. To this is perhaps due the fact that for that particular hour our curve shows a singular form.

Perhaps it cannot be excluded that there is an effect due to the competition between the decay provoked by the rise in the layers of the atmosphere on the one hand, and on the other the diminution of the vertical component of the Earth's magnetic field leading to a lowering in the cut-off in the primary (*). The problem is not fully resolved and further series of measurements will be necessary in order to confirm the supposed influence of the Sun on the Cosmic Radiation incident on the Earth.

8. – Conclusion.

From our analysis we can draw the following conclusions:

a) It seems that in order to correct the measurements of the intensity of Cosmic Radiation by means of the meteorological factors, it is sufficient to know the height of the isobars at 50, 100, 200, 300, 500, 700 and 850 mb, and

(*) As is well known, the upwards displacement of the Ionosphere in the Earth's magnetic field gives rise to induced currents which tend to diminish the field. In our hemisphere there is a minimum in the horizontal component of the field at about 11.00^{h} local time.

the pressure at sea level. In fact, even with insufficient data (i.e. without that relative to the 50 mb layer), we have obtained with our calculations a range spectrum which corresponds very well to that found experimentally if one applies a factor of 2.2. If one takes account of the fact that most of the mesons are produced at about 50 mb it would seem reasonable to suppose that if this is also included in the calculations, one can arrive at a spectrum which is in good agreement with that obtained experimentally.

b) In the registration of the total intensity with a low cut-off, it is necessary to take account of the solar acivity.

* * *

We are indebted to Professor G. Puppi for useful discussions and for having supervised the work.

Thanks are also due to Mr. Giorgio Salmaso who helped in carrying out the calculations.

RIASSUNTO

Si sono eseguite diverse correlazioni sulle misure di intensità di raggi cosmici, effettuate in Padova con tre diversi dispositivi. Si fa un'analisi dei dati atmosferici e si discute l'effetto stagionale presentato dai coefficienti di correlazione.

Search for the Electronic Decay of the Positive Pion (*).

H. L. Anderson (+)

Scuola di Perfezionamento in Fisica Nucleare dell'Università - Roma

C. M. G. Lattes (×)

Enrico Fermi Institute for Nuclear Studies
The University of Chicago - Chicago

(ricevuto il 24 Luglio 1957)

Summary. — A double focussing magnetic spectrometer of high transmission (1.8%) and good resolution (3.0%) was used in a search for the electronic decay of the positive pion. No evidence was found. The fraction of decays of the type $\pi \to e+\nu$ was found to be $f=(-0.4\pm9.0)\cdot10^{-6}$. The result appears to be statistically significant and thereby allows only a 1% probability that f could have a value greater than $2.1\cdot10^{-5}$. From a search for electrons of momentum 60.3 MeV/c we could conclude that the fraction of decays of the type $\pi \to e+\gamma+\nu$ was $f_\gamma=(-2.0\pm1.6)\cdot10^{-4}$ assuming tensor interaction determines the spectrum. Much lower limits for this last process have been recently reported by Cassels and by Lokanathan.

1. – Introduction.

The normal decay of the charged pion is into a muon and a light neutral particle, presumed to be a neutrino. An alternative possibility, the decay into an electron instead of the muon, has never been observed. This seems par-

(*) Experimental work carried out at The Enrico Fermi Institute for Nuclear Studies, The University of Chicago, under a joint program of the Office of Naval Research and the Atomic Energy Commission.

(+) Fulbright Lecturer and Guggenheim Fellow on leave from The University of Chicago.

(×) «On leave from Centro Brasileiro di Pesquisas Físicas» «and from Universidade do Brasil».

ticularly strange in view of the fact that the muon appears to have just those properties which would be expected of a more massive electron. Thus, the scattering of muons by nuclei is mostly an effect of the Coulomb field. What anomalies have been observed in the scattering seem to find their explanation in the inelastic processes which can be induced by the electromagnetic behavior of the muon (1). That this can hardly be different from that of an electron of muonic mass has been demonstrated in several ways. The energy levels of the μ-mesic atoms bear the correct relationship to those of an electron with augmented mass (2). In fact, the electric charge distribution of the heavy nuclei as determined from the μ-mesic X-ray measurements is just that which is found from the scattering of high energy electrons. Moreover, observations of the precession of polarized muons in a magnetic field have confirmed the fact that their gyromagnetic ratio is, to within 0.24%, not different from that of the electron (3). In addition, the production of μ-meson pairs by high energy γ-rays seems to proceed with the Bethe-Heitler cross-section calculated for a heavy electron (4).

While these evidences point to an identical electromagnetic behavoir of the muon and the electron and to the absence of other strong interactions, it is remarkable that also in the weak interaction which it exhibits with the neutrino field the behaviour of the muon is closely the same as that of the electron. Thus, GODFREY (5) was able to demonstrate the close identity of the coupling strength involved in the μ capture reaction

$$\mu^- + {}^{12}\mathrm{C} \rightarrow {}^{12}\mathrm{B} + \nu$$

and the β-decay process

$${}^{12}\mathrm{B} \rightarrow {}^{12}\mathrm{C} + \mathrm{e}^- + \nu$$

involving the same nuclear levels. This experiment, among many others, has served to reinforce the idea that a single « universal » Fermi interaction sufficed to explain not only μ capture, β-decay and μ-decay (6), but also pion decay as well.

(1) G. N. FOWLER: *Nuclear Physics*, **3**, 121 (1957).

(2) V. L. FITCH and J. RAINWATER: *Phys. Rev.*, **92**, 789 (1953).

(3) T. COFFIN, R. L. GARWIN, L. M. LEDERMAN, S. PENMAN and A. M. SACHS: *Phys. Rev.*, **106**, 1108 (1957).

(4) G. E. MASEK, A. J. LAZARUS and W. K. H. PANOFSKY: *Phys. Rev.*, **103**, 374 (1956).

(5) T. N. K. GODFREY: *Phys. Rev.*, **92**, 512 (1953).

(6) O. KLEIN: *Nature*, **161**, 897 (1948); G. PUPPI: *Nuovo Cimento*, **5**, 587 (1948); **6**, 194 (1949); T. D. LEE, M. ROSENBLUTH and C. N. YANG: *Phys. Rev.*, **75**, 905 (1949); J. TIOMNO and J. A. WHEELER: *Rev. Mod. Phys.*, **21**, 153 (1949).

The inclusion of the pion decay in this class of processes follows from its strong interaction with the nucleon field. The decay is supposed to proceed as a two step process, in the first of which the pion transforms into a nucleon-antinucleon pair, which then annihilate in a typical β-decay process according to the scheme

$$\pi^+ \to \mathrm{p} + \bar{\mathrm{n}} \to \mathrm{e}^+ + \nu \,. \tag{1}$$

Since the pion is pseudoscalar, this transition is forbidden except for the pseudoscalar and the axial vector β-couplings. This will be the case provided that the order in which the particles are written in the interaction term is the conventional one (pnev) ([7]). The smallness of the electronic decay of the pion appears, from this point of view, as evidence for the smallness of these couplings. Analyses of the data of β-decay have shown, in fact, that the dominant couplings are the scalar and tensor. In his review ([8]) MICHEL quotes values for vector and axial vector couplings zero or small, with no evidence to show that the pseudovector coupling strength is not zero also. These analyses are, however, open to re-examination in view of the recent discovery that parity is not always conserved in these processes ([9]).

Unfortunately, there is no satisfactory method for calculating the transition rate in accordance with the scheme (1). The calculations of STEINBERGER ([10]) and of RUDERMAN and FINKELSTEIN ([11]) involve divergent integrals and can give results differing by several orders of magnitude depending on the cut-off procedure used. Insofar as it can be supposed that the only difference between the muon and the electron is the mass, the calculation of the relative transition probability $f = \pi \to \mathrm{e} + \nu / \pi \to \mu + \nu$ may be made independent of the field theoretic uncertainties; only the masses of the particles enter. For pseudoscalar coupling of the fermions these authors obtain $f = 5.4$, a result which is roughly equal to the ratio of phase space available and certainly not in accord with the observations. The axial vector coupling, on the other hand, discriminates strongly against low mass particles giving $f = 12 \cdot 10^{-5}$. The experiments have been directed at finding the electron and determining the value of f.

In a previous attempt to find an electronic decay of the pion, FRIEDMAN and RAINWATER ([12]) examining pion endings in photographic emulsion could

([7]) G. MORPURGO: *Nuovo Cimento*, **5**, 1159 (1957).

([8]) L. MICHEL: *Rev. Mod. Phys.*, **29**, 223 (1957).

([9]) C. S. WU, E. AMBLER, R. W. HAYWARD, D. D. HOPPER and R. P. HUDSON: *Phys. Rev.*, **105**, 1413 (1957).

([10]) J. STEINBERGER: *Phys. Rev.*, **76**, 1180 (1949).

([11]) M. RUDERMAN and R. FINKELSTEIN: *Phys. Rev.*, **76**, 1458 (1949).

([12]) H. L. FRIEDMAN and J. RAINWATER: *Phys. Rev.*, **84**, 684 (1949).

report zero or one such decay in 1419 muonic decays. This was sufficient to rule out the pseudoscalar coupling but could not be decisive for the axial vector case. Subsequently, LOKANATHAN and STEINBERGER [13] using counters sensitive to the higher energy and shorter lifetime of the π-decay electrons to discriminate against those from μ-decay, obtained $f = (-3 \pm 9)\cdot 10^{-5}$. The axial vector coupling appeared unlikely in view of this result, but only to the extent of 1.7 standard deviations, not really enough to be decisive. Moreover, with the addition of a suitable amount of pseudoscalar to the axial vector coupling, an arbitrarily small value of f could be explained. However, as TREIMAN and WYLD [11] have shown, even if by chance this happened to be the case, there would still remain the difficulty of explaining why the radiative decay process $\pi \to e+\nu+\gamma$ should thus far have escaped detection [15].

The present experiment was undertaken to pursue even more exhaustively the search for the π-e decay. The chief experimental problem was to distinguish the electrons from π-decay from those of the μ-decay. Since the electrons from a two body decay of the pion would have a unique energy, well above the end point of the continuous μ-e spectrum, the magnetic spectrometer is the detector of choice. This frees the method from the fundamental limitation of the counter telescope of LOKANATHAN and STEINBERGER, which retains some sensitivity for the μ electrons at all usable absorber thicknesses through the detection of their bremsstrahlung. Our electronics were arranged to be particularly selective to those events which had a time dependence appropriate to the π-decay. This made it possible to include in our search for the π-e decay, a search for the π-e-γ process as well.

2. – Spectrometer.

We adapted for our use the magnetic spectrometer described by STOKER, HOK, HAAN and SIZOO [16] for the analysis of β-spectra. This is a shaped field, iron core, double focussing spectrometer of the SIEGBAHN-SVARTHOLM [17] type

---

[13] S. LOKANATHAN and J. STEINBERGER: *Suppl. Nuovo Cimento*, **1**, 151 (1955).

[14] S. B. TREIMAN and H. W. WYLD, jr.: *Phys. Rev.*, **101**, 1552 (1956).

[15] The result of FRIEDMAN and RAINWATER [12] applies equally to the radiative decay of the pion. During the writing of this paper, two new results on the process $\pi \to e+\nu+\gamma$ have been announced. CASSELS, at the 1957 Rochester Conference, reported an experiment giving $f_\gamma = (3 \pm 7)\cdot 10^{-6}$ (assuming tensor interaction and the e^+, γ correlations predicted thereby). LOKANATHAN, in a preprint to appear in *Phys. Rev.* reported $f_\gamma = (-27 \pm 45)\cdot 10^{-6}$ under the same assumptions.

[16] P. H. STOKER, ONG PING HOK, E. F. HAAN and G. J. SIZOO: *Physica*, **20**, 337 (1954).

[17] A. HEDGRAN, K. SIEGBAHN and N. SVARTHOLM: *Proc. Phys. Soc.*, A **63**, 960 (1950).

characterized by high transmission and good resolution. In this instrument the electrons are focussed in the central part, normally kept evacuated. The coils are external to the central region, and the iron magnetic return circuit is external to the coils. To preserve the high transmission of the design of STOKER *et al.* ([16]), we retained their pole shape but extended the range by

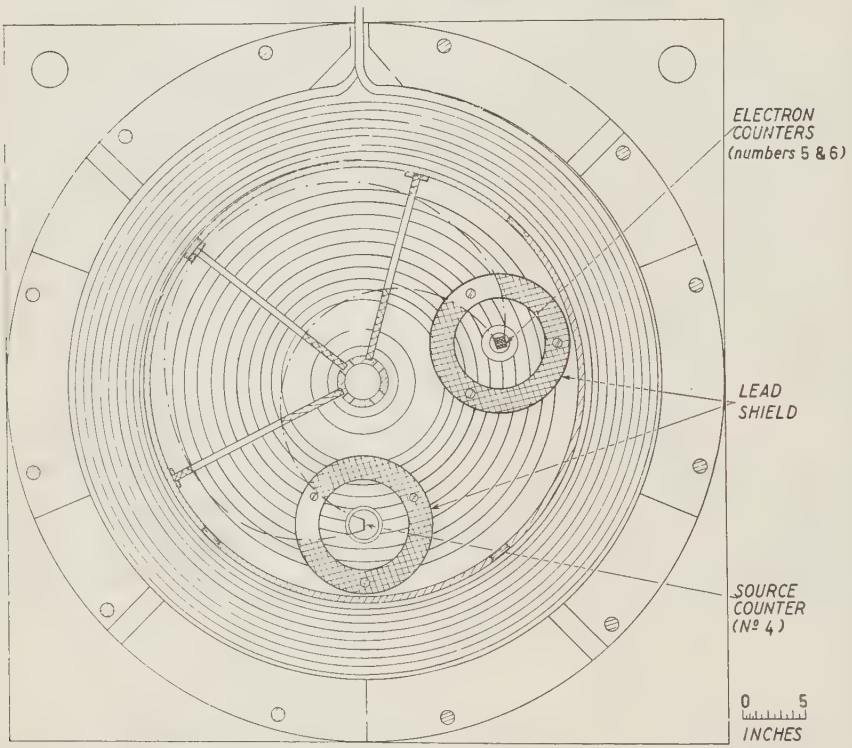

Fig. 1. – Sectional view of the spectrometer. Pions enter through the brass collimator, traverse counters no. 2 and no. 3, are slowed by the polyethylene moderator and come to rest in counter no. 4. Electrons emerging from counter no. 4 are brought to focus and detected by means of a triple coincidence of 4, 5 and 6.

increasing very much the amount of copper and current in the coils, as well as the amount of iron in the magnetic return circuit. In this way we were able to reach a momentum of 100 MeV/c without encountering serious saturation effects. Since we were dealing with high energy electrons, we required baffles and shields several radiations length in thickness.

A sectional view of the spectrometer is given in Fig. 1. A plan view, showing the shielding and baffling and indicating the extreme usable orbits is given in Fig. 2. The central poles were machined from two Armco iron disks 1.52 m in diameter. This included a central portion to accomodate the brass cylinder which determined the spacing of the poles, a shaped field region which

followed a template cut to the prescriptions of STOKER *et al.* [16], a place for the stainless steel cylinder which, with its rubber gasket, formed the external vacuum envelope, then a recess for the coils and, finally, a flat section for the magnetic return circuit and bolting holes. Additional iron in the form of

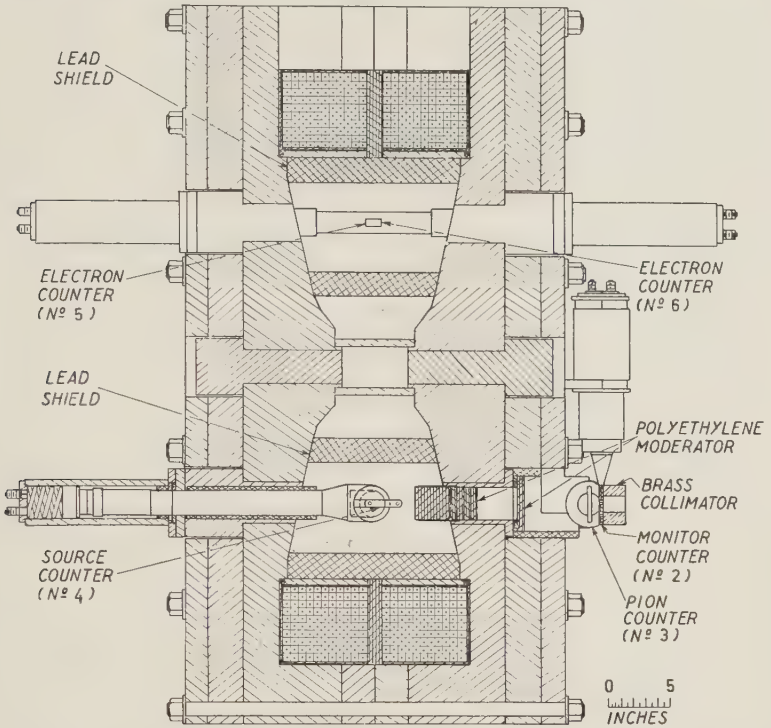

Fig. 2. – Sectional plan view of the spectrometer showing the extreme electron trajectories.

low carbon steel plates were added to reduce saturation in the iron and to keep low the stray fields external to the instrument. Total iron amounted to about 9 metric tons.

The coils were made up from double pancake spirals following the scheme used for the Chicago synchrocyclotron [18]. Here, a total of 120 turns of 1.22 cm square copper tubing with a 0.63 cm diameter hole for water cooling were employed in each of the two coils. With 1300 amperes we could obtain, without excessive overheating, a field of 11.7 kG at the central orbit (30.5 cm radius) capable of focussing electrons of momentum 109.5 MeV/c.

Holes were provided through the poles at the source and detector positions. Referring to Fig. 1, the lower right hand hole was used for the entrance

[18] H. L. ANDERSON, J. MARSHALL, L. KORNBLITH, L. SCHWARCZ and R. H. MILLER: *Rev. Sci. Instr.*, **23**, 707 (1952).

of the pion beam into the instrument. This had to pass through a monitor counter (no. 2), the pion counter (no. 3), an external polyethylene moderator, a thin aluminium window which served for vacuum seal, an internal polyethylene moderator with thickness adjusted so that in the end most of the pions came to rest in the source counter (no. 4), some-times called the target. The target was a strip of plastic scintillator 2.54 cm wide, 1.9 cm thick and 7.2 cm long. Held at an angle of 45° to the axis of the pion beam its axial extension in the spectrometer was only 5.08 cm. This scintillator was viewed with the help of a lucite light pipe extending through the lower left hand hole by means of an RCA 14 stage photomultiplier, which was thereby removed from the presence of strong magnetic fields. Further magnetic shielding of the photomultiplier was afforded by means of a double mu-metal shield inside a 6 mm thick iron container. The end of the light-pipe on which the source counter was supported was made hollow, the better to define the volume in which the pions came to rest and from which electrons could emerge and enter proper spectrometer orbits.

The detector consisted of two plastic scintillators, each 25 mm wide and 50 mm long, e.g. of the same radial and axial extension as the source, set inside a single lucite light-pipe which extended across the spectrometer through the upper holes. Aluminum reflectors were fitted so that the light from the first scintillator was recorded in counter no. 5 while that from the second in no. 6. Since the scintillators were rather thick, 19 mm, particles with range smaller than this would not be recorded as a coincidence in these two counters. The possible background from low energy electrons, pions, and protons was greatly reduced thereby.

The isolation of the detector from the direct radiation from the source, required in this experiment, was provided by 5 cm thick lead shields surrounding both the source and the detector. In addition to the openings in the lead shields, three baffles were provided to define the location of the extreme usable orbits. These were made of 13 mm thick lead and served to limit the entrance of unwanted particles into the detector. Lead was chosen because the need to keep low the background due to the entrance of unwanted electrons to the detector outweighted the need to keep low the effects of scattering. Since we were interested in finding an electron with energy higher than any of those normally present we were not greatly troubled by the energy loss which can occur in scattering, the principal effect of this being to allow a high energy electron to be mistaken for one having lower energy. More important the multiple Coulomb scattering, particularly that which takes place at the openings in front of the source and detector. The principal effect of this was to broaden somewhat the effective size of the source and detector. This made difficult a precise analysis of the μ-e spectrum, but did not diminish the detectability of the π-electrons.

3. – Calibration.

The range of the spectrometer was great enough to permit its use with many α-particle emitters. We used the α-particles of ^{239}Pu to determine the transmission, resolution, and absolute energy calibration of the instrument. These α-particles have an energy of 5.15 MeV, corresponding to a magnetic rigidity, expressed in terms of the momentum of a singly charged particle, of 97.96 MeV/c. A source of the α-particles having negligible thickness but ample intensity was kindly prepared for us by Mr. Ray Barnes and Mr. Paul Fields of the Argonne National Laboratory. This was distributed rather uniformly on an aluminium backing over an area 2.54 cm wide by 7.2 cm long. When located at the median plane of the source of our experiment, it corresponded quite closely to the electron source it was supposed to simulate. Moreover, we found by the use of a 6 mm diameter α source of this type, that the response of the spectrometer was rather independent of the radial and axial positioning, provided this remained within the 25 mm by 50 mm area defined by the detector. Outside this area the response fell rapidly. Thus, we suppose that the response of the spectrometer found with these α-particles would correspond quite closely to that which would obtain for the electrons, once due allowance was made for the loss of energy of the electrons in emerging from the interior of the source.

Our plastic scintillation detector was not sensitive to these α-particles, so we replaced it with a thallium activated cesium iodide crystal, obtained from the Harshaw Chemical Co., having the same surface dimensions but of thickness 3 mm. With this it was easy to observe the α-particles focussed by the spectrometer. From the counting rate observed as a function of magnet current we obtained the response curve given in Fig. 3. In this curve the response is plotted, with its maximum normalized to unity, as a function of $(p - p_0)/p_0$, the relative deviation of the particle momentum p from that of the momentum setting p_0 of the spectrometer. In plotting this curve the small deviations from linearity in the relation between magnet current and magnetic field were taken into account. The resolution full width at half maximum is seen to be 3.0%, a value not very different from that which is due to the radial extension of the source and the detector. Although the resolution curve is not as symmetrical as it should be, the cut-off is rather sharp for momenta lower than that for which the spectrometer is set. This helps discriminate against the μ electrons when the instrument is set above the end-point of this spectrum. The rather appreciable resolution width of our spectrometer was needed to accomodate to the spread in energy brought about because the electrons came from various depths in the source. This point will be discussed in more detail below.

The maximum response occurred at a current of 1138 amperes, thereby

establishing one point of the momentum calibration. We obtained the remainder by measuring the magnetic field at the central orbit as a function of

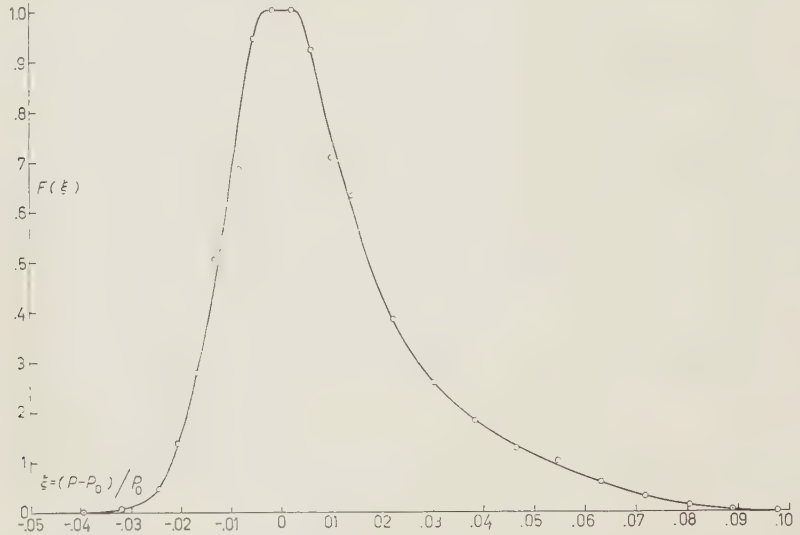

Fig. 3. - Momentum response of the spectrometer as obtained by observing α-particles of ^{239}Pu (97.96 MeV/c).

current by means of a rotating coil type fluxmeter made by the Rawson Instrument Co. Thus, the calibration of the spectrometer relied only on the linearity of the fluxmeter response but not on the absolute calibration supplied by the manufacturer. A check of the calibration was provided by the observation of the end point of the μ-e spectrum which is at 52.85 MeV/c. Because of this we could be confident that our setting of the spectrometer could be set on the π-e peak to within ½%. The full calibration curve is given in Fig. 4. The departure from linearity is less than 1% to 900 amperes (79 MeV/c), at 1140 amperes (98 MeV/c) it is only 3%. These evidences indicate

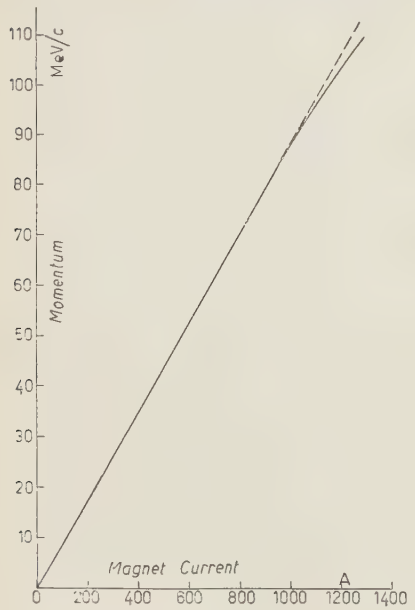

Fig. 4. – Calibration curve of the spectrometer. The dotted line is the linear extension of the lower part to show the effect of saturation.

that saturation effects can have only a minor influence on the present experiment.

The transmission of the spectrometer was obtained from the maximum counting rate, 12 500 counts per minute, and the knowledge of the number, $70 \cdot 10^4$ disintegrations per minute, of the α-particle source. The latter number was obtained by counting the α-particle tracks in emulsion exposed for a known time directly above the source. From these numbers we deduced that the transmission of our spectrometer was about 1.8%, a value somewhat poorer than the figure 2.8% given by STOKER *et al.* [16]. This loss in intensity of 35% was more than compensated for by the four times larger source area which we used.

4. – Arrangement.

The positive pions for this experiment were obtained from the Chicago synchrocyclotron. The most convenient beam seemed to be the one at 75 MeV. This was first focussed by a pair of quadrupole magnets of 10 cm aperture, then passed through a suitably oriented hole in the 3.7 m steel shield and then deflected through 90° by means of a wedge magnet arranged to give an approximate vertical and horizontal focussing of the beam at the source position of the spectrometer. The intensity of positive pions from the cyclotron is a maximum near 75 MeV yet this energy is low enough to allow the pions to be brought to rest within a suitably small volume without excessive losses due to the effects of multiple scattering and nuclear collisions. The normal intensity of the beam obtained in this way, after passing through a brass collimator which limited its cross-section to 38 mm × 64 mm, was $1.2 \cdot 10^6$ per minute.

The manner of introducing the pions into the spectrometer may be seen in Fig. 1. The idea was to have the pions come to rest and decay inside a block of scintillation plastic at the source position of the spectrometer. By viewing this with a photomultiplier (counter no. 4) we could observe the pions entering the source as well as the electrons leaving. The spectrometer accepted electrons from the source emerging at an angle of 90° with respect to the direction of the entering pions, the emergence of the electrons being from the same face as the entrance of the pions. Electrons of the proper momentum were brought to focus at the detector so that a triple coincidence T_{456} served to identify electrons originating at the source and reaching the detector. The electrons from μ-decay were readily detected in this way and served for the adjustment of the counters and as a means of standardizing the measurements.

The observations were monitored with the doubles coincidence count D_{24} which measures pions traversing no. 2 and reaching the source (counter no. 4).

To avoid an excessive counting rate the sensitive area of no. 2 was reduced by using two 6.3 mm diameter disks of 6 mm thick scintillator plastic near the center of the beam, these being imbedded in insensitive lucite. With this composite counter all the pions passed through the same thickness of material, but the counting rate was reduced by a factor of 12 to $1.2 \cdot 10^1$ per minute under normal conditions.

5. – Adjustment.

To bring the pions to rest in the target we used as moderator, polyethylene plastic disks, the optimum thickness of which was determined from a range curve. This was obtained from a measurement of the ratio of the double coincidences D_{34}/D_{23} as a function of polyethylene thickness. Counter no. 3 was a full area counter, able to count all the pions in the beam, so that the ratio D_{34}/S_3 gave directly the fraction of pions in the beam which entered the target and is the quantity plotted in Fig. 5. The arrow points to the thickness of polyethylene (12.8 g/cm²) used throughout the experiment. From the curve we estimated that the number of pions stopping in the target was 10^5 per minute.

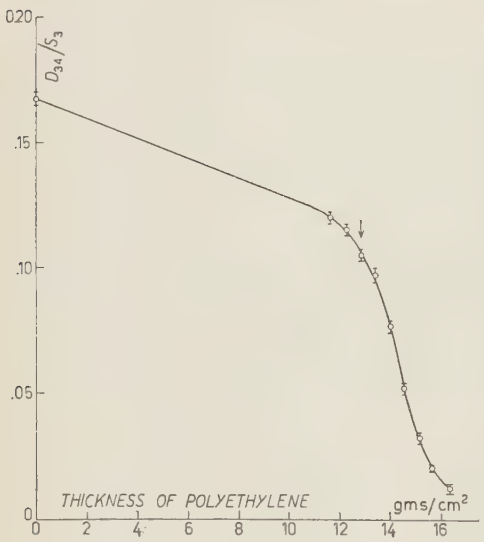

Fig. 5. – Range curve of the pions in polyethylene. The arrow points to the thickness of polyethylene used in the experiment to bring the pions to rest in the target.

We also observed directly the π-μ endings in emulsion exposed at various depths inside a simulated scintillator block. A dummy target was made up of 3.2 mm layers of scintillator plastic so that 200 μm emulsion could be sandwiched within at various depths. Several exposures were made, exposing in each case no more than two emulsion layers at one time so as to disturb as little as possible the density distribution of the material in the dummy target. The result is given in Fig. 6. From the integral under the curve we obtained the figure 70% as the fraction of pions entering the target which come to rest within. This was in agreement with what was estimated with somewhat less confidence from the range curve.

These results enabled us to account for the counting rates observed for

the electrons from μ-decay. Under normal operating conditions we had 10^5 pions per minute coming to rest within the target. Virtually all of these decayed into muons. Since the range of the muons is only 1.4 mm in scintillator plastic, most of these, about 95%, came to rest and decayed within the target. Of the electrons which were emitted in this process 1.8% were within the acceptance angle of the spectrometer. From the shape of the spectrum, Fig. 7, and the resolution curve, Fig. 3, we were able to deduce the momentum fraction of the electrons accepted by the spectrometer as being 4.7% at the 450 ampere setting (39.9 MeV/c). Thus, we could expect a counting rate for T_{456} of 82 per minute. We can understand the observed rate of 65 per minute if we suppose that the counters were each about 92% efficient, as seems reasonable.

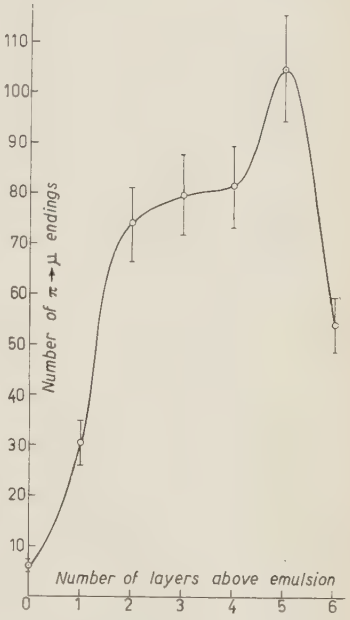

Fig. 6. – Distribution of $\pi \to \mu$ endings in the target. Plotted as ordinate is the number of endings in 1 cm² of 200 μm emulsion per 25000 counts of D_{23}, for various numbers n of 3.18 mm thick layers of scintillator placed above and at an angle of 45° to the pion beam.

6. – μ-electron spectrum.

Following T_{45}, over the range of the spectrometer gave the spectrum of the μ-electrons. The data given in Fig. 7 were obtained with counter 3 in anticoincidence with 4, 5, 6 in order to reduce the accidental coincidences between singles in 4 and doubles in 5, 6. Since this would reduce the sensitivity to π-electrons the anticoincidence was removed for the points above 56 MeV/c. The general features of the μ-electron spectrum are easily recognized, the intensity falling rather abruptly by a factor of about 400 in the vicinity of the expected end point. Scattering may account for some of the counts observed above 60 MeV/c, but the larger part must have been due to accidentals. We write,

$$A_{4,56} = 2TDS_4D_{55} \,. \tag{2}$$

With the pulse width $T = 10^{-8}$ s, a duty factor of the cyclotron $D = 150$, a singles rates in 4 $S_4 = 3 \cdot 10^5$ per minute and a doubles rate in 5, 6 due to fast neutrons from the cyclotron $D_{56} = 10$ per minute, we find for the accidentals rate $A_{4,56} = 0.15$ counts per minute, rather close to that observed.

The curve given in Fig. 7 is not useful for a precision determination of the

shape of the μ-electron spectrum, mainly because of the scattering which the electrons may suffer, particularly from the lead at the openings near the source as well as near the detector. The effect depends on the energy of the electrons and is difficult to estimate in a precise way. The dominant effect, multiple Coulomb scattering from the walls of the openings, increases the apparent width of the source and detector, making the resolution somewhat wider than that observed with α-particles. The shape of the upper end of the spectrum depends on this as well as on the loss of energy which the electrons undergo in emerging from the source.

Fig. 7. Electron spectrum obtained by observing the triples T_{456} per 10^5 D_{24}. To reduce accidental coincidences in the μ electron spectrum, anti-coincidence in no. 3 was added for the counts below 55 MeV/c.

7. – Energ loss of electrons.

We were able to measure directly this energy loss by observing the height of the pulse in no. 4 which produced the triple coincidence T_{456}. For this, we photographed the traces appearing on the screen of a Tectronix 517 fast scope with equipment kindly lent to us by Dr. Leona Marshall and Mr. Joseph Fischer of our laboratory. Observing, in this way, the pulse height distribution of the electrons recorded by the spectrometer at each of some 9 settings between 44 and 52 MeV/c, it became possible to obtain the spectrum near the end point corrected for the energy loss in the source. The loss due to bremsstrahlung is missed but this amounts to less than 0.2 MeV on the average and may be neglected for the purpose here.

Comparing this curve with that obtained by folding in our resolution function, Fig. 3, with the theoretical μ-electron spectrum having $\varrho_{\text{Michel}} = 0.65$, we obtained a good agreement once some allowance for the effects of scattering were made. The position of the end point is rather independent of the uncertainties here and was found to be within $\frac{1}{2}\,\%$ of the accepted value. We

could, therefore, set with some confidence the current in the spectrometer at which we could expect to observe the π-electrons.

We used the energy loss data to obtain the expected π-electron energy distribution from our source. This is plotted in Fig. 8. The fact that electrons losing less than 0.6 MeV would not be recorded by our coincidence circuits was automatically taken into account in this curve. The dotted curve in the same figure is a replot of the momentum response of the spectrometer obtained from Fig. 3 but corresponding to a setting at 760 amperes. The overlap of the two curves shows that 55% of the π-electrons would be recorded at this current setting. At 750 amperes the overlap was 52%. Both numbers would be somewhat higher if the resolution broadening due to scattering were taken into account.

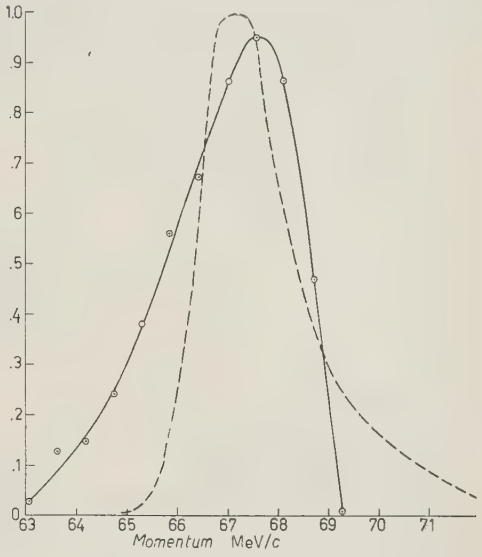

Fig. 8*a*. – Momentum distribution expected for the π electrons due to energy loss in the source (full curve). The points were obtained from the pulse height distribution in no. 4 due to μ-electrons observed at 450 amperes. For μ-electrons, the initial energy was taken to be 69.8 MeV. The dotted curve is the momentum response of the spectrometer for a current setting of 760 amperes.

Because of their broader distribution in momentum the spectrometer measures 1/12 as many of the μ-electrons at 450 amperes as it does of π-electrons at 760 amperes. A simple subtraction, performed using the highest four points of the data shown in Fig. 7 gives a preliminary value of $f=(4\pm4)\cdot10^{-5}$, a result not much better and hardly more useful than that of LOKANATHAN and STEINBERGER [13].

8. – Delayed coincidence measurements.

A considerable reduction in the accidental rate was obtained in the observations made with counter 3 in delayed coincidence with the simultaneous triples count in 4, 5, 6. The pulses from all counters were shaped by means of clipping lines at the anodes of the photomultiplier tubes to have a width fairly close to 10 mμs. We were able to verify, by means of delay curves, that the channel width for observing T_{45} was indeed twice this amount. A typical delay curve obtained by delaying the pulses from no. 4 with respect

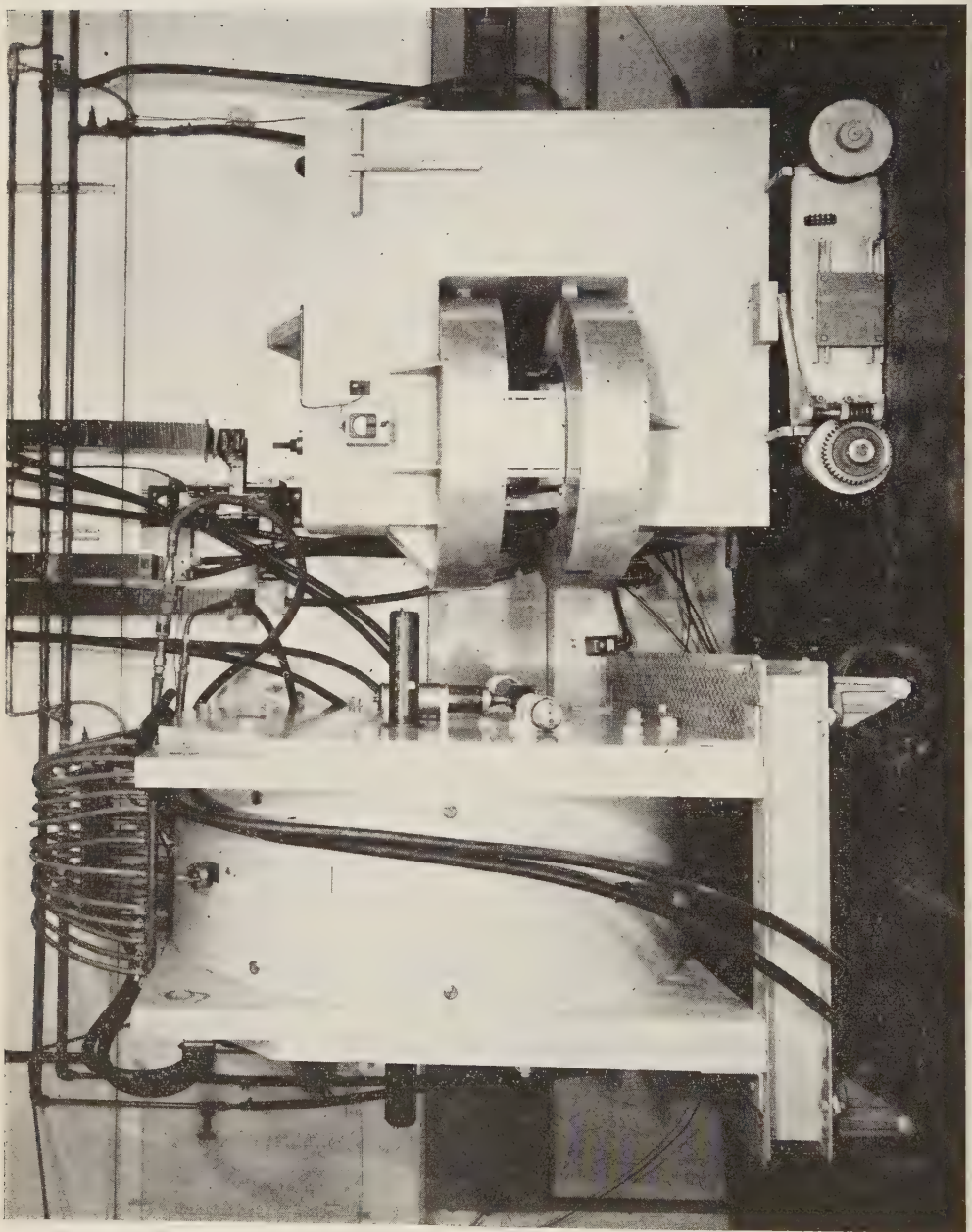

to those from 5, 6 is given in Fig. 9. All the timing of the pulses was set from delay curves of this type. In particular, the delay in no. 3 was set by observing the coincidences due to pions traversing no. 3 and no. 4, then delaying the pulse in no. 3 until D_{34} fell to the accidentals rate. Typically, this delay amounted to 20 mμs, although it was varied somewhat from this value in accordance with changes in the delay curves observed from time to time, particularly when changes in the photomultipliers and the voltages at which they were operated were made.

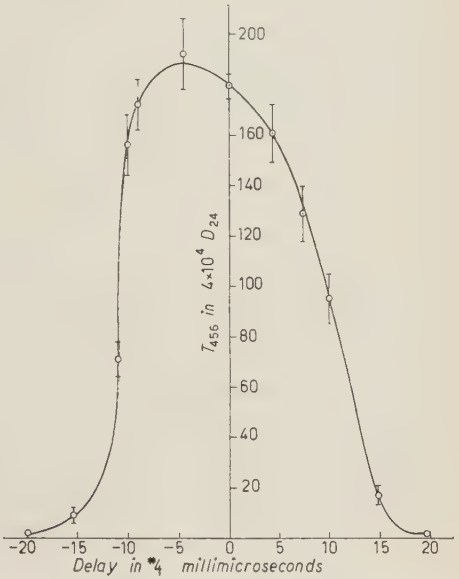

Fig. 9. – Delay curve obtained by delaying counter no. 4 with respect to 5, 6 in channel C.

The fraction of π-e events which would be recorded in a channel whose time response as a function of the delay t is $A(t)$, wa given by,

$$(3) \qquad a_1 = \int_{-\infty}^{\infty} A(t) \exp\left[-\left(\frac{t+t_0}{\tau}\right)\right] \mathrm{d}t \,.$$

Here, where the quantity $A(t)$ is obtained from the delay curves and normalized such that $\int_{-\infty}^{\infty} A(t)\,\mathrm{d}t = 1$, t_0 is the delay added to the pion pulse (in counter no. 3) and τ is the lifetime of the pion decay, taken to be 25.5 mμs ([19]). For $t_0 = 0$, a_1 turned out, variously, to be between 1.03 and 1.12. In a particular case (Run III) we used $t_0 = 20$ mμs and had $a_1 = 0.455$. To catch an additional fraction we added 27.9 mμs in a second channel for which we then had $a_1 = 0.164$. A further 28 mμs delay was added to the pion pulse arriving in a third channel so that a further fraction amounting to 0.055 would be recorded there. The total fraction of π-e events which would be recorded in all three channels was, thus, 0.774. With this arrangement, a comparison of the counting rates in the three channels gives some possibility for distinguishing the π-decay electrons from other processes having a different time relationship.

The arrangement used is indicated in Fig. 10. Five quadruple coincidence circuits were constructed, as nearly alike as possible. Circuit A was used to record the monitor count D_{21}, circuit B for the triples count T_{456}, while circuits C, D, F were used for the delayed coincidence quadruples Q_{3456}. In

([19]) W. L. Kraushaar: *Phys. Rev.*, **86**, 513 (1952).

various runs we interchanged the order of C, D and F, so as to reduce somewhat the effect of differences in the response of these. The circuits were similar to some used previously in this laboratory ([20]) as modified by DAVIDON and FRANK ([21]). A preferable procedure would have been to form separately D_{34} and T_{456} and then taking the delayed coincidence of these two; except for the difficulty of forming a fast enough triggered output from the first set of coincidence circuits.

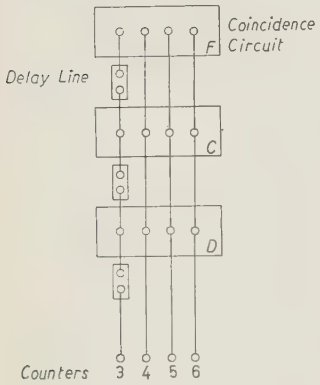

Fig. 10. – Block diagram of the quadruple coincidence circuits showing the manner of delaying the pulse from no. 3.

With our arrangement the accidentals rate due to singles S_3 and triplets T_{456} is given by,

$$A_{3,456} = (T' + T'')DS_3T_{456}\,. \tag{4}$$

At 450 amperes T_{456} is due to μ-electrons and was 65 per minute under normal conditions ($D_{24} = 13 \cdot 10^3$ per minute). Taking the duty factor $D = 150$, $S_3 = 12 \cdot 10^5$ per minute, and the sum of the pulse widths T' from no. 3 and T'' from the smallest of either 4, 5 or 6, to be 20 mμs, we see that we could expect $A_{3,456}$ about 4 counts per minute. The true quadruples counts due to the π-μ-e decay can only be about 0.6 counts per minute (less, in the first

TABLE I. – *Total counts obtained in th*

Run		I	I	II	II	II	II	II
Amperes		450	750	450	760	450	650	700
MeV/c		39.9	66.4	39.9	67.3	39.9	57.6	62.0
Configuration		*FDC*	*FDC*	*FDC*	*FDC*	*CFD*	*CFD*	*CFD*
Minutes		279.6	2512.8	21.7	363.6	31.4	74.5	311.7
A	D_{24}	$2.5 \cdot 10^6$	$23.6 \cdot 10^6$	$0.3 \cdot 10^6$	$5 \cdot 10^6$	$0.4 \cdot 10^6$	$1 \cdot 10^6$	$4 \cdot 10^6$
B	T_{456}	11953	358	1644	57 (*a*)	1644 (*b*)	21 (*c*)	32 (*d*)
C	Q_{3456}	1044	21	68	1	164	1	0
D	Q_{3456}	1078	35	75	2	88	1	1
F	Q_{3456}	1600	34	231	11	192	0	7

(*a*) For $3.5 \cdot 10^6$ D_{24}
(*b*) For $0.3 \cdot 10^6$ D_{24}
(*c*) For $0.5 \cdot 10^6$ D_{24}
(*d*) For $2.5 \cdot 10^6$ D_{24}
(*e*) For $0.5 \cdot 10^6$ D_{24}
(*f*) For $4.0 \cdot 10^6$ D_{24}

([20]) M. GLICKSMAN, H. L. ANDERSON and R. L. MARTIN: *Proc. National Electronics Conference*, **9**, 483 (1953).

([21]) W. C. DAVIDON and R. B. FRANK: *Rev. Sci. Instr.*, **27**, 15 (1956).

channel) due to the narrow width of the channels, here 1/100 of the lifetime of the μ-decay. Thus, the observed quadruples rate at 450 amperes is primarily due to accidentals and can be taken as an experimental measure of the coefficient by which T_{456} should be multiplied to give the number of accidentals expected at some other setting of the spectrometer. The accidental quadruples rate is seen to be about 1/16 of the triples rate. Since, as we have seen, most of the triples counts above 60 MeV/c are themselves accidentals we could expect a somewhat smaller ratio. We found, in fact, counting rates of the order of 1 in 100 minutes so that it was necessary to count for many hours to take advantage of the improved sensitivity of our arrangement.

9. – Search for π-electrons.

We looked for the electrons from pion decay by setting the spectrometer at 760 amperes (67.3 MeV/c) and also at 750 amperes (66.4 MeV/c). These measurements were always interlaced with measurements of the μ-electrons at 450 amperes (39.9 MeV/c) and sometimes with measurements at 830 amperes (73.3 MeV/c), above the π-electron position, at and 650 amperes (57.6 MeV/c), below the π-electron position, above the end point of the μ-electron spectrum, but where might be found electrons from the process $\pi \to e+\nu+\gamma$. The results are summarized in Tables I and II.

ctrons from the decay of the pion.

	II	II	II	II	III	III	III	III
0	450	650	760	830	450	650	760	830
.3	39.9	57.6	67.3	73.3	39.9	57.6	67.3	73.3
F	*DCF*	*DCF*	*DCF*	*DCF*	*DCF*	*DCF*	*DCF*	*DCF*
.6	46.5	155.3	358.6	285.7	57.4	741.5	616.8	621.0
0^6	$0.6\cdot10^6$	$2\cdot10^6$	$4.5\cdot10^6$	$3.6\cdot10^6$	$0.7\cdot10^6$	$8\cdot10^6$	$7\cdot10^6$	$7\cdot10^6$
(*f*)	3161	92	87	76	3748	404	182	132
	172	4	2	4	252	13	16	4
	208	2	3	4	275	11	6	8
	186	4	2	1	277	6	5	8

In the first run we concentrated the search at a single current 750 amperes, hoping to reveal the presence of the π-electrons by the decreasing counting rates observed in the channels arranged in the order *FDC* of in-

TABLE II. –

Run	I–*FDC*	I–*FDC*	II–*FDC*	II–*FDC*	II–*CFD*	II–*CFD*	II–*CFD*	II
Amperes	450	750	450	760	450	650	700	
Minutes	111.8	106.7	72.3	72.3	78.5	74.5	77.9	
B T_{456}	4781	15.2 ±0.8	5480	16.3±2.2	5480	42±9	12.8±2.3	2
C Q_{3456}	417±13	0.89±0.20	227±27	0.2±0.2	410±32	1±1	0 ±0.25	
D Q_{3456}	341±13	1.49±0.25	250±29	0.4±0.3	220±23	1±1	0.3±0.3	
F Q_{3456}	640±16	1.44±0.25	770±51	2.2±0.7	480±35	0±1	1.8±0.7	

creasing delays. When nothing significant was found we carried out further runs changing the order of delays in the channels and changing the current setting of the spectrometer. There was no evidence whatever for a positive effect. The problem which remained was to give a measure of the uncertainty to be associated with our lack of success.

10. – Data reduction.

The reduction of the data was carried out by the method of least squares. We illustrate the procedure by taking the case of Run III. In this, besides the measurement at 450 amperes, used to standardize the run, we made measurements at each of three currents; below, at and above the π-electron position. In each case the delayed quadruple count was observed in each of three non overlapping delayed channels, giving a total of nine measurements to be accounted for. We considered that each count $\underline{m}$ observed with statistical error n arose from two contributions. One part due to the electrons which might be expected at the given setting of the spectrometer, and a second due to accidentals. The equations are of the form,

$$ax + cz = m \pm n\,, \tag{5}$$

where x is the number of π-electrons which would enter the acceptance angle of the spectrometer under conditions in which 5000 μ-electrons would be recorded as the triples T_{456}, with the current at 450 amperes. This is multiplied by a product of factors $a = a_1 a_2 a_3$; such that a_1 is the time acceptance of the channel as given by (3); a_2 is the sensitivity of the channel, being its triples count $T_{456}/10^6 D_{24}$ measured at 450 amperes, divided by 5000; a_3 is the

ed per 10^6 D_{21}.

D	II-*DCF*	II-*DCF*	II-*DCF*	II-*DCF*	III-*DCF*	III-*DCF*	III-*DCF*	III-*DCF*
50	450	650	760	830	450	650	760	830
1	77.5	77.7	79.7	81.6	82.0	92.7	88.1	88.7
2.1	5268	46±5	19.3 ±2.1	21.1 ±2.5	5354	50.5 ±2.5	26.0 ±1.9	18.9±1.6 0
0.4	287±22	2±1	0.45±0.31	1.11±0.57	360±23	1.62±0.45	2.28±0.57	0.57±0.29
0.5	347±24	1±0.7	0.67±0.38	1.11±0.57	393±24	1.37±0.42	0.86±0.35	1.14±0.40
0.5	310±23	2±1	0.45±0.31	0.28±0.28	396±24	1.87±0.50	0.71±0.32	1.14±0.40

momentum acceptance of the spectrometer given by

$$a_3 = \int_0^\infty Q(p) F\left(\frac{p - p_0}{p_0}\right) \mathrm{d}p \,, \tag{6}$$

previously referred to as the overlap. $Q(p)$ is the distribution in momentum of the electrons emitted from the source, normalized so that $\int_0^\infty Q(p)\,\mathrm{d}p = 1$.

$F((p - p_0)/p_0)$ is the momentum response of the spectrometer plotted in Fig. 3. For the π-electrons as we could expect to find them at 760 amperes, these functions are plotted together in Fig. 8 and give $a_3 = 0.55$, as has already been mentioned. At 650 amperes there is some uncertainty about the distribution function, so we rewrite the first terms as $b\ y$ with $b = a_1 a_2$ and $y = a_3 x$. At 830 amperes $a_3 = 0$ so the first term in (5) does not appear at all.

The accidentals are estimated in the factor c from the accidentals observed at 450 amperes. Subtracting a small correction Q_T of true quadruples expected from the π-μ-e decay from the observed quadruples $Q_{3456}(450)$ observed at 450 amperes, we multiply by the ratio triples count at current setting S to that at 450 amperes, thus,

$$c = [Q_{3456}(450) - Q_T][T_{456}(S)]/T_{456}(450) \,. \tag{7}$$

By itself, c does not give a correct estimate of the accidentals rate for currents S above the μ-electron end point. This is because the triples count obtained there arises, at least in part, from the accidental coincidences between the counts in no. 4 and those in 56, in accordance with estimates given above. Such accidental triples are somewhat less effective in producing an accidental quadruple than are true triples.

For this reason we multiply c by a proportionality factor z whose value may then be adjusted to give a best fit to the data by the least squares criterion. Here we have supposed that the same factor z serves for all the circuits

at all the currents used in a given run, and that any differences in response to accidentals will have been already included in the factor c.

For Run III, with configuration $DC'F$ we obtained the following nine equations:

					check
650 A	circuit C			$0.172y + 2.56z = 1.62 \pm 0.45$	(1.59)
	D			$0.455y + 2.84z = 1.37 \pm 0.42$	(1.37)
	F			$0.057y + 2.86z = 1.87 \pm 0.50$	(1.98)
760 A	C	$0.090x$		$+ 1.39z = 2.28 \pm 0.57$	(0.96)
	D	$0.250x$		$+ 1.54z = 0.86 \pm 0.35$	(0.98)
	F	$0.031x$		$+ 1.55z = 0.71 \pm 0.32$	(1.11)
830 A	C			$1.00z = 0.57 \pm 0.29$	(0.72)
	D			$1.11z = 1.14 \pm 0.40$	(0.80)
	F			$1.12z = 1.14 \pm 0.40$	(0.81)

The solution of this set of equations by the method of least squares gave the following results:

$$x = -0.53 \pm 1.6$$
$$y = -1.51 \pm 1.2$$
$$z = 0.72 \pm 0.11$$

Reinserting these values in the left hand side of the above equations gave the values shown in the parentheses. These serve to check the goodness of the fit and the statistical significance of the data.

For Run I with configuration FDC the equations are:

				check
750 A	circuit C	$0.027x + 1.23z = 0.89 \pm 0.20$		(1.06)
	D	$0.089x + 1.28z = 1.49 \pm 0.25$		(1.06)
	F	$0.272x + 1.97z = 1.44 \pm 0.25$		(1.55)

with solutions:

$$x = -0.61 \pm 1.7$$
$$z = 0.87 \pm 0.18\,.$$

For Run II with configuration FDC the equations are:

				check
760 A	circuit C	$0.026x + 0.51z = 0.2 \pm 0.2$		(0.20)
	D	$0.069x + 0.58z = 0.4 \pm 0.3$		(0.55)
	F	$0.247x + 2.11z = 2.2 \pm 0.7$		(1.96)

with solutions:

$$x = 8.0 \pm 7.1$$
$$z = 0.0 \pm 0.7 .$$

For Run II with configuration CFD the equations are:

					check
650 A	circuit	C	$0.424y + 2.87z = 1$	± 1	(0.7)
		D	$0.042y + 1.25z = 1$	± 1	(0.4)
		F	$0.150y + 3.44z = 0$	± 1	(1.1)
700 A		C	$0.424y + 0.84z = 0$	± 0.3	(0.0)
		D	$0.042y + 0.37z = 0.3$	± 0.3	(0.1)
		F	$0.150y + 1.00z = 1.8$	± 0.7	(0.3)
750 A		C	$0.223x + 1.89z = 0$	± 1	(0.79)
		D	$0.022x + 0.82z = 0$	± 1	(0.30)
		F	$0.079x + 2.26z = 1$	± 1	(0.83)
760 A		C	$0.234x + 1.12z = 0.8$	± 0.4	(0.52)
		D	$0.024x + 0.49z = 1.0$	± 0.5	(0.18)
		F	$0.082x + 1.34z = 1.0$	± 0.5	(0.51)

In writing the equations for the run at 700 amperes we neglected any difference in the yield of electrons which there might be at this setting as compared with 650 amperes. We obtained the following solutions:

$$x = \quad 0.56 \pm 1.7$$
$$y = -0.60 \pm 0.65$$
$$z = \quad 0.35 \pm 0.17$$

For Run II configuration DCF the equation are:

					check
650 A	circuit	C	$0.151y + 2.03z = 2$	± 1	(1.3)
		D	$0.386y + 2.55z = 1$	± 0.7	(2.2)
		F	$0.053y + 2.23z = 2$	± 1	(1.1)
760 A		C	$0.084x + 1.83z = 0.45$	± 0.31	(0.79)
		D	$0.213x + 1.04z = 0.67$	± 0.38	(0.48)
		F	$0.029x + 0.91z = 0.45$	± 0.31	(0.45)
830 A		C	$1.89z = 1.11$	± 0.57	(0.81)
		D	$1.12z = 1.11$	± 0.57	(0.48)
		F	$0.98z = 0.28$	± 0.28	(0.41)

with solutions:

$$x = 0.15 \pm 2.0$$
$$y = 2.9 \pm 2.0$$
$$z = 0.42 \pm 0.13 .$$

The overall fit of the data may be judged from the point of view of the χ^2 criterion. In all, 36 equations have been fitted with 13 variables yielding $\chi^2 = 29$, a value not excessively greater than the number of degrees of freedom 23. In our equations we used as the eror assigned to the observed count, only the uncertainty based on the total number of counts recorded. In a counting experiment involving rather complicated electronic equipment used over a long period of time, this must certainly be an underestimate. Drifts and changes in the sensitivity of the equipment occur and in spite of the use of interlacing of the measurements and careful monitoring, some additional uncertainty enters. In view of this, we believe that the fit obtained is good and that our method for reducing the data is justified.

Some increase in the stated error seems indicated. We choose this to be the amount which brings χ^2 down to its expectation value. A 12% increase applied uniformly to all the errors as given above has just this effect and should serve to improve the statistical significance of our final result. This has been done in giving the weighted averages obtained from the above solutions,

(8) $$\overline{x} = -0.04 \pm 0.92$$

(9) $$\overline{y} = -0.77 \pm 0.62 .$$

We do not observe a positive effect, either for $\pi \to e + \nu$ or for $\pi \to e + \nu + \gamma$.

11. – π-e decay.

The fraction f of π-e to π-μ decays may be obtained from the value of $\overline{x}$, provided the momentum fraction G_μ of μ-electrons accepted by the spectrometer is known. Since our analysis for $\overline{x}$ refers to a counting rate $R_\mu = 5000$, we write,

(10) $$f = \frac{1}{5000} G_\mu \overline{x} r ,$$

where the subscript μ refers to values at 450 amperes. The factor r is the fraction of μ which do not escape from the source before decaying and is about 0.95. We may obtain G_μ from the observed μ-electron spectrum, as follows:

For the counting rate with the spectrometer set at p_0 we write,

$$R(p_0) = N\int_0^\infty Q'(p)F\left(\frac{p-p_0}{p_0}\right)\mathrm{d}p = NG(p_0)\,. \tag{11}$$

The distribution function of the μ-electrons is supposed normalized so that $\int_0^\infty Q'(p)\,\mathrm{d}p = 1$. Neglecting the variation of Q' over the range of F we may take it outside the integral in (11). Since $H = \int_0^\infty F((p-p_0)/p_0)\,\mathrm{d}p/p_0$ is a constant for the spectrometer, independent of p_0, we have,

$$J = \int_0^\infty R(p_0)\,\mathrm{d}p/p_0 = NH\int_0^\infty Q'(p_0)\,\mathrm{d}p_0 = NH\,. \tag{12}$$

Thus,

$$G_\mu = R_\mu H/J\,. \tag{13}$$

From the data of Fig. 7 we obtain $R_\mu/J = 1.27$, while from Fig. 3, $H = 0.037$, giving $G_\mu = 0.047$. This should be increased by about 10% to take account of the broadening due to electron scattering since this affects the μ-electron response somewhat more than that of the π-electrons. Finally,

$$f = 0.98\cdot 10^{-5}\,\overline{x}\,. \tag{14}$$

Our result for the fraction of $\pi \to \mathrm{e} + \nu$ decays is

$$f = (-0.4 \pm 9.0)\cdot 10^{-6}\,.$$

This appears to be statistically significant and thereby allows only a 1% probability that f could be greater than $2.1\cdot 10^{-5}$.

12. – π-e-γ decays.

We can obtain some information about the process $\pi \to \mathrm{e} + \gamma + \nu$ from our value of $\overline{y}$. We write

$$f_\gamma = \frac{r}{5\,000}\,\frac{G_\mu}{G_\gamma}\,\overline{y}\,, \tag{15}$$

where G_γ, in analogy with G_μ, is the fraction of π-γ electrons accepted by the

spectrometer at 650 amperes. We need to know the distribution function $Q''(p)$ of these electrons. Then,

$$G_\gamma = \int_0^\infty Q''(p)\,\mathrm{d}p F\left(\frac{p-p_\gamma}{p_\gamma}\right) = Q''(p_\gamma)p_\gamma H\,, \tag{16}$$

where $p_\gamma = 60.3$ MeV/c, account having been taken of the 3.0 MeV average energy loss in the source.

The value of f_γ will depend on what is taken for the distribution function. Since we are dealing with a three body decay of relativistic particles the distribution may be expected to be similiar to that of the μ-electrons. We obtain an order of magnitude by taking $G_\gamma = G_\mu$. Then $f_\gamma = (-1.5 \pm 1.2)\cdot 10^{-4}$. The result is not very different if the distribution given by EGUCHI [22] assuming tensor interaction is taken, from which $G_\mu/G_\gamma = 1.36$ and we would then have

$$f_\gamma = (-2.0 \pm 1.6)\cdot 10^{-4}\,.$$

Recently, CASSELS [15] has reported a much lower limit than this by looking for e-γ coincidences in the π-decay, giving $f_\gamma = (3 \pm 7)\cdot 10^{-6}$ assuming tensor interaction and the e-γ correlations predicted thereby. A lower limit than ours has also been reported by LOKANATHAN [15].

13. – Conclusions.

The non-occurence of any kind of electronic decay of the pion is now established well below the limits set by the explanations thus far offered in terms of an effect of mass alone. We may conclude that there is a more essential difference which distinguishes the electron from the muon in its interaction with the neutrino field. Within the framework of the idea that the electron interacts with the pion through the intermediary of a nucleon antinucleon pair, our result implies that not only the pseudoscalar, but also the axial vector coupling must be quite small.

Recently, MORPURGO [7] has proposed a way of understanding the behavior of the pion within the framework of the universal Fermi interaction. His idea is to forbid the process $\pi \to e + \nu$ by supposing that only the scalar and tensor (possibly also the vector) couplings intervene. For the π-μ decay, on the other hand, he supposes that the order in which the factors must be written in the Fermi interaction is different than for the electron. With a suitable choice

---

[22] T. EGUCHI: *Phys. Rev.*, **102**, 879 (1956).

the π-μ decay becomes allowed. With this scheme f may be made arbitrarily small and the value of $f_\gamma \simeq 10^{-5}$, not inconsistent with present experimental limits.

* * *

We received a great deal of help in carrying through this experiment from our students, especially Mr. RICHARD MILLER and Mr. TADAO FUJII, whose skill, patience and intelligence were invaluable to us. We are grateful to Mr. PAUL FIELDS and Mr. RAY BARNES of the Argonne National Laboratory for the plutonium source they prepared and loaned to us. Dr. LEONA MARSHALL and Mr. JOSEPH FISCHER placed kindly at our disposal their pulse height analyzer. We also want to credit Mr. CLOVIS BORDEAUX for the long steady operation of the cyclotron. One of us (H.L.A.) profited from interesting discussions with Dr. G. MORPURGO and wishes to thank the Guggenheim Foundation for a Fellowship and the Institute of Physics « Guglielmo Marconi », Rome, for the hospitality which made the completion of this work possible.

RIASSUNTO (*)

Uno spettrometro magnetico con doppia focalizzazione, dotato di elevato potere trasmissivo (1.8%) e buona risoluzione (3.0%), è stato usato per rivelare il decadimento elettronico del pione positivo. Non si è scoperta alcuna prova. La frazione di decadimenti del tipo $\pi \to e+\nu$ fu trovata essere $f=(-0.4\pm9.0)\cdot10^{-6}$. Il risultato appare statisticamente significativo e perciò consente solo una probabilità dell'1% che f possa avere un valore superiore a $2.1\cdot10^{-5}$. Dalla ricerca di elettroni di momento 60.3 MeV/c si potrebbe concludere che la frazione di decadimenti del tipo $\pi \to e+\gamma+\nu$ sia stata $f_\gamma=(-2.0\pm1.6)\cdot10^{-4}$, assumendo che l'interazione tensoriale determini lo spettro. Per questo processo CASSELS e LOKANATHAN hanno riferito recentemente limiti assai inferiori.

(*) *Traduzione a cura della Redazione.*

IL NUOVO CIMENTO Vol. VI, N. 6 1° Dicembre 1957

A General Treatment of Expanding Systems (*).

II. - Application to Multiple Meson Processes.

Y. Takahashi and H. Umezawa (+)

Department of Physics, State University of Iowa - Iowa City, Iowa, U.S.A.

(ricevuto il 24 Luglio 1957)

Summary. — The general theory proposed in the previous paper will be applied to multiple meson processes. This is a field theoretical justification of the Landau theory of multiple meson production, based on a hydrodynamical analogy. According to our calculation, mesons enclosed in a narrow disk will expand in the direction perpendicular to the disk and give a sharp angular distribution in favor of recent experimental data.

1. – Introduction.

In photographic emulsions, events have been observed in which a primary particle produces a large « star » believed to be due to a collision with a nucleus in the emulsion. There is no doubt that many mesons can be produced in the collision of one nucleon with a nucleus.

For many years, there was a controversy about the mechanism of this phenomenon, the question being whether the meson production was « multiple » or « plural ». The plural hypothesis has been advocated specially by Heitler [1], while the multiple hypothesis has been suggested by a number of authors, Heisenberg, Lewis-Oppenheimer-Wouthuysen (LOW), Fermi, and Landau [2-5].

(*) This work is supported in part by the National Science Foundation.

(+) Present address: (Y.T.) Dublin Institute for Advanced Studies, Dublin, Ireland. (H.U.) Department of Physics, University of Tokyo, Tokyo, Japan.

(1) W. Heitler and L. Jánossy: *Proc. Phys. Soc. London*, **62**, 669 (1949).

(2) W. Heisenberg: *Zeits. f. Phys.*, **101**, 533 (1936); *Naturwiss.*, **39**, 69 (1952).

(3) H. W. Lewis, J. R. Oppenheimer and S. A. Wouthuysen: *Phys. Rev.*, **73**, 127 (1948).

(4) E. Fermi: *Progr. Theor. Phys.*, **5**, 570 (1951); *Phys. Rev.*, **81**, 681 (1951).

(5) L. D. Landau: *Izv. Acad. Nauk SSSR, Ser. Fig.*, **17**, 51 (1953); S. Z. Belen'kji and L. D. Landau: *Suppl. Nuovo Cimento*, **3**, 15 (1956).

We shall concentrate here on the discussion of the detailed mechanism of the multiple production of mesons (*).

Historically speaking, the multiple mechanism was first predicted by HEISENBERG, in connection with the applicability of the present quantum field theory (2). HEISENBERG's original discussion is essentially on the classical non-linear theory, but a refined version appeared later.

An orthodox field-theoretical calculation for this process was carried out by LOW, which was based on the Bloch-Nordsieck transformation (3).

A third type of multiple meson theory has been developed by FERMI (4) and modified by LANDAU *et al.* (5), who assume a thermal equilibrium state of mesons at the first stage of meson production. All these theories are reviewed by LEWIS (6). We shall not repeat here the detailed ideas of these theories.

A question now arises as to what relation exists between LOW's and Fermi-Landau's theories; in other words, how can Fermi-Landau's thermodynamical treatment be understood in terms of the orthodox field theory?

The first clue of this question has been achieved by one of the authors, who has introduced statistical ideas into the S-matrix theory, starting with a general expression of the S-matrix for multiple meson production (7). Once it is proved that the S-matrix for meson production can be approximated by the most probable distribution of mesons, one can apply the method of statistical mechanics for thermal equilibrium. This has been worked out by EZAWA *et al.*, BARUT and DOMOKOS (8-10). One of the significant features of the ETU theory is to show that there is an essential difference of behavior of the produced mesons between the first (renormalizable) and the second (unrenormalizable) kinds of interactions. We thus come back to the original question by HEISENBERG, namely, how the multiple meson process is related to the applicability of the present quantum field theory.

In order to answer this question, we have first to formulate the field theory so as to be able to treat the multiple process even qualitatively and to see how the prediction of the field theory differs from experimental results in this high energy region. In this connection, we must notice that LEWIS and

---

(*) This is of course not to exclude the possibility of the plural mechanism. As is emphasized by Heitler himself, the plural hypothesis is not an antithesis of the multiple hypothesis but a possible mechanism which cannot be always disregarded.

(6) H. W. LEWIS: *Rev. Mod. Phys.*, **24**, 241 (1952); *Proc. Rochester Conference* (1957).

(7) Y. TAKAHASHI: *Can. Journ. Phys.*, **34**, 378 (1956); *Nuovo Cimento*, **4**, 531 (1956); *Can. Journ. Phys.*, **35**, 489 (1957).

(8) H. EZAWA, Y. TOMOZAWA and H. UMEZAWA: *Nuovo Cimento*, **5**, 810 (1957). This paper will be quoted as ETU.

(9) A. O. BARUT: private communication.

(10) G. DOMOKOS: private communication.

COCCONI emphasized in the Rochester Conference that no serious effort has been made to develop a theory suitable for comparison with the experimental data and that the recent information demands a more detailed theoretical analysis of the possibility of a bremsstrahlung model (LOW) ([6]).

As will be discussed in the following sections, our formulation for expanding systems seems to be appropriate to handle the multiple meson process, especially the production process suggested by LANDAU ([11]).

We shall here summarize the qualitative features of recent experiments ([12]).

The multiplicity of the produced mesons does not contradict Fermi's prediction

$$\overline{N} \sim E^{\frac{1}{4}} ,$$

where E is the total energy of the incident nucleons in the center of mass system, and the average meson energy is about 1 GeV for a primary energy of $2 \cdot 10^4$ GeV. All the charged particles are included in two cones, one backward and one forward, of half-angle approximately 20°, in the center of mass system. From the distribution of μ-mesons underground, one can estimate the angular distribution of multiple pions as $1/\theta$ for small angles, where θ is the angle between the incident nucleon and the produced pion.

2. – Qualitative discussion.

The basic postulates of Fermi are the following ([4]):

1) When two fast nucleons collide, their kinetic energy will be suddenly released in a small volume Ω surrounding the two nucleons and a high concentration of energy will be established within the volume of this size.

2) The energy concentration lasts a very short time and is rapidly converted into mesons or other particles that fly away with a speed approximating that of light. During the short time a statistical equilibrium will be reached.

3) The small volume Ω in which the statistical equilibrium is reached is determined by the dimensions of the pion cloud, whose radius is of the order $\varkappa^{-1}$, where $\varkappa$ is the meson mass. The volume will be contracted, however, due to the nucleon velocity, namely

$$\Omega = \frac{4\pi}{3} \varkappa^{-3} \frac{2M}{E} , \tag{2.1}$$

([11]) Y. TAKAHASHI and H. UMEZAWA: *Nuovo Cimento*, **6** (1957). This paper will be quoted as I hereafter.

([12]) Recent experimental data on the multiple meson production are summarized by J. NISHIMURA. J. NISHIMURA: *Soryushiron-Kenkyu* (*Japanese*), **14**, 145 (1957). See also ([6]).

where M is the nucleon mass and E the total energy of the two colliding nucleons in the center of mass system.

LANDAU revised Fermi's idea in the following way ([5]):

1) In the collision of two nucleons a compound system arises and energy is released in a small volume Ω, Lorentz-contracted in the transverse direction. A statistical equilibrium is established in the system.

2) The second stage of the collision consists in the expansion of the system. This stage is examined *hydrodynamically* considering the expansion as motion of an ideal fluid. (The stage of expansion).

3) With the expansion of the system, the interaction of particles decreases and the mean free path increases. When the mean free path becomes comparable with the linear dimensions of the system, the system disintegrates into separate particles. (The stage of break-up).

It has been discussed by KOBA that Landau's revision would be actually needed to explain the production ratio of pions and K-mesons ([13]).

We shall calculate here the average meson number in field theoretical fashion by using a formulation of expanding systems, which is proposed in our first paper.

Keeping Fermi-Landau's original idea, we shall start with a free-meson model enclosed in a volume Ω (a disk flat in the x_3-direction) and treat the expansion process by the aid of the method in paper I. Although our formulation in I is concerned with a three-dimensional expansion, one can easily reformulate it so as to be suitable for our problem by putting

$$\lambda_1 = 1\,, \qquad \lambda_2 = 1\,, \qquad \lambda_3 = \lambda \gg 1\,, \tag{2.2}$$

$$\begin{cases} L_1' = L_1\,, \\ L_2' = L_2\,, \\ L_3' = \lambda L_3\,, \end{cases} \tag{2.3}$$

$$L_1' = L_2' = L_3' = L\,, \tag{2.4}$$

$$\begin{cases} \Omega = L_1 L_2 L_3\,, \\ V = L_1' L_2' L_3' = \lambda \Omega\,. \end{cases} \tag{2.5}$$

Here Ω is the volume in which a thermal equilibrium is established in the first stage of the collision. V, on the other hand, is the volume in which all

([13]) Z. KOBA: *Progr. Theor. Phys.*, **15**, 461 (1956).

the mesons become free to fly away. Following Landau's idea, we shall take

$$\text{(2.6)} \qquad \begin{cases} V = \dfrac{4\pi}{3}\varkappa^{-3}, \\ \Omega = V\dfrac{2M}{E}, \end{cases}$$

where $2M/E$ is a Lorentz-contraction factor, E is the total energy of the colliding particles with mass M in the center of mass system.

The pressure acting on the wall of the volume Ω is, according to ETU,

$$\begin{aligned} \text{(2.7)} \quad P_i &= -\frac{1}{\Omega}\frac{\partial H[\Omega]}{\partial \lambda_i} = -\frac{1}{\Omega}\int \mathrm{d}^3x \frac{\partial \varphi_\Omega(x)}{\partial x_i}\frac{\partial \varphi_\Omega(x)}{\partial x_i} = \\ &= -\frac{1}{\Omega}\sum_{\boldsymbol{p}}\frac{p_i^2}{2\omega_p}\{a(\boldsymbol{p})a(-\boldsymbol{p})\exp[-2i\omega_p t] + \\ &+ a^*(\boldsymbol{p})a^*(-\boldsymbol{p})\exp[2i\omega_p t] + a^*(\boldsymbol{p})a(\boldsymbol{p}) + a(\boldsymbol{p})a^*(\boldsymbol{p})\} = \\ &= -\frac{1}{(2\pi)^3}\int \mathrm{d}\boldsymbol{p}\frac{p_i^2}{2\omega_p}\{a(\boldsymbol{p})a(-\boldsymbol{p})\exp[-2i\omega_p t] + a^*(\boldsymbol{p})a^*(-\boldsymbol{p})\exp[2i\omega_p t] - \\ &+ a^*(\boldsymbol{p})a(\boldsymbol{p}) + a(\boldsymbol{p})a^*(\boldsymbol{p})\}, \qquad (i = 1, 2, 3), \end{aligned}$$

where the summation is replaced by an integration. Since the average value of the momentum p_3 is much larger than p_1 or p_2, because, due to the uncertainty principle,

$$\text{(2.8)} \qquad \begin{cases} \langle p_3\rangle \sim \dfrac{\lambda}{L} = \varkappa^{-1}\dfrac{E}{2M}, \\ \langle p_1\rangle = \langle p_2\rangle \sim \dfrac{1}{L} = \varkappa^{-1}, \end{cases}$$

the pressure P_3 becomes much larger than P_1 or P_2. It is thus clear that in the volume Ω mesons will be produced in the x_3-direction due to the large pressure P_3.

Since the first line of the right hand side of the equation (2.7) does not give any contribution to the average value of the pressure, we may omit it in view of the fact that the definition of the pressure operator (2.7) makes sense only when the average value is taken (see ETU). The average value of the second line contains an infinite number which means an infinite pressure. We have to subtract this term from physical necessity. The subtraction will be actually carried out in the next section.

Bearing the above intuitive picture in mind, let us carry out the detailed calculation in the next section.

3. – Quantitative discussion.

The calculation of the average number of particles produced into the volume V is straightforward.

According to the idea qualitatively discussed in the previous section, we

shall take into account the effect of the volume change (or the pressure effect) by perturbation theory (*).

The interaction Hamiltonian in this case is, according to equation (I.2.20):

$$\mathcal{H}(t) = \int_{\Omega} \mathrm{d}^3x \mathcal{H}(x) = -\tfrac{1}{2}\Lambda(\lambda) \int_{\Omega} \mathrm{d}^3x \frac{\partial \varphi_{\Omega}(x)}{\partial x_3'} \frac{\partial \varphi_{\Omega}(x)}{\partial x_3} = \tag{3.1}$$

$$= -\tfrac{1}{2}\Lambda(\lambda) \sum_{n} \frac{p_3^2}{2\omega_p} \{a(\boldsymbol{p})a(-\boldsymbol{p}) \exp[-2i\omega_p t] +$$

$$+ a^*(\boldsymbol{p})a^*(-\boldsymbol{p}) \exp[2i\omega_p t] + a^*(\boldsymbol{p})a(\boldsymbol{p}) + a(\boldsymbol{p})a^*(\boldsymbol{p})\},$$

where $\Lambda(\lambda) = 1 - 1/\lambda^2$. The number operator in the interaction picture is, as was given in (I.3.10):

$$N_0(t) = \sum_{n} \{(C_\lambda(\boldsymbol{p}))^2 a^*(\boldsymbol{p})a(\boldsymbol{p}) + (S_\lambda(\boldsymbol{p}))^2 a(\boldsymbol{p})a^*(\boldsymbol{p}) - \tag{3.2}$$

$$- S_\lambda(\boldsymbol{p})C_\lambda(\boldsymbol{p})a^*(\boldsymbol{p})a^*(-\boldsymbol{p}) \exp[2i\omega_p t] -$$

$$- S_\lambda(\boldsymbol{p})C_\lambda(\boldsymbol{p})a(\boldsymbol{p})a(-\boldsymbol{p}) \exp[-2i\omega_p t]\}.$$

The number operator in the Heisenberg picture is therefore, in the first order of the perturbation expansion:

$$N(t) = U^{-1}(t)N_0(t)U(t) = \left(1 + i\int_{\infty}^{t} \mathcal{H}(t')\,\mathrm{d}t'\right) N_0(t) \left(1 - i\int_{\infty}^{t} \mathcal{H}(t')\,\mathrm{d}t'\right) = \tag{3.3}$$

$$= N_0(t) + i\int_{\infty}^{t} [\mathcal{H}(t'),\ N_0(t)]\,\mathrm{d}t'.$$

Omitting terms which give no contribution to the spur calculation, we have

$$\left\{\begin{array}{l} [\mathcal{H}(t'),\ N_0(t)] \cong \tfrac{1}{2}\Lambda(\lambda) \sum_{n,n'} \frac{p_3^2}{2\omega_p} S_\lambda(\boldsymbol{p}')C_\lambda(\boldsymbol{p}') \cdot \\ \cdot [\{a^*(\boldsymbol{p}')a^*(-\boldsymbol{p}') \exp[2i\omega_p t] + a(-\boldsymbol{p}')a(\boldsymbol{p}') \exp[-2i\omega_p t]\} \cdot \\ \cdot \{a(\boldsymbol{p})a(-\boldsymbol{p}) \exp[-2i\omega_p t] + a^*(\boldsymbol{p})a^*(-\boldsymbol{p}) \exp[2i\omega_p t]\}] \cong \\ \cong -\Lambda(\lambda) \sum_{n} \frac{p_3^2}{2\omega_p} S_\lambda(\boldsymbol{p})C_\lambda(\boldsymbol{p}) \cdot \{\exp[2i\omega_p(t-t')] - \exp[-2i\omega_p(t-t')]\} \cdot \\ \cdot \{a^*(\boldsymbol{p})a(\boldsymbol{p}) + a(\boldsymbol{p})a^*(\boldsymbol{p})\}\ (^+)\,. \end{array}\right. \tag{3.4}$$

(*) *Note added in proof*: the calculation without recourse to the perturbation theory is carried out by H. Ezawa.

(+) $\cong$ signifies an equality apart from the terms which vanish in the spur calculation.

Due to the relation

$$\int_{-\infty}^{t} \exp\left[\pm 2i\omega_p(t-t')\right] \mathrm{d}t' = \pm \frac{i}{2\omega_p}, \tag{3.5}$$

we have

$$-i \int_{-\infty}^{t} [\mathscr{H}(t'), N_0(t)] \, \mathrm{d}t' \cong \Lambda(\lambda) \sum_n \frac{p_3^2}{2\omega_p^2} S_\lambda(\boldsymbol{p}) C_\lambda(\boldsymbol{p}) \{a^*(\boldsymbol{p}), a(\boldsymbol{p})\}. \tag{3.6}$$

Therefore

$$N(t) \cong \sum_{\nu} [a^*(\boldsymbol{p}) a(\boldsymbol{p}) + \xi(\boldsymbol{p}) \{a^*(\boldsymbol{p}), a(\boldsymbol{p})\}], \tag{3.7}$$

where

$$\xi(\boldsymbol{p}) \equiv (S_\lambda(\boldsymbol{p}))^2 + \Lambda(\lambda) \frac{p_3^2}{2\omega_p^2} S_\lambda(\boldsymbol{p}) C_\lambda(\boldsymbol{p}) \quad (*). \tag{3.8}$$

The average number is consequently

$$\bar{N} = \mathrm{Trace}\,[N(t)\varrho_0]/\mathrm{Trace}\,[\varrho_0] = \tag{3.9}$$

$$= \sum_n \left\{ \frac{1}{\exp[\beta\omega_p] - 1} + \xi(\boldsymbol{p}) \frac{\exp[\beta\omega_p] + 1}{\exp[\beta\omega_p] - 1} \right\},$$

where the relations

$$\begin{cases} \mathrm{Trace}\,[a^*(\boldsymbol{p}) a(\boldsymbol{p}) \varrho_0]/\mathrm{Trace}\,[\varrho_0] = \dfrac{1}{\exp[\beta\omega_p] - 1}, \\ \mathrm{Trace}\,[\{a^*(\boldsymbol{p}), a(\boldsymbol{p})\}\varrho_0]/\mathrm{Trace}\,[\varrho_0] = \dfrac{\exp[\beta\omega_p] + 1}{\exp[\beta\omega_p] - 1}, \end{cases} \tag{3.10}$$

have been used.

The summation in (3.9) can be approximated by integration, namely

$$\bar{N} = \frac{\Omega}{(2\pi)^3} \int \mathrm{d}p \, \frac{1}{1 - \exp[-\beta\omega_p]} \{\exp[-\beta\omega_p] + \xi(\boldsymbol{p})(1 + \exp[-\beta\omega_p])\} = \tag{3.11}$$

$$= \frac{\Omega}{(2\pi)^3} \int \mathrm{d}\boldsymbol{k} \, \frac{1}{1 - \exp[-\beta\omega_k]} \{\exp[-\beta\omega_k] + \xi(\boldsymbol{k})(1 + \exp[-\beta\omega_k])\}.$$

(*) Notice an identity

$$(C_\lambda(\boldsymbol{p}))^2 - (S_\lambda(\boldsymbol{p}))^2 = 1.$$

The first term in (3.11) is the one which is expected by Fermi's simple model, while the second is the correction coming from the volume change (or the pressure) effect. The integration in (3.11) is rather complicated, but one can roughly estimate it under the following simplifications:

1) The meson mass $\varkappa$ may be neglected.

2) The term which does not vanish at $\beta \to \infty$ must be omitted.

3) The parameter λ may be put equal to infinity, which means that the large volume V is infinite.

The first simplification will be justified by the consideration that in the case of an extremely high energy, all the particles are extremely relativistic in the center of mass system so that the mass may be negligible compared to their kinetic energy. The second is related to the definition of the vacuum. The subtraction of this term is necessary in order to make the pressure finite, as one can readily see from the equation (2.7). The third is justified as follows: The mesons in the volume V are interacting with each other due to their statistical correlation even in our free-meson model. Since the interaction due to the statistics is of short-range, it becomes negligible if the distance between mesons becomes larger than the meson's Compton wave length. It is considered therefore that the mesons travel as free particles when the radius of the system exceeds the meson's Compton wave length.

If one takes into account the above facts, the equation (3.11) can be remarkably simplified as follows:

$$\bar{N} = \frac{\Omega}{(2\pi)^3} \int_0^\infty k^2 \, \mathrm{d}k \exp\left[-\beta\omega_k\right] \cdot 2\pi \int_0^\pi \sin\theta \, \mathrm{d}\theta \, \eta(\theta) \quad (*) \,, \tag{3.12}$$

where

$$\eta(\theta) \equiv 1 + 2\xi(\boldsymbol{k})\big|_{\substack{\lambda\to\infty \\ \varkappa\to 0}} \,, \tag{3.13}$$

$$= \frac{1}{\sin\theta}\left\{1 - \frac{1}{2}\cos^2\theta + \frac{1}{4}\cos^4\theta\right\} \,,$$

and $k_3 \equiv k\cos\theta$.

The angular distribution $N(\theta)$ defined by

$$\bar{N} \equiv 2\pi \int_0^\pi \sin\theta \, \mathrm{d}\theta N(\theta) \,, \tag{3.14}$$

(*) The classical statistics is taken for the sake of simplicity.

becomes

$$N(\theta) = \frac{\Omega}{(2\pi)^3}\int_0^\infty k^2\,\mathrm{d}k\,\exp\left[-\beta\omega_k\right]\eta(\theta) = \frac{\Omega}{4\pi^3}\,\beta^{-3}\eta(\theta)\,. \tag{3.15}$$

The function $\eta(\theta)$ has large values for small angles θ, as is seen in Fig. 1.

For small angles, we have

$$N(\theta) \sim 1/\theta\,, \tag{31.6}$$

which is in good agreement with the data obtained from the distribution of μ-mesons underground.

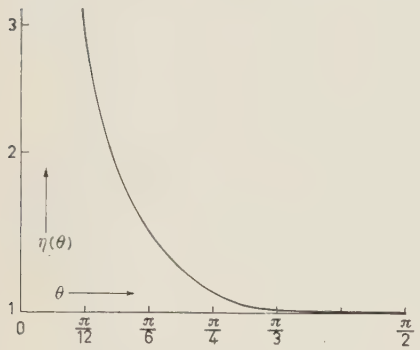

Fig. 1.

Using the relation

$$\int_0^\pi \eta(\theta)\,\sin\theta\,\mathrm{d}\theta = \frac{27}{32}\,\pi\,, \tag{3.17}$$

we have

$$N = \frac{27}{64}\,\frac{\Omega}{\pi}\,\beta^{-3}\,, \tag{3.18}$$

and

$$\Delta E = \int_0^\infty \omega_k N(\boldsymbol{k})\,\mathrm{d}\boldsymbol{k} = -\frac{\partial N}{\partial\beta} = \frac{81}{64}\,\frac{\Omega}{\pi}\,\beta^{-4}\,. \tag{3.19}$$

We see in the equation (3.19) that the temperature of our theory is lower than Fermi's when ΔE are the same, as is expected from the fact that the meson system $S[\Omega]$ expands adiabatically into the larger volume V.

The multiplicity is from (3.18) and (3.19)

$$N = 3\left(\frac{\Delta E}{M}\right)^{\frac{3}{4}}\Big/\left(\frac{E}{M}\right)^{\frac{1}{4}}\,, \tag{3.20}$$

where we have taken

$$\Omega = \frac{4\pi}{3}\,\varkappa^{-3}\,\frac{2M}{E}\,. \tag{3.21}$$

and E is the total nucleon energy in the center of mass system. The dependence of the average number on the energies E and ΔE is the same as Fermi's, but the angular dependence is not, as was shown in the equation (3.15).

4. – Conclusion and discussion.

There are a number of questions concerning the multiple meson process, for instance,

1) How can the thermal equilibrium be established in the first stage of the nucleon collision?
2) How does the established thermal equilibrium state decay into separate particles?
3) How is the behavior of produced mesons different from the prediction of present quantum field theory?

As was shown in a previous paper ([7]), the S-matrix for the multiple meson production can be written in a similar fashion as the equation determining the temperature of a gas. This would answer the first question.

This paper was devoted to discuss the second question. We have calculated the average number of produced mesons, keeping Fermi-Landau's idea and shown that it gives a narrow angular distribution in the direction of the incident particles. Our calculation was carried out, however, under the assumptions that the free-meson-model would be a fairly good approximation and the expansion effect could be taken into account by the perturbation approximation (*). The results we obtained in this paper are:

1) The multiplicity which is almost the same as Fermi's. (It differs only by a factor 2.)
2) The angular distribution of Fig. 1, which can be approximated by $N(\theta) \sim 1/\theta$ for small angles.

The model with which we start might be too simple to get a quantitative agreement with the experiments, but it has a very good attitude to explain the characteristics of the multiple meson production. As experimental data will become accurate, one can always refine our model, and attack the third question, namely how the applicability of the present field theory can be connected with this phenomenon.

(*) See the foot-note page 1387.

RIASSUNTO (*)

Applicheremo la teoria generale proposta nel precedente lavoro a processi di produzione multipla dei mesoni. Daremo una giustificazione, basata sulla teoria dei campi, della teoria di Landau della produzione multipla dei mesoni, basata su una analogia idrodinamica. Secondo i nostri calcoli, i mesoni racchiusi in un piccolo disco si espanderanno in direzione perpendicolare al disco dando una distribuzione angolare netta d'accordo con recenti dati sperimentali.

(*) *Traduzione a cura della Redazione.*

The Čerenkov Effect Produced by Single Particles in Gases.

A. Ascoli-Balzanelli (*) and R. Ascoli

Istituto di Fisica dell'Università - Torino
Istituto Nazionale di Fisica Nucleare - Sezione di Torino

(ricevuto il 3 Agosto 1957)

Summary. — The problem of the detection by means of photomultipliers of the Čerenkov radiation produced by single particles in gases is studied. It is shown that a high efficiency may be obtained with not too big detectors, provided that each pulse due even to one photoelectron may be detected. Experiments are described, which show that such an use of a photomultiplier is possible, and that an efficiency in agreement with the developed theory has been obtained with an 80 cm long detector filled with air at N.T.P. These experiments allow also a good determination of the number of emitted photons, and the result is in agreement with Tamm's theory. Some results obtained with freon 12 instead of air are also reported.

1. – Introduction.

In two previous works [1,2] we have given a preliminary account of a series of researches on the Čerenkov effect produced by single particles of cosmic rays in gases, by means of a photomultiplier.

The main purposes of these researches are:

1) To study a detector sensible only to particles having a velocity greater than a threshold value very near to the velocity of light in vacuum.

(*) Istituto di Meccanica Razionale dell'Università, Torino.

[1] A. Ascoli-Balzanelli and R. Ascoli: *Nuovo Cimento*, **10**, 1345 (1953).

[2] A. Ascoli-Balzanelli and R. Ascoli: *Nuovo Cimento*, **11**, 562 (1954).

2) To verify the agreement between theory and experiment for the Čerenkov effect in gases. Such a comparison may be interesting because of the dependance of this effect on the velocity, which is quite different than in usual phenomena.

Meanwhile similar experiments have been carried out by BARCLAY and JELLEY [3] in air making use of a 6 m high detector [4].

In the present work we study in general the problem of the detection of Čerenkov radiation in gases by photomultipliers and we show that by a careful use of the photomultiplier it is possible to obtain a good efficiency in the detection, without employing too big detectors. This happens if the photomultiplier is used in conditions in which each pulse due even to one photoelectron is detected. Our experiments show that such an use of a photomultiplier is possible: this fact has been established executing the absolute calibration of the height of the photomultiplier pulses by means of a light source.

Moreover an efficiency of the same order than in Barclay and Jelley's detector has been obtained in air with an only 80 cm high detector. The experiments have also allowed a rather good comparison with Frank and Tamm's theory and the results are in good agreement with the theory. Most of the experiments have been done with air, but some proofs have been made also with Freon 12.

The problem of avoiding spurious coincidences due to showers in this type of detector is also discussed.

2. – Theory of the Čerenkov-radiation detectors with gases.

2 1. *Čerenkov effect in gases.* – In the case of gases the formulae of Frank and Tamm's theory can be simplified, observing that $n - 1 \ll 1$, where n is the refractive index of the gas; moreover, for the particles which produce the effect it is $1 - \beta \ll 1$ ($V = \beta c$ being the velocity of the particles). It is useful to introduce the variable $\gamma = 1/\sqrt{1-\beta^2}$; so $\beta \simeq 1 - 1/2\gamma^2$.

Then the results of the theory, which concern our study may be expressed as follows:

a) The effect begins for $\beta_m = 1/n$, that is

$$\gamma_m \cong \frac{1}{\sqrt{2(n-1)}} \,. \tag{1}$$

[3] F. R. BARCLAY and J. V. JELLEY: *Nuovo Cimento*, **2**, 27 (1955).

[4] Lately, experiments with a detector with CO_2 at a pressure of 13.1 atm have been done by R. J. HANSON and D. C. MOORE; *Nuovo Cimento*, **4**, 1558 (1956).

b) The maximum emission angle ϑ_M, which is obtained when β tends to 1, is given by:

$$\cos \vartheta_M = \frac{1}{n} ,$$

that is:

$$\vartheta_M \cong \sqrt{2(n-1)} . \tag{2}$$

c) The average number of photons, emitted in the circular frequency range $\Delta\omega$ by a particle of velocity $v = \beta c$, for unit of path length, is:

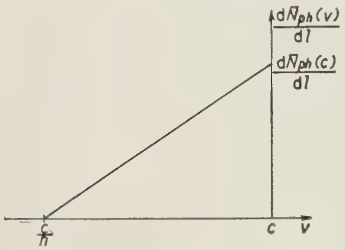

Fig. 1. – Average number of photons emitted per unit of path length as a function of the particle velocity, in the case of Čerenkov effect in gases. In the case of air at N.T.P. it is: $c/n = 0.999\,71\ \mathrm{d}\bar{N}_{\mathrm{ph}}(c)/\mathrm{d}l = 0.50/\mathrm{cm}$.

$$\frac{\mathrm{d}\bar{N}_{\mathrm{ph}}(v)}{\mathrm{d}l} = \frac{e^2}{\hbar c}\,\frac{\Delta\omega}{c}\left(1 - \frac{1}{\beta n^2}\right) \cong \tag{3}$$

$$\cong 2\,\frac{e^2}{\hbar c}\,\frac{\Delta\omega}{c}\,(n-1)\left(1 - \frac{1-\beta}{n-1}\right) \cong$$

$$\cong 2\,\frac{e^2}{\hbar c}\,\frac{\Delta\omega}{c}\,(n-1)\left(1 - \frac{1}{n-1}\,\frac{1}{2\gamma^2}\right) ,$$

having supposed n constant in the considered requency range. Thus in the case of gases $\mathrm{d}\bar{N}_{\mathrm{ph}}(v)/\mathrm{d}l$ is a linear function of the particle velocity, which is equal to zero as $\beta \simeq 1/n$ and reaches its maximum value:

$$\frac{\mathrm{d}\bar{N}_{\mathrm{ph}}(c)}{\mathrm{d}l} = \frac{2e^2}{\hbar c}\,\frac{\Delta\omega}{c}\,(n-1) , \tag{4}$$

as β tends to 1 (see Fig. 1). It appears that this maximum value is proportional to $(n-1)$. We will consider the radiation between 3 000 Å and 7 000 Å.

Then it is:

$$\frac{2e^2}{\hbar c}\,\frac{\Delta\omega}{c} = 872 .$$

In the case of air at N.T.P. we have:

$n-1$	β_m	γ_m	$E_{\mu m}$	ϑ_M	$\mathrm{d}\bar{N}_{\mathrm{ph}(c)}/\mathrm{d}l$
0.000 29	0.999 7	41.2	4.4 GeV	1° 25′	0.50/cm

where $E_{\mu m}$ is the threshold energy of the effect for μ-mesons.

2 2. *Photomultiplier efficiency. Optical system efficiency.* – We observe that the number of photons emitted per unit frequency range is constant for the Čerenkov radiation (formula (3)). It is then convenient to plot the photomultiplier efficiency per unit frequency range as a function of the frequency (see Fig. 2). From the area of the obtained diagram it is easy to deduce the total photomultiplier efficiency η_{pm} for the Čerenkov radiation emitted in a given frequency range.

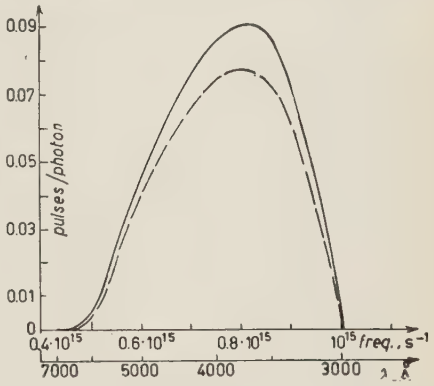

Fig. 2. - —— photomultiplier efficiency (pulses/photon) as a function of the radiation frequency (*S*-4 response); ---- efficiency of the system photomultiplier-aluminized mirror (pulses/photon). In the same diagram the Čerenkov spectrum is an horizontal line.

Such a deduction neglects the loss in the optical system. To take into account such a loss, each ordinate of the diagram must be multiplied by the efficiency of the optical system at the corresponding frequency. We have made the calculation in the case of a photocathode of spectral response curve *S*-4 (which holds also for the EMI 6260 photomultipliers), in the case in which all the light is reflected once by an aluminized mirror. The photocathode efficiency measured with a standard tungsten source has been assumed to be 30 μA/lumen. The results are: photomultiplier efficiency for the Čerenkov radiation emitted between 3000 Å and 7000 Å:

neglecting the loss in the optical system . . .	pm =	0.051 pulses/photon
taking into account the loss in the mirror . . .		0.043 pulses/photon
optical system efficiency (aluminized mirror)		0,84

2 3. *Theoretical efficiency of a Čerenkov detector.* – We call l the path length of the particles in the detector, $\overline{N}_{ph}(v) = (d\overline{N}_{ph}(r)/dl)l$ the average number of photons emitted by a particle of velocity r, $\overline{N}_e(r)$ the corresponding average number of photoelectrons emitted from the photo-cathode.

Being η_0 the optical system efficiency, we have

$$\overline{N}_e(v) = \eta_{pm}\eta_0\overline{N}_{ph}(v) \tag{5}$$

and using (3)

$$\overline{N}_e(v) = \frac{2e^2}{\hbar c}\frac{\Delta\omega}{c}(1-n)\left(1-\frac{1}{n-1}\frac{1}{2\gamma^2}\right)l\eta_{pm}\eta_0 .$$

As $v \to c$ we have

$$\overline{N}_e(c) = \frac{2e^2}{\hbar c}\frac{\Delta\omega}{c}(n-1)l\eta_{pm}\eta_0 . \tag{6}$$

So it is:

$$\overline{N}_e(v) = \overline{N}_e(c)\left(1 - \frac{1}{n-1}\frac{1}{2\gamma^2}\right). \tag{7}$$

With a given detector the highest efficiency $\eta_M(v)$ is obtained if the photomultiplier is used in conditions in which each pulse due even to one photoelectron is detected.

In this case the efficiency is equal to the probability that no photoelectron is emitted. Thus it is:

$$\eta_M(v) = 1 - \exp\left[-\overline{N}_e(v)\right], \tag{8}$$

where $\overline{N}_e(v)$ is obtained from (7) and (6) ([5]).

From this result we see that, using the photomultiplier in the assumed conditions, a high efficiency may be obtained with a small number of photoelectrons. For example, with an 80 cm long detector filled with air at N.T.P., assuming $\eta_{pm}\eta_0 = 0.043$, it is:

$$\overline{N}_{ph} = 40\,, \qquad \overline{N}_e = 1.72\,,$$

$\eta_M(c) = 1 - \exp[-1.72] = 0.82$. With a detector of double length or filled with a gas of double refractive index we obtain: $\overline{N}_{ph} = 80$, $\overline{N}_e = 3.44$, $\eta_M(c) = 1 - \exp[-3.44] = 0.968$.

With the previous suppositions the average number of electrons $\overline{N}_{er}(v)$ in each revealed pulse can be also calculated easily from:

$$\overline{N}_{er}(v) = \frac{\overline{N}_e(v)}{\eta_M(v)}\,.$$

We will now find the average value $\eta_{M\mu}$ of η_M for μ-mesons of cosmic rays.

In the case of gases of refractive index not greater than 1.003 the mesons producing the Čerenkov radiation have an energy greater than 1.4 GeV. Therefore the frequency of the particles per unit interval of γ is given with good approximation by $f(\gamma) = a/\gamma^2$, where a is a constant. Then the frequency

([5]) This result takes into account that not every electron emitted from the photocathode produces a pulse, for this loss is already computed in the photomultiplier efficiency.

of the detected particles is given from:

$$(9)\quad \int_{\gamma_m}^{\infty} f(\gamma)(1-\exp[-\bar{N}_e(v)])\,d\gamma = a\int_{\gamma_m}^{\infty}\frac{1}{\gamma^2}\left\{1-\exp\left[-\bar{N}_e(c)\left(1-\frac{1}{n-1}\,\frac{1}{2\gamma^2}\right)\right]\right\}d\gamma =$$

$$= \frac{a}{\gamma_m} - a\sqrt{\frac{2(n-1)}{\bar{N}_e(c)}}\exp[-\bar{N}_e(c)]\int_0^{\sqrt{\bar{N}_e(c)/(2(n-1))}\,1/\gamma_m}\exp[u^2]\,du =$$

$$= a\sqrt{2(n-1)}\left[1-\frac{\exp[-\bar{N}_e(c)]}{\sqrt{\bar{N}_e(c)}}\int_0^{\sqrt{\bar{N}_e(c)}}\exp[u^2]\,du\right],$$

where in the last step we have used (1).

The frequency of the particles which may produce Čerenkov effect is given by:

$$(10)\quad \int_{\gamma_m}^{\infty} f(\gamma)\,d\gamma = a\sqrt{2(n-1)}\,.$$

The we obtain $\eta_{M\mu}$ dividing (9) by (10):

$$(11)\quad \eta_{M\mu} = 1 - \frac{\exp[-\bar{N}_e(c)]}{\sqrt{\bar{N}_e(c)}}\int_0^{\sqrt{\bar{N}_e(c)}}\exp[u^2]\,du\,.$$

The value of $\eta_{M\mu}$ is plotted in Fig. 3 as a function of $\bar{N}_e(c)$ (6). Even in the case of μ-mesons of cosmic rays we calculate the average number of electrons $\bar{N}_{er\mu}$ in each revealed pulse from

$$\bar{N}_{er\mu} = \frac{\bar{N}_{e\mu}}{\eta_{M\mu}},$$

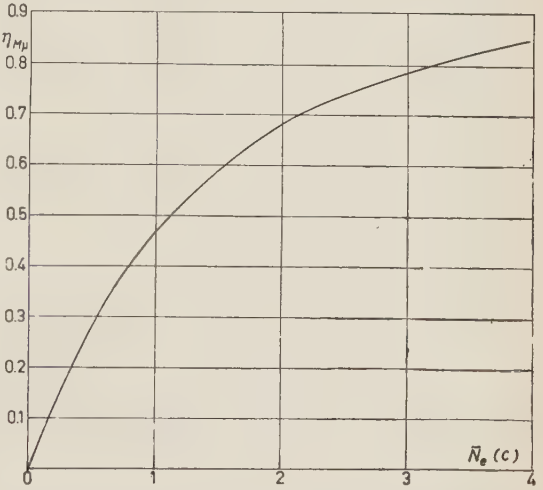

Fig. 3. Maximum overall efficiency $\eta_{M\mu}$ for cosmic-ray μ-mesons of a Čerenkov gas detector, as a function of the average number of electrons $\bar{N}_e(c)$ produced by a particle of velocity near c. It is supposed that all the pulses due even to one electron are detected.

where $\bar{N}_{e\mu}$ is the average number of photoelectrons produced by each particle.

(6) For a table of the function $\int_0^x e^{u^2}\,du$, see: JAHNKE-EMDE: *Tafeln höherer Funktionen* (Stuttgart, 1952), p. 26.

It is:

$$N_{e\mu} = \int_{\gamma_m}^{\infty} \frac{a}{\gamma^2} \bar{N}_e(c)\, d\gamma \Big/ \int_{\gamma_m}^{\infty} \frac{a}{\gamma^2} d\gamma = \frac{2}{3} \bar{N}_e(c) ,$$

so that

$$\bar{N}_{e\mu} = \frac{2}{3} \frac{N_e(c)}{\eta_{M\mu}} . \tag{12}$$

3. – Study of the optical system.

In designing a Čerenkov detector it is important to place the photomultiplier out of the particles path. In fact, if even the pulses due to one photoelectron are detected, the particles which pass through the cathode are directly revealed with an efficiency near unity, probably on account of Čerenkov effect in the glass envelope of the photomultiplier (7).

Also the necessity of avoiding the use of refractive systems along the path of the particles is evident, so that the simplest optical system consists in a specular surface, which reflects the light in the direction of the photocathode.

Let us suppose that the detector must be sensible to the particles the direction of which makes an angle lesser than a given α_M with the axis of the detector. Then the produced rays form with such an axis an angle at most equal to $\varphi = \alpha_M + \gamma_M$.

We have studied in particular a case in which $\alpha_M + \vartheta_M$ is relatively wide, that is $\varphi = \alpha_M + \vartheta_M = 12°$. Our purpose was to design a detector having a circular section as great as possible with the condition that all the luminous rays produced in a given path length l are converged on a photocathode of given diameter. In such a case the photomultiplier must be placed at a relatively small distance from the mirror, in comparison with the mirror diameter since we want to place the photomultiplier out of the particles path. So the axis of the mirror must form a wide angle with the axis of the detector. In these conditions the astigmatism of the optical system cannot be neglected, if we make use of a spherical mirror. It is necessary, therefore, to search the reflected rays graphically and we have found that there is no convenient solution.

On the contrary good results are obtained using a paraboloidic mirror with its axis parallel to the detector axis; with such a mirror the construction of the reflected rays is also simplified: the rays parallel to the axis of the de-

(7) This supposition is confirmed by recent experiments of U. Amaldi and L. Mezzetti: see U. Amaldi: *Sugli impulsi prodotti da raggi cosmici nei fotomoltiplicatori* (to be published in *Nuovo Cimento*).

tector converge all in the focus of the parabolic mirror; the rays forming an angle φ with the axis of the detector will form, after reflection, cones of amplitudes φ with their vertices on the mirror and the axes of which pass all through the focus.

Practically to design the mirror it is convenient to study the rays laying in the plane π, which contains the axes of the detector, of the paraboloid and of the photomultiplier.

To this purpose we have designed a parabola (see Fig. 4) and then we have proceeded by attempts: firstly we have assumed arbitrarily the position of the points A and B which limit the used portion of the mirror; so the diameter D of the detector is determined on the diagram. Then the rays reflected from A and B (which are in the most unfavourable conditions to be caught by the photocathode) were considered and the least photocathode was traced, able to collect these rays. To this purpose we have joined A and B with the focus F of the parabola. Then we have drawn two straight-lines from A and from B forming an angle φ with AF and BF.

The intersections H and K of these lines delimit the least photocathode, as requested.

Now the ratio between the diameter D of the detector and the diameter d of the photocathode can be measured.

Changing the position of A and B and proceeding as before it is easy to obtain by attempts the maximum value of D/d.

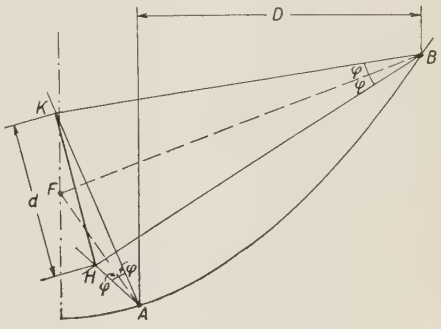

Fig. 4. – Design of the optical system (plane π of the detector axis and photomultiplier axis); D detector diameter; d photocathode diameter; $\varphi = \alpha_M + \theta_M$ maximum angle formed with the detector axis by the light rays to be collected. The represented solution gives the maximum value for D/d ($D/d = 1.78$) having assumd $\varphi = 12°$.

At last the scale of the diagram was fixed in order to give to d the value corresponding to the photomultiplier to be used. In our case ($\varphi = \alpha_M + \theta_M = 12°$) we have found $(D/d)_{\max} = 1.78$ (see Fig. 4). We have chosen, however, a solution with $D/d = 1.6$, with the axis of the photomultiplier normal to the axis of the detector. It is easy to see that practically all the rays which do not lay in the plane π are in more favourable conditions to be conveyed in the direction of the photocathode so that the choice made using the explained method, is apt even for these latter rays.

For a given l and a given θ_M, the rays emitted from the particles will form a spot of light of radius $l \operatorname{tg} \theta_M$ on the basis of the detector, where the paraboloidic mirror is situated. If this spot is small compared to the mirror, the number of particles for which not all the light falls on the mirror is negligible.

On the contrary if the spot is great compared to the mirror (as is our case), an optical device must be disposed to avoid this loss of light.

To this purpose a cylindrical specular tube of diameter D and length l was used.

By such a device the angle that a ray forms with the axis of the detector is conserved after reflection on the cylindrical mirror, so that all the rays (the ones directly, the others after reflection) fall on the paraboloidic mirror and are reflected towards the photocathode ([8]).

Naturally, using the cylindrical mirror, the light produced in a path length 1 can be collected only for the particles which travel internally through the whole length of the specular tube.

4. – Use of the photomultiplier in the best conditions.

As it was already explained, a good efficiency of the detector is obtained only if the photomultiplier is used in conditions in which each pulse due even to one photoelectron is detected.

To this purpose, the main points to be considered are:

a) *Reduction of the background.* – This is obtained by the following means:

1) Cooling the photomultiplier.

2) Employing coincidence circuits with resolving-time as small as possible.

3) Reducing the duration of the pulses before the discrimination. This means to derive the pulses with a low time-constant and to use an amplifier with a small rise time and a correspondingly fast discriminator. After discrimination the pulses may be lengthened if required.

This mean for the reduction of the background is the most important of the three. In fact, if the decay time-constant of the photomultiplier pulses is not sufficiently low, many of the observed pulses result from the superposition of several small pulses due to the dynodes (the rate of the pulses produced by the dynodes is much greater than that due to the photocathodes).

With the use of a sufficiently low time-constant the probability of the superposition of two or more pulses is reduced to a practically negligible value.

([8]) In this study we have neglected the hole in the surface of the cilindrical mirror, which is necessary to let the rays hit the photocathode after reflection on the paraboloidic mirror.

b) *Absolute calibration of the pulse height.* – In order to obtain an absolute calibration of the pulse height, we have drawn the pulse spectrum due to the illumination of the photocathode by a weak light source placed inside the detector. These pulses are due certainly to single photoelectrons.

The method 3) has allowed us to reduce the background to suc ha degree

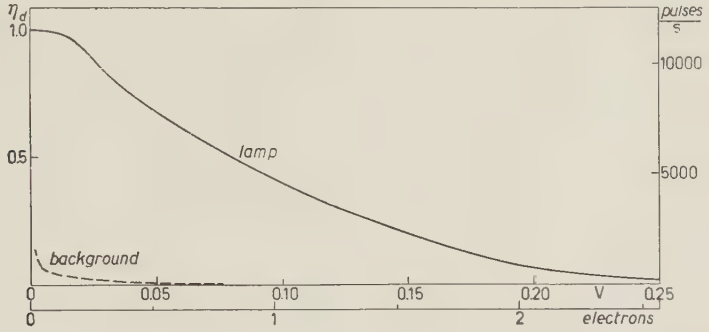

Fig. 5. – —— Pulse height spectrum due to a light source; – – – – Pulse height spectrum due to the background (right hand scale). The left hand scale gives the fraction $\eta_d(V)$ of detected pulses as a function of the discrimination V. The scale of the pulse height in volt refers to the photomultiplier output. The scale in electrons is obtained after evaluation of the area of the pulse height spectrum due to the light source.

as to permit us to obtain the spectrum of the lamp even without refrigerating the photomultiplier.

The pulse spectra, due to the lamp and to the background respectively, are represented in Fig. 5.

The photomultiplier was an EMI 6260, supplied with 1650 V, at a temperature of about 12 °C.

The rise-time, of the amplifier was of 0.02 μs and the decay time constant was of 0.05 μs. Fig. 5 shows that even with a weak light source (about 10000 pulses/s), the background is negligible.

The average height of the pulses produced by one electron which leaves the photocathode may be deduced with good precision from the spectrum due to the lamp.

In our case the average height is found to be 0.097 V.

The ordinate of the spectrum corresponding to a discrimination 0 gives the number of pulses produced by the lamp.

So the fraction $\eta_d(V)$ of pulses that is detected using a pulse height discrimination V is obtained dividing the corresponding ordinate by the ordinate corresponding to the discrimination 0.

From Fig. 5 we see that there is an interval near zero in which $\eta_d(V)$ is practically constant and very near 1; moreover the fact is very important

that such values of $\eta_d(V)$ may be obtained with discriminations for which the background is sufficiently small.

The reduction of the effect of the background and the knowledge of the height distribution of the pulses due to one photoelectron allows us to choice the appropriate discrimination in order to detect practically all the pulses due to one photoelectron.

Another advantage of working with such a discrimination is that the results are not dependent on the fluctuations of the gain of the system. This happens on account of the constancy of $\eta_d(V)$ in the neighbourhood of this discrimination.

When measurements are made with other discrimination values, care must be taken to control the constancy of the gain of the system.

In this case also the absolute calibration with the lamp is useful: the discrimination value must be adjusted at intervals in order to obtain always the same height for the pulses due to the lamp. To this purpose it is sufficient to adjust the discrimination in such a way as to keep $\eta_d(V)$ unchanged. This assures that the overall gain too remains unchanged.

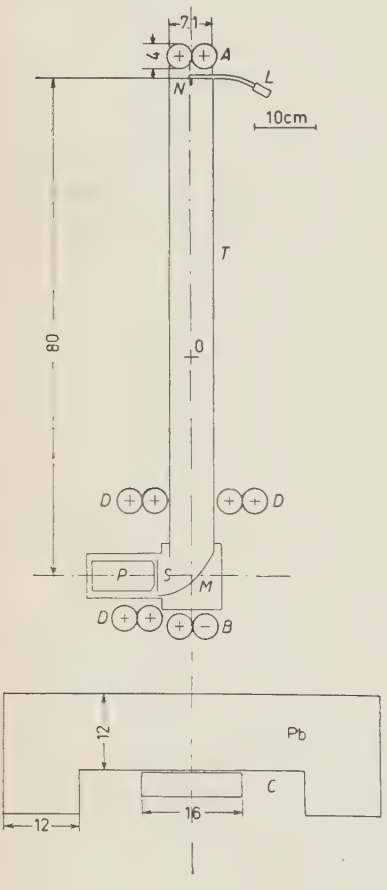

Fig. 6. – Diagram of the apparatus: T, internally aluminized specular tube; P, photomultiplier; M, parabolic aluminized mirror; S, movable shutter; L, small lamp collected to the detector through a copper pipe. O, track of the rotation axis of the apparatus; N, internally black lid; A and B, sets of two 8 cm long counters; C, set of four 16 cm long counters under a 12 cm thick lead-absorber Pb; D, set of six anticoincidence counters; the four counters over the photomultiplier are 40 cm long, the two counters under the photomultiplier are 8 cm long.

5. – Description of apparatus.

As it was described briefly in a previous work ([2]), our detector (Fig. 6) consists of an 80 cm long specular tube T having a diameter of 7.1 cm; the photomultiplier P is situated at the bottom with its axis perpendicular to the axis of the tube.

The Čerenkov radiation is converged on the photocathode by the previously described parabolic mirror M). A movable dark shutter

S set before the photocathode may be operated from outside the detector. The top of the tube is closed by a black lid N.

The light of a small lamp L is conveyed to the top of the detector through a small copper pipe, to allow the above mentioned controls. The whole device is contained in a gas- and lightt-ight envelope. The apparatus is completed by a Geiger counter telescope.

Counters A and B have an area of 8×8 cm^2.

Previous experiments ([2]) have shown that many coincidence pulses are due to showers, a particle of which hits the photocathode, while others hit counters A and B.

To avoid this effect we have decided to reveal only penetrating particles and to this purpose we have added the counters C, set under 12 cm of lead.

This addition was not entirely sufficient. Therefore we have used counters D of large area as anticoincidence counters. The whole device, except counters C, can turn round a horizontal axis of trace 0. The following coincidences were recorded: $A+B$, $A+B+P$, $A+B+P+C$, $A+B+P+C+D$.

To reduce the chance-coincidence rate in the coincidence between P and $A+B$, we have taken advantage of the fact that the photomultiplier pulses come without sensible delay.

This allows to reduce the length of the pulses coming from the coincidence between A and B (so we have used a pulse length of 0.25 μs, whereas a pulse engtth of 1.1 μs was used for the pulses coming from the photomultiplier).

16. – Experiments and results.

The most of our experiments (837.4 hours) have been made with air at natural pressure. Some experiments (94 hours) have been made with freon 12 (dicloro difluoro methane CCl_2F_2) at natural pres-

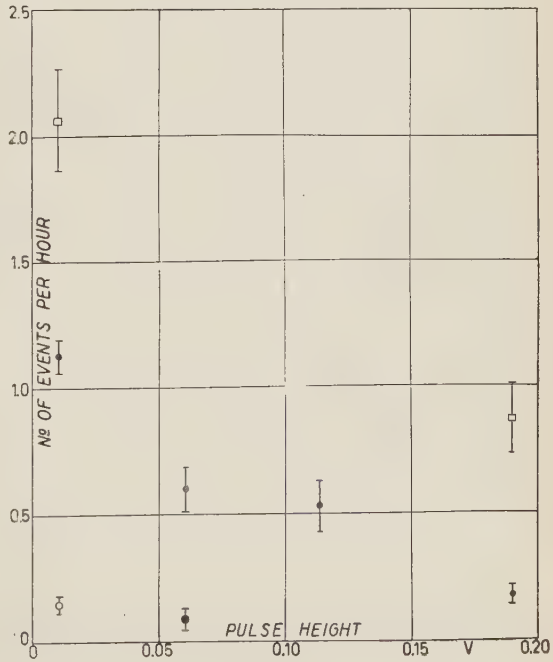

Fig. 7. – Experimental results for the rate $(A+B+P+C) - (A+B+P+C+D.)$ ⊙ air, open shutter; ● air, closed shutter; ○ air, invertde detector; □ freon 12, open shutter. The pulse height discriminations in volts are referred to the photomultiplier output.

sure: this gas was used because of its rather high refractive index (of the order of 1.0011) and of its incombustibility.

The experiments were made with different discriminations, corresponding to photomultiplier pulse-heights of 0.01 V, 0.06 V, 0.113 V, 0.19 V ([9]).

The discrimination 0.01 V has been chosen according to the criteria given at the end of Sect. 4, so that practically all the pulses due to one photoelectron are detected. With such a discrimination the background varied between 350 and 700 pulses/s, so that the expected chance-coincidence rate with the counter telescope was from one in eight days to one in four days, which is negligible in this experiment.

Some proofs were made with the photomultiplier open, some with the shutter closed and others with the detector inverted and the shutter open.

All the proofs were alternated with one another.

The results are given in the following table and those of the column d are plotted in Fig. 7.

TABLE I.

	Discriminated pulse height Volt	Pulse counting rate: pulses-hour				Total duration hours
		a $A+B+P$	b $A+B+P+C$	c $A+B+P+C+D$	d $(A+B+P+C)-(A+B+P+C+D)$	
air open	0.01	3.20±0.11	1.31 ±0.07	0.189±0.027	1.126±0.066	258.2
	0.06	2.16±0.17	0.68 ±0.09	0.079±0.032	0.60 ±0.09	76.1([10])
	0.113	1.49±0.16	0.69 ±0.01	0.16 ±0.05	0.53 ±0.10	60.5
	0.19	0.99±0.08	0.33 ±0.05	0.15 ±0.03	0.181±0.035	149.4
air closed	0.06	0.84±0.11	0.22 ±0.057	0.13 ±0.04	0.088±0.036	68.1 ([10])
air inverted	0.01	0.79±0.08	0.244±0.043	0.099±0.027	0.145±0.033	131.1
freon 12 open	0.01	4.60±0.31	2.26 ±0.22	0.19 ±0.06	2.06 ±0.21	47
	0.19	2.44±0.23	1.02 ±0.15	0.15 ±0.06	0.87 ±0.14	47

([10]) Measurements made without the two anticoincidence counters under the photomultiplier.

([9]) These values have been periodically adjusted with the lamp calibration as explained in Sect. 4.

The coincidence rate of the counter telescope $A+B+C$ was also measured and it was found to be 10.5/hour ([11]).

Other experiments had been made in 1954 without anticoincidence counters and without counters under lead. The results are given in a previous work of us ([2]).

7. – Discussion.

7·1. *General considerations.* – The comparison between the experiments with open and closed shutter shows that most of the recorded pulses are due to light produced from particles passing through the detector. The comparison between the measurements made with straight and inverted detector shows that this light is due to a directional effect, that is to Čerenkov effect.

7·2. *Comparison with Tamm's theory.* – The most convenient way to compare the results with Tamm's theory is to study the frequency of the detected particles for the pulse height discrimination 0.01 V, in the case of air. This frequency is obtained subtracting column d of Table I for inverted detector from column d for inverted detector and its value is (0.98 ± 0.07)/hour.

We remember that with the discrimination 0.01 V practically all the pulses due to one electron are detected, so that the theory developed in Sect. 2 can be applied.

We calculate at first the theoretical frequency of the particles having a velocity sufficient to produce Čerenkov effect. We consider that the measured frequency $A+B+C$ of the particles detected by the counter telescope is 10.5/h and that 24% of them can produce Čerenkov effect (this results from the consideration of the spectrum of μ-mesons and from the fact that any particle revealed by the telescope must pass through 12 cm of Pb).

Then the particles detected by the telescope and able to produce Čerenkov effect have a frequency of 2.54/hour.

From this value it is easy to calculate the rate of particles that pass through the whole length of the tube and it is found to be 1.28/hour.

To calculate the theoretical value of the detector efficiency η_{M_μ} for these particles we have taken for η_{pm} the value of 0.0507 corresponding to the photocathode sensitivity of 30 μA/lumen, given from the constructors. It is reasonable to assume that this value may be more probably lower than greater with a standard error of ~ 5 μA/lumen. We have assumed $\eta_0 = 0.795$, starting from a mirror efficiency of 0.84 (see Sect. 2) and taking into account that some rays undergo more reflections.

([11]) The coincidence rate $A+B$ was constantly controlled and it was 19.5/hour.

So we have

$$\eta_{\text{pm}}\eta_0 = 0.040 ,$$

and from (6) it results

$$\bar{N}_e(c) = 1.6 .$$

Substituting in (11) we obtain

$$\eta_{M_\mu} = 0.61 .$$

Thus the theoretical frequency of the events due to particles that pass through the whole length of the tube is $\eta_{M_\mu} \cdot 1.28/\text{hour} = 0.78/\text{hour}$.

We must add to this value the frequency of the events due to particles that pass but through a portion of the tube.

This frequency has been calculated to be 0.39/hour. This value was found subdividing the particles in groups and attributing a different detection efficiency to each group, according to the path length of the particles in the tube.

So a total value of 1.17/hour is obtained.

This value may be more probably lower than greater with a standard error of ~ 0.11/hour, the error being due chiefly to the uncertainty in the value of η_{pm}.

This theoretical value results in good agreement with the experimental value (0.98 ± 0.07)/hour.

With an inverse procedure we have also deduced the number of emitted photons from the experimental results, to compare it directly with the theory.

In this manner we obtain the value 0.51 ± 0.05 for the detector efficiency η_{M_μ} for particles that pass through the total length of the tube. Thus it results for these particles $\bar{N}_e(c) = 1.18 \pm 0.18$.

Finally we obtain $d\bar{N}_{\text{ph}}(c)/dl = 0.37/\text{cm}$, this value being more probably greater than lower with a standard error of ~ 0.09/cm, chiefly due to uncertainty in the photocathode efficiency.

The result is in good agreement with the theoretical value 0.50/ cm.

7·3. *Comparison with the theory developed in Sect.* 2·3. – We have taken into consideration the pulse height spectrum in the case of air (see Fig. 7) to study the average height of the pulses. The comparison of this spectrum with the spectrum of the lamp assures us that it is unlike that the average number of electrons in the pulses $\bar{N}_{\text{er}_\mu}$ may be greater than ~ 1.5 (and it cannot be lesser than 1).

For $\bar{N}_{\text{er}_\mu} = 1.5$ applying the theory developed in Sect. 2 3 (in particular using formulae (11) and (12)), we find the value $\eta_{M_\mu} = 0.52$ for the detector efficiency for particles that pass through the whole length of the tube.

The experimental value of $\eta_{M_\mu}(0.51 \pm 0.05)$ shows that in the experiment a good efficiency was obtained, with regard to the pulse height.

7·4. *Results with freon* 12. – The results with freon 12 have not been quantitatively examined because of the poor statistics, the possibility of instrumental errors and the uncertainty in the refractive index. However the results are sufficient to show a strong increase of the counting rates in comparison with air, expecially in the case of higher pulses. This proves that with freon 12 there is an increase in the frequency of the detected events, and an increase in the average height of the pulses, as it must be, owing to the higher refractive index.

7·5. *Considerations on the spurious coincidences.* – Previous experiments [2] were made without counters under lead and without anticoincidence counters. The frequency of the events with closed shutter or with inverted detector was of the same order as the frequency of the studied events. This fact may also be seen comparing with one another the frequencies of column *a* of Table I.

It was rather difficult in these experiments to reduce the frequency of such spurious coincidences to a negligible value.

As the frequency of chance coincidences is at most of the order of one in 4 days, the events with closed shutter or inverted detector may only be explained as due to showers, in which some particles hit the counters and one hits the photocathode and is directly revealed from the same.

This assumption is confirmed by the fact that a strong reduction is obtained eliminating the soft component showers with a lead absorber. Results with lead absorber, but without anticoincidence counters, are written in column *b* of Table I. We see that the fraction of spurious coincidences is reduced to $\frac{1}{4}$.

A stronger reduction is obtained adding the anticoincidence counters (column *d* of Table I). In this way the fraction of spurious coincidences is reduced to $\frac{1}{7}$.

The remaining rate with closed shutter or inverted detector (of the order of 1/7 hours) cannot be explained again as due to chance-coincidences, and therefore will be due to coincidences produced by special cases of showers.

8. – Conclusions.

The most important results are:

a) It is possible to use a photomultiplier in conditions in which each pulse due to one photoelectron is detected, while the background remains sufficiently small (see Sect. **4**).

b) The developed theory about Čerenkov-radiation detectors for gases shows the possibility of obtaining a high efficiency with not too big detectors,

(see Sect. 2), provided the photomultiplier is used in the above mentioned conditions.

In our experiments, using an 80 cm high detector, we have obtained nearly the same efficiency as BARKLAY and JELLEY ([3]) have obtained with a 6 m high detector, and this efficiency is in agreement with the developed theory (see Sections 3, 4, 5, 6, 7).

c) The quantity of light produced by Čerenkov effect is in agreement with Tamm's theory within the experimental errors (of the order of 23 %) (see Sect. 7).

* * *

We wish to express our gratitude to Professor G. WATAGHIN for his kind interest throughout this work. We also wish to thank Dr. Ing. F. CARELLO for having cared the construction of the parabolic mirror, and the operation of aluminising the inside of the mirror and of the reflecting tube in the laboratories of the Carello Fausto e C. Co. We thank also Mr. A. FERRERO for having operated the apparatus in our absence, in particular for having predisposed and accomplished the measurements with freon.

RIASSUNTO

Si studia in generale il problema della rivelazione mediante fotomoltiplicatori dell'effetto Čerenkov prodotto da singole particelle in gas. Si mostra che è possibile costruire rivelatori di dimensioni non eccessive aventi un elevato rendimento, purchè si riveli ogni impulso dovuto anche a un solo fotoelettrone. Si descrivono esperimenti che mostrano che è possibile usare un fotomoltiplicatore in tali condizioni, e che con un rivelatore ad aria a pressione atmosferica lungo 80 cm, è stato ottenuto un rendimento non inferiore a quello prevedibile con la teoria sviluppata. Questi esperimenti permettono inoltre una determinazione relativamente buona del numero di fotoni emessi, e il risultato è in buon accordo con la teoria di Tamm. Si riportano anche alcuni risultati ottenuti usando freon 12 invece di aria.

IL NUOVO CIMENTO Vol. VI, N. 6 1° Dicembre 1957

On the Nucleon-Nucleon Interaction with Energy Higher than 10^{14} eV.

P. Ciok, M. Danysz, J. Gierula, A. Jurak, M. Mięsowicz, J. Pernegr

Institute of Nuclear Research - Warsaw and Krakow

J. Vrána and W. Wolter

Physical Institute of the Czechoslovak Academy of Science - Prague

(ricevuto il 4 Agosto 1957)

Summary. — A jet $0+14\alpha$ of the energy $3.3\cdot10^{14}$ eV is described. It was found that the distribution of charged particles is asymmetric in center of mass system but becomes symmetric when the neutral particles have been taken in consideration. The information about the neutral particles was obtained from the development of the electronic component of the shower. The angular distribution in center of mass system is strongly anisotropic and near to Heisenberg's distribution. The energy of the secondary particles in center of mass system is of the order of a few GeV and transversal momenta given for two secondaries are of the order of several hundred MeV/c. The inelasticity coefficient is ~ 0.1.

1. – Description of the event.

In the course of systematic scanning for photon-electron cascades on $\frac{1}{3}$ of the I-stack of stripped emulsions irradiated on high altitude during the Po-Valley Expedition 1955 a jet $0+14\ \alpha$ of very high energy has been found. The two cones of the jet are very distinct; the narrow cone with the opening angle of some 10^{-4} radians contains 10 tracks, the diffuse cone with the opening angle of some 10^{-2} radians contains 4 tracks (Fig. 2). The length of the jet in one pellicle of the emulsion is about 3000 μm, the whole event is observable in 26 pellicles i.e. in the length of about 8 cm in our part of the block.

On this length two secondary interactions have been found (see Sect. 6). Besides these interactions of secondaries another interaction appears at the

point B (Fig. 1) in the narrow cone at the distance of about 4200 μm from A. In this part of the jet the individual tracks of the narrow cone are yet distinguishable and therefore the type of this interaction cannot be established with certainty. Measurements in about twenty cuts at distances between 6 and 40 mm from A have been made in order to construct target diagrams. From the latter and from the measurements of grain density in the vicinity of B we obtained the situation as presented in Fig. 1. It is not possible to decide whether the interaction B is of the type $0+3$ (n or p) or $0+4$ (n or p).

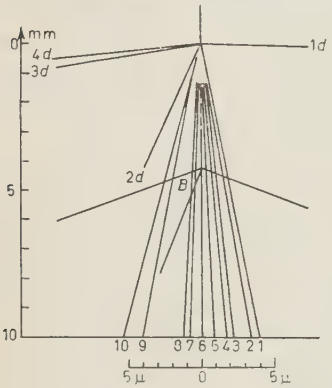

Fig. 1. – Event's drawing.

All the tracks of interaction B are within the cone with the opening angle 10^{-2} radians. From the fact that both jets (A and B) have a similar angular divergence it may be concluded that their energies are also comparable and that they probably are produced by the interaction of two nucleons of the same primary α-particle. This assumption is also supported by the fact that the direction of one of the tracks (No. 6) crosses accurately both points A and B. Assuming this interpretation as correct and using the principle of charge conservation, we conclude that it is most likely that 12 particles were produced in interaction A and 2 charged particles in interaction B. Track No. 6 which we assume as the axis of both jets and one of the tracks from jet A have been therefore excluded from the analysis of particles produced in jet A. The very small multiplicity of produced particles in the interaction B is rather unusual.

2. – Measurements of angles.

The angles have been measured on all tracks in relation to track No. 6 which represents the assumed direction of flight of the primary α-particle. The results of these measurements are given in Table I.

3. – Electron pairs.

The scanning for pairs of charged particles was made in a cone of 0.14 radians covering the whole jet to the distance of 6 cm from A. Further scanning was difficult because of the large development of the cascades in this region. The distribution of the distances between each pair and the nearest

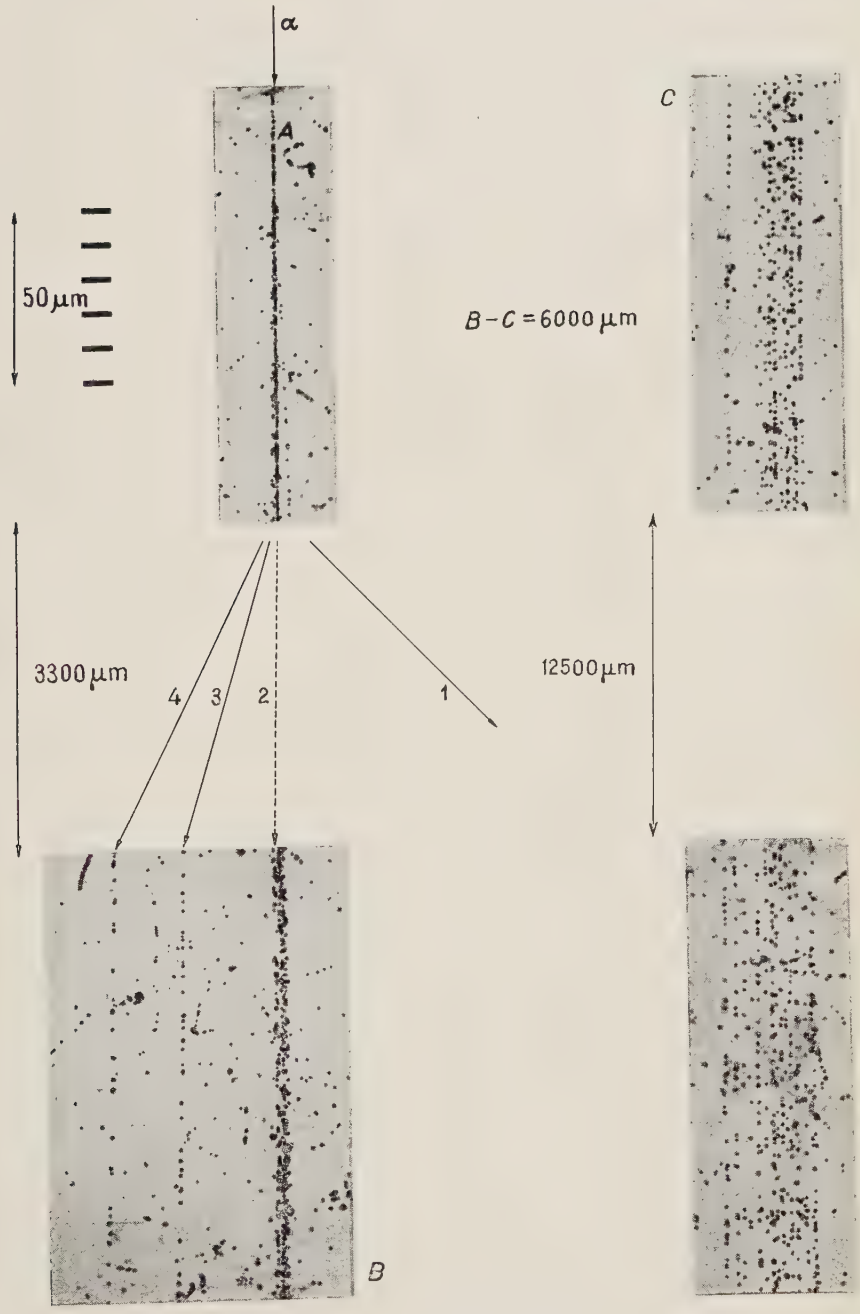

Fig. 2. – Event's microphotography.

TABLE I. – *The angular distribution of tracks.*

No.	θ (rad) angle in L. system	$\bar{\theta}$ angle in C.M. system transformed with $\gamma = 420$	Secondary interactions
6	axis		
7	$0.7 \cdot 10^{-4}$	3.3°	
5	$1.1 \cdot 10^{-4}$	5.3°	0+16p, $E_p = 2 \cdot 10^{12}$ eV
8	$1.8 \cdot 10^{-4}$	8.6°	
2	$3.7 \cdot 10^{-4}$	17.7°	
1	$3.9 \cdot 10^{-4}$	18.5°	
9	$4.2 \cdot 10^{-4}$	20.0°	
4	$4.8 \cdot 10^{-4}$	22.8°	
10	$5.4 \cdot 10^{-4}$	25.5°	3+18p, $E_p = 1 \cdot 10^{12}$ eV
3	$10.0 \cdot 10^{-4}$	41.5°	
2*d*	$0.8 \cdot 10^{-2}$	154.5°	
4*d*	$1.6 \cdot 10^{-2}$	164.3°	
3*d*	$1.9 \cdot 10^{-2}$	166.5°	
1*d*	$5.1 \cdot 10^{-2}$	174.7°	

TABLE II. – *Electron pairs.*

No.	x (μm) distance of the origin of the pair from the beginning of the jet	the angular θ (rad) coordinate of the origin of the pair	Energy (eV) of the pair
1	415	$6.0 \cdot 10^{-2}$	$1 \cdot 10^{9}$
2	6120	$0.9 \cdot 10^{-2}$	$2 \cdot 10^{10}$
3	7200	$0.4 \cdot 10^{-2}$	$6 \cdot 10^{9}$
4	7600	$1.3 \cdot 10^{-2}$	$8 \cdot 10^{9}$
5	17780	$2.3 \cdot 10^{-2}$	$4 \cdot 10^{10}$
6	23460	$0.2 \cdot 10^{-2}$	$2 \cdot 10^{10}$
7	29400	$3.0 \cdot 10^{-2}$	$5 \cdot 10^{9}$
8	34680	$0.2 \cdot 10^{-2}$	$3 \cdot 10^{10}$
9	36800	$0.9 \cdot 10^{-2}$	$2 \cdot 10^{9}$
10	38070	$0.4 \cdot 10^{-2}$	$2 \cdot 10^{10}$
11	51070	$0.4 \cdot 10^{-2}$	$5 \cdot 10^{8}$
12	28010	$9.4 \cdot 10^{-4}$	$3 \cdot 10^{12}$
13	33880	$1.8 \cdot 10^{-4}$	$1 \cdot 10^{12}$
14	37330	$6.8 \cdot 10^{-4}$	$6 \cdot 10^{11}$
15	43760	$6.9 \cdot 10^{-4}$	$7 \cdot 10^{11}$

electron track was analysed in order to distinguish the bremsstrahlung pairs. From the 15 pairs found, one is considered to be a bremsstrahlung pair (No. 11). In Table II the following data on the pairs are summarised: the distance of the point of origin of each pair from the beginning of the jet (x), the angle θ in relation to the axis of the jet, the energy of each pair which was estimated from profile measurements along the track.

The energies of rather low energetic pairs ($\sim 10^9$ eV) were evaluated according to Borsellino's formula $\omega_{\prime\prime}=4\,mc^2/E_{\mathrm{ph}}$ [1], assuming equiparation of energy. For pairs of higher energy the influence of scattering was taken into account [2]. The energies of pairs No. 12-15 (Table II) producing electron-photon cascades were additionally estimated from the analysis of these cascades.

4. – Number of charged and neutral particles.

In the diffuse cone scanned for a length of 6 cm 11 pairs were found. As was stated above we assume that from these 11 pairs only one (No. 11) is a secondary bremsstrahlung pair. Assuming that the pairs were produced by photons emitted at the points A and B of the interaction, and taking for the conversion length the value 3.75 cm, we have calculated that 14 photons are emitted in the diffuse cone from interactions A and B. In the narrow cone 4 pairs were found for the same length of scanning. Considering a small correction for the finite average length of flight of π^0-meson of energy of about $5\cdot 10^{12}$ eV (about 1 cm, assuming $\tau_{\pi^0}\approx 10^{-15}$ s) we obtain the number of about 3 π^0-mesons emitted in the narrow cone. We can therefore obtain the following numbers of particles emitted in the narrow and in the diffuse cones:

	Narrow cone	Diffuse cone
Charged particles	8 ÷ 10	4 ÷ 6
π^0-mesons	3	7
Total	11 ÷ 13	11 ÷ 13

The apparent assymmetry in the number of particles in the diffuse and narrow cones therefore disappears if we take into consideration not only the charged but also the neutral particles. The rather high value (between 0.7 and 0.8) of the ratio $R=\pi^0/(\pi^{\pm}+\mathrm{K}^{\pm})$ is noticeable.

[1] A. Borsellino: *Phys. Rev.*, **89**, 1023 (1953).
[2] E. Lohrmann: *Nuovo Cimento*, **2**, 1029 (1955).

5. – Evaluation of the primary energy.

In many papers dealing with jets the method of $\theta_{\frac{1}{2}}$ angle is used for estimation of the primary particle energy ($\theta_{\frac{1}{2}}$ is the half angle of the cone containing half of the emitted particles). If we assume the symmetrical angular distribution in the center of mass system, we can evaluate the angle $\theta_{\frac{1}{2}}$ as the geometrical mean value of all laboratory angles of a given jet. For isotropic and monoenergetic distribution in center of mass system we can estimate the value of γ (the energy of the nucleon in center of mass system), for cases of small laboratory angles, simply taking $\gamma = 1/\theta_{\frac{1}{2}}$. The method described above is in this case equivalent with the often used first approximation of the Castagnoli's [3] method ($\ln \gamma = \ln \cot \theta_{\frac{1}{2}}$). However, if we have jets with anisotropic or not monoenergetic distribution we can only in special cases [4,5] calculate the γ values from $\theta_{\frac{1}{2}}$ in a simple way. For instance for a strong anisotropic angular distribution which follows from Heisenberg's theory and which should be valid for $\gamma > 20$, the primary energy calculated by $\theta_{\frac{1}{2}}$ must be reduced by a factor 0.5, i.e. $\gamma = 0.5/\theta_{\frac{1}{2}}$. Information about the type of distribution in the center of mass system can be obtained from the integral angular distribution $F(\theta)$ in the laboratory system by plotting $\log F(\theta)/(1-F(\theta))$ vs. $\log \operatorname{tg} \theta$ [6]. These plots are straight lines for typical distributions, for example for isotropic distribution or Heisemberg of Landau distributions. The last two distributions differ from the isotropic one by their slopes.

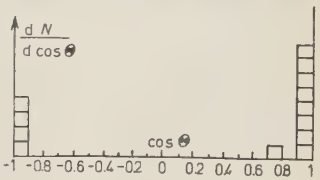

Fig. 3. – Circles - the integral angular distribution of charged particles in L-system. The stright Line corresponds to Heisenberg's distribution for $\gamma = 420$.

The $\log F/(1-F)$ vs. $\log \operatorname{tg} \theta$ for our case is given on Fig. 3 (circles). The straight line corresponds to Heisenberg's distribution for $\gamma = 420$. Taking into account the asymmetry of emission of charged particles, discussed in Sect. 4, we may explain the deviation of experimental points from linearity by lack of charged particles in the diffuse cone. This means that our distribution is near to Heisenberg's and so we are able to use the formula $\gamma = 0.5/\theta_{\frac{1}{2}}$. It is also evident that the angular distribution in the narrow cone is most representative for the distribution in the whole jet. Therefore the value of $\theta_{\frac{1}{2}}$ can be obtained by plotting a straight line with Heisenberg's slope on the experimental points of the narrow cone only. Thus we take for the total number of charged particles the double number of tracks in the narrow cone. From

(3) C. Castagnoli, G. Cortini, C. Franzinetti, A. Manfredini and D. Moreno: *Nuovo Cimento*, **10**, 1539 (1953).

(4) K. Symanzik in W. Heisenberg: *Kosmische Strahlung*, **2**, 7 (Berlin, 1953).

(5) L. v. Lindern: *Zeits. f. Naturfor.*, **11***a*, 340 (1956).

(6) N. M. Duller and W. D. Walker: *Phys. Rev.*, **93**, 215 (1954).

this procedure we obtain the value of $\theta_{\frac{1}{2}}=1.2\cdot10^{-3}$ and $\gamma=420$ with the limits of statistical errors $^{+280}_{-180}$ calculated for Heisenberg's distribution according to the formula $\Delta\log\gamma=0.7/\sqrt{n_s}$ (5). This corresponds to the energy of the primary α-particle $3.3\cdot10^{14}$ eV/nucleon.

It is worth noting that the direct calculation of γ from the data in Table I gives a not much differing value of 460. If we consider the necessarity of rejecting one track and do this for every track successively we obtain the lower and the upper limits of $\gamma-370$ and 645 respectively. These values are in the limits of statistical errors of the value $\gamma=420$, which we consider as the most probable.

6. – Secondary interactions.

Besides the interaction B which was attributed to one nucleon of the primary α-particle, there have been found in the narrow cone of the jet two interactions of secondaries: Interaction $(0+16p)$ on track No. 5 and interaction $(3+18p)$ on the track No. 10. The energy of the primaries of these interactions estimated from the angular distribution amounts to $2\cdot10^{12}$ eV and $\sim1\cdot10^{12}$ eV respectively. From these measurements as well as from the energies of the observed pairs it appears that the mean energy of the particles in the narrow cone can be considered as $\sim2.3\cdot10^{12}$ eV. In the diffuse cone this value based on the energy evaluation of the pairs would be $3\cdot10^{10}$ eV. Taking these values and $\gamma=420$ we can construct the distribution in center of mass system (Table I and Fig. 4) by means of the formulae given in the paper of SCHEIN et al. (7). The energies of the secondary particles in center of mass were calculated on the same basis and are of the order of few GeV. The estimation of energy of the secondary interactions and of the electron pairs permitted the evaluation of the fraction of energy transferred by the primary nucleon to the produced particles. This fraction is ~0.1. At present we have information about transversal momenta of only few particles. As examples we can give the transversal momenta of the interacting particles No. 5 and No. 10 which are 220 MeV/c and 540 MeV/c respectively.

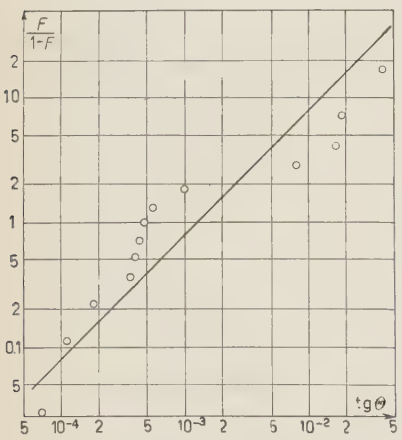

Fig. 4. – Angular distribution in C.M. system.

(7) M. SCHEIN, R. G. GLASSER and D. M. HASKIN: *Nuovo Cimento*, **2**, 647 (1955).

7. – Conclusions.

From this investigation we see that for energies $\sim 10^{14}$ eV pro nucleon the analysis of the electron component give us very valuable information. The investigation of the electron component completes the analysis of the angular distribution and together with the analysis of secondary interactions gives us in the above described case of a very high energy nucleon-nucleon interaction a rather consistent picture. We see from our example that we could improve our knowledge of the distribution in emission of particles in the center of mass system. In this region of primary energies ($\sim 10^{14}$ eV), where we could expect the energies of secondaries of 10^{10} eV or more, the scattering measuraments are of limited meaning and the investigation of the electron component is of great value.

Summarising the results from the above described event we conclude:

1) The distribution of charged particles is asymmetric in respect to the median plane in the center of mass system (Fig. 4), but it becomes symmetric when we take also the neutral particles in consideration. This information coud be obtained by investigation of the electron component of the shower. The rather high fluctuation in the distribution of charged particles is noticeable.

2) The angular distribution in the center of mass system is strongly anisotropic.

3) The energy of secondary particles in the center of mass system is of the order of a few GeV.

4) The inelasticity coefficient is approximately 0.1.

* * *

The authors wish to express their thanks to Mrs. H. Mosz and Miss Z. Czachowska for their help in following and measuring the electron cascades and to Mr. T. Coghen for help in the course of this investigation.

RIASSUNTO (*)

Si descrive un getto $0+14\alpha$ di energia $3.3 \cdot 10^{14}$ eV. Si è trovato che la distribuzione delle particelle cariche è asimmetrica nel sistema del centro di massa, ma diventa simmetrica se si considerano le particelle neutre. Le informazioni sulle particelle neutre furono ottenute dallo sviluppo della componente elettronica dello sciame. La distribuzione angolare nel sistema del centro di massa è fortemente anisotropica e prossima alla distribuzione di Heisenberg. L'energia delle particelle secondarie nel sistema del centro di massa è dell'ordine di qualche GeV e i momenti trasversali dati per due secondari sono dell'ordine di parecchie centinaia di MeV/c. Il coefficiente di inelasticità è ~ 0.1.

(*) *Traduzione a cura della Redazione.*

IL NUOVO CIMENTO Vol. VI, N. 6 1° Dicembre 1957

The Study of Polarizations of Secondary Muons in K-Meson Decay Processes.

S. Furuichi, S. Sawada and M. Yonezawa

Department of Physics, Hiroshima University - Hiroshima

(ricevuto il 6 Agosto 1957)

Summary. — To get the knowledge of weak interactions acting in the K-meson decay processes having the muons in their decay products, the authors have investigated the polarization of the emitted muons in these processes, taking the view-point that the weak Fermi interaction is participating for the decay processes and the neutrino associated is of two components. For the determination of the type of weak interaction in $K_{\mu 3}$-meson it is useful to analyse the longitudinal polarization of muons. Although our main interest is in the type determination of weak interactions, we also examine the spin of the K-meson and our analysis shows that the polarization of muons is in general not complete for spin 1 $K_{\mu 2}$-mesons in contrast with spin 0 $K_{\mu 2}$-mesons.

1. – Introduction.

About the various weak processes the peculiarity of the magnitude of the weak interaction—the effective coupling constants of almost all decay processes are falling in a confined region irrespectively of the mode of the weak process—has been noticed [1]. Basing on this suggestive fact several investigations have been performed, which are titled as « Universality of weak Interaction » [2].

[1] S. Ogawa: *Prog. Theor. Phys.*, **13**, 1387 (1955).

[2] O. Klein: *Nature*, **161**, 897 (1948); K. Iwata, S. Ogawa, H. Okonogi, B. Sakita and S. Oneda: *Prog. Theor. Phys.*, **13**, 19 (1955); A. Wakasa and S. Oneda: *Nuclear Physics*, **1**, 445 (1956); S. Ogawa: *Prog. Theor. Phys.*, **10**, 487 (1956); S. Gotô: *Prog. Theor. Phys.*, **17**, 107 (1957); Ref. [1].

SOCIETÀ ITALIANA DI FISICA

TERZO CONGRESSO INTERNAZIONALE SUI FENOMENI D'IONIZZAZIONE NEI GAS

tenuto a Venezia dall'11 al 15 giugno 1957

RENDICONTI

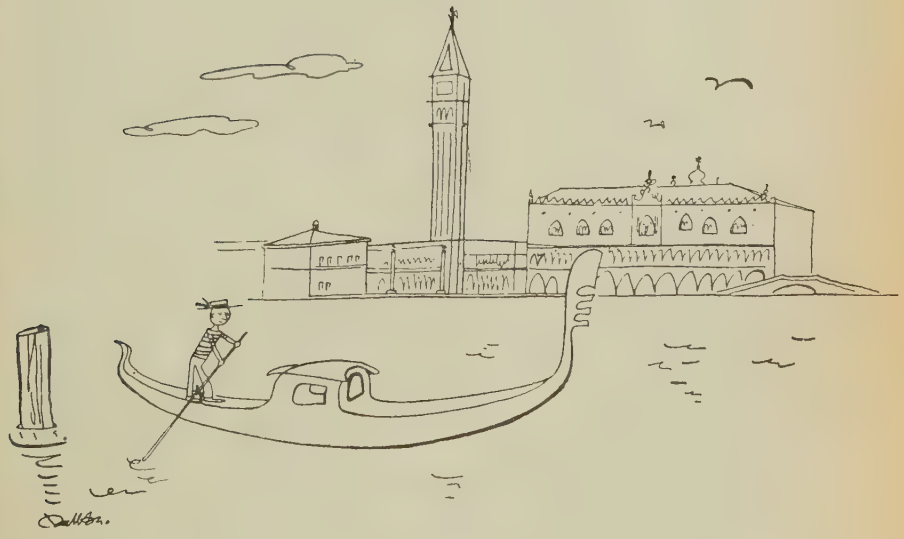

MILANO OTTOBRE 1957

SOCIETÀ ITALIANA DI FISICA

RENDICONTI
DEL
III CONGRESSO INTERNAZIONALE
SUI
FENOMENI DI IONIZZAZIONE NEI GAS

Venezia, 11-15 Giugno 1957

Questi *Rendiconti* sono pubblicati in edizione ciclostilata. Le bozze sono state rivedute dagli Autori e molte figure sono state riprodotte tipograficamente. Il volume è stato apprestato con molta cura. Non si prevede di pubblicare i *Rendiconti* in edizione tipografica: il volume ciclostilato costituisce quindi l'edizione definitiva dei *Rendiconti*. Esso è preparato solo in 400 esemplari.

Il volume è posto in vendita a $ 12 o equivalentemente a L. 7 500 la copia: nel prezzo sono comprese le spese postali di spedizione raccomandata. Chi desidera acquistare il volume è pregato di inviare la somma suddetta, a mezzo assegno bancario o vaglia postale, al seguente indirizzo:

prof. UGO FACCHINI
presso la Società Italiana di Fisica
Via Saldini, 50 Milano

e indicare chiaramente a quale indirizzo va spedito il volume.

Taking the view point that all weak processes are realized by the weak Universal Fermi Interaction, the most promising one which can produce any kind of weak interactions (weak Boson-Fermion Interaction etc.), the authors have studied the workability of this model and some analyses have been performed of the decay processes $K_{\mu 3}$ and K_{e3} ([3,4]). The analyses have been carried out about their secondaries' energy spectra and angular correlations.

Recently it became clear that the invariance law for space reflection is violated in the weak decay processes accompanying the neutrino ([5]) (β-decay, π-μ-decay and μ-e-decay), and the experimental data show us that the violation of parity conservation occurs as maximum asymmetry. From these experimental information LEE and YANG have proposed the two component theory of the neutrino ([6]). The agreement of the experimental data with this theory seems to be rather satisfactory at present and the theory is very attractive in understanding the reason of the vanishing small mass of the neutrino. We shall base our analysis on this theory.

Now if the neutrinos in $K_{\mu 2}$, $K_{\mu 3}$ and K_{e3} decay processes are of the two-component type, the parity non-conservation is also observed in these events. Then the resulting muons are in general polarized. If the $K_{\mu 2}$ meson is a spin 0 particle, the polarization of the secondary muon is, as noted by LEE and YANG ([7]), complete, while in the case of spin 1 $K_{\mu 2}$ the polarization is generally not complete and dependent on the decay interaction. A similar situation is also expected in the $K_{\mu 3}$ and K_{e3} processes. If we pick up the very low energy muons, these muons might show a nearly complete polarization along the direction of the neutrino momentum in the case of spin 0 $K_{\mu 3}$. Further, when we take the polarization in the direction of the muon propagation, we shall find that it is critically dependent on the interaction taking place. Thus the investigation of the polarization of the secondary muon will serve to clarify the type of weak interaction.

We have proceeded to analyse the energy spectrum of the secondary muon

([3]) S. FURUICHI, T. KODAMA, S. OGAWA, Y. SUGAHARA, A. WAKASA and M. YONEZAWA: *Prog. Theor. Phys.*, **17**, 89 (1957).

([4]) S. FURUICHI: *Nuovo Cimento* (to be published).

([5]) C. S. WU, E. A. AMBLER, R. W. HAYWARD, D. D. HOPPES and R. P. HUDSON: *Phys. Rev.*, **105**, 1913 (1957); R. L. GARWIN, L. M. LEDERMAN and M. WEINRICH: *Phys. Rev.*, **105**, 1415 (1957); J. I. FRIEDMAN and V. L. TELEGDI: *Phys. Rev.*, **105**, 1681 (1957); A. ABASHIAN, R. K. ADAIR, R. COOL, A. ERWIN, J. KOPP, L. LEIPNER, T. W. MARRIE, D. C. RAHN, R. R. RAW, A. M. THORNDIKE and W. L. WHITTEMORE: *Phys. Rev.*, **105**, 1927 (1957); H. FRAUENFELDER, R. BOBONE, E. VON GOELER, N. LEVINE, H. R. LEWIS, R. N. PEACOCK, A. ROSSI and G. DE PASQUALI: *Phys. Rev.*, **106**, 386 (1957).

([6]) T. D. LEE and C. N. YANG: *Phys. Rev.*, **105**, 1671 (1957).

([7]) Ref. ([5]).

in the $K_{\mu 3}$-events ([8]). Unfortunately, the obtained experimental spectrum is not so well determined owing to the scanning difficulty of the experimental detection of the secondary muon, in contrast with the electron spectrum in K_{e3}-events ([9]). So it seems to be very difficult to give a conclusive assertion for the particular type of interaction for the $K_{\mu 3}$ case. However, the polarization of the muon will be found to be more critically dependent on the type of interaction than its energy distribution. Hence the investigation of the polarization in the $K_{\mu 3}$ process will be a good tool to make clear the decay interaction.

In this paper we shall make the analysis mainly of the polarization of muons in (spin 0) $K_{\mu 3}$ processes for the purpose of decay interaction analysis. The measurement of polarization of secondary muons seems to be rather easy by means of μ-e angular correlation measurements. Besides the investigation of decay interaction we shortly discuss the spins of $K_{\mu 2}$ and $K_{\mu 3}$ mesons from the polarization of muons. We shall give the expressions for polarization in Sect. 3 and some features of the polarization will be discussed there. The polarized muon will experience depolarization in slowing down in the matter. The magnitude of the depolarization is intimately connected with the experimental possibility of the present analysis. We discuss this problem briefly in Sect. 4.

2. – Matrix elements.

In the following analysis we assume the decay modes as $K^+_{\mu 3} \to \mu^+ + \bar{\nu} + \pi^0$ and $K^+_{\mu 2} \to \mu^+ + \bar{\nu}$, and the neutrino to be of two-component. The application of the information obtained about these processes to other modes ($K^+_{\mu 3} \to \mu^+ + \nu + \pi^0$ etc.) is simple and immediate.

In the derivation of the matrix elements we make the assumption that the lepton interaction is a point interaction ([10]) (which stands for our assumption that the weak Fermi interaction between baryon and lepton is participating in the decay). No further restriction other than this point interaction assumption for lepton interaction as well as proper Lorentz invariance requirements is imposed for the transition matrix.

There is no direct suggestion as to the spin of the $K_{\mu 3}$-meson. However current experiments about 0, τ and K_{e3}-mesons strongly indicate that these particles

([8]) S. FURUICHI, Y. SUGAHARA, A. WAKASA and M. YONEZAWA: *Nuovo Cimento*, **5**, 285 (1957).

([9]) Ref. ([8]); C. ALEXANDER, R. H. W. JOHNSTON and C. O'CEALLAIGH: private communication. We thank Prof. C. O'CEALLAIGH for his sending the manuscript before publication.

([10]) In the sense of Feynman diagram.

are spin 0 particles ([11]), and it is highly probable that these particles (decay modes) are the alternative decay modes of $K_{\mu 3}$-meson. We proceed in the analysis assuming that the $K_{\mu 3}$-meson is a spin 0 particle. The application of the present method to the high spin case is immediate, but the number of independent types of interaction is much increased and the expression becomes too lengthy and is of no practical use.

For the spin 0 $K_{\mu 3}$-meson the effective transition matrix is given by

$$(1) \qquad M \sim F_{\mathrm{S}}\bar{\psi}^{(\mu)}(p)\psi^{(\nu)}(q)\Phi(k)\varphi^{*}(l) + F_{\mathrm{V}}\bar{\psi}^{(\mu)}(p)\gamma_{\mu}\psi^{(\nu)}(q)k_{\mu}\Phi(k)\varphi^{*}(l) + \\ + F_{\mathrm{T}}\bar{\psi}^{(\mu)}(p)\,(\gamma_{[\mu}\gamma_{\nu]}/2)\psi^{(\nu)}(q)k_{\mu}(p+q)_{\nu}\Phi(k)\varphi^{*}(l)\,,$$

where $\Phi(k)$, $\varphi(l)$, $\psi^{(\mu)}(p)$ and $\psi^{(\nu)}(q)$ are the wave function of K-meson, pion, muon and neutrino, and k_λ, l_λ, p_λ and q_λ are their 4-momenta respectively. The two component wave function $\psi^{(\nu)}$ is safely replaced by $\frac{1}{2}(1-\gamma_5)\varphi^{(\nu)}$ where $\varphi^{(\nu)}$ is the ordinary 4-component neutrino wave function. F's are the invariant functions of independent momenta. Here k_λ and $(p+q)_\lambda$ are taken as two independent momenta.

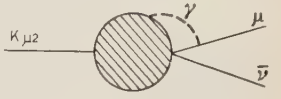

Fig. 1. – Diagram for the high spin (> 1) $K_{\mu 2}$ decay. Waved line denotes the photon.

Here we also give the matrix elements for the $K_{\mu 2}$-meson. Under the assumption of the point interaction for leptons, the $K_{\mu 2}$-meson with its spin higher than 1 can decay only through the diagram in Fig. 1 which violates the one point interaction assumption for leptons, and in this case it seems to be very difficult to reconcile the theoretical calculation to the observed life-time and branching ratio. As for the $K_{\mu 2}$-meson our interests are mainly in the relation between spin and polarization. So we take the cases of spin 0 and 1 for this meson.

The matrix elements are given as:

Spin 0 $K_{\mu 2}$

$$(2a) \qquad M \sim F'_{\mathrm{S}}\bar{\psi}^{(\mu)}(p)\psi^{(\nu)}(q)\,\Phi(k)\,.$$

Spin 1 $K_{\mu 2}$

$$(2b) \qquad M \sim F'_{\mathrm{V}}\bar{\psi}^{(\mu)}(p)\gamma_{\mu}\psi^{(\nu)}(q)\,\Phi_{\mu}(k) + F'_{\mathrm{T}}\bar{\psi}^{(\mu)}(p)\,(\gamma_{[\mu}\gamma_{\nu]}/2)\psi^{(\nu)}(q)k_{\mu}\Phi_{\nu}(k)\,.$$

It is necessary for the computation to introduce the spin projection operator in the direction ξ for Dirac particles (muons). This was given by Tol-

([11]) See, for example, Y. Eisenberg, E. Lomon and S. Rosendorf: *Nuovo Cimento*, **4**, 610 (1956); J. Orear: *Phys. Rev.*, **106**, 834 (1957); W. D. Walker and W. D. Shephard: *Phys. Rev.*, **101**, 1810 (1956); Ref. ([8]).

HOECK [12] and its covariant form is

$$\sum(\xi) = \tfrac{1}{2}(1 + i\gamma_5\gamma_\mu s_\mu)\,, \tag{3}$$

where $s_\mu = (\boldsymbol{s}, is_0)$ is

$$\begin{cases} \boldsymbol{s} = \xi + \dfrac{\boldsymbol{p}(\xi\cdot\boldsymbol{p})}{m_\mu(p_0 + m_\mu)} \\ s_0 = \dfrac{\xi\cdot\boldsymbol{p}}{m_\mu} \end{cases} \tag{4}$$

and $p_\mu = (\boldsymbol{p}, ip_0)$ is the momentum-energy of muon and m_μ is its mass. It is noted that $s_\mu p_\mu = 0$. For the case of $\xi = \boldsymbol{p}/p$ (the muon propagation direction) $\sum$ is reduced to the familiar form

$$\sum(\boldsymbol{p}/p) = \tfrac{1}{2}(1 + \boldsymbol{\sigma}\cdot\boldsymbol{p}/p)\,. \tag{5}$$

It can be easily seen that $\sum(\xi)$ commute with the Dirac projection operator and Hamiltonian of the free Dirac field.

The polarization along the direction, ξ, $P(\xi)$ (precisely speaking, $P(\xi)$ is the « degree of polarization »: in the following we abbreviate it simply « polarization ») is defined as

$$P(\xi) = \frac{a(\xi) - a(-\xi)}{a(\xi) + a(-\xi)}\,, \tag{6}$$

where $a(\xi)$ is the transition probability to a final state with muons polarized in the direction of ξ and $a(-\xi)$ is the corresponding one in the reversed direction $-\xi$.

If the polarization measurement is performed in terms of μ-e angular correlation the expression of the angular distribution of the emitted electrons from muons with polarization P is given by [13]

$$N(\cos\theta)\,\mathrm{d}\theta = (1 + P\alpha\cos\theta)\,\mathrm{d}\theta, \tag{7}$$

where

$$\alpha = \frac{1}{3}\frac{2\,\mathrm{Re}\,[C_\mathrm{V}C_\mathrm{A}^*]}{C_\mathrm{V}'^2 + C_\mathrm{A}'^2}\,,$$

and θ is the angle between the momentum of the electron and the polarization direction of the muon.

[12] H. A. TOLHOECK: *Rev. Mod. Phys.*, **28**, 277 (1956).
[13] Ref. [7].

3. – Expressions of polarization and discussions.

In this section we give the expressions of polarization of the secondary muon with the matrix element given in the preceeding section. As noted before, our main intention is to supply the information which may be useful for the determination of the interaction type of (spin 0) $K_{\mu 3}$ decay process.

There may be two directions along which the measurement of the polarization of muon produces fruitful results, the neutrino- and muon-propagation direction. For the determination of the type of interaction, it seems convenient to take the polarization along the direction of the muon momentum, since this dependence of the polarization on the type of interaction is more prominent than the one along the direction of the neutrino momentum and in the later case the experimental confirmation of the neutrino direction is also required in each of the events. Thus we discuss the longitudinal polarization of the muon.

3·1. *Polarization of the muon for a fixed muon momentum and* μ-ν *angle in the* $K_{\mu 3}$ *case.* – First we discuss the polarization of the muon for a fixed muon momentum and muon-neutrino angle. The expression of polarization is given by

$$P(\boldsymbol{p}/p,\, p_0,\, \theta) =$$

$$= [-F_S^2 A + F_V^2 m_K^2 B + F_T^2 m_K^2 C + 2\,\mathrm{Im}\,(F_S F_V^*) m_K m_\mu \cos\theta - 2\,\mathrm{Re}\,(F_S F_T^*) m_K D +$$

$$+ 2\,\mathrm{Im}\,(F_V F_T^*) m_K^2 m_\mu E][F_S^2 a + F_V^2 m_K^2 b + F_T^2 m_K^2 c + 2\,\mathrm{Im}\,(F_S F_V^*) m_K m_\mu +$$

$$+ 2\,\mathrm{Re}\,(F_S F_T^*) m_K d + 2\,\mathrm{Im}\,(F_V F_T^*) m_K^2 m_\mu e]^{-1},$$

$$A = p - p_0 \cos\theta, \qquad a = p_0 - p\cos\theta,$$

$$B = p + p_0 \cos\theta, \qquad b = p_0 + p\cos\theta,$$

$$C = p^2(p_0\cos\theta - 2q\cos\theta - p) + 2p_0 pq + q^2(p_0\cos\theta - p),$$

$$c = p^2(p_0 - 2q - p\cos\theta) + q^2(p_0 - p\cos\theta),$$

$$D = p(q - p_0) + (p^2 - p_0 q)\cos\theta, \qquad d = (p_0 q - p^2)\cos\theta + (p_0 - q)p\cos\theta,$$

$$E = p + q\cos\theta, \qquad e = q + p\cos\theta,$$

where θ is the angle between the muon and neutrino momenta. q is the magnitude of the neutrino momentum and is given by $m_K(W - p_0)(m_K - p_0 + p\cos\theta)^{-1}$

and $W = (m_K^2 + m_\mu^2 - m_\pi^2)(2m_K)^{-1}$, where m_K and m_π are the masses of K-meson and pion respectively.

The apparent advantage of this expression is that we do not need the details of structure of the invariant functions F in the calculation, while its disadvantage is that the neutrino propagation direction is required to be known in the experiment for comparison with theory. Such an experiment in order to detect the secondary neutral pion and hence determine the neutrino direction is in progress [14]. But it may take much time before it produces available data. In Fig. 2 we show the energy dependence of polarization for a pure interaction S, V and T [15] at angle $\theta = 90°$ and $160°$.

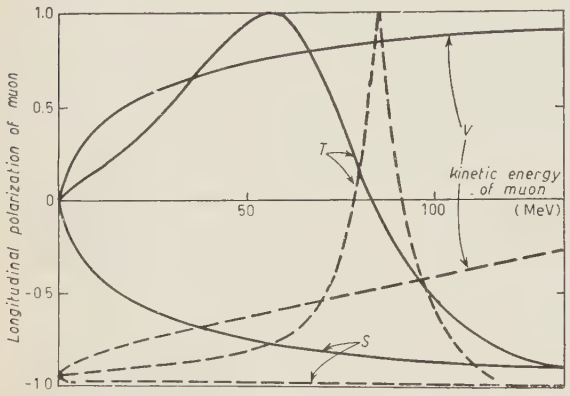

Fig. 2. – The dependence of polarization on energy. The curves are given for pure interaction S, V and T of spin 0 $K_{\mu 3}$. Angles are 90° and 160°. The solid line is for 90° and the dashed line is for 160°.

In the case of the energy spectrum or the angular correlation the most dominant contribution is that of the final state density while in the case of polarization the behavior is completely determined by the matrix element. This is the reason why the analysis of polarization may be considered to be useful for the determination of interaction.

3·2. *Polarization integrated over the* μ-ν *angle in the* $K_{\mu 3}$-*case.* – In the comparison of the preceeding calculation with experiment, it is necessary to determine the neutrino propagation direction. This task, however, is not so easy. The experimental technique is somewhat restricted. For example a large bubble chamber must be used and a large number of events must be accumulated.

The practically most useful analysis will be that of the polarization integrated over the μ-ν angle. In the calculation of integrated polarization, the information or the assumption about F is required.

We approximate it by a momentum independent constant as in our previous

(14) D. I. MAYER: Private communication.

(15) The terms scalar (S), vector (V) and tensor (T) should not be taken literally, since « scalar » contains scalar and pseudoscalar interactions in the ordinary sense. However we use it for simplicity.

discussions of energy spectra ([16]). This approximation may be less serious for the polarization calculation than for that of the energy distribution owing to the definition (6) of polarization itself. The integrated longitudinal polarization of muon is given by

$$
\begin{aligned}
P(\boldsymbol{p}/p,\, p_0) = \\
&= [-F_S^2\{(m_K p_0 - m_\mu^2)I_3 - p_0 I_2\} + F_V^2 m_K^2\{(2p_0^2 - m_\mu^2 - m_K p_0)I_3 + p_0 I_2\} - \\
&- F_T^2 m_K^2\{m_K^2(m_K p_0 - m_\mu^2)(W - p_0)^2 I_5 - m_K^2(W p_0 + p_0^2 - 2m_\mu^2)(W - p_0)I_4 + \\
&+ p^2(2m_K W - m_K p_0 - m_\mu^2)I_3 - p_0 p^2 I_2\} - \\
&- 2\ \mathrm{Im}\ (F_S F_V^*) m_K m_\mu\{(m_K - p_0)I_3 - I_2\} - \\
&- 2\ \mathrm{Re}\ (F_S F_T^*) m_K\{m_K(m_K p_0 - m_\mu^2)(W - p_0)I_4 - m_K(W p_0 - m_\mu^2)I_3 + p^2 I_2\} + \\
&+ 2\ \mathrm{Im}\ (F_V F_T^*) m_K^2 m_\mu\{m_K(m_K - p_0)(W - p_0)I_4 - (p^2 + m_K W - m_K p_0)I_3\}] \cdot \\
&\cdot\ p^{-1}[F_S^2(m_K^3 I_3 - I_2) + F_V^2 m_K^2\{(2p_0 - m_K)I_3 + I_2\} + \\
&+ F_T^2 m_K^2\{m_K^3(W - p_0)^2 I_5 - m_K(m_K W + m_K p_0 - 2m_\mu^2)(W - p_0)I_4 + \\
&+ m_K(2p_0 W - p_0^2 - m_\mu^2)I_3 - p^2 I_2\} + 2\ \mathrm{Im}\ (F_S F_V^*) m_K m_\mu I_3 + \\
&+ 2\ \mathrm{Re}\ (F_S F_T^*) m_K\{m_K^2(W - p_0)I_4 - (m_K W - m_\mu^2)I_3 + p_0 I_2\} - \\
&- 2\ \mathrm{Im}\ (F_V F_T^*) m_K^2 m_\mu\{m_K(W - p_0)I_4 - (m_K - p_0)I_3 + I_2\}]^{-1},
\end{aligned}
$$

where

$$
I_n = \int_0^\pi p \sin\theta\, \mathrm{d}\theta\, (m_K - p_0 + p\cos\theta)^{-n}\,.
$$

([15]) In connection with this approximation it should be noted that our intention is to explain the various experimental data by the most simple form of interaction and by the least number of parameters. As presented in our previous paper our discussion on the energy spectrum starts from the assumption that the invariant function can be expanded as

$$
F = a + b(p + q)_\mu k_\mu / M^2 + \dots\,,
$$

and the convergence of this expression is so good that it can be replaced by the first term only.

If we do not put the above restriction on F, we can fit the arbitrary curve of the energy spectrum by appropriately choosing the momentum dependence of F, since F can be an arbitrary invariant function of momentum. However this is not our concern. Any statement about « higher momentum dependent terms » in the previous paper should be taken in the frame-work of approximation, i.e. $a > b$.

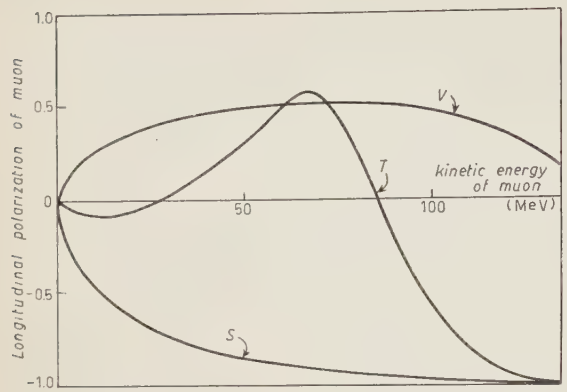

Fig. 3. – Integrated polarization for the spin 0 $K_{\mu 3}$.

In Fig. 3, we give the energy dependence of the polarization for pure interactions. The curves retain the features of the (unintegrated) distributions for large angles.

Finally we will also give the value of the polarization integrated over a certain interval of muon energy in Table I.

In the analysis of the integrated polarization the investigation of the low energy muon (0 ÷ 40 MeV) is of particular interest. The polarization integrated over this energy interval is — 0.67 for S, 0.41 for V and — 0.001 for T. When the qualitative data about polarization of the low energy muon become available, we may discriminate S and V by the sign of the polarization, from the information about π-μ-e decay, assuming the conservation of the lepton number.

TABLE I. – *Polarization integrated over angle and energy.*

Energy range / Type	0÷20	20÷40	40÷60	60÷80	80÷100	100÷102	120÷134	Total
S	—0.54 (5.2)	—0.73 (11.5)	—0.83 (17.0)	—0.92 (21.0)	—0.94 (23.0)	—0.97 (18.5)	—0.99 (3.8)	—0.88
V	0.30 (10.1)	0.47 (17.8)	0.54 (21.3)	0.57 (21.3)	0.54 (17.8)	0.48 (10.4)	0.47 (1.3)	0.50
T	—0.07 (13.4)	0.05 (18.2)	0.37 (12.9)	0.58 (8.9)	—0.24 (12.1)	—0.83 (23.1)	—0.99 (11.4)	—0.23

Figures in brackets are the distribution-weight in the concerned interval of energy, the total of which is normalized to 100. They can be used to get the polarization integrated over an energy range wider than 20 MeV. It is given by $\Sigma N_i P_i / \Sigma N_i$ where P_i is the polarization in the energy interval i and N_i is the corresponding figure in brackets.

3·3. *The relation between the polarization of the muon and the spin of* $K_{\mu 2}$ *and* $K_{\mu 3}$. – There is abundant experimental evidence which supports the idea that only one kind of K-meson exists and that its spin is zero. It is interesting to obtain the non-negative evidence about the possibility of spin 0 for $K_{\mu 2}$ and $K_{\mu 3}$-mesons.

Let us discuss briefly here the relation between the polarization of secondary muons and the spin of $K_{\mu 2}$ and $K_{\mu 3}$-mesons.

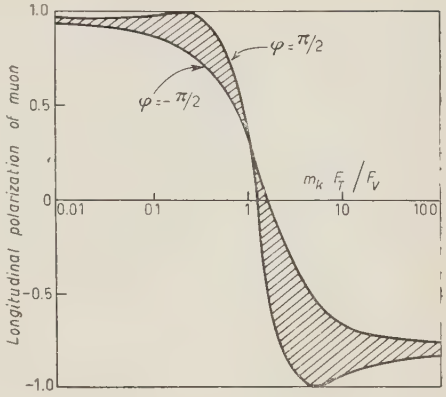

Fig. 4. – The relation between coupling constants and polarization in spin 1 $K_{\mu 2}$: The shadowed region is the permitted region.

$K_{\mu 2}$-meson. – If the spin of the $K_{\mu 2}$-meson is zero, the secondary muon is, as noted by LEE and YANG, completely polarized along the direction of the anti-neutrino propagation. If the spin of the K-meson is 1, the secondary muon is also in general polarized, and the polarization is dependent on the interaction. There are two independent types of interaction for spin 1 $K_{\mu 2}$-meson which are specified as F'_V and F'_T, and the polarization of secondary muons is determined by the relative magnitude of effective constants and their relative phase φ. The expression for polarization is

$$(10) \quad P(\boldsymbol{p}/p) = [2m_K^2 - m_\mu^2 + (F'_T/F'_V)^2 m_K^2(2m_\mu^2 - m_K^2) + 2(F'_T/F'_V)m_\mu m_K^2 \sin\varphi] \cdot$$
$$\cdot [2m_K^2 + m_\mu^2 + (F'_T/F'_V)^2 m_K^2(2m_\mu^2 + m_K^2) + 6(F'_T/F'_V)m_\mu m_K^2 \sin\varphi]^{-1}.$$

In Fig. 4 we sketch the relation between coupling constants and polarization.

Only for an accidental combination of F'_V and F'_T the polarization is complete and in this case we can not make any difference between spin 0 and spin 1. However it is noted that we can expect that the polarization will be never complete for the spin 1 $K_{\mu 2}$ if the time reversal invariance is violated ([17]).

$K_{\mu 3}$-meson. – In the $K_{\mu 3}$-process the number of the independent types of interaction is much increased owing to the increase of the independent momenta and it seems to be somewhat difficult to get the information to discriminate the spin 0 from 1 for $K_{\mu 3}$. However, in case of spin 0 ($K_{\mu 3}$-meson), there is still some feature whose experimental analysis is interesting. If we measure the polarization (along the anti-neutrino direction) at $\theta = 180°$, it becomes 1 independent from the muon momentum. It is necessary for the experimental analysis to estimate the lower limit of polarization when θ is near 180°. We check this and find it very difficult to exclude the possibility to have the polarization differing far from 1. However if we choose the relative phase of parameters to fit the experimental energy distribution of

([17]) Ref. ([4]). Time reversal invariance restricts the phase φ to $(2n+1)\pi/2$.

muons which shows a preponderance in the low energy region ([18]), we can obtain the lower limit. This is about 0.98 for muon energy $\lesssim 50$ MeV at $\theta = 175°$ and the average polarization will be 0.9 at the same angle.

In the tentative analysis of experimental data up to now for (spin 0) $K_{\mu 3}$-meson decay, scalar and/or vector type of interaction seems to be favourable, while the $K_{\mu 2}$ (if it is of spin 0) mode is allowed only for scalar and/or vector type of interaction ([19]). It may be worthwhile to note that both $K_{\mu 2}$ and $K_{\mu 3}$ decay may simultaneously be caused by the existence of scalar or/and vector type of Fermi interaction, violating parity-conservation.

4. - Depolarization of the muon in passing through the matter.

In order to assure the workability of our analysis for the experiment it is necessary that the stopping material is not a perfect depolarizer for high-energy muons, if we use the type of experiments of μ-e angular correlation for the measurement of the polarization of muons. It is very important to estimate the order of depolarization which the muons experience in the matter. For the analysis of experimental data the precise information about depolarization is necessary to draw conclusions; however the theoretical prediction is very complicated and difficult, and the depolarization seems to be dependent on the characteristics of the local field of each material, particularly at low energy. It is recommended to make the experiments of the depolarization with high energy muons coming from high energy pion decay. Such an experiment will supply the information which is necessary for the analysis of $K_{\mu 2}$ and $K_{\mu 3}$-mesons.

In this section we count some possible origins of the depolarization and a rough check is given. The following origins for depolarization are considered:

a) muonium formation;

b) external magnetic field;

c) multiple scattering due to molecular and atomic fields;

d) Coulomb excitation of the electron;

e) bremsstrahlung of muons.

Since the information of depolarization in the low energy (< 4 MeV) region

([18]) Ref. ([9]); S. TAYLOR: Private communication, for which we are much indebted to him.

([19]) Strictly speaking, under parity conservation, $K_{\mu 2}$ can decay through scalar (or V) type of interaction when $K_{\mu 3}$ decays via pseudoscalar (or PV) type.

is now rapidly increasing, our main interest is in high energy behavior of depolarizations. It is expected that *a*) and *d*) are only dominant in the low energy region and the correction for the external field *b*) can experimentally be estimated. As to *c*) we remark that the cross-section is extremely small for muons, and sometimes this may be excluded by careful examination of the muon tracks. Thus, we only estimate the contribution to the depolarization due to multiple scattering by fixed nuclear electromagnetic field.

The relative order of magnitude, A, of nuclear magnetic interaction to charge interaction is given by ([20])

$$A \simeq \frac{p\mu}{eZ} = \frac{p}{2M} \cdot \frac{\mu}{Z\mu_N}, \tag{12}$$

where Ze and μ are the charge and magnetic moment of the nucleus; μ_N is the nuclear magneton, M is the nucleon mass and p is the momentum of muon. If we take the momentum p as 200 MeV/c ($\sim$ muon momentum in $K_{\mu 2}$), $A \simeq 0.01$ for Cu and 0.03 for Xe. Thus the contribution to the scattering from the nuclear magnetic moment is expected to be very small, and we only consider the case of scattering by nuclear charge. This problem has been studied by HAYAKAWA ([21]).

When the initial muon is completely polarized along its momentum, its polarization along the initial direction η after being scattered is given by

$$\left\{\begin{aligned} &\eta = 1 - \frac{2g^2 \sin\theta}{f^2 + g^2}, \\ &f^2 + g^2 = \frac{1}{4} q^2 \operatorname{cosec}^4 \frac{\theta}{2} \left[1 - v^2 \sin^2 \frac{\theta}{2} - \pi v^2 q \sin \frac{\theta}{2} \left(1 - \sin \frac{\theta}{2}\right)\right], \\ &2g^2 = \frac{1}{2} q^2 \operatorname{cosec}^2 \frac{\theta}{2} \cdot \\ &\qquad \cdot \left[\{1 - (1 - v^2)^{\frac{1}{2}}\}^2 \cos^2 \frac{\theta}{2} - \pi v^2 q \sin \frac{\theta}{2} \left(1 - \sin \frac{\theta}{2}\right) \{1 - (1 - v^2)^{\frac{1}{2}}\}\right], \end{aligned}\right. \tag{13}$$

where q is Ze^2/v and v is the muon velocity, and θ is the scattering angle.

The decrease of polarization when the muon passes through the distance x is obtained by multiplying the scattering cross-section by the second term of (13) and integrating it over x. Rewriting this expression by using the

([20]) R. G. NEWTON: *Phys. Rev.*, **103**, 385 (1956).

([21]) S. HAYAKAWA: *Soryushi-Ron-Kenkyu* (mimeographed circular in Japanese), **14**, 513 (1957).

momentum loss formula we get the decrease of polarization δ, while the velocity of the muon V decreases to V'

$$(14) \qquad \delta \cong \pi Z m_e/m_\mu \int_{V'}^{V} \frac{\mathrm{d}v}{v} \frac{1}{\sqrt{1-v^2}} \cdot$$

$$\cdot \left\{ \frac{3}{8}(1-\sqrt{1-v^2})^2 - \frac{Z}{137} v(1-\sqrt{1-v^2}) \left(\frac{1}{3} - \frac{\pi}{16} \right) \right\} \left| \log \left\{ \frac{2m_e v^2}{I_0 Z(1-v^2)} \right\} - v^2 \right|^{-1},$$

where I_0 is the ionization energy of the hydrogen atom.

Integration of (12) from 152 to 4 MeV gives 0.0018 for Cu and 0.0030 for Xe.

This shows that the muons keep their initial polarization direction almost completely in the interaction with nuclear charge. The upper limit of depolarization may rather be given by the estimation of interaction with the nuclear magnetic moment. However even if the magnetic interaction acts as a perfect depolarizer (although this may not be the case), the polarization of stopped muons will be still ~ 1 as noted before.

The situation is favorable for the experiment. However, to avoid an unseen depolarization factor, it is desired to proceed with standard experiments of depolarization. We repeat that the π-μ-e correlation should be measured in the material with which $K_{\mu 3}$ and $K_{\mu 2}$ experiments will be performed.

5. – Summary and remarks.

In this paper we have investigated the polarization of secondary muons from $K_{\mu 2}$ and $K_{\mu 3}$ decay processes, aiming to add some new information on the decay interactions. The general expressions obtained are lenghty and the comparison with the experiment seems to be a tedious task. However, there are some features of which a detection is interesting:

a) For the purpose of decay interaction analysis in $K_{\mu 3}$ processes the measurement of longitudinal polarization may be convenient. The analysis of longitudinal polarization integrated over the angle may serve to make clear the type of interactions. The analysis of low energy muons ($0 \sim 40$ MeV) is interesting.

b) In $K_{\mu 2}$ decay process the polarization measurement may give some information to discriminate between spin 0 and spin 1 possibilities. It must be remarked that for spin 1 K-mesons, the polarization is generally not complete, i.e. $|P| < 1$, and it will never be complete when the time reversal invariance is violated.

To draw a definite conclusion from the expermiental data the detailed information of depolarization is required. The necessary information of the depolarization of high energy muons will be supplied by performing the experiment using the muon from pion decay which is polarized completely ([22]). It were desirable to perform such an experiment besides the polarization analysis proposed in this paper.

* * *

The authors would like to express their sincere thanks to Dr. S. OGAWA for his valuable discussion and careful reading of the manuscript. They also thank Prof. K. SAKUMA for his interest in this work. One of the authors (M.Y.) is indebted to the Yukawa-Yomiuri Fellowship for financial aid.

([22]) If we choose the muons which are emitted from the high energy pions in the direction of the pion momentum, these muons will be completely polarized along their motion.

Note added in proof.

After we have submitted this paper to this journal, there appears the article by J. WERLE (*Nucl. Phys.*, **4**, 171 (1957)), where the analysis same with our discussion in Sect. **3** is developed. The investigation of muon polarization along pion direction is helpful for the purpose of decay interaction analysis. The analysis of the polarization along this direction will be published in this journal. The analysis has been done without the assumption about effective coupling constants.

Besides the polarization along muon and pion propagation directions, the study of the muon polarization to the decay plane is interesting, since it can supply the information about the validity of time-reversal invariance in $K_{\mu 3}$: This has been noted by J. J. SAKURAU and also by J. WERLE. The authors thank them for their kind sending the preprints.

RIASSUNTO (*)

Allo scopo di rilevare le interazioni deboli agenti nei processi di decadimento dei mesoni K fra i cui prodotti di decadimento figurano muoni, gli autori hanno esaminato la polarizzazione dei muoni emessi in questi processi partendo dal punto di vista che l'interazione debole di Fermi sia partecipe dei detti processi e il neutrino associato sia a due componenti. Per la determinazione del tipo dell'interazione debole nei mesoni $K_{\mu 3}$ è utile analizzare la polarizzazione longitudinale dei muoni. Per quanto lo scopo principale fosse quello di determinare il tipo delle interazioni deboli, abbiamo esaminato anche lo spin del mesone K e la nostra analisi mostra che la polarizzazione dei muoni è generalmente incompleta per i mesoni $K_{\mu 2}$ di spin 1 in contrasto coi mesoni $K_{\mu 2}$ di spin 0.

(*) *Traduzione a cura della Redazione.*

Production directe de paires d'électrons par les électrons de grande énergie. Modèle de formation de la trace initiale des paires d'électrons. Elimination des faux tridents.

R. Weill, M. Gailloud et Ph. Rosselet

Laboratoire de Recherches Nucléaires, E.P.U.L. - Lausanne

(ricevuto il 7 Agosto 1957)

Summary. — We have measured the mean free path for direct électron pair production by electrons in the energy region: 2 to 8 GeV, 8 to 32 GeV, 32 to 150 GeV. The obtained values are less than those foreseen by Bhabha's theory. The desagreement is not imputable to energy underestimations. We describe a three dimensional model of track formation in nuclear emulsion which accounts for the ionization variation observed at the beginning of electron pairs of more than ten GeV. This indicates that our energy determinations using methods described in a previous paper, are correct: while energies evaluated on the basis of dipole effect theory can be overestimated by 100 times. The number of unresolvable « bremsstrahlung » pairs produced on the track of an electron of known path and energy has been calculated. Errors inherent to Koshiba and Kaplon's method are thus eliminated.

1. – Introduction.

Le problème de la mesure du libre parcours moyen de production directe des paires d'électrons par des électrons de haute énergie a déjà fait l'objet d'un grand nombre de travaux (références [1-9]). La situation actuelle dans,

(1) W. H. Barkas, R. W. Deutsch, F. C. Gilbert et C. E. Violet: *Phys. Rev.* **86**, 59 (1952).

(2) M. Avan et L. Avan: *Compt. Rend. Acad. Sc. Paris*, **241**, 1284 (1955).

(3) M. F. Kaplon et M. Koshiba: *Phys. Rev.*, **97**, 193 (1955); **100**, 327 (1955).

(4) S. L. Leonard: *Bull. Am. Phys. Soc.*, **1**, 167 (1956).

(5) J. E. Naugle et P. S. Freier: *Phys. Rev.*, **92**, 1086 (1953), **104**, 804 (1956).

(6) E. Lohrmann: *Nuovo Cimento*, **3**, 820 (1956).

(7) M. M. Block, D. T. King et W. W. Wada: *Phys. Rev.*, **96**, 1627 (1954).

(8) A. Debenedetti, C. M. Garelli, L. Tallone et M. Vigone: *Nuovo Cimento*, **4**, 1151 (1956).

(9) R. Weill, M. Gailloud et Ph. Rosselet: *Helv. Phys. Acta*, **29**, 437 (1956); M. Gailloud, R. Weill et Ph. Rosselet: *Helv. Phys. Acta*, **30**, 280 (1957).

ce domaine apparaît confuse: certains auteurs ont obtenu des résultats expérimentaux qui s'accordent avec les valeurs théoriques calculées par BHABHA [10] et RACAH [11], alors que d'autres ont mesuré des libres parcours moyens inférieurs à ceux prévus par la théorie. Nous avons des raisons de croire que ces divergences proviennent, pour une certaine part, d'erreurs commises dans l'application des méthodes de mesure de l'énergie des paires d'électrons. Nous apportons ici des arguments nouveaux qui justifient les déterminations d'énergie au-delà de 10 GeV faites suivant une méthode que nous avons décrite dans un précédent article [12]. D'autre part, nous montrons que l'élimination des paires de bremsstrahlung non résolubles (faux tridents) a été faite jusqu'ici par un procédé qui peut conduire à des erreurs. Nous avons établi une méthode de correction plus précise et plus directe, dont nous exposons le principe.

2. – Identification des tridents et mesure de l'énergie des paires d'électrons.

Nous avons étudié les trajectoires d'électrons dans des cascades électrophotoniques produites dans un lot de 108 émulsions pelées faisant partie d'un vol au Texas (1955). Seuls les événements qui mettent en jeu une énergie totale supérieure à 20 GeV ont été retenus; parmi 9 cascades étudiées, 7 sont engendrées par un photon, 2 par un électron. Etant donné la rareté de ces phénomènes, nous avons été contraints de suivre les trajectoires sur des distances pouvant aller jusqu'à 4 cm, de manière à observer un nombre suffisant de tridents. Trois classes de trajectoires ont été constituées, d'après l'énergie des électrons primaires: de 2 à 8 GeV, de 8 à 32 GeV, de 32 à 150 GeV. La largeur de chaque classe représente à peu près la perte d'énergie moyenne d'un électron ayant l'énergie supérieure de cette classe sur un parcours de 4 cm dans l'émulsion.

Les méthodes utilisées pour la mesure de l'énergie des électrons ont été décrites ailleurs [9,12]. Rappelons brièvement que la diffusion multiple relative a été mesurée chaque fois que l'on disposait, sur une longueur suffisante, de traces distantes de 1 à 20 μm; dans ces conditions, la diffusion parasite due aux dislocations de la gélatine (spurious scattering) s'élimine [12]. L'angle d'ouverture à l'origine des paires d'électrons a été déterminé soit par mesure directe si l'énergie est inférieure à 20 GeV, soit par mesure de la variation de l'ionisation sur la trace initiale si l'énergie dépasse 10 GeV [9]. Dans un précédent mémoire [12], nous avions tenté une interprétation de cette variation

[10] H. B. BHABHA: *Proc. Roy. Soc.*, A **152**, 559 (1935).
[11] G. RACAH: *Nuovo Cimento*, **14**, 93 (1937).
[12] R. WEILL, M. GAILLOUD et PH. ROSSELET: *Nuovo Cimento* **6**, 413 (1957).

sur la base du modèle unidimensionnel de formation de trace imaginé par Della Corte [13]. Les calculs ont été poursuivis à l'aide d'un modèle plus élaboré à trois dimensions dont le principe est exposé ci-dessous.

3. – Application d'un modèle tridimensionnel de formation des traces à l'étude de la variation de l'ionisation à l'origine des paires d'électrons (*).

Soit un système de référence xyz et une trajectoire située dans le plan xy et parallèle à x. Nous considérons les grains de bromure d'argent cubique, de côté d, ayant leurs arêtes parallèles aux axes de coordonnées. $\bar{d}$ est la longueur moyenne de la trajectoire dans un grain sphérique de diamètre d_0 où $d_0 = \frac{3}{2}\bar{d}$ est le diamètre moyen du grain réel. Les centres des grains sont supposés distribués dans des plans perpendiculaires à l'axe x, la distance minimum entre deux plans étant d_0. La répartition des plans le long des trajectoires, identique à celle des grains dans le modèle unidimensionnel d'O'Ceallaigh [14], est caractérisée par une loi de Poisson tronquée. Si $\delta + d_0$ est l'espace moyen suivant l'axe x entre deux plans consécutifs, la probabilité d'avoir n plans sur une longueur x de trajectoire est:

$$p(n) = \frac{\left(\frac{x - nd_0}{\delta}\right)^n \left(\frac{1}{n!}\right) \exp - \left[\frac{x - nd_0}{\delta}\right]}{\sum_{m=0}^{x/d_0} \left(\frac{x - md_0}{\delta}\right)^m \frac{\exp - [(x - md_0)/\delta]}{m!}} . \tag{1}$$

La probabilité $p(x)\,\mathrm{d}x$ pour qu'un grain développable soit à l'origine d'une lacune de longueur comprise entre x et $x + \mathrm{d}x$ dans l'émulsion non développée est:

$$P(x, P_{1d})\,\mathrm{d}x = \frac{\mathrm{d}x}{\delta} P_{1'} \sum_{n=0}^{x/d_0} p(n)(1 - P_{1'})^n . \tag{2}$$

$P_{1d} = \pi\, q$ est la probabilité d'avoir un grain développable dans un des plans définis ci-dessus, q étant la probabilité pour un grain d'un plan de toucher la trajectoire, et π la probabilité conditionnelle qu'il soit impressionné. Si j est la densité des centres de grains dans un plan et ϱ l'espace moyen entre

(*) Ce calcul a été presenté au colloque international de photographie corpusculaire de Strasbourg, Juillet 1957.

(13) M. Della Corte, M. Ramat et L. Ronchi jr.: *Nuovo Cimento*, **10**, 509, 958 (1953).

(14) C. O'Ceallaigh: *C.R. Congrès de Bagnères*, p. 73 (1953); *Suppl. Nuovo Cimento*, **12**, 412 (1954).

bords de grains (de côté d), suivant une direction parallèle à y ou z on a:

$$q = j \cdot d^2 = \frac{d}{d + \varrho} .$$

Nous postulons que par unité de parcours le trajet moyen d'une particule dans l'AgBr est le même dans notre modèle et dans l'émulsion réelle, et que, par conséquent, les nombres de grains rencontrés sont égaux:

$$\frac{q}{\delta + d_0} = \frac{1}{\Delta} .$$

D'après les données du Dr. WALLER de la Maison Ilford, la distance moyenne entre centres Δ est de 0.38 μm ([15]) et $d_0 = 0{,}27$ μm.

Les deux expressions ci-dessus montrent que ϱ dépend du paramètre δ. Dans l'émulsion développée le diamètre D du grain d'argent est supérieur à celui d_0 du grain d'AgBr: $D = (1+f)d_0$. La distribution des longueurs de alcunes s'obtient à partir de l'expression (2) par:

$$P(x, P_{1d}, f)\,\mathrm{d}x = P(x + f d_0, P_{1d}, 0)\,\mathrm{d}x , \tag{3}$$

d'où l'on déduit la longueur moyenne des lacunes G. Les spectres tirés de la relation (2) se confondent pratiquement avec des exponentielles si $x > d_0$ pour toutes les valeurs de P_{1d} comprises entre 0 et 1 et des valeurs de δ allant de 0 à 0.47 μm. Ceci indique que la longueur moyenne des lacunes est indépendante du développement lorsque f est supérieur à 1 ([13,14]), ce qu'a confirmé l'expérience ([16]). Ayant adopté une valeur de δ, la relation (3) permet d'établir le graphique donnant G en fonction de P_{1d}. Mesurant G pour les traces au plateau on en déduit les valeurs de P_{1d} et π correspondantes, ainsi que la courbe donnant G^* ([+]) en fonction de P_{1d}.

La densité de grains par unité de parcours est égale à $P_{1d}/(\delta + d_0)$; la densité de blobs g s'en déduit au moyen de la relation établie par O'CEALLAIGH ([14]), ce qui permet d'obtenir g^* ([+]) en fonction de P_{1d}.

Le problème dans le cas d'une paire d'électrons se traite formellement de la même façon que ci-dessus; soient 2 trajectoires parallèles à l'axe x, dans le plan xy, séparées par une distance y. Il suffit de remplacer P_{1d} dans l'expression (3) par P_{2d}, probabilité pour qu'un plan traversé par deux trajectoires présente un ou deux grains développables: soient A et B l'intersection des

([15]) J. H. WEBB: *Phys. Rev.*, **74**, 511 (1948).

([16]) G. FATZER, R. WEILL, M. GAILLOUD et CH. HAENNY: *I^er Colloque Intern. de Photographie corpusculaire*, Strasbourg (1957); *Rev. Sc. Instr.* (sous presse).

([+]) L'astérisque indique que la grandeur est rapportée a sa valeur au plateau.

deux trajectoires avec un plan parallèle à $0yz$. P_{2d} se calcule en considérant toutes les positions possibles de A et B pour lesquelles un ou deux grains sont rendus développables; pour $y < d$:

$$(4)\quad \begin{cases} P_{2'} = \dfrac{[(2\pi-\pi^2)(y)](d-y)+2\bar{\pi}\varrho(1-\exp[-y/\varrho])-\{y+\varrho(\exp[-\varrho/y]-1)\}(2\bar{\pi}-\bar{\pi}^2)}{\varrho+d}, \\ P_{2d} = P_{1'}\cdot\left|\left(\dfrac{2\pi-\pi^2}{\bar{\pi}}\right)(y)+\dfrac{y}{d}\left\{2-\pi-\left(\dfrac{2\bar{\pi}-\pi^2}{\pi}\right)(y)\right\}+\dfrac{\varrho}{d}(1-\exp[-y/\varrho])\bar{\pi}\right|, \end{cases}$$

$\overline{\pi^2}(y)$ est la moyenne quadratique de la probabilité de développement pour un grain sphérique de diamètre d_0 traversé par 2 trajectoires séparées par une distance y. $\overline{\pi^2}(y)$ se calcule à partir de la relation de Demers [17]:

$$(5)\quad \begin{cases} \overline{(2\pi-\pi^2)}(y) = \bar{\pi}\left(2\beta\dfrac{1}{2}\sqrt{d_0^2-y^2}\right), \\ \bar{\pi}(\beta d_0) = 1-\dfrac{2}{\beta^2 d_0^2}(1-\exp[-\beta d_0](\beta d_0+1)), \\ \beta = \dfrac{\alpha}{\varepsilon}\dfrac{dE}{dR}. \qquad [13] \end{cases}$$

Nous avons tenu compte du processus de recombinaison étudié par Della Corte [13] qui diminue d'environ 10 % la valeur de $(2\pi-\pi^2)$. Connaissant $\bar{\pi}$ et P_{1d} pour les traces au plateau, on peut calculer P_{2d} en fonction de y, ce qui permet de construire $G^*(y)$ et $g^*(y)$. Les calculs ont été effectués pour $\delta = 0$; 0.04 et 0.12 μm, ce qui correspond à $\bar{\pi} = 0.09$ 0.09 et 0.08. Dodd et Waller [18] donnent $\bar{\pi} = 0.11$ à 0.13, et Bailliard 0.09 [19].

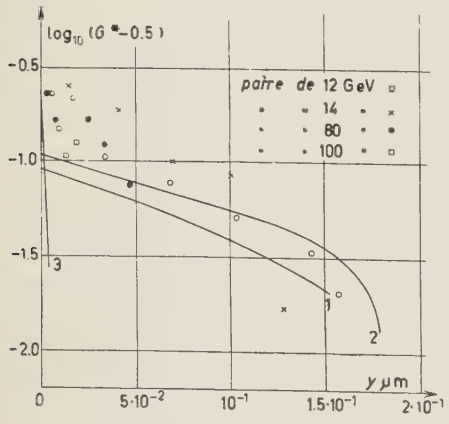

Fig. 1. – Longueur moyenne des lacunes relative au plateau G^* en fonction de l'écartement des trajectoires y μm. Valeurs calculées sur la base du modèle tridimensionnel de formation des traces. Courbe 1: $\delta = 0$; Courbe 2: $\delta = 0.04$ et 0.12 μm; Courbe 3: effet dipôle.

[17] P. Demers: *Can. Journ. Res.*, A **25**, 223 (1947).
[18] E. C. Dodd et C. Waller: *Photographic Sensitivity* (London, 1951).
[19] J. P. Bailliard: Communication privée.

Les valeurs de $G^*(y)$ et $g^*(y)$ s'accordent avec nos valeurs expérimentales pour y compris entre 10^{-2} et $2 \cdot 10^{-1}$ μm; pour $y \simeq 2 \cdot 10^{-1}$ μm, $g^* = \sim 2$ (Fig. 1 et 2). L'écartement y des trajectoires a été déterminé par l'intermédiaire de la relation de BORSELLINO ([20]) à partir de l'énergie mesurée par dif-

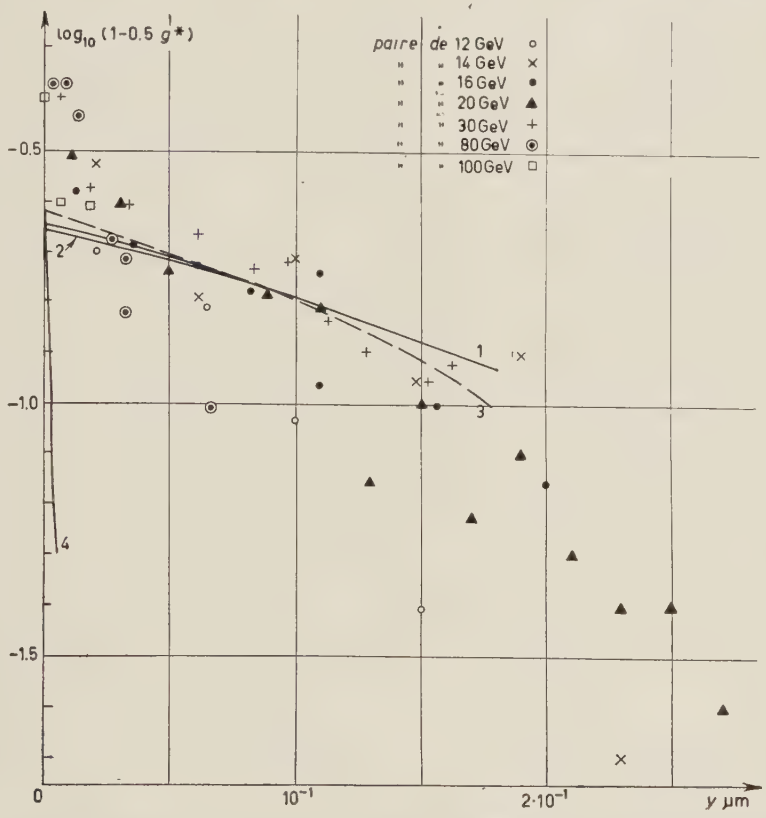

Fig. 2. Densité moyenne de lacunes relative au plateau g^* en fonction de l'écartement des trajectories y μm. Valeurs calculées sur la base du modèle tridimensionnel de formation des traces. Courbe 1: $\delta = 0$; Courbe 2: $\delta = 0.4$; Courbe 3: $\delta = 0.12$ μm; Courbe 4: effet dipôle.

fusion multiple relative. La variation de l'ionisation sur la trace initiale des paires d'électrons peut donc être interprétée dans les limites définies ci-dessus, sur la base d'un effet géométrique de dispersion des grains autour des trajectoires.

PERKINS ([21]) et ČUDAKOV ([22]) ont donné une autre interprétation de cette

([20]) A. BORSELLINO: *Phys. Rev.*, **89**, 1023 (1953).
([21]) D. H. PERKINS: *Phil. Mag.*, **46**, 1146 (1955).
([22]) A. E. ČUDAKOV: *Compt. Rend. Acad. Sci. U.R.S.S.*, **19**, 651 (1955).

même variation: d'après eux les deux électrons doivent être considérés comme formant une seule entité ionisante tant que l'écartement des trajectoires est inférieur à $3 \cdot 10^{-3}$ μm. Introduisant la perte d'énergie unitaire d'un dipôle ([22]) dans la relation de Demers ([17]) on peut calculer P_{1d} en fonction de y. Les valeurs de g^* et G^* obtenues de cette manière sont en désaccord avec celles résultant de l'expérience (Fig. 1 et 2).

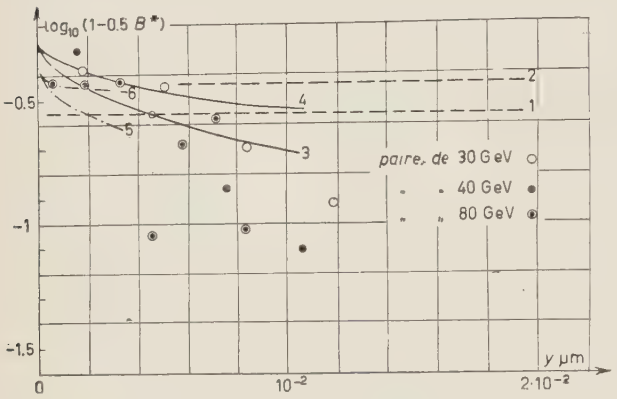

Fig. 3. – Longueur totale de blobs relative au plateau B^* en fonction de l'écartement des trajectoires y μm, mesuré pour des cellules comprises entre 30 et 50 μm. Valeurs calculées sur la base du modèle de formation des traces. Courbe 1: $\delta=0$; Courbe 2: $\delta=0.04$ et 0.12 μm. Effet dipôle: selon YEKUTIELI: courbe 3 pour $\delta=0$, courbe 4 pour $\delta=0.04$ et 0.12 μ=; selon ČUDAKOV: courbe 5 pour $\delta=0$, courbe 6 pour $\delta=0.04$ et 0.12 μm.

Nous avons constaté d'autre part que la longueur totale de blobs relative au plateau B^*, mesurée sur des cellules de 30 à 50 μm à partir de l'origine des paires de plus de 30 GeV, croît avec l'éloignement pour atteindre une valeur constante à environ 100 à 200 μm du sommet (voir Fig. 3). Cette variation ne peut être mise en évidence par les mesures de densité et longueur moyenne de lacunes, par suite des fluctuations statistiques qui nécessitent dans ce cas l'emploi de cellules d'environ 200 μm. Ce phénomène qui se manifeste sur des distances 10 fois plus courtes que celui considéré auparavant, résulte vraisemblablement de l'effet dipôle. En effet, les valeurs de B^* obtenues à partir des calculs de ČUDAKOV ([22]) et YEKUTIELI ([23]) (courbes 3 à 6 Fig. 3) sont en accord avec les valeurs mesurées.

En résumé, d'après notre expérience, l'énergie des paires d'électrons peut être déterminée à l'aide des méthodes suivantes:

1) pour $E > 10$ GeV: la variation de la densité g^* ou de la longueur moyenne G^* des lacunes relatives au plateau est mesurée pour des cellules de 200 μm sur une longueur pouvant aller jusqu'à quelques millimètres de la trace initiale. La courbe d'étalonnage donnée dans un précédent mémoire ([12]) permet de déduire l'énergie. Notre modèle tridimensionnel n'est pas suffisamment précis pour être appliqué au calcul de la valeur de l'énergie. D'autre part,

([23]) G. YEKUTIELI: *Nuovo Cimento*, **5**, 1381 (1957).

l'utilisation des théories de l'effet dipôle conduit dans ce cas à des surestimations de l'ordre de 100 fois.

2) Pour $E > 30$ GeV: la variation de la longueur totale de blobs B^* relative au plateau est mesurée pour des cellules de 30 μm environ jusqu'à 200 μm de l'origine. Les expressions de Čudakov [22] et Yekutieli [23] permettent de calculer la valeur de l'énergie.

4. – Calcul du nombre de faux tridents.

On définit généralement un trident comme étant une paire d'électrons produite soit directement par l'électron considéré (vrai trident, phénomène qui nous intéresse), soit par un photon de rayonnement converti sur la trace photographique de cet électron à l'intérieur des limites de résolution spaciale (faux tridents, phénomène parasite). Le calcul du libre parcours moyen λ de production de vrais tridents nécessite donc la connaissance du nombre moyen de faux tridents créés sur la longueur de trajectoire étudiée. Soient pour une classe d'énergie donnée:

n_{r_i}: le nombre total de paires (tridents compris) observées sur une trajectoire de longueur l_i;

n_i: le nombre total de photons de freinage convertis sur la longueur l_i;

ν_{fi}: le nombre de faux tridents produits sur l_i;

ν_{vi}: le nombre de vrais tridents créés sur l_i;

$f_i = \nu_{fi}/n_i$: la fraction des photons de rayonnement donnant lieu aux faux tridents, sur la longueur l_i.

Un calcul approché de f_i a été effectué par Koshiba et Kaplon [3]. Jusqu'ici les divers auteurs ont procédé de la manière suivante: ils mesurent $N = \nu_{fi} + \nu_{vi}$ et n_{vi}, et calculent

$$\nu_{fi} = \frac{N_i - n_{r_i} f_i}{1 - f_i} .$$

L'application du principe du maximum de vraisemblance [9] donne:

$$\lambda = \frac{\sum_i l_i}{\sum_i \nu_{vi}} . \tag{6}$$

Cette méthode peut conduire, dans le cas d'électrons de grande énergie, à des valeurs erronnées de λ. Par suite de la multiplication rapide des tridents

le long de la trajectoire étudiée, une certaine fraction difficile à calculer des paires dénombrées provient d'électrons secondaires, ce qui entraîne à une surestimation de la valeur de n_{vi}.

Nous avons éliminé cet inconvénient en calculant, sur la base des sections efficaces de radiation et de conversion données par Bethe-Heitler, le nombre moyen de faux tridents: $\nu_{fi} = n_i f_i$ produits par l'électron considéré, en fonction de son énergie E et du trajet qu'il parcourt l_i: λ s'obtient dès lors à partir de la seule mesure de N_i [9]:

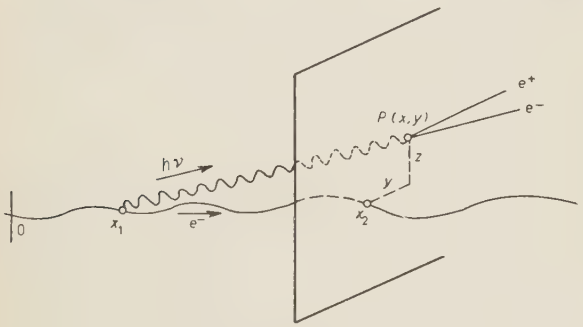

Fig. 4.

$$(7) \qquad \lambda = \frac{\sum_i l_i}{\sum_i (N_i - \nu_{fi})} .$$

Notre calcul repose sur les bases suivantes (voir Fig. 4). Soient:

$\Phi_{\text{rad}}(E, E_\gamma)\,\mathrm{d}E_\gamma\,\mathrm{d}x_1$: la probabilité pour qu'un électron d'énergie cinétique E émette un photon d'énergie E_γ sur le parcours $\mathrm{d}x_1$. Nous admettons ici que l'influence des phénomènes d'interférence signalés par FERRETTI [24] est négligeable, étant donné que l'orientation du cristal de bromure d'argent par rapport à la trajectoire considérée varie d'un grain à l'autre.

$\varphi_{\text{paire}}(E_\gamma) \exp[-(x_2 - x_1)\varphi_{\text{paire}}(E_\gamma)]\,\mathrm{d}x_2$: la probabilité pour que le photon d'énergie E_γ émis sur $\mathrm{d}x_1$ en x_1, soit converti dans un plan yz, perpendiculaire à la trajectoire, d'abcisse comprise entre x_2 et $x_2 + \mathrm{d}x_2$.

$Q(E, x_2 - x_1, y, z)\,\mathrm{d}y\,\mathrm{d}z$: la probabilité pour que l'origine de la paire d'électrons soit dans l'élément $\mathrm{d}y\,\mathrm{d}z$ au point $P(y, z)$ de ce plan. Nous choisissons l'axe y parallèle au plan de l'émulsion; l'axe z lui est sensiblement perpendiculaire, le calcul étant fait pour des trajectoires faiblement inclinées.

Les grandeurs ayant la dimension d'une longueur sont exprimées en longueurs de rayonnement ($X_0 = 29$ mm dans l'émulsion nucléaire).

D'après notre expérience, la limite de résolution d'une paire d'électrons dans l'émulsion développée est d'environ 0.2 μm au grossissement de 1000 ×; en d'autres termes, nous considérons qu'une paire est comptée comme trident si son sommet est à l'intérieur d'un prisme droit axé sur la trajectoire, de 0.4 μm de côté. En raison de la contraction de l'émulsion suivant son épaisseur

[24] B. FERRETTI: *Nuovo Cimento*, **7**, 118 (1950).

(coefficient de contraction: 2.2), le prisme correspondant dans l'émulsion non développée a une section droite rectangulaire de petit côté $y_{\max} = 0.4\ \mu$m, de grand côté $z_{\max} = 0.88\ \mu$m. Le nombre moyen n_i de photons convertis sur la longueur l_i et le nombre moyen de faux tridents ν_{l_i} sont donnés respectivement par:

$$(8) \qquad n_i = \int_{2m_e c^2}^{E} \Phi_{\text{rad}}(E, E_\gamma)\varphi_{\text{paire}}(E_\gamma)\,\mathrm{d}E_\gamma \int_0^{l_i}\mathrm{d}x_2 \int_0^{x_2} \exp\left[-(x_2 - x_1)\varphi_{\text{paire}}(E_\gamma)\right]\mathrm{d}x_1\,,$$

$$(9) \qquad \nu_i = \int_{2m_e c^2}^{E} \Phi_{\text{rad}}(E, E_\gamma)\varphi_{\text{paire}}(E_\gamma)\,\mathrm{d}E_\gamma \cdot$$

$$\cdot \int_0^{l_i}\mathrm{d}x_2 \int_0^{x_2} \exp\left[-(x_2 - x_1)\varphi_{\text{paire}}(E_\gamma)\right]\mathrm{d}x_1 \cdot 4 \int_0^{y_{\max}} \int_0^{z_{\max}} Q(E, x_2 - x_1, y, z)\,\mathrm{d}y\,\mathrm{d}z\,,$$

$m_e c^2$ est l'énergie au repos de l'électron.

L'intégration de ces expressions a été effectuée pour les conditions suivantes:

1) $\Phi_{\text{rad}}(E, E_\gamma)$: expression (2.11.5) dans B. Rossi, p. 49 [25] (effet d'écran total);

2) $\varphi_{\text{paire}}(E_\gamma)$: pour $E_\gamma > 260$ MeV: $\varphi_{\text{paire}}(E_\gamma) = \frac{7}{9}$ (effet d'écran total), pour $E_\gamma < 260$ MeV: expression obtenue en intégrant les relations (2.19.4) et (2.19.5) dans B. Rossi, p. 80 [25]. (effet d'écran nul);

3) $$Q(E, x_2 - x_1, y, z) = \frac{1}{2\pi}\,\frac{1}{\sigma_y \sigma_z}\,\exp\left[-\frac{1}{2}\left(\frac{y^2}{\sigma_y^2} + \frac{z^2}{\sigma_z^2}\right)\right],$$

avec:

$$\sigma_y = \sigma_z = (x_2 - x_1)\sqrt{\frac{1}{3}\langle\theta^2_{\text{diff}}\rangle + \frac{1}{2}\langle\theta^2_{\text{ouv}}\rangle}\,,$$

$\langle\theta^2_{\text{diff}}\rangle$ = moyenne des carrés des angles projetés des tangentes à la trajectoire de l'électron en x_1 et x_2.

$\frac{1}{2}\langle\theta^2_{\text{ouv}}\rangle$ = moyenne des carrés des angles d'émission projetés des photons de freinage.

La distribution des déviations projetées de l'électron résultant de la diffusion multiple et celle de l'angle d'émission projeté des photons de freinage

---

[25] B. Rossi: *High Energy Particles* (New York, 1952).

(Borsellino) ont été assimilées à des gaussiennes de variances:

$$\frac{1}{3}\langle\theta^2_{\text{diff}}\rangle = \frac{1}{3}\,\frac{x_2 - x_1}{E^2}\left(K\sqrt{\frac{3\pi}{4}}\,\frac{\pi}{180}\sqrt{290}\right)^2:$$

$$\frac{1}{2}\,\theta^2_{\text{mult}} = \frac{1}{2}\left[1.1\,q(E, E_\gamma, \bar{Z})\,\frac{m_e c^2}{E}\,\ln\frac{E}{m_e c^2}\right]^2 \text{ (tirée de la formule de Stearns)}$$

où: K est la constante de diffusion multiple utilisée dans les mesures sagittales en l'absence de coupure. La distance moyenne parcourue par les photons rayonnés par l'électron sur une longueur de rayonnement ($X_0 = 29$ mm) est d'environ $0.3\,X_0$; Molière donne pour une cellule de $0.3\,X_0$: $K = 32$ MeV degré (100 μm)$^{-\frac{1}{2}}$. Dans ce calcul, nous négligeons l'influence de la perte d'énergie de l'électron sur ce parcours;

$q\,(E, E_\gamma, \bar{Z}) = 0.77$. Nous avons admis la valeur de $q(E, E_\gamma, \bar{Z})$ donnée dans B. Rossi (voir [25]), fig. 2.11.5) pour les conditions: $Z = 13$, $E = 5$ GeV, $E_\gamma/E = 0.1$. Le spectre de bremsstrahlung variant sensiblement comme $1/E_\gamma$, chaque photon emporte en moyenne 1/10ème de l'énergie de l'électron. Le facteur 1.1 tient compte de la déviation moyenne de l'électron au moment de l'émission du photon. En effet, nous nous intéressons ici à l'angle d'émission du photon par rapport à la direction de l'électron après le choc, alors que la formule de Stearns donne l'angle entre le photon émis et la direction de l'électron avant le choc.

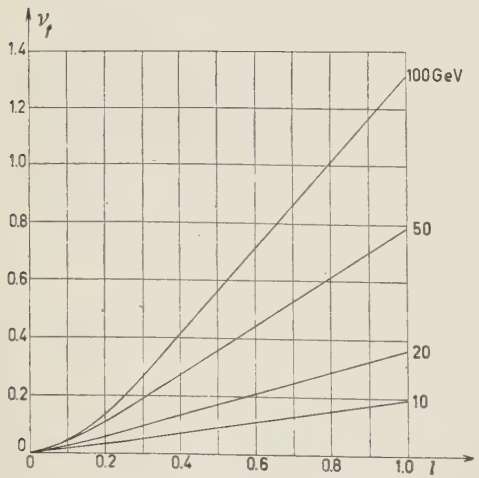

Fig. 5. – Nombre moyen de faux tridents ν_f produits sur la longueur l (en longueurs de rayonnement: 2.9 cm dans l'émulsion). En paramètre, l'énergie des électrons.

Nous avons construit (voir Fig. 5 et 6) les graphiques donnant ν_{fi} et $f_i = \nu_{fi}/n_i$ en fonction de l_i, l'énergie E étant en paramètre. Les valeurs calculées par Koshiba et Kaplon sont représentées par les courbes en trait interrompu de la Fig. 6.

Il est important d'étudier la répercussion des diverses approximations que nous avons faites dans le calcul de ν_{fi} et n_i. L'erreur commise en remplaçant la distribution de Molière par une gaussienne est négligeable (< 1%); nous avons majoré la constante de diffusion multiple habituelle de 5% pour tenir compte de la suppression de la coupure. L'approximation de la distribution

de Borsellino par une gaussienne de même variance entraîne une surestimation de ν_{fi} d'environ 32% à 10 GeV et 4% à 20 GeV, et une sousestimation de ν_{fi} d'environ 8% à 50 GeV et 5% à 100 GeV. On peut le voir facilement comme suit, en négligeant l'effet de la contraction de l'émulsion. Etant donnée la distance parcourue en moyenne par les photons de freinage ($0.3\,X_0$), seuls ceux émis dans un cône d'ouverture $5\cdot10^{-5}$ radian donnent lieu à des faux tridents. Dans ces conditions les gaussiennes qui donneraient la même proportion de photons émis dans ce cône que la formule de Borsellino ont des variances égales à $5\langle\theta^2_{\text{ouv}}\rangle$ pour 10 GeV, $1.3\langle\theta^2_{\text{ouv}}\rangle$ pour 20 GeV, $0.5\langle\theta^2_{\text{ouv}}\rangle$ pour 50 GeV et $0.55\langle\theta^2_{\text{ouv}}\rangle$ pour 100 GeV. Il suffit d'introduire ces valeurs à la place de $\langle\theta^2_{\text{ouv}}\rangle$ dans les expressions de σ_y et σ_z pour avoir les nombres et proportions correspondant de faux tridents à l'aide de (8) et (9) (page 9) ce qui conduit aux erreurs indiquées ci-dessus. La Fig. 6 montre que les valeurs de f_i données par KOSHIBA et KAPLON sont trop grandes, ces auteurs ayant omis le facteur $\sqrt{3\pi/4}$ dans le calcul de $\langle\theta^2_{\text{diff}}\rangle$ et pris pour K une valeur trop petite étant donnée la longueur de cellule à considérer ici ($0.3\,X_0$). D'autre part ils ont négligé l'influence de la contraction de l'émulsion ainsi que la variation de $\varphi_{\text{paire}}(E_\gamma)$ avec l'énergie, et ils ont utilisé à tort dans le calcul de $\langle\theta^2_{\text{ouv}}\rangle$ la valeur de $q(E, E_\gamma, \bar{Z})$ donnée par ROSSI pour $E_\gamma/E = 0.5$.

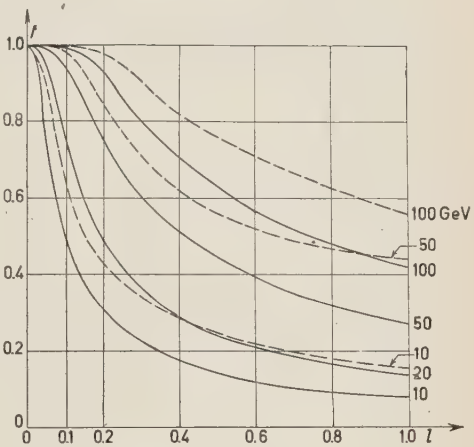

Fig. 6. – Fraction moyenne f des photons de freinage convertis en faux tridents sur la longueur l (en longueurs de rayonnement: 2.9 cm dans l'émulsion); en paramètre l'énergie de l'électron. D'après nos calculs ——; selon KOSHIBA et KAPLON – – –.

Il y a lieu de remarquer que ces erreurs s'ajoutent à l'erreur de méthode signalée auparavant. Les valeurs du libre parcours moyen λ de vrais tridents déterminées sur la base des calculs de KOSHIBA et KAPLON sont donc surestimées de plus de 30%.

Divers auteurs ([26-28]) ont mis en doute la validité des sections efficaces de radiation et de création de paires calculées par Bethe-Heitler aux très hautes énergies de l'électron ($E > 20$ GeV). Il se peut que la variation en $1/E_\gamma$ du

([26]) L. LANDAU et J. POMERANČUK: *Compt. Rend. Acad. Sci. U.R.S.S.*, **92**, No. 3 (1953); **92**, 735 (1953).

([27]) F. DYSON: *Proceedings Sixth Anunal Rochester Conference*, O. IX, 29 (1956).

([28]) A. B. MIGDAL: *Phys. Rev.*, **103**, 1811 (1956).

spectre de bremsstrahlung soit à remplacer par une divergence en $1/E\sqrt{E_\gamma}$ au dessous d'une valeur critique E_γ, croissant avec l'énergie E. Une estimation grossière à partir des données de MIGDAL [28] indique que les valeurs de n_{ii} et ν_{ii} obtenues dans ces conditions sont inférieures à celles calculées auparavant, l'écart maximum étant d'environ 40 %. Nous sommes en train de reconsidérer l'intégration des expressions (8) et (9) sur la base des calculs plus récents de FEINBERG [29].

5. – Résultats et conclusions.

La Fig. 7 réunit les principales valeurs publiées de λ (*) (rectangles blancs) ainsi que nos résultats expérimentaux récents (rectangles hachurés). Les courbes théoriques ont été établies sur la base des sections efficaces sans (trait continu) et avec effet d'écran (trait interrompu) calculées par BHABHA [10].

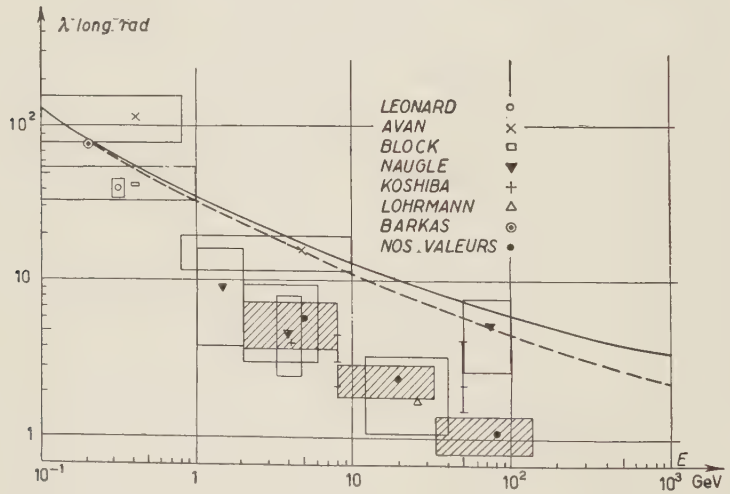

Fig. 7. – Libre parcours moyen λ de création de paires d'électrons par des électrons. Théorie Bhabha: sans effet d'écran ——, effet d'écran total – – –. Le côté horizontal des rectangles correspond à la classe, tandis que le côté vertical représente l'erreur sur λ.

Dans le tableau ci-dessous, L est la longueur totale des trajectoires étudiées par classe d'énergie, N le nombre correspondant de tridents identifiés et ν_f le

(29) E. FEINBERG: *Progrès des sciences physiques*, Tome **58**, 193 (1956).

(*) Les résultats publiés par le groupe de Turin [8] ont été omis car ils ne nous permettent pas de calculer les valeurs de λ.

nombre calculé de faux tridents. Pour mettre en évidence l'incompatibilité des valeurs mesurées (λ_{mes}) et des valeurs calculées d'après BHABHA ($\lambda_{théor}$), nous donnons dans ce même tableau le rapport de la probabilité P d'avoir la complexion observée, si le libre parcours moyen était égal à $\lambda_{théor}$, à la probabilité maximum P_{max} ($\lambda = \lambda_{mes}$) d'obtenir cette même complexion (9). L'erreur statistique sur λ_{mes} est calculée pour un intervalle de confiance à 68 %.

TABLE I.

Energie E	L	N	ν_f	λ_{mes} (long. ray.)	$\lambda_{théor}$ (long. ray.)	P/P_{max}
2 ÷ 8 GeV	105.0 cm	10	3.6	5.6 ± 1.8	$14 < \lambda < 25$	$1.5 \cdot 10^{-1}$
8 ÷ 32 GeV	67.8 cm	18	8.3	2.4 ± 0.6	$8 < \lambda < 14$	$1.6 \cdot 10^{-3}$
32 ÷ 150 GeV	26.4 cm	19	10.8	1.1 ± 0.3	$5 < \lambda < 8$	10^{-2}

Le désaccord entre les résultats expérimentaux et la théorie de Bhabha s'accentue au fur et à mesure que l'énergie E croît; ce désaccord ressort également de l'examen de la Fig. 7, si l'on considère l'ensemble des mesures effectuées; ceci d'autant plus que les valeurs publiées nous paraissent surestimées en raison des erreurs inhérentes à la méthode appliquée et des erreurs sur les facteurs correctifs utilisés. NAUGLE et FREIER [5] ont objecté que les écarts ci-dessus pouvaient être imputables à une sousestimation systématique des valeurs de l'énergie des paires d'électrons, au délà de 10 GeV. Le fait qu'un modèle tridimensionnel de formation de traces rende compte de la variation d'ionisation sur la trace initiale des paires d'électrons nous permet de réfuter cette objection.

* * *

Nous exprimons notre gratitude à Monsieur le Professeur CH. HAENNY pour l'intérêt qu'il a porté à notre travail. Les intégrations et calculs numériques relatifs à la correction pour faux tridents ont été effectués à l'Institut de Mathématiques appliquées de l'E.P.U.L. Nous adressons nos vifs remerciements à Monsieur le Professeur CH. BLANC et Monsieur le Docteur P. BANDERET pour leur précieuse collaboration. Le groupe de dépouillement de notre laboratoire a apporté une large contribution aux mesures. Nous remercions le Fonds National Suisse de la Recherche Scientifique qui a financé ces recherches.

RIASSUNTO (*)

Abbiamo misurato negli intervalli d'energia $2 \div 8$ GeV, $8 \div 32$ GeV, $32 \div 150$ GeV il cammino libero medio per la produzione diretta di coppie di elettroni da parte di elettroni. I valori ottenuti sono inferiori a quelli previsti dalla teoria di Bhabha. Il disaccordo non è imputabile a sottovalutazioni dell'energia. Descriviamo un modello tridimensionale per la formazione delle tracce nelle emulsioni nucleari che rende ragione della variazione di ionizzazione osservata all'inizio delle tracce di coppie di elettroni di oltre 10 GeV. Ciò indica che le nostre determinazioni dell'energia fatte applicando metodi descritti in un precedente lavoro sono corrette, mentre le energie calcolate in base alla teoria dell'effetto di dipolo possono essere in eccesso fino a 100 volte. Il numero delle coppie di bremsstrahlung non risolvibili prodotte sulla traccia di un elettrone di traccia ed energie note è stato calcolato. Risultano così eliminati gli errori insiti nel metodo di Koshiba e Kaplon.

(*) *Traduzione a cura della Redazione.*

IL NUOVO CIMENTO Vol. VI, N. 6 1° Dicembre 1957

Energy Spectrum of Pions and Polarization of Muons and Electrons in the $K_{\mu 3}$ and K_{e3} Decay (*).

S. W. McDowell (+)

Department of Mathematical Physics, University of Birmingham

(ricevuto il 10 Agosto 1957)

Summary. — In this paper two aspects of the $K_{\mu 3}$ and K_{e3} decay are discussed: the energy density of final states and the longitudinal polarization of the muons and electrons. It is assumed that the fermion pair is produced through a Fermi interaction which can be of scalar, vector or tensor type. The two-component theory of the neutrino is used. The energy spectra and polarization depend in general on three complex parameters. However, if the theory is to be invariant under time reversal, the parameters must be real. With the values of the parameters determined from the energy spectrum one can predict the polarization. This provides a good check of the two-component theory.

Introduction.

The nature of the interactions involved in $K_{\mu 3}^{+}$ and K_{e3}^{+} decay has so far been investigated through the energy spectrum of the μ-mesons and electrons emitted.

Since these are three-body decays, more information can be obtained from the determination of the complete sharing in energy amongst the particles. Although the pion energy has not been measured so far, we hope that this information may become available.

On the other hand, an important consequence of the non-conservation of

(*) This work has been done under the auspices of the Conselho Nacional de Pesquísas of Brazil.

(+) On leave of absence from the Centro Brasileiro de Pesquísas Físicas.

parity in weak interactions is that μ-mesons and electrons from $K_{\mu 3}$ and K_{e3} decay will in general be partially polarized along their direction of motion. The orientation and energy dependence of the polarization depend on the nature of the interactions.

In this paper we are concerned with a theoretical treatment of these two subjects.

1. – General assumptions.

Assuming that there exists only one K-meson having different decay modes (parity not being conserved in some of them), present evidence strongly favours the assignment of spin zero. Therefore we restrict our analysis to the case of a spinless K-meson. Our discussion of the polarization is carried out on the basis of the two-component theory of the neutrino as formulated by YANG and LEE [1]. In this theory, the spin of the neutrino is always parallel to its momentum while the spin of the antineutrino is always anti-parallel to its momentum. This theory is equivalent to the conventional one if the neutrino field, ψ_ν, is restricted to eigenfunctions of γ_5 belonging to the eigenvalues -1, so that $((1-\gamma_5)/2)\psi_\nu = \psi_\nu$. We further assume that in a definite decay process either a neutrino or an anti-neutrino is produced. The magnitude of the polarization should be the same in either case, but would have different sign.

If the results of β-decay [2,3] are interpreted according to the two component theory, one concludes that a neutrino is produced with the positron [4] while an anti-neutrino is produced with the electron, in accordance with the principle of conservation of leptons (*).

Applying this principle to the process:

$$\mu^+ \to e^+ + \nu + \bar{\nu}\,,$$

[1] T. D. LEE and C. N. YANG: *Phys. Rev.*, **105**, 1671 (1957).

[2] C. S. WU, E. AMBLER, R. W. HAYWARD, D. D. HOPPES and R. P. HUDSON: *Phys. Rev.*, **105**, 1413 (1957).

[3] H. FRAUENFELDER, R. BOBONE, E. VON GOELER, N. LEVINE, H. R. LEWIS, R. N. PEACOCK, A. ROSSI and G. PASQUALI: *Phys. Rev.*, **106**, 386 (1957).

[4] E. AMBLER, R. W. HAYWARD, D. D. HOPPES and E. P. HUDSON: *Further experiments on β-decay of polarized nuclei* (to be published).

(*) Recent experiments in β-decay [5] seem to indicate that the two component theory may not be valid, but the situation is still unclear. In the last section our problem is briefly discussed within the broader framework of the four-component theory.

[5] W. B. HELMANSFELDT, D. R. MAXSON, P. STÄHELIN and J. S. ALLEN: *Electron neutrino angular correlation in the positron decay of* ^{35}A (to be published).

one concludes that μ^- like e^- should be an anti-particle. Experiments on the polarization of μ-mesons and electrons from K-meson decay will provide a check on the validity of the principle of conservation of leptons. On the basis of this principle the processes should be:

$$K_{e3} \to \mu^+ + \nu + \pi^0 ,$$

$$K_{\mu 3} \to e^+ + \nu + \pi^0 .$$

These combinations are assumed in our analysis. All conclusions on polarization refer to them.

It should be noted that as far as energy distribution is concerned the spin state of the neutrino is irrelevant.

In principle, the only requirement upon the interactions is that they must be invariant under proper Lorentz transformations. However, we assume that the fermion pair is produced through a Fermi interaction, the whole process involving closed baryon loops of which an example is given in Fig. 1. Radiative corrections are negligible. Moreover, we assume that the factor in the transition matrix element arising from the internal processes can be expanded in a power series in the initial and final momenta; we retain only the leading term of this expansion for each type of Fermi interaction. This is the procedure adopted by FURUICHI *et al.* [6] in their analysis of the μ-meson and electron energy spectra.

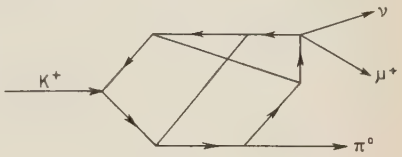

Fig. 1.

We summarize our assumptions as follows:

1) The K-meson is a spinless particle.

2) The neutrino is described by the two-component theory of Yang and Lee, or equivalently in terms of the Dirac spinor ψ_ν satisfying the condition:

$$\frac{1-\gamma_5}{2}\psi_\nu = \psi_\nu . \tag{1}$$

3) The decay modes of $K^+_{\mu 3}$ and K^+_{e3} are:

$$K^+_{\mu 3} \to \mu^+ + \nu + \pi^0 , \tag{2a}$$

$$K^+_{e3} \to e^+ + \nu + \pi^0 . \tag{2b}$$

[6] S. FURUICHI, T. KODAMA, S. OGAWA, Y. SUGAHARA, A. WAKASA and M. YONEZAWA: *Prog. Theor. Phys. (Japan)*, **17**, 1, 89 (1957).

4) A primary Fermi interaction is involved in the production of the fermion pair. An expansion of the matrix element in powers of the four-momenta of the decay products is assumed possible and only the leading term for each type of Fermi interaction is retained.

2. – Matrix elements.

The transition matrix elements for processes in which μ-mesons (electrons) are produced with spin parallel or anti-parallel to their momenta can be written as:

$$M_{\pm} = (2\pi)^4\,\delta^4(p_K - p_\pi - p - p_\nu)\,\bar{\psi}_\nu O_j \psi_{\pm} A^j(p)\,, \tag{3}$$

where ψ_ν is a spinor for a neutrino with momentum p_ν and $\psi_{\pm}$ is a spinor for a muon (electron) with momentum p and spin parallel (+) or anti-parallel (—) to $\boldsymbol{p}$. The O_j's are covariant Dirac matrices and $A^j(p)$ are covariant functions of the momenta, which taking into account hypothesis 4) and the conservation laws, reduce to:

$$\text{Scalar} \quad (O_j = I) \qquad A^j = \frac{1}{M}\, g_s\,, \tag{4a}$$

$$\text{Vector} \quad (O_j = i\gamma_\alpha) \qquad A^j = -\frac{i}{M^2}\,(g_V p_K^\alpha + g_{V'} p_\pi^\alpha)\,, \tag{4b}$$

$$\text{Tensor} \quad (O_j = i\sigma_{\alpha\beta}) \qquad A^j = \frac{1}{M^3}\, g_T p_K^\alpha p_\pi^\beta\,, \tag{4c}$$

for three possible types of Fermi interaction; axial vector and pseudo-scalar couplings are equivalent to vector and scalar by virtue of condition 1). The g's are dimensionless constants and M is the K-meson mass. Throughout this paper we use natural units such that $\hbar = c = 1$. The transition rate into an element of phase space is given by:

$$\mathrm{d}T_{\pm} = (2\pi)^4\,\delta^4(p_K - p_\pi - p - p_\nu)\,\mathrm{Tr}\cdot\left[\not{p}_\nu O_j \frac{1 \pm \boldsymbol{\sigma}\cdot\boldsymbol{\epsilon}}{2}\,(\not{p} + m)\bar{O}_i\,\frac{1-\gamma_5}{2}\right]\cdot \tag{5}$$

$$\cdot\,\frac{A^j A^{i*}}{(2\pi)^9}\,\frac{\mathrm{d}^3p_\pi\,\mathrm{d}^3p\,\mathrm{d}^3p_\nu}{2M\cdot 2E_\pi\cdot 2E\cdot 2E_\nu}\,,$$

where $(1 \pm \boldsymbol{\sigma}\cdot\boldsymbol{\epsilon})/2$ is the spin projection operator for the state $\psi_{\pm}$, $\boldsymbol{\epsilon}$ is a unit vector in the direction of motion of the muon (electron). As is shown in the appendix, invariance under time reversal implies that all g's must be either

real or pure imaginary depending on the parity of the K-meson. In general, they may be complex. However, since the strong interactions are invariant under time reversal, it is evident from the assumed decay mechanism that $g_{\nu}g_{\nu'}^{*}$ is real.

3. – Energy distribution.

Integrating expression (5) over the whole of momentum space one obtains

$$T_{\pm} = \iint \mathrm{Tr}\cdot\left[\mathfrak{p}_{\nu}O_j\,\frac{1}{2}\pm\boldsymbol{\sigma}\cdot\boldsymbol{\epsilon}\,(\mathfrak{p}+m)\bar{O}_i\,\frac{1-\gamma_5}{2}\right]\frac{A^{j}A^{i*}}{(4\pi)^3}\,\frac{1}{M}\,\mathrm{d}E\,\mathrm{d}E_{\bar{\pi}}\,, \tag{6}$$

where the integrand is a function of E and $E_{\bar{\pi}}$ only, because of the conservation of energy and momentum.

The total transition rate is given by:

$$T = T_{+} + T_{-} = \iint \varrho(E, E_{\bar{\pi}})\,\mathrm{d}E\,\mathrm{d}E_{\bar{\pi}}\,, \tag{7}$$

where $\varrho(E, E_{\bar{\pi}})$ is the probability density for an event to take place in which the energy of the pion and muon (electron) are respectively E_{π} and E. We give below the expressions for $\varrho(E, E_{\bar{\pi}})$ in the K-meson rest system for each type of Fermi interaction:

$$\varrho_S = 2\,|g_S|^2(W_{\bar{\pi}}-E_{\pi})/(4\pi)^3M^2\,, \tag{8a}$$

$$\varrho_V = 2\,[\,|g_V+g_{V'}|^2[2EE_{\nu}-M(W_{\bar{\pi}}-E_{\bar{\pi}})]M+|g_{V'}|^2m^2(W_{\bar{\pi}}-E_{\bar{\pi}})- \\ -2(g_V+g_{V'})g_{V'}^{*}m^2E_{\nu}]/(4\pi)^3M^4\,, \tag{8b}$$

$$\varrho_T = 2\,|g_T|^2\,[[(E-E_{\nu})^2-m^2](W_{\bar{\pi}}-E_{\bar{\pi}})M+2m^2E_{\nu}^2]/(4\pi)^3M^5\,, \tag{8c}$$

where $W_{\bar{\pi}} = (1/2M)(M^2+\mu^2-m^2)$ is the maximum pion energy, μ and m are the pion and muon (electron) masses. Numerical values are given in Tables I and II. The numbers represent the relative probabilities of finding events inside the corresponding energy intervals. The last row and column give the frequency distribution of pions and muons (electrons). The vector interaction has been calculated for $g_{V'}=0$. We have taken $M = 965\ \mathrm{m}_e$, $\mu = 264.5\ \mathrm{m}_e$, $m_{\mu} = 207\ \mathrm{m}_e$.

One observes very distinct behaviour for the probability densities corresponding to the various interactions. For a given μ-meson or electron energy, ϱ_S decreases linearly whereas ϱ_V increases linearly with pion energy. For a

given pion energy, ϱ_V is constant. Vector coupling suppresses the probability of the electron (also, to a lesser extent, of the μ-meson) and neutrino to go off in opposite directions, hence the probability density is small near the extreme end of the electron (μ-meson) spectrum and greatest in between; just the opposite trend is evidenced by ϱ_T since, due to the factor $(E - E_\nu)^2$ the probability density is large at extreme energies and small at intermediate ones.

In calculating the Tables I and II, we have omitted the second term of (4*b*) because it can be split into two terms: one of the form of the first term, the other giving a contribution of the form of a scalar interaction. Using conservation of momentum and the Dirac equation, one obtains the result that

$$\overline{\psi}_\nu \gamma_\alpha \psi p_\pi^\alpha = \overline{\psi}_\nu \gamma_\alpha \psi p_K^\alpha - m \overline{\psi}_\nu \psi \, .$$

It is important to realize that in the vector interaction the constants g_V and $g_{V'}$ are likely to be of the same order of magnitude. The difference between ϱ_V calculated for each term separately is small of order of magnitude $(m/M)^2$

TABLE I.

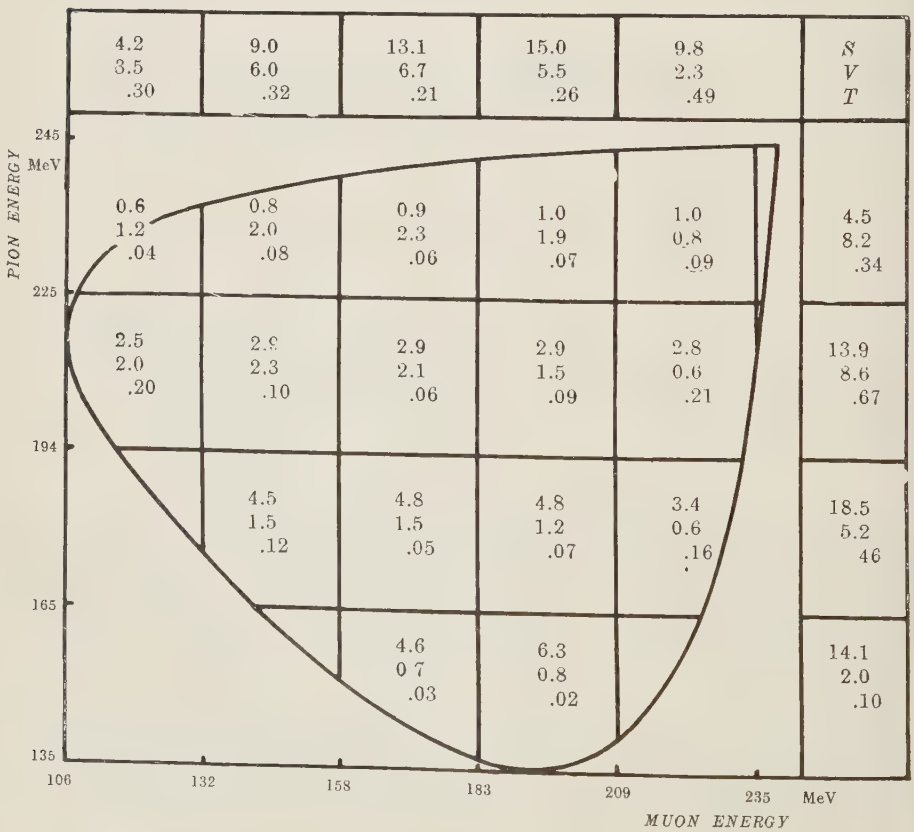

TABLE II.

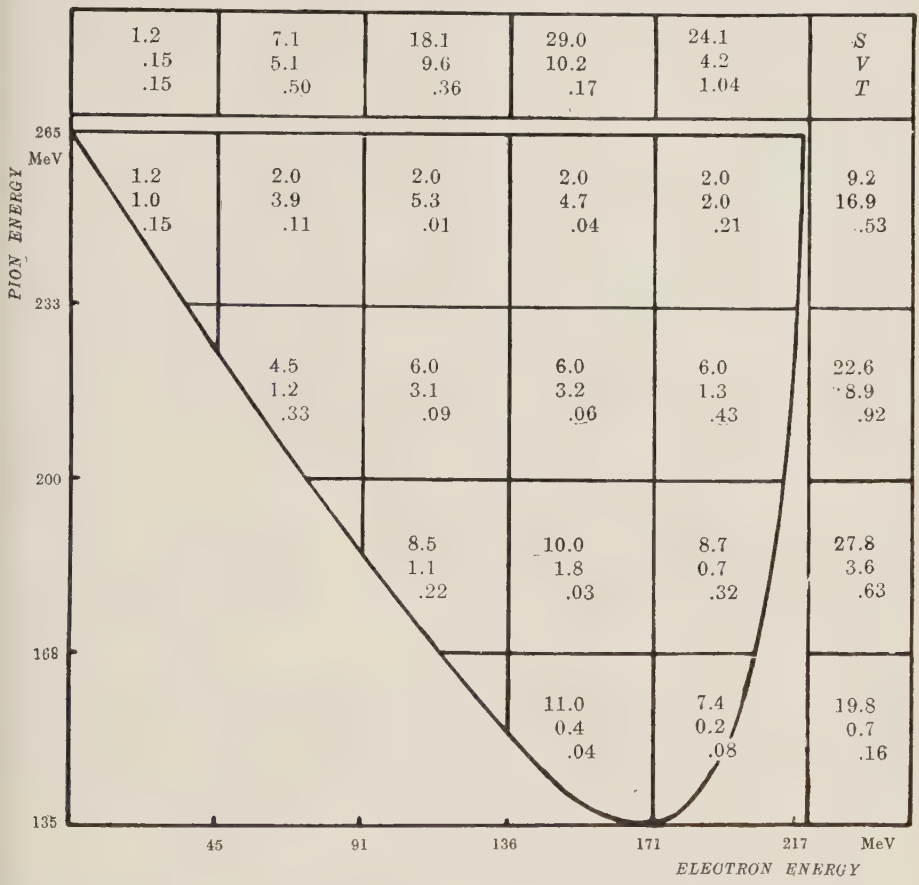

(cf. 8*b*) and therefore negligible for K_{e3}-decay; for $K_{\mu 3}$-decay the V'-coupling favours highly energetic pions even more than V-coupling (see Fig. 2). For the most general combination of interactions, the probability density is given by

$$\varrho(E, E_\pi) = \varrho_S + \varrho_V + \varrho_T + 2\,\mathrm{Re}\,(\varrho_{SV} + \varrho_{VT} + \varrho_{TS})\,, \tag{9}$$

where

$$\varrho_{SV} = 2m\,[g_S(g_V + g_{V'})^* E_\nu - g_S g_{V'}^* (W_\pi - E_\pi)]/(4\pi)^3 M^3\,, \tag{10a}$$

$$\varrho_{VT} = 2m\,[(g_V + g_{V'}) g_T^*\,[M(W_\pi - E_\pi) - E_\nu(M - E_\pi)]M - \\ - g_{V'} g_T^* [(E - E)_\nu (W_\pi - E_\pi) M - m^2 E_\nu]]/(4\pi)^3 M^4\,, \tag{10b}$$

$$\varrho_{TS} = 2 g_T g_S^*\,[(E - E_\nu)(W_\pi - E_\pi) M - m^2 E_\nu]/(4\pi)^3 M^4\,. \tag{10c}$$

The total pion spectrum shows much greater differences in the case of the K_{e3}-decay due to the fact that the electron energies are almost completely in the relativistic range. Because of this, the behaviour of the matrix elements for the different types of interaction are very different and influence the shape

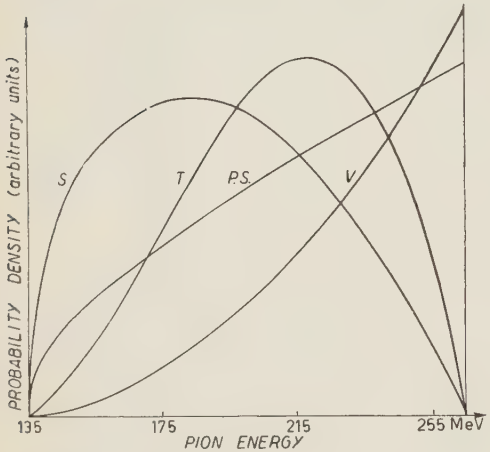

Fig. 2. – Energy distribution of pions in $K_{\mu 3}$-decay.

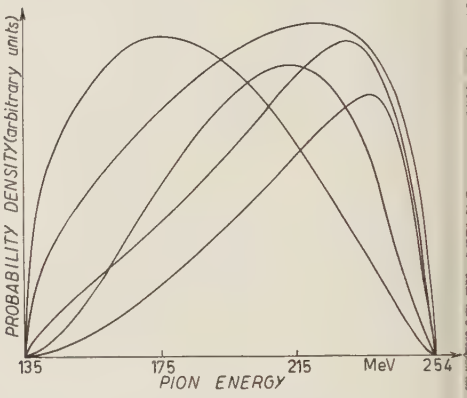

Fig. 3. – Energy distribution of pions in K_{e3}-decay.

of the spectra decisively. On the other hand, in the $K_{\mu 3}$ case the phase space factor is more effective. Curves for the pion spectrum due to S, V, V' and T coupling and to phase space alone, are shown in Fig. 2 and 3. In general, the pion spectrum $\mathrm{d}T/\mathrm{d}E_\pi = \int \varrho \, \mathrm{d}E$ is given by (*)

$$(11)\qquad \frac{\mathrm{d}T}{\mathrm{d}E_\pi} = \frac{2}{(4\pi)^3}\left\{\left| g_S - \frac{m}{M} g_{V'}\right|^2 Q_S + |g_V + g_{V'}|^2 Q_V + |g_T|^2 Q_T + \right.$$
$$\left. + 2\,\mathrm{Re}\left[\left(g_S - \frac{m}{M} g_{V'}\right)(g_V + g_{V'})^* Q_{SV} + (g_V + g_{V'})^* g_T Q_{VT}\right]\right\},$$

where

$$(12a)\qquad Q_S = (W_\pi - E_\pi)\,\delta E/M^2\,,$$

$$(12b)\qquad Q_V = [2EE_\nu - \tfrac{1}{6}(\delta E)^2 - M(W_\pi - E_\pi)]\,\delta E/M^2\,,$$

$$(12c)\qquad Q_T = \{[(E - \bar{E}_\nu)^2 + \tfrac{1}{3}(\delta E)^2 - m^2]M(W_\pi - E_\pi) +$$
$$+ 2m^2[E_\nu^2 + \tfrac{1}{12}(\delta E)^2]\}\delta E/M^5\,,$$

(*) In its centre of mass system the fermion pair is produced in the following states of angular momentum and parity:

Scalar coupling: $0^\pm$
Vector coupling: $0^\pm$, $1^\mp$
Tensor coupling: $1^\mp$

This explains why the interference term Q_{TS} vanishes.

(12*d*) $\quad Q_{SV} = m\bar{E}_\nu \delta E / M^3 ,$

(12*e*) $\quad Q_{VT} = m[M(W_\pi - E_\pi) - E_\nu(M - E_\pi)]\delta E / M^4 ,$

(12*f*) $\quad Q_{TS} = 0$

and $E = M - E_\pi - \bar{E}_\nu$ and $E_\nu = M((W_\pi - E_\pi)(M - E_\pi))/(M^2 - 2ME_K - \mu^2)$, are the average energies of the muon (electron) and neutrino for a given pion energy and $\delta E = (2M(W_\pi - E_\pi))/(M^2 - 2ME_\pi + \mu^2)(E_\pi^2 - \mu^2)^{\frac{1}{2}}$ is the phase space factor.

Numerical values for the expressions (12) are given in Tables III and IV. The electron mass was neglected in these calculations.

TABLE III. – *Numerical values* ($\times 10^2$) *for pion spectrum in* $K_{\mu 3}$*-decay.*

E_π/M	Q_S	Q_V	Q_T	Q_{SV}	Q_{VT}
.30	2.36	.29	.014	.75	— .016
.33	3.02	.54	.042	1.05	— .054
.36	3.15	.83	.074	1.22	— .105
.39	2.92	1.12	.099	1.30	— .163
.42	2.42	1.44	.114	1.18	— .224
.45	1.69	1.70	.109	1.14	— .265
.48	.815	1.65	.071	.53	— .237
.51	.032	.24	.0053	.06	— .030

TABLE IV. – *Numerical values* ($\times 10^2$) *for pion spectrum in* K_{e3}*-decay.*

E_π/M	Q_S	Q_V	Q_T
.30	3.16	.06	.019
.33	3.94	.21	.047
.36	4.26	.42	.082
.39	4.22	.71	.115
.42	3.85	1.08	.138
.45	3.20	1.52	.143
.48	2.31	2.04	.124
.51	1.20	2.65	.077

4. – Polarization of muons and electrons.

An important consequence of non-conservation of parity in $K_{\mu 3}$ and K_{e3}-decay is that the muons and electrons will in general be partially polarized along their direction of motion. Polarization in other directions should arise if the motion of the pion is observed.

If dT_+/dE, dT_-/dE are the transition rates to states in which the muon (electron) spin and momentum are respectively parallel and anti-parallel, the polarization is given by

$$P = \left(\frac{dT_+}{dE} - \frac{dT_-}{dE}\right) \Big/ \left(\frac{dT_+}{dE} + \frac{dT_-}{dE}\right). \tag{13}$$

In the two component theory of the neutrino, the polarization and, in particular, its sign, depends mainly on the commutators of the Dirac operators O_j involved in the covariant product $\bar{\psi}_\nu O_j \psi$ with the operator γ_5. Let us consider

$$\bar{\psi}_\nu O_j \psi = \psi_\nu \frac{1+\gamma_5}{2} O_j \psi = \psi_\nu O_j \frac{1 \pm \gamma_5}{2} \psi ,$$

where the upper sign corresponds to the scalar and tensor operators which commute with γ_5 and the lower one to the vector operator which anti-commutes with γ_5. Remembering that for plane waves

$$\gamma_5 \psi = \frac{\boldsymbol{\sigma} \cdot \boldsymbol{p}}{E + \gamma_0 m} \psi ,$$

so that

$$\frac{1 \pm \gamma_5}{2} \psi = \frac{1 \pm \boldsymbol{\sigma} \cdot \boldsymbol{p}/(E + \gamma_0 m)}{2} \psi , \tag{14}$$

one can see that for sufficiently large values of the energy, the matrix element M_- is small in the case of scalar or tensor coupling and M_+ in the case of vector coupling. Therefore, the polarization should be large in either case but oriented in opposite senses.

These considerations apply particularly to the electrons from K_{e3}-decay. For most of the spectrum, $E \gg m$ and the polarization is essentially equal to the velocity of the electron. In fact, for each type of coupling, the magnitude of the electron polarization (derived from (16) below) is of the form $(p/E)[1 + O(m/M)]$. Since $m/M \sim .001$, the second term is negligible and the polarization just equals the velocity of the electron even at low energies. (The same result has been obtained for the electrons in β-decay ([7,8])). Therefore, for S and T or V coupling the polarization rises from zero to a value close to unity within a few MeV, and apart from a small region at low energies, is practically complete.

However, a mixture of vector with scalar and (or) tensor interactions will produce only partial polarization.

On the other hand, for $K_{\mu 3}$-decay, since the maximum energy of the muon

([7]) J. D. Jackson, S. B. Treiman and H. W. Wyld: *Phys. Rev.*, **106**, 169 (1957).
([8]) L. Landau: *Nuclear Physics*, **3**, 1, 127 (1957).

is only about $2\,m$, its mass cannot be neglected and from (14) only, one cannot draw a definite conclusion. For the scalar and vector interactions, the polarization is given by

$$P_S = Mp/(ME - m^2)\,,$$

$$P_{V'} = -\,Mp/(ME - m^2)\,,$$

$$P_V = -\,(M - 2E)p/[(M - 2E)E + m^2]\,.$$

The absolute values of P_S and $P_{V'}$ increase monotonically with energy to a value of .996 at maximum energy. For V-coupling, the polarization reaches a maximum of about 56 % at $E \cong .36M$ and then decreases to 21 % at maximum energy. The expression for the polarization for tensor coupling is somewhat involved. The peculiar behaviour exhibited in this case (see Fig. 4) can be understood by observing that

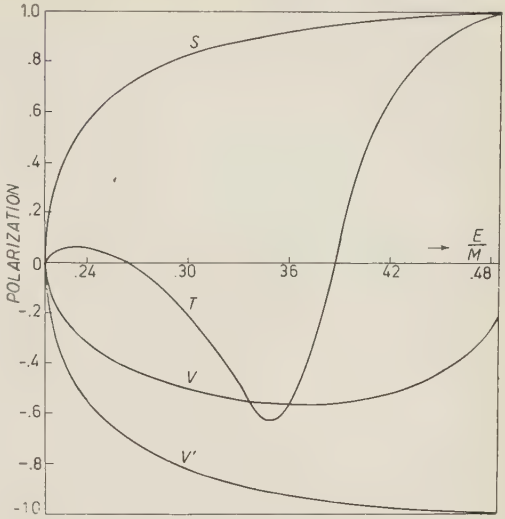

Fig. 4. – Polarization of muons in $K_{\mu 3}$-decay.

15) $$i_\nu \overline{\psi}\sigma_{\alpha\beta}\psi p_K^\alpha p_\pi^\beta = \overline{\psi}_\nu \psi [p_K^\alpha (p_\alpha - p_{\nu\alpha}) - m^2] - m\overline{\psi}_\nu \gamma_\alpha \psi p_\pi^\alpha\,.$$

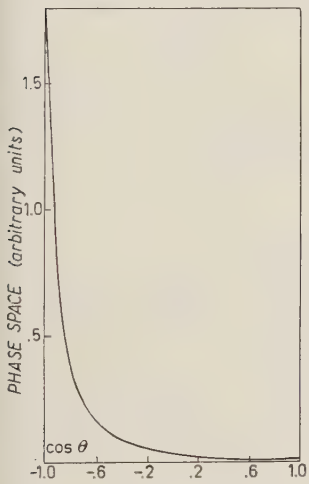

Fig. 5. – Angular correlation between the direction of motion of fast muons and neutrinos due to phase space alone.

The first term is a scalar coupling multiplied by a factor which reduces to $[M(E - E_\nu) - m^2]$ in the K-meson rest system . This term gives a small contribution in the intermediate energy region where $\bar{E}_\nu = E - m^2/M$. (As has already been pointed out, the energy spectrum has a minimum in this region). The second term is then predominant, and, as it is of vector type V', the polarization is negative. At higher energies, as $\bar{E}_\nu$ approaches zero, the first term increases causing the polarization to become positive and large.

Curves for the polarization corresponding to these interactions are shown in Fig. 4. It is interesting that at high energies the polarization is large and positive for S and T, large and negative for V'-coupling, but small for V-coupling. This can be explained in the following way. As is shown in Fig. 5, the angular correlation between fast muons and neutrinos due to phase space alone is strongly peaked backwards. From conservation

of angular momentum when the muons move in opposite direction to the neutrinos, they are completely polarized in their direction of motion. Therefore, the phase space factor enhances the contribution of the matrix element giving a large right-handed polarization at maximum energy in the case of S and T coupling (cf. (14)). However, for vector coupling the matrix element and phase space factor favour opposite spin alignments. The net result is small polarization for V-coupling. For V'-coupling the matrix element strongly dominates whihc accounts for the large polarization.

For the most general combination of interactions

$$P\frac{\mathrm{d}T}{\mathrm{d}E}=\left(\frac{\mathrm{d}T_+}{\mathrm{d}E}-\frac{\mathrm{d}T_-}{\mathrm{d}E}\right),$$

is given by an expression analogous to (11), viz:

$$(16)\qquad P\frac{\mathrm{d}T}{\mathrm{d}E}=\frac{2}{(4\pi)^3}\left\{\left|g_S-\frac{m}{M}g_{V'}\right|^2 D_S+|g_V+g_{V'}|^2 D_V+|g_T|^2 D_T+\right.$$

$$\left.+2\,\mathrm{Re}\left[\left(g_S-\frac{m}{M}g_{V'}\right)(g_V+g_{V'})^* D_{SV}+(g_V+g_{V'})g_T^* D_{VT}+g_T\left(g_S-\frac{m}{M}g_{V'}\right)^* D_{ST}\right]\right\},$$

where

$$(17a)\qquad D_S=\left\{\frac{p}{E}(W_\pi-\bar{E}_\pi)\,M+\frac{1}{2}m^2\frac{\delta E_\pi}{E}\right\}\delta E_\pi/M^3,$$

$$(17b)\qquad D_V=\left\{-\frac{p}{E}[2E\bar{E}_\nu-(W_\pi-\bar{E}_\pi)M]+\frac{1}{2}m^3\frac{\delta E_\pi}{E}\right\}\delta E_\pi/M^3,$$

$$(17c)\qquad D_T=\left\{\frac{p}{E}\left([(E-\bar{E})_\nu^2-m^2](W_\pi-\bar{E}_\pi)M+2m^2\bar{E}_\nu^2+\right.\right.$$

$$-\frac{1}{3}\left(\frac{\delta E_\pi}{2}\right)^2\left[(W_\pi-E_\pi)-2\left(E-E_\nu-\frac{m^2}{M}\right)\right]M\Big)+$$

$$\left.\left.+\frac{1}{2}m^2\frac{\delta E_\pi}{E}\left(p^2-2\bar{E}_\pi\bar{E}_\nu-\frac{1}{3}\left[p\,\delta E_\pi+\bar{E}_\nu^2-\left(\frac{\delta E_\pi}{2}\right)^2\right]\right)\right\}\delta E_\pi/M^3,$$

$$(18a)\qquad D_{SV}=m\,\delta E_\pi^2/2M^3,$$

$$(18b)\qquad D_{VT}=m\left\{\frac{p}{E}[2E\bar{E}_\nu-(W_\pi-\bar{E}_\pi)M]-\frac{1}{2}m^2\frac{\delta E_\pi}{E}+\right.$$

$$\left.+\frac{1}{2}\left(E-\frac{4}{3}\bar{E}_\nu\right)\delta E_\pi\right\}\delta E_\pi/M^4,$$

$$(18c)\qquad D_{ST}=\left\{\frac{p}{E}\left[(E-\bar{E}_\nu)(W_\pi-\bar{E}_\pi)-\frac{1}{3}\left(\frac{\delta E_\pi}{2}\right)^2\right]-\frac{2}{3}m^2\frac{\bar{E}_\pi}{M}\frac{\delta E}{E_\pi}\right\}\delta E_\pi/M^3.$$

In these expressions,

$$p = (E^2 - m^2)^{\frac{1}{2}} ;$$

$$\bar{E}_\pi = M - E - \bar{E}_\nu ;$$

$$\bar{E}_\nu = M(M - E)(W - E)/(M^2 - 2ME + m^2) ;$$

$\delta E_\pi = 2Mp(W E)/(M^2 - 2ME + m^2)$ and $W = M - W_\pi = (M^2 + m^2 - \mu^2)/2M$ is the maximum energy of the muon (electron). The absolute values of the coefficients of p/E in the first terms of the expressions (17) are the energy distributions of the mesons or electrons for the corresponding couplings. They have been obtained and tabulated by FURUICHI *et al.* (6).

TABLE V. – *Numerical values* ($\times 10^2$) *for the polarization and energy distribution of* μ*-mesons in* $K_{\mu 3}$*-decay. The upper figures correspond to* $P(dT/dE)$*, the lower ones to* dT/dE.

E/M	D_S	D_V	D_T	D_{SV}	D_{VT}	D_{TS}
.27	.43	— .23	.003 5	.09	— .030	— .072
	.78	.70	.066 4	.66	— .210	— .220
.30	1.52	— .61	— .012 3	.33	.103	— .110
	1.84	1.21	.060 2	1.09	— .259	— .262
.36	2.47	— .69	— .018 6	.53	.164	.063
	2.68	1.26	.034 9	1.17	— .156	— .038
4.2	2.65	— .43	.046 8	.57	.194	.390
	2.74	.84	.071 5	.91	.015	.348
.48	.149	— .006	.022 4	.032	.015	.058 6
	.151	.023	.022 7	.039	.012	.057 9

The muon spectrum is also given by formula (16) provided the lower figures for the D's in the above table are used.

5. – Four component theory.

The predictions of the two component theory are equivalent to a particular case ($f = 0$) of a more general interaction for which the transition matrix is proportional to:

$$g\bar{\psi}_\nu \frac{1 + \gamma_5}{2} O_i \psi + f\bar{\psi}_\nu \frac{1 - \gamma_5}{2} O_i \psi , \tag{19}$$

where ψ_ν is here a four-component Dirac spinor. The transition rate to a state ψ_- corresponding to the second term is equal to the transition rate to the state ψ_- corresponding to the first. Since there is no interference between these two terms, the energy spectrum is simply obtained by adding to the expression we have given an identical expression with the g's substituted by f's, and the generalization of (16) is

$$P\frac{\mathrm{d}T}{\mathrm{d}E}=\left(P\frac{\mathrm{d}T}{\mathrm{d}E}\right)_g-\left(P\frac{\mathrm{d}T}{\mathrm{d}E}\right)_f, \tag{20}$$

where on the right hand side $P(\mathrm{d}T/\mathrm{d}E)$ is to be calculated by means of (16) with the constants g or f as indicated.

6. – Concluding remarks.

The following discussion is based on the validity of our assumptions 1) and 4). If higher powers of momenta were not neglected in (3), the correct expression for the probability density corresponding to each coupling should differ from that we have calculated only by a factor of the form $[1+f(E_\pi)]$. Therefore, the dependence on E (the muon or electron energy) is correctly given by our expressions ([9]). Moreover, since the internal processes essentially involve nucleon propagators, one might expect the magnitude of $f(E_{\bar{\nu}})$ to be small compared with unity and the results of our approximation not to differ appreciably from those of a more rigorous treatment.

The expressions for ϱ given in (8) and (10) are linearly independent functions of E and $E_{\bar{\nu}}$. Also, integrating with respect to either of these variables, one obtains linearly independent functions of the other. Therefore, in principle, from the $\mathrm{K}_{\mu 3}$-decay it is possible to determine the magnitudes of $(g_S-(m/M), g_V)$, (g_V+g_V') and g_T, and the relative phases of these parameters. For K_{e3} since only the interference between the scalar and tensor interactions is appreciable, one can determine only the relative phase of g_S and g_T.

If our parameters are found to be complex (note that a small relative phase is not significant), one has two alternatives for interpreting this result:

(i) Invariance under time reversal is violated.

(ii) The two component theory or the law of conservation of leptons is not valid (in both cases the number of real parameters at our disposal is doubled).

([9]) A. Pais and S. B. Treiman: *Phys. Rev.*, **105**, 1616 (1957). The authors establish the general form of the angular correlation between the pion and neutrino directions of motion, which is connected with the probability density being a polynomial of second degree in powers of E.

With the values of our parameters determined from the energy distribution, one can use formula (16) to calculate the polarization. If the result of such a calculation is inconsistent with the experimentally observed polarization, this implies a failure of the two component theory or of the conservation of leptons (even if the parameters are real). On the other hand if there is a good agreement between the theoretical predictions and the experimental results, then complex values of the parameters imply violation of time reversaly invariance.

One notes that the foregoing considerations provide a more powerful test of the two-component theory or conservation of leptons than of time reversal invariance.

* * *

The author is very glad to express his thanks to Dr. R. H. Dalitz for his stimulating assistance, to Professor R. E. Peierls for most helpful discussions and to Dr. Nina Byers for many valuable suggestions.

Appendix

Invariance under time reversal.

Since $S = 1 - iM$ it follows from the unitarity of the S-matrix that

$$i(M_{ab} - M^*_{ba}) = \sum_c M_{ac} M^*_{bc} .$$

Taking a and b to be (K) and (π, μ, e) states, the order of magnitude of the right-hand side is given by the square of the coupling constant for weak interactions or else the product of such a coupling constant and e^4 (an electromagnetic interaction between μ^+ and π^0 is of fourth order in e). Therefore, one can neglect it and take

$$M_{ab} = M^*_{ba} . \tag{21}$$

Invariance under time reversal implies that

$$M_{ba} = M_{-a-b} , \tag{22}$$

where $-a$, $-b$ are the time reversed states corresponding to a, b. Using the Majorana representation of the Dirac matrices, under time reversal one has

$$\boldsymbol{p} \to -\boldsymbol{p}; \qquad \psi \to \gamma_0\gamma_5\psi^*; \qquad \overline{\psi} \to \overline{\psi}^*\gamma_5\gamma_0 . \tag{23}$$

Therefore, for a particular choice of coupling, it follows that

$$M_{\alpha} \sim \overline{\psi}_{\nu}^{*}\gamma_5\gamma_0 O_j\gamma_0\gamma_5\psi^{*}A^{j}(-\boldsymbol{p}) = \overline{\psi}_{\nu}^{*}\gamma_5 O_j\gamma_5\psi^{*}A^{j}(\boldsymbol{p}) = \varepsilon[\overline{\psi}_{\nu}O_j\psi A(\boldsymbol{p})^{*}]^{*} ,$$

where $\varepsilon = 1$ if the coupling is scalar or tensor and $\varepsilon = -1$ if it is vector. The first step follows from parity conservation in strong interactions. The last one is a consequence of our definitions of O_j in (4) according to which, in this representation, the O_j's are all real. Therefore invariance under time reversal requires that

$$\varepsilon A^{j}(\boldsymbol{p})^{*} = A^{j}(\boldsymbol{p}) , \tag{24}$$

which implies that all g's are real. Remembering that for pseudo-scalar bosons the field operators $\varphi(t)$ transform under time reversal into $-\varphi^{\dagger}(-t)$ while for scalar bosons $\varphi(t) \to \varphi^{\dagger}(-t)$ one sees that the above result is valid only for odd parity K-meson. For even parity K-meson, the above expression for M_{ba} must be multiplied by (-1) and, as a consequence, it follows that the g's must be pure imaginary.

RIASSUNTO (*)

Si discutono nel presente lavoro due aspetti dei decadimenti $K_{\mu 3}$ e K_{e3}, la densità d'energia degli stati finali e la polarizzazione longitudinale dei muoni e degli elettroni. Si assume che la coppia di fermioni sia prodotta per una interazione di Fermi che può essere di tipo scalare, vettoriale o tensoriale. Si impiega la teoria del neutrino a due componenti. Gli spettri energetici e la polarizzazione dipendono in genere da tre parametri complessi. Tuttavia, perchè la teoria risulti invariante rispetto all'inversione del tempo, i parametri debbono essere reali. Con i valori dei parametri risultanti dallo spettro d'energia si può predire la polarizzazione. Ciò fornisce una buona verifica della teoria a due componenti.

(*) *Traduzione a cura della Redazione.*

On the Decay of ^{113}Sn and ^{121}Te.

K. S. Bhatki, R. K. Gupta, S. Jha and B. K. Madan

Tata Institute of Fundamental Research - Bombay

(ricevuto il 18 Agosto 1957)

Summary. — By the coincidence studies of ^{113}Sn and by studying ^{113}Sn sources completely separated from ^{113}In, the existence of a level at 650 keV in ^{113}In resulting in the emission of 258 keV γ-ray has been established. This state is fed by the electron capture transition in ^{113}Sn to the extent of about 3.5%. The decay energy of ^{113}Sn leading to the 650 keV state has been calculated to be 36 keV. In the decay of ^{121}Te^m and ^{121}Te γ-rays of energy 70 keV and 1130 keV have been observed.

1. – Introduction.

The results of scintillation spectrometer studies of the radiations from carrier-free sources of ^{113}Sn and ^{121}Te are presented here. In the decay of ^{113}Sn, the existence of a radiation of 258 keV energy has been established by radiochemical and coincidence studies. The decay energy of this isotope has been measured by the measurements of the ratio of the K and L electron capture probabilities. In the decay of ^{121}Te, γ-radiations of energy 70 keV and 1130 keV have been detected.

2. – The 260 keV γ-rays from ^{113}Sn.

Although the existence of a γ-ray of about 260 keV energy in the decay of ^{113}Sn has been suspected before [1], the investigations of Thomas *et al.* [2]

[1] J. M. Cork, A. E. Stoddard, C. E. Branyan, W. J. Childs, D. W. Martin and J. M. Leblanc: *Phys. Rev.*, **84**, 596 (1951).

[2] D. A. Thomas, S. K. Haynes, C. D. Broyles and H. C. Thomas: *Phys. Rev.*, **82**, 961 (1951).

and AVIGNON (3) showed that the electron capture in ^{113}Sn leads only to the first excited state of ^{113}In at 392 keV, which is an isomer decaying with a half-life of 1.7 hrs. Recently GARDNER *et al.* (4) found that the scintillation γ-ray of 258 keV. They estimated the spectrometer study of ^{113}Sn shows the intensity of this γ-ray to be about 12% of the intensity of the 392 keV γ-ray. They suggest that this γ-ray arises from the branching of the decay of the 392 keV isomeric state through an intermediate state at 258 keV or 134 keV.

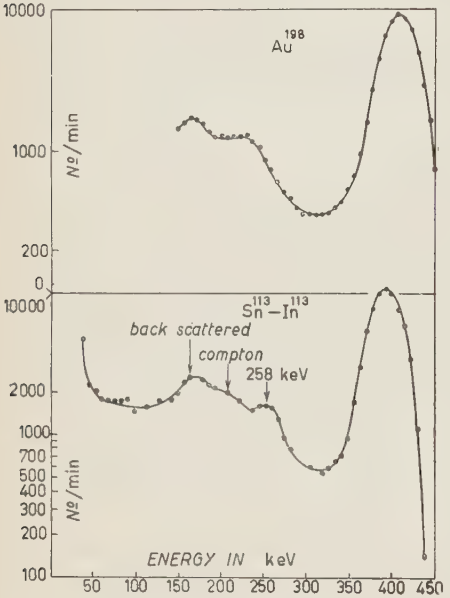

Fig. 1. – The γ-ray spectrum of ^{113}Sn and ^{198}Au taken in an identical geometry in a scintillation spectrometer.

3. – Present studies of ^{113}Sn.

The source of ^{113}Sn, for the present studies, was obtained by the deuteron bombardment of indium in the cyclotron of the Birmingham University. The carrier free tin was separated from indium by a method developed by BHATKI *et al.* (5). In Fig. 1 is reproduced the spectrum of the γ-rays from ^{113}Sn studied in a scintillation spectrometer with a NaI(Tl) crystal of 2 in. height and 1½ in. diameter, fixed to a 6292 Du Mont multiplier. In Fig. 1 is given also the spectrum of the γ-radiation from ^{198}Au, which emits mainly 411 keV γ-rays, taken in an identical geometry. From the comparision of the two spectra, one can see that there is a γ-ray of energy 258 keV emitted from ^{113}Sn. Since this γ-ray comes from a source of ^{113}Sn, prepared by (d, 2n) reaction on indium, from which it is chemically separated, and it has already been observed from a pile irradiated tin source (4), the assignment of this γ-ray to ^{113}Sn becomes certain.

4. – Further studies on the 258 keV γ-rays.

A source of ^{113}Sn was purified from the 1.7 hr indium daughter product, and whitin five minutes of the completion of the separation, the spectrum of the γ-rays was taken in a scintillation spectrometer. The spectrum, after

(3) P. AVIGNON: *Ann. de Phys.*, **1**, 10 (1956).
(4) G. GARDNER and J. I. HOPKINS: *Phys. Rev.*, **101**, 999 (1956).
(5) K. S. BHATKI and P. RADHAKISHNA: *Proc. Ind. Acad.*, **45**, 30 (1957).

correcting for the growth of the indium isomer (which emits a 392 keV γ-ray) is reproduced in Fig. 2. One can see that the 258 keV γ-ray appears very prominently. From this, after subtracting the Compton contribution of the 392 keV γ-rays, one can get the intensity of the 258 keV γ-rays.

The same source was studied from time to time for about 20 hrs. It was found that the 258 keV γ-rays remained constant within the errors of measurement. From the spectrum taken after the 1.7 hr activity had reached equilibrium with ^{113}Sn (not shown), the intensity of the 392 keV γ-ray was obtained. After correcting for the difference in the photoelectric efficiencies of the 392 keV γ-ray and the 258 keV γ-ray, it was found that the 258 keV γ-ray is about 5% of the 392 keV γ-ray in intensity.

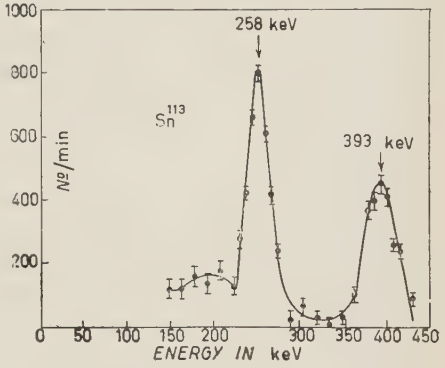

Fig. 2. – The spectrum of γ-rays from ^{113}Sn, taken five minutes after it had been completely separated from ^{113}In^{m}.

If the conclusion that the 258 keV γ-ray originates from a level in ^{113}In is correct, one should be able to observe this in coincidence with the K X-rays of indium. In Fig. 3 is reproduced the spectrum of γ-rays from a tin source in coincidence with the indium K X-rays. One can see that, as expected, the 392 keV peak does not appear, but the 258 keV peak does. The coincidence experiment thus substantiates the conclusions arrived at from the radiochemical experiment. In the spectrum in Fig. 3, there is a hump at about 160 keV. It could not be decided whether this peak was due to a γ-ray or it arose entirely as a result of back-scattering.

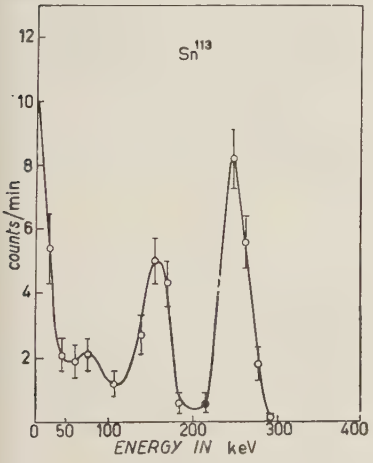

Fig. 3. – The spectrum of γ-rays in coincidence with the KX-rays of indium.

An attempt was made to measure the number of KX-rays of indium in coincidence with the 258 keV γ-ray. The counter heads of two scintillation counter spectrometers were placed at right angles to each other and a source of ^{113}Sn, mounted on an anti-Compton source-holder, was placed symmetrically before them. One channel accepted the full photo-peak of the 258 keV γ-ray and the other channel accepted the full X-ray peak. If the number of disintegrations leading to the state which de-excites by the emission of the 258 keV γ-ray is N, and N_K the number

of K captures leading to the same state, the number of γ-rays I_γ, accepted by the first channel, is given by

$$I_\gamma = N(1 - \chi)\varepsilon_\gamma S_1$$

and the coincidence rate is given by

$$I_{\gamma X} = N_K(1 - \chi)\varepsilon_\gamma \varepsilon_X S_1 S_2 \omega_K \exp[-\mu_X t],$$

where ε_γ and ε_X are the photo-electric efficiencies of the γ-rays and the X-rays, S_1 and S_2 are the solid angles subtended by the source at the two counters, $\exp[-\mu_X t]$ is the transmission of the X-rays through the cover of the crystal, $\omega_K = 0.85$ is the K fluorescence yield in indium and

$$\chi = \frac{\text{total number of the conversion electrons of the 260 keV } \gamma\text{-rays}}{\text{total number of conversion electrons and } \gamma\text{-rays}},$$

Then

$$N_K/N = (I_{\gamma X}/I_\gamma)(1/\omega_K \varepsilon_X S_2 \exp[-\mu_X t]).$$

The number of 258 keV γ-rays, I_γ, is calculated from the number of the 392 keV γ-rays, making use of the ratio of the intensities of the two γ-rays. The ratio P_L/P_K, where P_L is the probability of the L electron captures leading to the state from which the 260 keV γ-ray originates, and P_K the probability of the K electron captures leading to the same state, can be calculated from the ratio N_K/N. The average value of P_L/P_K has been found to be $2.23^{+1.12}_{-0.88}$ from which the decay energy of ^{113}Sn has been calculated ([6]) to be 36^{+1}_{-4} keV.

5. – Discussion.

It is clear from the results of this work that the electron capture decay of ^{113}Sn leads to the 392 keV state and also to another level. The fact that the decay energy of ^{113}Sn to the new level is only 36 keV shows that this level cannot be accommodated below the 392 keV level; it must lie above. Our result is different from that of THOMAS *et al.* ([2]), who find that the decay energy of ^{113}Sn to the 392 keV state is only about 40 keV. The result of THOMAS *et al.* depends on the value of the K conversion coefficient of the 392 keV γ-rays. Although the theoretically predicted value of the K conversion coefficient for the 392 keV M_4 transition in indium is only 0.45, the

([6]) H. BRYSK and M. E. ROSE: *ORNL* (1830), January 1955.

experimentally found values are 0.39 ([8]), 0.5 ([3]) and 0.9 ([9]). The higher value of α_K would reduce the value of P_L/P_K, found by measuring the intensity of the γ-rays and the K X-rays, and so reduce the value of the decay energy. The decay energy from the value of P_L/P_K found by AVIGNON ([3]), who measured α to be 0.5, is not inconsistent with our measurement. The result of POOLE *et al.* ([7]), who studied the inner breamsstrahlung in coincidence with the K X-ray and found the end point at about 100 keV, is very difficult to reconcile with the results of this work. From our results, it can be concluded that in ^{113}In there is a level at 650 keV which is fed by about 3.5% of the

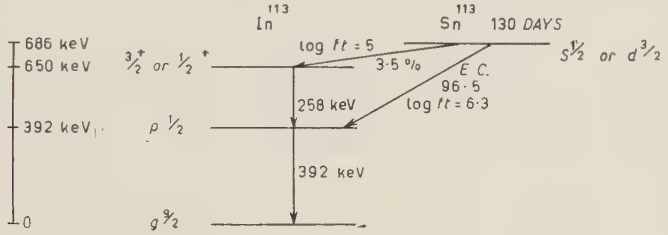

Fig. 4. – A tentative decay scheme of ^{113}Sn. (*)

electron capture transition. This state de-excites by the emission of the 258 keV γ-ray, followed by the isomeric transition of the 392 keV γ-ray. From these considerations, the following decay scheme can be proposed.

The log ft for the transition to the 392 keV state has been calculated ([10]) to be 6.3, which is consistent with the first forbidden transition of the type $\Delta J = \pm 0, 1$, yes. The log ft for the transition to the 650 keV state has been calculated to be 5 which is consistent with the allowed transition of the type $\Delta J = \pm 1, 1$, no. Recently ACHAR *et al.* ([11]) have studied ^{113}Sn in a β-ray spectrometer. They find that the intensity of the conversion electron line of the 258 keV γ-ray is about 0.3% of the intensity of the conversion line of the 392 keV γ-ray. Taking into account that the unconverted part of the 258 keV γ-rays is 5% of the unconverted part of the 392 keV γ-rays and assuming the conversion coefficient of the latter to be 0.45 ([9]), the conversion coefficient of the 258 keV γ-rays comes out to be about $2.7 \cdot 10^{-2}$. This value of the conversion coefficient is consistent with the M_1 character of the 258 keV γ-rays.

(*) *Note added in Proof:* The parity of the 650 keV state is odd in Fig. 4.

([7]) R. G. JUNG and M. L. POOL: *Bull. Am. Phys. Soc.*, **1**, 171 (1956).
([8]) I. V. ESTULIN and E. M. MOISEEVA: *Soviet Physics JETP*, **1**, 463 (1955).
([9]) M. GOLDHABER and R. D. HILL: *Rev. Mod. Phys.*, **24**, 179 (1952).
([10]) J. K. MAJOR and L. C. BIEDENHARN: *Rev. Mod. Phys.*, **26**, 321 (1954).
([11]) W. T. ACHOR, W. E. PHILIPS, J. I. HOPKINS and S. K. HAYNES: *Bull. Am. Phys. Soc.*, **2**, 259 (1957).

The 392 keV state is without doubt a $p_{\frac{1}{2}}$ state from which one can conclude that the 650 keV state has a spin and parity $\frac{1}{2}^-$ or $\frac{3}{2}^-$. One would normally expect the ground state of ^{113}Sn to be $s_{\frac{1}{2}}$ or $d_{\frac{3}{2}}$. Although this makes the electron capture transition to the 392 keV level first-forbidden and consistent with our log *ft* value of 6.3, this requires the electron capture transition to the 650 keV $\frac{1}{2}^-$ or $\frac{3}{2}^-$ state also to be first-forbidden. The log value of 5 for this transition seems then to be anomalous.

6. – Studies with ^{121}Te.

It has been found ([9,12]) that ^{121}Te decays by electron capture to the states of ^{121}Sb at 506 keV and 575 keV with the intensities of 13% and 87% respectively. These states de-excite by the emission of 560 keV and 575 keV γ-rays. The estimated decay energy of this isotope by the method of Way and Wood ([13]) was found to be about 1200 keV, and it was suspected that other γ-rays may be emitted in the decay of ^{121}Te.

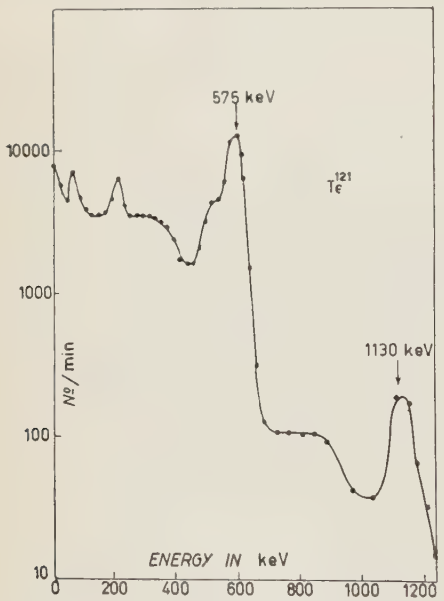

Fig. 5. – The spectrum of γ-rays from ^{121}Te, ^{121}Te^m and ^{123}Te^m in a scintillation spectrometer.

The tellurium isotopes of mass 121 and 123 in the ground and isomeric states were made by deuteron bombardment of antimony in the cyclotron of the Birmingham University. The tellurium isotopes in the carrier free state were separated from antimony. The γ-rays from ^{121}Te, ^{121}Te^m, and ^{123}Te^m were studied in a scintillation spectrometer. The spectrum of the γ-rays is reproduced in Fig. 5. Along with the 160 keV γ-rays from ^{123}Te^m and the 214 keV γ-rays from ^{121}Te^m (the highly converted γ-rays of energy 82 keV and 89 keV from the two isomers do not appear), there are the well known γ-rays of energy 506 keV and 575 keV from ^{121}Te. At the end of the spectrum, there is a peak corresponding to a γ-ray of energy 1130 keV. If this γ-ray is due to ^{121}Te, is hitherto unreported. The ratio of the intensity of this γ-ray and the 575 keV

([12]) M. Goldberg and S. Frankel: *Phys. Rev.*, **100**, 1350 (1955).
([13]) K. Way and M. Wood: *Phys. Rev.*, **94**, 121 (1954).

γ-ray remained unchanged as the source strength was reduced, showing that this peak did not arise due to any piling-up effects. The absorption experiment in lead showed that the 1130 keV peak height was reduced less than the 575 keV peak. Repeated chemical purifications to remove any traces of zinc and the elements formed by the deuteron bombardment on the common impurities in the antimony target material did not bring about any change in the relative intensities of 575 keV and 1130 keV peaks. This peak with the same intensity was also observed in a tellurium sample, irradiated in the Harwell pile, and left to decay away for about 8 months, from which traces of antimony and iodine had been removed. One is thus reasonably certain that this γ-ray originates in ^{121}Te either in the ground or the isomeric state. This question could not be decided as the source was about a year old when this study was made, and the ^{121}Te produced in the ground state had completely decayed. The intensity of the 1130 keV γ-ray was found to be about 5% of the intensity of the 575 keV γ-ray.

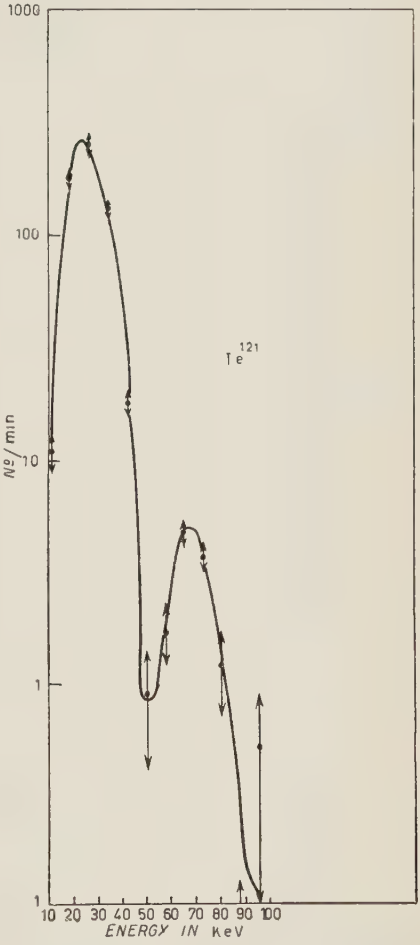

Fig. 6. – The spectrum of γ-rays in coincidence with the 506 keV γ-ray from ^{121}Te showing the presence of a 70 keV γ-ray.

The coincidence studies did not reveal any γ-rays in coincidence with the 1130 keV γ-ray in the region of 400 keV to 800 keV, nor were any γ-rays found in coincidence with either the 506 keV γ-ray or 575 keV γ-ray in the region of 400 keV to 800 keV.

No one has reported any transition between the 575 keV and the 506 keV levels in ^{121}Sb. With the multiplier units and the source kept away from the walls and scattering materials like lead, the spectrum was scanned in the low energy region in coincidence with the 506 keV γ-ras and the 575 keV γ-ray. In coincidence with the 506 keV γ-ray, a peak at 70 keV was observed; this peak did not appear when the region was scanned in coincidence with the 575 keV γ-ray. The 70 keV γ-ray was found to be about 2% of the 575 keV γ-ray in intensity. The low energy spectrum of ^{121}Te in coincidence with the 506 keV γ-ray is shown in Fig. 6.

The number of K X-rays in coincidence with the 1130 keV γ-ray and the singles count of the this γ-ray gave the ratio of the probability of the K electron captures and the L electron captures leading to the state from which the 1130 keV γ-ray originates. This ratio was found to be rather low indicating that the decay energy to this state must be large in comparison with the K-binding energy. If this state had originated from the electron capture in the ground state of ^{121}Te, the decay energy should have been about 100 keV, since the empirical estimate of the ground to ground decay energy is about 1200 keV. This leads us to the surmise that possibly there is some electron capture decay branching in the 115 day isomeric state of ^{121}Te. A tentative decay scheme is given in Fig. 7.

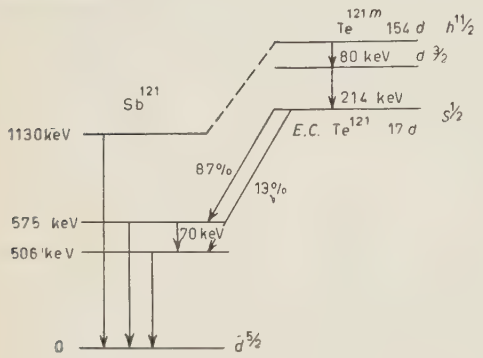

Fig. 7. – A tentative decay scheme of ^{121}Te^m.

* * *

Our thanks are due to the authorities of the Birmingham University, who produced these isotopes for us. We are grateful to Mr. A. T. Rane, who helped in the chemical separations and to Dr. P. Radhakrishna for his co-operation in solving the problem of chemical purifications. We are thankful to Dr. B. V. Thosar and Mr. B. Saraf for their co-operation.

RIASSUNTO (*)

Con lo studio delle coincidenze del ^{113}Sn e studiando sorgenti di ^{113}Sn completamente liberate da ^{113}In è stato identificato nel ^{113}In un livello a 650 keV risultante nell'emissione di raggi γ di 258 keV. Tale stato è alimentato per circa il 3.5% dalla transizione per cattura d'elettrone nel ^{113}Sn. L'energia di decadimento del ^{113}Sn che porta allo stato di 650 keV è stata calcolata in 36 keV. Nel decadimento del ^{121}Te^m e del ^{121}Te sono stati osservati raggi γ di 70 keV e 1130 keV d'energia.

(*) *Traduzione a cura della Redazione.*

IL NUOVO CIMENTO Vol. VI, N. 6 1° Dicembre 1957

Coupling Constant Invariants in β-Decay

S. Kahana (*) and D. L. Pursey

Tait Institute of Mathematical Physics, University of Edinburgh

(ricevuto il 18 Agosto 1957)

Summary. — The principle recently used by Pauli (1) and Pursey (2) is extended and applied to single β-decay without lepton conservation, and to β-decay with non-vanishing neutrino mass. Identities are found between the coupling constant invariants for Pauli's (1) general interaction, and it is shown that these involve at most 35 independent real constants. Conditions are given for invariance under space inversion, time reversal, particle-antiparticle conjugation, and for four interesting special theories, including lepton conservation and the two-state neutrino theory. A brief discussion is given of how experimental knowledge of the invariants, in particular those occurring in single β-decay, can be used to check the various special cases.

1. – Introduction.

Recently, Pauli (1) and independently Pursey (2) used a little-known principle to show that β-decay processes can depend on the coupling constants only through certain combinations which are invariant under a transformation group generated by a group of unitary transformations of the theory. In this paper we are concerned primarily with the properties of these invariants, and what can be deduced from measurements of them, but we also find it necessary to state a more general form of the principle in order to be able to handle single β-decay in the case when leptons are not conserved. We also give a new application of the principle to derive some of the general features of Enz' (3) results on β-decay with non-zero neutrino mass.

(*) Present Address: Department of Mathematics, McGill University, Montreal.

(1) W. Pauli: *Nuovo Cimento*, **6**, 204 (1957).

(2) D. L. Pursey: *Nuovo Cimento*, **6**, 266 (1957).

(3) C. Enz: *Nuovo Cimento*, **6**, 250 (1957).

We feel it may be helpful to say that in our opinion Sect. 2, 4 and 5 are of primarily theoretical interest while Sect. 3, 6 and 7 may be of interest also for the interpretation of experimental results.

2. – The fundamental principle.

PAULI's statement of the fundamental principle is as follows:

The S-matrix elements of any process are invariant (up to a phase) under any unitary transformation of the theory which leaves the initial and final states unaltered.

By leaving the initial and final states unaltered, we mean that the unitary operator of the transformation commutes with all the operators whose eigenvalues define the states; the state *vectors* may be multiplied by phase factors. If the relative phase of the initial and final state vectors is unaltered, the S-matrix element is strictly invariant, that is it is not even multiplied by a phase factor.

The principle as stated is adequate for the published applications ([1,2]), but is not sufficient for the discussion of single β-decay in the case when leptons are not conserved, for no final state of the system is invariant under the complete group of transformations used by PAULI ([1]). The difficulty is overcome by using the following generalization of the principle:

The average over given sets of initial and final states of the squared modulus of the S-matrix element for any process is invariant under any unitary transformation which leaves the sets of initial and final states invariant.

The wider applicability of this version is gained at the expense of the connection between the phase change of the S-matrix element and the change in relative phase of the initial and final states.

It is still possible to imagine situations in which applications of the principle similar to those already made ([1,2]) seem impossible. For example, in single β-decay the principle would appear to be inapplicable if the plane of polarization of the neutrino were detected. However, the term *plane of polarization of the neutrino* has no observational meaning until an experiment has been described to measure it. This measurement must work through some neutrino interaction whose coupling constants will also be changed by the unitary transformations considered. The whole experiment, including both production and detection of the neutrino, is defined in terms of initial and final states or sets of states which are unaltered by the unitary transformations, and the predicted results depend on the coupling constants only through invariants built from those of both the production and the detection interactions. The non-invariant neutrino states are intermediate, are not directly observed, and are summed over in the course of calculation.

A similar argument applies to the problem of observing whether the emitted light neutral particle is a neutrino or an antineutrino if leptons are not conserved. This case has been discussed in more detail by ENZ ([3]).

These remarks imply that the possibility of a natural and unambiguous experimental definition of, for example, the plane of polarization of the neutrino depends on special properties of the neutrino interactions. The same is true for the experimental definition of plane of polarization of electromagnetic radiation, or equivalently for the experimental distinction between $\boldsymbol{E}$ and $\boldsymbol{H}$. Suppose all particles carry both a normal electric charge and a magnetic (monopole) charge. If the ratio of magnetic to electric charges is the same for all particles, it is possible to redefine the fields and charges by a canonical transformation so that all the redefined magnetic charges vanish. In this case, we have the normal theory, with a natural definition of $\boldsymbol{E}$ and $\boldsymbol{H}$ which is experimentally unambiguous. However if the ratio of magnetic to electric charge is different for different particles, this is no longer so. An attempt to define $\boldsymbol{E}$ and $\boldsymbol{H}$ in the normal way will give results which depend on the test particle, and will be different for different particles.

3. – Definition of invariants.

This section is primarily concerned with explaining our notation, which we try to keep as close to established usage as possible.

The coupling constants are defined by specifying the interaction hamiltonian density to be

$$H_{\text{int}} = \sum_j \bar{\psi}_p O_j \psi_n \bar{\psi}_e O_j [(C_j + C_j' \gamma_5)\psi_\nu + (D_j + D_j' \gamma_5)\gamma_5 \psi_\nu^c] + \text{h. c.} \tag{1}$$

Here j ranges over the usual five interaction terms S, V, T, A and P: where we do not wish to be specific we may also distinguish different interactions by arabic numerals 1, ..., 5. The adjoint $\bar{\psi}$ and « charge » conjugate ψ^c of a field ψ are as defined by PAULI ([1,4]). The coupling constants C_j and C_j' are the same as those used by LEE and YANG ([5]) and most other authors; they differ from those used by PAULI ([1]). The coupling constants D_j and D_j' are defined in the way most convenient for the present paper, and also differ from the corresponding ones defined by PAULI ([1]). The relationship between Pauli's ([1])

([4]) W. PAULI: Article in *Niels Bohr and the Development of Physics* (London, 1955).
([5]) T. D. LEE and C. N. YANG: *Phys. Rev.*, **104**, 254 (1956).

constants $g_{\mathrm{I},j}$, $f_{\mathrm{I},j}$, $g_{\mathrm{II},j}$, $f_{\mathrm{II},j}$ and ours is as follows:

$$(2)\qquad \begin{cases} g_{\mathrm{I},j} = C_j^*, & f_{\mathrm{I},j} = C_j'^*, \\ g_{\mathrm{II},j} = -D_j'^*, & f_{\mathrm{II},j} = D_j^* . \end{cases}$$

It is convenient to define two sets of two-component column matrices ξ_j and η_j by

$$(3)\qquad \xi_j = \begin{pmatrix} C_j + C_j' \\ D_j + D_j' \end{pmatrix}, \qquad \eta_j = \begin{pmatrix} C_j - C_j' \\ D_j - D_j' \end{pmatrix}.$$

We shall use ζ or ζ_j when we do not wish to distinguish between a ξ and a η. The usual Pauli spin matrices, operating in the space of the vectors ζ, will be denoted by ϱ_1, ϱ_2, ϱ_3 (collectively, $\boldsymbol{\varrho}$). By ζ^+, $\tilde{\zeta}$ and $\tilde{\zeta}^+$ we shall mean respectively the row matrix hermitian conjugate to ζ, the row matrix $\zeta^T\varrho_2$ where ζ^T is the transpose of ζ, and the column matrix $\varrho_2\zeta^*$ hermitian conjugate to $\tilde{\zeta}$.

For the invariance group we shall generally supplement PAULI's [1] four parameter unitary transformation of the neutrino field by a phase change of the electron field. This generates the coupling constant transformations

$$(4)\qquad \xi_j \to \xi_j' = \exp[i(\varphi+\theta)]A\xi_j\,; \qquad \eta_j \to \eta_j' = \exp[i(\varphi-\theta)]A\eta_j\,;$$

where θ and φ are independent and $\boldsymbol{A}$ is a general 2×2 unimodular unitary matrix. Pauli's transformation is given by $\varphi = 0$.

Apart from the phase factors, the transformations of the ζ_j are identical with those of the spinor representation of the three-dimensional rotation group [6]. It follows that the only quantities which are invariant up to a phase are products of factors such as $\zeta_j^+\zeta_k$ and $\tilde{\zeta}_j\zeta_k$.

All quantities which are completely invariant under the transformations (4) must be products of factors of the four basic types

$$(5)\qquad \xi_j^+\xi_k\,, \qquad \eta_j^+\eta_k\,, \qquad \xi_j^+\eta_k\eta_l^+\xi_m\,, \qquad \xi_j^+\tilde{\eta}_k^+\tilde{\eta}_l\xi_m\,.$$

These are not all independent: it is easy to show (most elegantly by using Fierz transformations for two-component spinors) that

$$(6)\qquad (\xi_j^+\tilde{\eta}_k^+\tilde{\eta}_l\xi_m) + (\xi_j^+\eta_l\eta_k^+\xi_m) = (\xi_j^+\xi_m)(\eta_k^+\eta_l)\,.$$

Further identities between the invariants (5) are obtained in Sect. 5.

If the group is restricted to Pauli's four parameter group, then quantities such as $\tilde{\eta}_j\xi_k$ are also invariant.

[6] This remark is due to Professor PAULI.

For the purposes of comparison with experiment, it is convenient to introduce the notations

$$(7)\qquad \begin{cases} K_{jk} = K_{kj}^* = \frac{1}{2}(\xi_k^+ \xi_j + \eta_k^+ \eta_j) = C_j C_k^* + C_j' C_k'^* + D_j D_k^* + D_j' D_k'^* , \\ L_{jk} = L_{jk}^* = \frac{1}{2}(\xi_k^+ \xi_j - \eta_k^+ \eta_j) = C_j C_k'^* + C_j' C_k^* + D_j D_k'^* + D_j' D_k^* , \end{cases}$$

$$(8)\qquad \begin{cases} I_{jk}^* - I_{kj}^* = \frac{1}{2} i(\tilde{\xi}_k \eta_j - \tilde{\eta}_k \xi_j) = -C_j D_k' + C_j' D_k + D_j C_k' - D_j' C_k , \\ -J_{jk}^* = J_{kj}^* = \frac{1}{2} i(\tilde{\xi}_k \eta_j + \tilde{\eta}_k \xi_j) = -C_j D_k + C_j' D_k' + D_j C_k - D_j' C_k' . \end{cases}$$

The invariants K_{jk} and L_{jk} and the quantities I_{jk} and J_{jk} (which are invariant if $\varphi = 0$ in (4) are identical with the quantities defined by PAULI [1].

K_{jk} and L_{jk} are the direct extension to the case of non-conservation of leptons of the quantities α_{jk} and β_{jk} introduced by CURTIS and LEWIS [7]. From the general form of the fundamental principle it follows at once that any calculation for single β-decay with lepton conservation is extended to the case of lepton non-conservation by making the substitutions $\alpha_{jk} \to K_{jk}$, $\beta_{jk} \to L_{jk}$.

4. – β-decay with non-zero neutrino mass.

If the neutrino mass is non-zero, the free neutrino hamiltonian density is not invariant under the unitary transformations which generate (4). If, however, we adopt the modified mass term

$$(9)\qquad \tfrac{1}{2}(\overline{\psi}_\nu,\ \psi_\nu C\gamma_5)\boldsymbol{\rho}^T \cdot (\boldsymbol{m} + \boldsymbol{m}'\gamma_5)\begin{pmatrix} \psi_\nu \\ \gamma_5 \psi_\nu^c \end{pmatrix},$$

then Pauli's unitary transformations generate linear transformations of the six mass parameters $\boldsymbol{m}$ and $\boldsymbol{m}'$. In (9), $\boldsymbol{\rho}$ is again the Pauli spin-matrix vector, now operating on the row and column matrices $(\overline{\psi}_\nu,\ \psi_\nu C\gamma_5)$ and $\{\psi_\nu,\ \gamma_5\psi_\nu^c\}$, and $\boldsymbol{m}$ and $\boldsymbol{m}'$ are two vectors in the same three-dimensional space as the vector $\boldsymbol{\rho}$.

As the notation suggests, the transformations of $\boldsymbol{m}$ and $\boldsymbol{m}'$ generated by the unitary transformations are given by

$$(10)\qquad \begin{cases} \boldsymbol{m} + \boldsymbol{m}' \to \exp[2i\theta] R(\boldsymbol{m} + \boldsymbol{m}') , \\ \boldsymbol{m} - \boldsymbol{m}' \to \exp[-2i\theta] R(\boldsymbol{m} - \boldsymbol{m}') , \end{cases}$$

[7] R. B. CURTIS and R. R. LEWIS: *Phys. Rev.*, to be published (1957).

where θ is as in (4), and R is that rotation operator operating on the vectors $\boldsymbol{m}$ and $\boldsymbol{m}'$ which is represented by the matrix A in (4) operating on the spinors ζ.

For hermiticity, $\boldsymbol{m}$ must be real and $\boldsymbol{m}'$ pure imaginary. If, in addition,

$$\boldsymbol{m} \wedge \boldsymbol{m}' = 0 , \tag{11}$$

then it is possible to find a transformation (10) which makes all the mass parameters vanish except m_3; it is easily seen that (9) is then just the normal mass term for a particle of mass m_3.

The only invariants which can be built from the mass parameters alone are $m^2 - m'^2$ and $(\boldsymbol{m}+\boldsymbol{m}')^2(\boldsymbol{m}-\boldsymbol{m}')^2$. If (11) is satisfied then the second of these reduces to the square of the first.

For single β-decay, the general form of the fundamental principle shows that observable effects can depend only on invariants built from the coupling constants together with the neutrino mass parameters. The terms independent of the neutrino mass can depend only on K_{jk} and L_{jk} defined by (7). Terms linear in the mass can depend only on $(\boldsymbol{m}+\boldsymbol{m}')\cdot(\xi_j^{-}\boldsymbol{\rho}\eta_k)$ and $(\boldsymbol{m}-\boldsymbol{m})\cdot(\eta_j^{-}\boldsymbol{\rho}\xi_k)$. For the standard representation in which the only non-vanishing mass parameter is $m_3 = m_\nu$, the only possible coefficients of the neutrino mass are $(\xi_j^{-}\varrho_3\eta_k)$ and $(\eta_j^{-}\varrho_3\xi_k)$. Half the sum of these gives the coefficient, found by ENZ [3],

$$K'_{kj} = C_j^* C_k - C_j'^* C'_k - D_j^* D_k + D_j'^* D'_k , \tag{12}$$

while half the difference gives

$$L'_{kj} = C_j'^* C_k - C_j^* C'_k - D_j'^* D_k + D_j^* D'_k , \tag{13}$$

which can be expected to occur for processes which do not conserve parity.

For double β-decay without neutrinos, Pauli's form of the principle shows that terms in the S-matrix element linear in m_ν must be proportional to $(\eta_j\varrho_3\eta_k)$ or $(\xi_j\varrho_3\xi_k)$. (This is a case where the initial and final state vectors are strictly invariant, so the S-matrix element cannot suffer any phase change). Suitable combinations of these invariants give the coefficients

$$\begin{cases} -I'^*_{jk} = C_j D'_k + C'_j D_k + D_j C'_k + D'_j C_k , \\ J'^*_{jk} = C_j D_k + C'_j D'_k + D_j C_k + D'_j C_k . \end{cases} \tag{18}$$

I'_{jk} and J'_{jk} are just the coefficients found by ENZ [3].

So long as we do not want to work to any higher order in perturbation theory, any additional powers of the neutrino mass must enter only through the invariant $m^2 - m^2 = m_\nu$.

Henceforth we shall deal only with the case of zero neutrino mass.

5. – Identities satisfied by the invariants.

Since the interaction involves 40 real coupling constants, and the observable combinations of them are invariant under a 5 parameter group, we expect the coupling constant invariants to involve at most 35 independent real constants. Obviously, many identities must exist among the invariants (4), and in (6) we have already found one set.

An obvious further set is

$$\left\{\begin{aligned} &(\xi_j^+\eta_k\eta_l^+\xi_m)(\xi_n^+\eta_p\eta_q^+\xi_r) = (\xi_j^+\eta_k\eta_q^+\xi_r)(\xi_n^+\eta_p\eta_l^+\xi_m)\,, \\ &(\xi_j^+\tilde\eta_k^-\tilde\eta_l\xi_m)(\xi_n^+\tilde\eta_p^+\tilde\eta_q\xi_r) = (\xi_j^+\tilde\eta_k^+\tilde\eta_q\xi_r)(\xi_n^+\tilde\eta_p^+\tilde\eta_l\xi_m)\,, \end{aligned}\right. \tag{15}$$

obtained by permuting scalar factors $\eta^+\xi$ and $\tilde\eta\xi$ between invariants.

A third set may be found by noting that at most two of the ζ's can be linearly independent. It follows at once that

$$\begin{vmatrix} \zeta_j^+\zeta_m & \zeta_j^+\zeta_n & \zeta_j^+\zeta_p \\ \zeta_k^+\zeta_m & \zeta_k^+\zeta_n & \zeta_k^+\zeta_p \\ \zeta_l^+\zeta_m & \zeta_l^+\zeta_n & \zeta_l^+\zeta_p \end{vmatrix} = 0\,. \tag{16}$$

If we make suitable choices for the ζ's, expand the determinant, and use (6), we find

$$\left\{\begin{aligned} &(\xi_j^-\tilde\eta_k^-\tilde\eta_l\xi_m)(\xi_p^-\xi_q) = (\xi_j^-\xi_q)(\xi_p^-\xi_m)(\eta_k^+\eta_l) - (\xi_p^-\eta_l\eta_k^-\xi_q)(\xi_j^+\xi_m) - \\ &\qquad - (\xi_p\eta_l\eta_k^-\xi_m)(\xi_j\xi_q) - (\xi_j^+\eta_l\eta_k^-\xi_q)(\xi_p\xi_m)\,, \\ &(\xi_j^+\tilde\eta_k^-\tilde\eta_l\xi_m)(\eta_p^+\eta_q) = (\xi_j^+\xi_m)(\eta_k^+\eta_q)(\eta_p^-\eta_l) + (\xi_j^+\eta_q\eta_p^+\xi_m)(\eta_k^-\eta_l) - \\ &\qquad - (\xi_j^+\eta_l\eta_p^+\xi_m)(\eta_k^+\eta_q) - (\xi_j^+\eta_q\eta_k^+\xi_m)(\eta_p^+\eta_l)\,, \end{aligned}\right. \tag{17}$$

and the analogous set

$$\left\{\begin{aligned} &(\xi_j\eta_l\eta_k^-\xi_m)(\xi_p^-\xi_q) = (\xi_j\xi_q)(\xi_p^+\xi_m)(\eta_k^-\eta_l) - (\xi_p^+\tilde\eta_k^-\tilde\eta_l\xi_q)(\xi_j\xi_m) - \\ &\qquad - (\xi_p^+\tilde\eta_k^+\tilde\eta_l\xi_m)(\xi_j^+\xi_q) - (\xi_j^+\tilde\eta_k^+\tilde\eta_l\xi_q)(\xi_p^-\xi_m)\,, \\ &(\xi_j^+\eta_l\eta_k^-\xi_m)(\eta_p^+\eta_q) = (\xi_j^+\xi_m)(\eta_p^+\eta_l)(\eta_k^+\eta_q) + (\xi_j^+\tilde\eta_p^+\tilde\eta_q\xi_m)(\eta_k^-\eta_l) - \\ &\qquad - (\xi_j^+\tilde\eta_p^+\tilde\eta_l\xi_m)(\eta_k^+\eta_q) - (\xi_j^+\tilde\eta_k^+\tilde\eta_q\xi_m)(\eta_q^+\eta_l)\,. \end{aligned}\right. \tag{18}$$

We demonstrate that this now gives a complete set of identities by showing how to express all the invariants in terms of 35 real constants.

Suppose that $\xi_1^+\xi_1$, $\eta_1^+\eta_1$, $\xi_1^+\eta_1\eta_1^+\xi_1$ and $\xi_1^+\tilde{\eta}_1^+\tilde{\eta}_1\xi_1$, are known and are all non-zero: these are all real, so that, by (6), they involve only three independent real constants. Now suppose $\xi_1^+\xi_j$, $\eta_1^+\eta_j$, $\xi_1^-\eta_j\eta_1^+\xi_1$ and $\xi_1^-\eta_1\eta_1^-\xi_j$ are also known for j running over the remaining four interactions: these involve 32 real constants, making 35 altogether. By use of (6) and (18) it is now possible to find $(\xi_j^+\eta_k\eta_l^+\xi_m)$ and $(\xi_j^-\tilde{\eta}_l^+\tilde{\eta}_k\xi_m)$, in the first place when two of the indices are 1, and then for arbitrary indices. Either (17) or (18) then gives $(\xi_j^+\xi_k)$ and $\eta_j^+\eta_k)$.

This is the least favourable case. If, for example, it is found that one of $\xi_1^-\eta_1\eta_1^-\xi_1$ and $\xi_1^-\tilde{\eta}_1^+\tilde{\eta}_1\xi_1$ is zero, then the above solution is not possible, but a more efficient one using at most 34 real constants (including the three $\xi_1^+\xi_1$, $\eta_1^+\eta_1$, $\xi_1^+\eta_1\eta_1^-\xi_1$) can be found.

It is obviously not practicable to check the identities (6), (15), (17) and (18) experimentally, but they may prove useful in deducing the values of invariants which it is impracticable to measure directly.

6. – Conditions for invariance and for other special cases.

The conditions for invariance under space inversion (P), time reversal (T) and particle-antiparticle conjugation (C) which were given by PURSEY [2] must be amplified before they are valid for the interaction (1). The generalized conditions are

$$\begin{aligned}
&P \textit{ invariance}: && L_{jk} = 0\,, && \text{(all } j,\ k),\\
&\quad \text{and } \textit{either} && I_{jk} = 0\,, && \text{(all } j,\ k),\\
&\quad \textit{or} && J_{jk} = 0\,, && \text{(all } j,\ k).\\
&T \textit{ invariance}: && K_{ik},\ L_{jk},\ I_{jk}\ I^*_{lm},\ J_{jk}\ J^*_{lm},\ I_{jk}\ J^*_{lm} && \text{all real}\\
& && && \text{(all } j,\ k,\ l,\ m).\\
&C \textit{ invariance}: && K_{jk},\ I_{jk},\ I^*_{lm},\ J_{jk},\ J^*_{lm} && \text{all real},\\
& && L_{jk},\ I_{jk},\ J^*_{lm}, && \text{all pure imaginary}\\
& && && \text{(all } j,\ k,\ l,\ m).
\end{aligned}$$

These conditions can be obtained by showing that if they are satisfied then (1) can be transformed by (4) into a form which is trivially invariant, and vice versa. For P invariance, there are two inequivalent trivially invariant

possibilities, namely $C_j' = D_j' = 0$ (all j) and $C_j' - D_j' = 0$ (all j), which cannot be transformed one into the other by (4). Only the second case is consistent with a parity conserving two-state neutrino theory.

We shall now consider the conditions for a number of interesting special cases.

Case A. This is defined by

$$\tilde{\xi}_j \xi_k = \tilde{\eta}_j \eta_k = 0\,, \qquad \text{(all } j,\ k\text{)}, \tag{19}$$

which is equivalent to

$$\begin{cases} K_{jk}K_{lm} + L_{jk}L_{lm} = K_{jm}K_{lk} + L_{jm}L_{lk}\,, \\ \text{and} \\ K_{jk}L_{lm} + L_{jk}K_{lm} = K_{jm}L_{lk} + L_{jm}K_{lk}\,, \qquad \text{(all } j, k, l, m\text{)}, \end{cases} \tag{20}$$

where K_{jk} and L_{jk} are the invariants measured in single β-decay defined by (7) above. The importance of this theory is that there exist *simple relations involving only those invariants occurring in single β-decay.* A special case is when the D and D' coupling constants vanish.

Case B. In this case, the light neutral particle emitted in β-decay, whether it is a neutrino or antineutrino, is always circularly polarized in the same sense. The condition for this is

$$\text{either} \quad \xi_j = 0\,, \quad \text{(all } j\text{)}, \quad \text{or} \quad \eta_j = 0\,, \quad \text{(all } j\text{)}, \tag{21}$$

or equivalently

$$\begin{cases} \text{either} \quad L_{jk} = \ \ K_{jk}\,, & \text{(all } j, k\text{)}\,, \\ \text{or} \quad\ \ L_{jk} = -K_{jk}\,, & \text{(all } j, k\text{)}\,. \end{cases} \tag{22}$$

This is a particular and rather exceptional case of a theory conserving leptons.

Case C: Lepton conservation. By lepton conservation we mean the impossibility of double β-decay without neutrinos. The condition is

$$\tilde{\xi}_j \eta_k = 0\,, \qquad \text{(all } j,\ k\text{)}, \tag{23}$$

or

$$I_{jk} = J_{jk} = 0\,, \qquad \text{(all } j,\ k\text{)}. \tag{24}$$

With the exception of the special Case *B*, lepton conservation also implies Case *A*.

Case D: Two state neutrino. In writing down the interaction (1) we have allowed for a four state neutrino theory. The most direct way of specializing to a two-state theory is to use the version due to WEYL ([8]) and other recent workers ([9]) rather than that of MAJORANA ([10]). The relationship between the two versions has been fully discussed by several authors ([11]).

The conditions for a two state theory are

$$\xi_j^+ \eta_k = 0\,, \qquad \tilde{\xi}_j \xi_k = \tilde{\eta}_j \eta_k = 0\,, \qquad \text{(all } j,\ k)\,, \tag{25}$$

or alternatively

$$\begin{cases} I_{jk}\ I_{lm}^* = \frac{1}{2}(K_{mk}K_{lj} - L_{mk}L_{lj} + K_{lk}K_{mj} - L_{lk}L_{mj})\,, \\ J_{jk}\ J_{lm}^* = \frac{1}{2}(K_{mk}K_{lj} - L_{mk}L_{lj} - K_{lk}K_{mj} + L_{lk}L_{mj})\,, \\ I_{jk}\ J_{lm}^* = \frac{1}{2}(K_{mk}L_{lj} - L_{mk}K_{lj} - K_{lk}L_{mj} + L_{lk}K_{mj})\,, \end{cases} \tag{26}$$

together with (20). This does not imply lepton conservation nor does it imply the polarized neutrino theory of Case *B* ([1]). Case *A* is always implied by a two-state theory. Except for a two-state theory which also satisfies *B*, the conditions (19) or (20) defining Case *A* are redundant in the definition of Case *D*.

Case *A* and *B* taken together imply both Cases *C* and *D*, and vice versa: this is the two-state theory envisaged by LANDAU, LEE, YANG and SALAM ([9]). Cases *A* and *C* together imply the possibility of choosing a representation in which $D_j = D_j' = 0$, (all j).

7. – Conclusion.

In this Section, we shall try very briefly to relate our considerations to experimental results, especially on single β-decay, which we hope will in time become available.

The most interesting theoretical questions are whether leptons are conserved and whether a two-state theory is adequate. Direct checks of these involve difficult experiments on double β-decay or of the type performed by DAVIS ([12]). However, it is possible to get some indirect evidence from single β-decay alone, by testing the conditions (20) and (22) for the special Cases *A* and *B*. If both conditions are satisfied, then leptons are conserved and a two

([8]) H. WEYL: *Zeits. f. Phys.*, **56**, 330 (1929).

([9]) L. LANDAU: *Nuclear Physics*, **3**, 127 (1957); T. D. LEE and C. N. YANG: *Phys. Rev.*, **105**, 1671 (1957); A. SALAM: *Nuovo Cimento*, **5**, 299 (1957).

([10]) E. MAJORANA: *Nuovo Cimento*, **14**, 171 (1937).

([11]) J. SERPE: *Physica*, **18**, 295 (1952); *Nuclear Physics*, **4**, 183 (1957); M. FIERZ: private communication from Professor PAULI; J. A. MCLENNAN: *Phys. Rev.*, **106**, 821 (1957); L. A. RADICATI and B. TOUSCHEK: *Nuovo Cimento*, **5**, 1693 (1957); K. M. CASE: *Phys. Rev.*, to be published (1957).

state theory is valid. If (22) is satisfied but not (20), then leptons are conserved but a two state theory is impossible. If (20) is satisfied but not (22), then further tests of lepton conservation and the two-state theory, involving the Davis type of experiment, will be necessary. If neither (20) nor (22) is satisfied, then leptons can not be conserved, and also the two-state theory is impossible.

If Case *A* is true but not Case *B*, we are faced with the problem of deciding whether leptons are conserved, or whether a two state theory is valid. A complete check on these points appears impossibly difficult, but we notice that for a two state theory the result of any experiment on neutrino capture (of a type equivalent to a double β-decay experiment with no neutrinos) can be predicted from information obtained from single β-decay and used in (26). It may in time be practicable to check the total probability for a positive result in the Davis ([12]) experiment in this way.

* * *

We wish to thank Professor W. PAULI for stimulating discussions, and for sending us a prepublication copy of his paper. We are also grateful to the many friends with whom we have discussed various aspects of this and related work, in particular Professor N. KEMMER and Dr. J. C, POLKINGHORNE of Edinburgh and Mr. L. CASTILLEJO, Dr. P. W. HIGGS and Dr. E. A. POWER of London. One of us (S.K.) wishes to thank the National Research Council, Ottawa, Canada, for the award of a Special Scholarship.

([12]) R. DAVIS: *Phys. Rev.*, **97**, 766 (1955).

Note Added in proof.

Since this paper was written, we hawe learnt of a paper by G. LÜDERS (to be published in *Nuovo Cimento*) which covers similar ground. We wish to thank Dr. LÜDERS for sending us a prepubblication copy of his paper, and for a valuable correspondence.

RIASSUNTO (*)

Il principio recentemente applicato da PAULI ([1]) e PURSEY ([2]) si estende e si applica al singolo decadimento β senza conservazione dei leptoni e al decadimento β con massa del neutrino non tendente a zero. Si trovano identità tra gli invarianti della costante d'accoppiamento per l'interazione generale di Pauli, e si dimostra che detti invarianti contengono al massimo 35 costanti reali indipendenti. Si danno le condizioni per l'invarianza rispetto all'inversione dello spazio, del tempo, della coniugazione particella-antiparticella e per quattro interessanti teorie speciali, includenti la conservazione dei leptoni e la teoria del neutrino a due stati. Si discute brevemente come la conoscenza sperimentale degli invarianti, in particolare di quelli che si presentano nel singolo decadimento β, possa essere usata per controllare i vari casi speciali.

(*) *Traduzione a cura della Redazione.*

A WF_6 Bubble Chamber (*).

E. D. Alyea jr., L. R. Gallagher, J. H. Mullins and J. M. Teem
California Institute of Technology - Pasadena, California

(ricevuto il 9 Maggio 1957)

Summary. — A small bubble chamber has been constructed for testing corrosive, high density liquids. Its successful operation with tungsten hexafluoride (WF_6) is described, together with some of the techniques necessary for handling this liquid and measurements of its physical properties. Some work on stannic chloride ($SnCl_4$) and stannic bromide ($SnBr_4$) is also summarized.

1. – Introduction.

D. Glaser first pointed out the possible advantages of a bubble chamber liquid of relatively high density and atomic number. High stopping power (approaching that of nuclear emulsions) and high γ-conversion efficiency are evident features of such liquids. Also, for particles possessing strong coupling with nuclei, interaction lengths would be comparable with the dimensions of a feasible size chamber of this type. In addition there exists the possibility of using coulomb scattering as well as bubble density to measure such dynamical quantities as particle momentum and velocity.

The first heavy liquid bubble chamber to be operated succesfully was the xenon chamber of Brown, Glaser and Perl [1]. While xenon has one major advantage among possible heavy liquids, namely that it is chemically inert, its extremely high cost and low production rate necessarily limit the number, as well as the size, of xenon chambers. For this reason it seemed worthwhile to investigate other high density liquids for bubble chamber use. To be feasible, such liquids should have reasonably low critical temperatures and pressures, low surface tension, transparency, and chemical stability at the operating temperature.

Among the first heavy liquids suggested by Glaser (in addition to xenon) were WF_6 and $SnCl_4$. We have investigated these two liquids and $SnBr_4$ for use in bubble chambers. These liquids are all corrosive and require special

(*) This work was supported in part by the U.S. Atomic Energy Commission.

(1) J. L. Brown, D. A. Glaser and M. L. Perl: *Phys. Rev.*, **102**, 586 (1956).

handling. However, providing proper techniques are used for purifying the liquid, corrosion seems to present no major problem in the case of WF_6. WF_6 is available commercially (2), and there does not appear to be any practical limit to the quantity available.

2. – Description of the bubble chamber.

To carry out the investigation of these liquids, a small corrosion resistant bubble chamber was constructed. The sensitive region is a cylinder 3.8 cm in diameter by 1.5 cm deep. Entering this cylinder are two tubes, one from the top 4.7 mm in diameter and one from the bottom 8.3 mm in diameter. The latter leads to the expansion apparatus 25 cm below (see Fig. 1-*a*). We

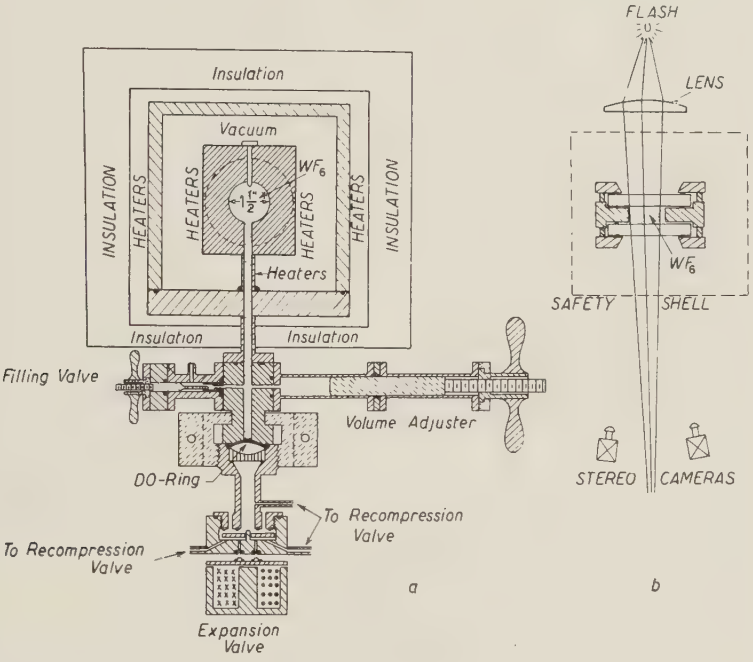

Fig. 1. – *a*) Diagram of bubble chamber; *b*) optical system.

have found that for successful operation of a chamber of this size and construction the expansion tube must be greater than 3 mm in diameter. Leading from the expansion tube are a filling valve and a piston which is used for adjusting and measuring liquid volume changes with a sensitivity of .004 cm^3. The top tube has been used to introduce into the chamber purifying agents and metal samples for corrosion tests.

The windows are quartz plates 1.27 cm thick. For temperatures below

(2) General Chemical Division, Allied Chemical and Dye Corporation, 40 Rector Street, New York 7, New York, USA. Present market price $ 15/lb.

200 °C, e.g. with WF_6, teflon « O » rings have been used to make the window seals. Alternatively, at any temperature flat gold gaskets may be employed between lapped metal surfaces and the quartz. With the exception of the top tube, which is sealed with a gold plug (*), all other seals are made at room temperature with teflon « O » rings.

The expansion diaphragm-« O » ring combination is machined from a singel piece of teflon. The flat portion is 0.76 mm thick and 3.8 cm in diameter. This diaphragm is backed by a hycar rubber disk and a perforated polyethylene piece. These are further supported by a perforated brass plate, which limits the excursion of the diaphragm under unbalanced pressures from the liquid side. The expansion system is fairly conventional, consisting of a pilot operated, d.c. solenoid activated, gas pop-valve. Reasonably fast recompression is accomplished with a commercial a.c. solenoid valve.

The use of any toxic, corrosive heavy metal compound necessitates certain precautions for the safety of personnel. Although we have never experienced leakage or breakage of this chamber, we have adopted the principle that any such chamber should be surrounded by an evacuated safety vessel capable of containing high pressures in the event of a disaster. The safety tank of the present chamber is constructed of stainless steel with quartz windows and designed to hold 40 atm. A fast closing, solenoid operated valve isolates the safety tank from the vacuum pump should the pressure rise above 100 μm.

The chamber heaters (see Fig. 1*a*) are controlled by thermistor regulated thyratron power supplies, temperatures being measured with thermo-couples located at appropriate points. The thermocouple which monitors the liquid temperature is located in the wall within 1.6 mm of the liquid.

While the bulk of the chamber is constructed of stainless steel, coatings on the inner walls provide further corrosion resistance. The heated portions of the chamber are gold plated to a thickness of about 20 μm. The valve, expansion cavity, and volume adjustor (with the exception of its monel piston) are ceramic coated to a thickness of about 50 μm. However, the above is not the best system for WF_6. Specifically, the ceramic coating is undesirable, and the gold plating is unnecessary. These coatings are probably necessary to prevent corrosion by $SnCl_4$ and $SnBr_4$ and were applied for that purpose. On the basis of our experience we would recommend the use of nickel-rich alloys, e.g. monel and inconel, or nickel for the construction of WF_6 bubble chambers.

The chamber is photographed with dark field illumination by a stereographic system consisting of two 16 mm movie cameras (see Fig. 1*b*). Unfortunately, some light reflected from the edge of the safety tank window enters the cameras, causing an annoying ring in the photographs shown below.

3. – Purification of tungsten hexafluoride.

Like many metal hexafluorides, WF_6 hydrolyses when exposed to water vapor, in this case forming HF and WOF_4. HF will etch glass to form H_2O and SiF_4, thus producing more water and initiating a chemical chain reaction. Since any bubble chamber requires transparent windows, we were initially

(*) We are indebted to D. F. Buckingham, D.D.S., for supplying this gold casting.

hesitant to consider operation with WF_6. However, our experience has shown that with proper techniques one can avoid this difficulty. First, initial outgassing at high temperatures will remove essentially all the water vapor from the system. Second, the distillation process employed greatly reduces any HF impurities that may be present in the WF_6. Finally, sodium fluoride can be placed in contact with the WF_6 to act as a getter for HF, and in addition any unoxidized metal in the system tends to remove HF without producingmore H_2O.

The purification system employed three stages of vacuum distillation through tubes filled with NaF pellets (see Fig. 2). Except for the steel WF_6 storage cylinder and its Cu connecting tube, the entire system is constructed, of monel or nickel. During distillation the liquid was evaporated at a temperature of about 0 °C and condensed at — 80 °C. Between distillations the WF_6 was kept frozen at — 80 °C while the system was evacuated through a cold trap at — 196 °C for about 10 min to remove HF. (Some WF_6 was lost in this process). Unless the NaF is thoroughly dry, it probably does more harm than good in reducing the HF contamination. We heated it to 1 040 °C in melting the powder into pellets and, furthermore, outgassed the entire system thoroughly at temperatures above 150 °C before beginning the distillation.

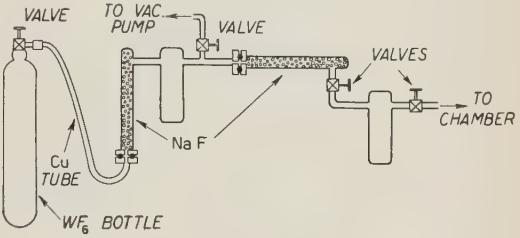

Fig. 2. — Purification and filling system.

While this system has been resonably satisfactory, an alternative method which is probably superior has been suggested by WEINSTOCK [3]. In this system the pumping to remove HF is done while the WF_6 is at — 100 °C, using an eutetic mixture of trichlorethylene and chloroform for the temperature control bath, and no getter is used.

4. — Chamber operation with WF_6.

This bubble chamber operated successfully with WF_6 on its initial trial, after previous testing with normal butane. Satisfactory electron tracks were observed over an operating temperature range from 136° to 150° C. The negative prints shown in Figs. 3 and 4 were obtained during a run at 149 °C with the California Institute of Technology Synchrotron. The chamber was placed 70 cm from a CH_2 target at an angle of 45° with respect to the 1 GeV bremsstrahlung beam. At this temperature the bubble density for relativistic electrons is 45-50 bubbles/cm. The change in pressure upon expansion is not known (*), but the n-butane operating temperature of this chamber that cor-

---

[3] B. WEINSTOCK and J. G. MALM: *Journ. of Inorg. and Nucl. Chem.*, **2**, 380 (1956), and B. WEINSTOCK: private communication.

(*) Although the gas in the pop-valve expands to one atmosphere in about 3 ms, there is obviously self-recompression of the liquid due to violent boiling around an inconel plug inserted in the top tube for corrosion tests. This boiling is seen in Fig. 3. Flash photographs taken early in the expansion cycle show that it originates in the space between the plug and the wall of the tube, and not from the surface of the inconel.

responds roughly to the lower temperature above is 115 °C. We have not yet observed an upper limit to the range of operating temperatures for WF_6 (the « fizz » limit, as it is called by Glaser), nor have we determined the lowest temperature for radiation sensitivity.

The synchrotron was an ideal source for studying chamber operation, since the X-ray beam could be extracted in about 100 μs. By varying the timing of the beam with respect to the expansion cycle, we measured the sensitive time of the chamber as 1.5 ms. Presumably the cut-off of the sensitive time is caused by self-recompression of the chamber. The rate of operation was once every 20 to 30 s, but it probably could be greater, since the liquid appears to reach thermal equilibrium in about 10 s. The photographs illustrate the behavior of different kinds of particles in a WF_6 bubble chamber. Several features are worthy of note in these examples. Differences in Coulomb scattering and bubble density between pions and protons are obvious near the ends of their tracks. π^+-mesons can be readily distinguished from π^-'s through their characteristic decay (*). The variation of bubble density with residual range is evident in these examples even though the operating temperature was so high that accurate bubble density (or gap counting) measurements were impossible within our resolution. Many cases of pair production in the chamber liquid have been seen, of which the examples included readily illustrate the use of such an instrument for the detection of γ-rays and π^0-mesons. The possibility of containing a shower for γ-ray energy measurement in a moderate size chamber is illustrated in the shower example.

5. – Effect of WF_6 on chamber materials.

After three months, including about 150 h at operating temperatures and several hours as high as 180 °C, the liquid and particularly one quartz window were somewhat dirty, as is apparent in Fig. 3. Although initial corrosion tests had indicated that the ceramic was only slightly affected by exposure for 150 h to pure WF_6 at 125 °C, we found after the WF_6 run that the ceramic coated parts of the chamber had been badly corroded. A large part of the background of single bubbles in the photographs came from boiling on foreign materials, which probably floated up from the ceramic below. When the chamber was disassembled, a thin black coating on the quartz and a similar coating on the gold were readily wiped off, and the quartz showed absolutely no sign of etching.

Our initial tests with teflon also indicated it to be essentially unaffected by pure WF_6. However, at the end of the run, we found that the teflon window gaskets had changed from their characteristic white to a light gray color. Furthermore, they had flowed rather badly, though they still retained their flexibility. The teflon gaskets at room temperature were apparently unaffected. However, after two days' exposure to the atmosphere, all teflon surfaces which had been exposed to WF_6 grew many thin « whiskers » up to 3 cm long. This would indicate that from a chemical standpoint, gold would be a better high temperature gasket material.

(*) Few π^- stars should be visible in WF_6 because of the short ranges of typical π^- star prongs.

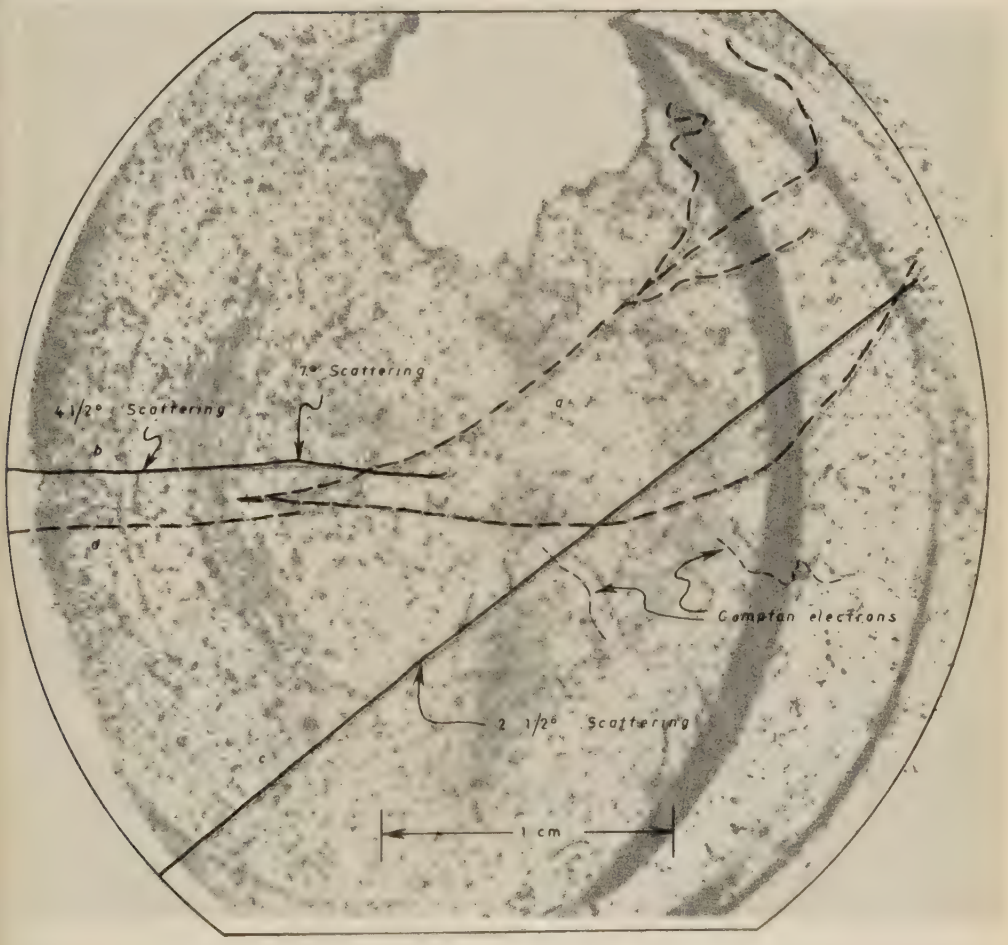

Fig. 3. - Low energy shower in WF_6 bubble chamber. This picture includes: *a*) a shower: $e^{\pm}$ pair, one of which emits bremsstrahlung (track bends down), second $e^{\pm}$ pair, one of which also emits bremsstrahlung; *b*) a stopping particle, probably a π^- meson; *c*) a high energy proton which scatters by $2\frac{1}{2}°$, and *d*) an electron which goes out of the chamber through the window.

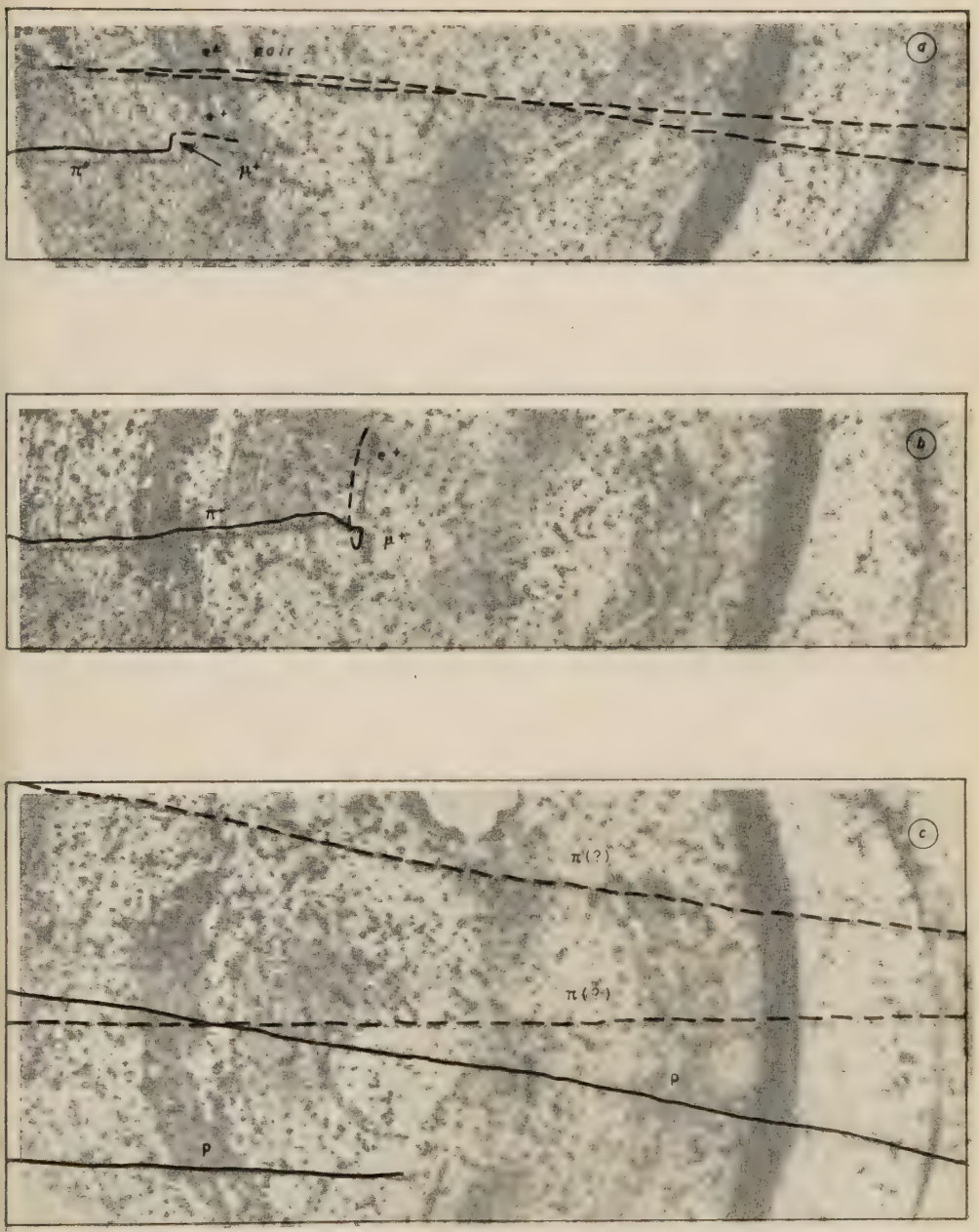

Fig. 4. – Various types of particles in WF$_6$ bubble chamber: a) high energy pair and $\pi^+ \to \mu^+ \to e^+$ decay: e^+ leaves chamber before stopping. b) [illegible] decay, e^+ leaves chamber. Note Coulomb scattering of proton (scattered proton is lowest track). c) a non-stopping proton and two probable π mesons.

Upon disassembling the expansion apparatus, we discovered small amounts of WF_6 between the teflon diaphragm and the hycar backing. Although the latter had been attacked, it had not been penetrated. Since the teflon was not cracked and appeared normal, it is possible that the WF_6 had penetrated this piece through microscopic pinholes, or had permeated the teflon itself.

Our experience has indicated that inconel X and monel acquire at most a very thin fluoride coating which apparently stops further action. Although we do not recommend copper, stainless steel, or ordinary steel for hot parts of the chamber, they do appear useful for some purposes, since their corrosion is also self-limited by a fluoride coating. Oxide coatings, however, should be avoided because of their role in $HF—H_2O$ chemical chain reactions.

6. – Physical properties of WF_6.

Tungsten hexafluoride in its pure state is a colorless liquid with a measured index of refraction at 145 °C of 1.28 ± .02. We have measured its critical temperature as (178.2 ± 0.5 °C) and the vapor pressure as a function of temperature from 10 to 30 atm. Extrapolation of our vapor pressure data above 30 atm with the function $p = C \exp[K/T]$, where C and K are empirical constants, yields a critical pressure of 46.3 atm. We believe this result to be accurate to ± 0.5 atm.

Some preliminary measurements were also made of the liquid density for temperatures near its operating point using volume measurements made with the calibrated piston. If we employ the law of corresponding states and use the critical temperature and pressure given above, we find a critical density of 1.40 g/cm³. Fig. 5 presents the results of our vapor pressure and density measurements, together with their extrapolation to the critical point and earlier measurements on WF_6 at lower temperatures ([1]).

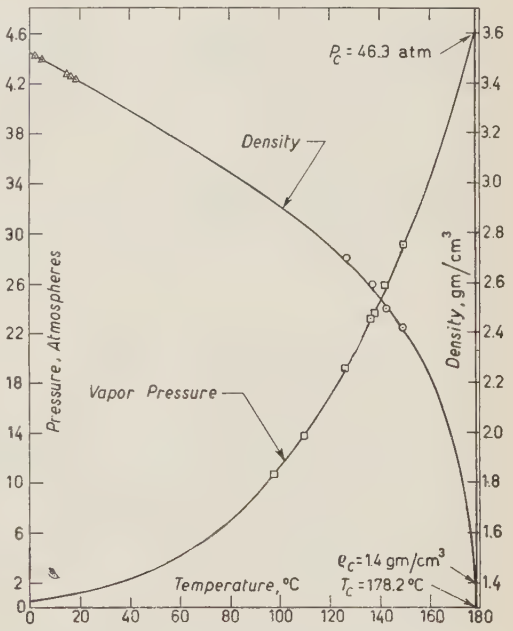

Fig. 5. – Vapor pressure and density of WF_6 vs. temperature.

Assuming an operating temperature of 149 °C, the liquid density from these preliminary measurements is 2.42 ± .10 g/cm³. We believe, however, that in a better chamber a lower operating temperature may be feasible, yielding a density perhaps as high as 2.6 g/cm³.

([1]) Quoted in GMELINS: *Handbuch der Anorganischen Chemie*, 8th Ed., vol. **54**, page 156.

We have compiled in Table I a comparison of some pertinent characteristics of several proven bubble chamber liquids at their operating temperatures.

TABLE I. – *Comparison of some bubble chamber liquids.*

Material	Oper. temp. °C	Oper. press. atmos.	Oper. dens. g/cm³	Rad. length (cm)	Stopping power rel. to. Al.	Range of 100 MeV π (cm)	Nuclear interact. length (cm)	Mult. scatt. coeff.
Propane	58	21	0.43	118	.22	57	97	1.06
Xenon	— 19	25	2.3	3.5(*)	.62	20	63	7.15
WF_6	149	29	2.4	3.8	.72	17	42	6.94
$SnCl_4$	270	20	1.4	8.6	.44	29	77	4.43
Nuclear emulsion	Room	Room	3.8	3.0	.98	12	26	7.64

(*) The radiation length in xenon is quoted in ref. (1) as 3.1 cm. Since different definitions are sometimes used for the radiation length (or cascade unit), we have calculated this quantity for all the above materials using equation (20) in Rossi: *High Energy Particles*, p. 54.

The analogous quantities are also listed for nuclear emulsion. The nuclear interaction length entries were calculated assuming geometrical cross sections for the various nuclei. The multiple scattering coefficient is defined as the factor $(\varrho \sum n_i Z_i^2/A)^{\frac{1}{2}}$ where the sum is taken over the number of i-th type atoms, n_i, of atomic number, Z_i, in the compound whose molecular weight is A and density ϱ. It should be noted that a direct comparison of this factor is meaningful only among the various liquids, since the accuracy of measurement is much greater in emulsions than in bubble chambers.

7. – Experience with other liquids.

Because of its availability, the first liquid that we tested was $SnCl_4$. These early tests were conducted in a « clean » glass chamber before the present chamber was constructed. Its glass bulb was immersed in a temperature bath consisting of Dow-Corning fluid 550, which our tests have shown to remain transparent to 400 °C when heated in an oxygen free atmosphere. $SnCl_4$ showed tracks from a RaBe source at a temperature of 270 °C, where its vapor pressure is 20 atm and density is 1.4 g/cm³. Radiation sensitivity was observed as low as 261 °C.

The success with $SnCl_4$ led us to try next the similar, but more dense liquid, $SnBr_4$. We estimated that this liquid would operate at a temperature between 380° and 400 °C. Breakage of the glass chamber delayed this test, and while the present chamber was being cons ructed we made a number of corrosion tests with $SnBr_4$ and WF_6. We found that among the metals, gold and rhodium were corrosion resistant to $SnBr_4$ at 400 °C, while aluminum, copper, nickel, inconel, and stainless steel were attacked. A ceramic coating applied to these metals does provide corrosion resistance; however, we have had some difficulty with chipping of the ceramic coating on sharp edges. Since the corrosion

tests with WF_6 were more encouraging, the work with the tin compounds was suspended.

The purification of the $SnBr_4$ presented another difficulty. Whenever the liquid was vacuum distilled into a glass tube, sealed, and heated to 400 C, a black coating was deposited on the walls (*). While the identity of this impurity was never determined, it apparently was removed by the heat treatment, because after redistillation no such effect was observed upon reheating the $SnBr_4$. The stannic bromide exhibits a greenish-amber color at temperatures above 250 °C, but reverts to the colorless state upon cooling.

8. – Recommendations.

Tungsten hexafluoride seems quite feasible as a bubble chamber liquid, furnishing a less expensive and more readily available substitute for liquid xenon. In at least one respect, i.e., in its stopping power, WF_6 would appear even superior to Xe. Reasonable safety precautions and proper handling techniques, however, must be observed in its use. A cylindrical bubble chamber 12 inches in diameter and 6.5 inches deep designed for use either with WF_6 or hydrocarbons is under construction here. As its design is somewhat unconventional, it will be described in detail elsewhere. Stannic chloride would also appear feasible, but less desirable because of its lower density and atomic number, higher operating temperature, and probably greater corrosion difficulties.

Both Xe and WF_6 lack free protons for target nuclei with which to study elementary particle interactions within the chamber. For photoproduction studies, however, we hope to use a high pressure hydrogen gas target passing through the chamber. For charged particle interactions we believe another approach should be considered. It would appear technically feasible to construct a double bubble chamber composed of a thin-walled hydrocarbon target chamber completely immersed in a heavy liquid chamber. Both would operate at the same temperature and possibly use the same expansion system. Xenon and ethylene would make one such possible combination, while WF_6 and a proper mixture of isopentane and normal butane could make another. The feasibility of the latter combination depends upon whether or not there would be a violent chemical reaction in the event of a disastrous mixing of the two liquids, but an ethylene-xenon double bubble chamber would obviously not suffer from this danger.

* * *

We would like to acknowledge the assistance of Messrs. J. T. Chang, R. L. Cohen, L. J. Fretwell jr., and D. E. Groom at various stages of this investigation. Mr. C. W. Friswold provided engineering advice.

We are especially indebted to Dr. B. Weinstock for helpful and enthusiastic advice on the handling of WF_6, and to Dr. N. R. Davidson for advice

(*) During operation of the glass chamber with $SnCl_4$ a thin, but similar black coating was observed to form on the walls, but this could have been a result of corrosion of the metal parts of the system.

on other chemical problems. Finally, we are grateful for the continuing interest and encouragement of Prof. R. F. BACHER throughout all phases of the heavy liquid bubble chamber program.

One of us, (J.H.M.) acknowledges financial assistance in the form of fellowships provided during different periods of this investigation by the Charitable and Educational Fund of the General Electric Company and by the Dow Chemical Corporation.

RIASSUNTO (*)

Una piccola camera a bolle è stata costruita per fare una prova dell'uso di corrosivi liquidi di grande densità. Si descrivono il funzionamento di questa camera a bolle con esafluoruro di tungsteno (WF_6). Vengono anche esposti alcuni procedimenti necessari per il lavoro con questo liquido, e qualche misura sulle sue proprietà fisiche. Inoltre si riassume qualche lavoro con cloruro di stagno ($SnCl_4$) e con bromuro di stagno ($SnBr_4$).

(*) *Traduzione a cura di* ROBERTO WALKER.

LETTERE ALLA REDAZIONE

(La responsabilità scientifica degli scritti inseriti in questa rubrica è completamente lasciata dalla Direzione del periodico ai singoli autori)

On the Perihelion Shift in Conformally Flat Space-Time.

A. Das

Department of Physics, Calcutta University - Calcutta, India

(ricevuto il 25 Maggio 1957)

In a recent note Pirani [1] investigated the motion of perihelion in conformally flat space-time according to Littlewood's [2] equations. Again, an identical problem had already been worked out independently by Gürsey [3]. But the results obtained by the two authors do not agree with each other. So, in this note, we re-investigate the same problem and ultimately support the result got by Pirani. We shall also extend the field equation.

Now, in a conformally flat space-time

$$\mathrm{d}s = g(r)\,\mathrm{d}s_0 \,. \tag{1}$$

where $\mathrm{d}s_0$ is a Minkowskian interval.

The field equation in absence of matter is

$$R = 0 \,, \tag{2}$$

where R denotes the curvature scalar. From (1) and (2) we get the appropriate solution

$$g(r) = 1 - m/r \,. \tag{3}$$

The corresponding geodesics evidently permit motion in the plane $\theta = \pi/2$. And the integrals of area and energy become respectively

$$r^2 \frac{\mathrm{d}\varphi}{\mathrm{d}s} = \frac{h}{(1 - m/r)^2} \,. \tag{4}$$

$$\frac{\mathrm{d}t}{\mathrm{d}s} = \frac{c}{(1 - m/r)^2} \,. \tag{5}$$

Making use of the last two equations and putting $r^{-1} = u$, the energy equation ultimately goes over into

$$\left(\frac{\mathrm{d}u}{\mathrm{d}\varphi}\right)^2 = \frac{2mu}{h^2} - \frac{E}{h^2} - u^2 - \frac{m^2}{h^2}\,u^2 = \left(1 + \frac{m^2}{h^2}\right)(u_1 - u)(u - u_2) \,. \tag{6}$$

Now we substitute

$$u = \frac{u_1 + u_2}{2} + \frac{u_1 - u_2}{2}\cos\xi \,.$$

The increase of the azimuth φ after a full revolution is furnished by

$$\varphi = \left(1 + \frac{m^2}{h^2}\right)^{-\frac{1}{2}} \cdot \int_{\xi=0}^{\xi=2\pi} \frac{\mathrm{d}u}{(u_1 - u)(u - u_2)} \simeq 2\pi - \pi\,\frac{m^2}{h^2} \,. \tag{7}$$

---

[1] F. A. E. Pirani: *Proc. Camb. Phil. Soc.*, **51**, 535 (1955).

[2] D. E. Littlewood: *Proc. Camb. Phil. Soc.*, **49**, 90 (1953).

[3] F. Gürsey: *Proc. Camb. Phil. Soc.*, **49**, 285 (1953).

The perihelion advance becomes one sixth the Schwarzchild's amount and in the wrong direction. This confirms the result obtained by PIRANI. The source of GÜRSEY's error is the equation (15) of his paper, where $r^2\omega\gamma$ should be replaced by $ur^2\omega\gamma$.

But in order to meet the known conditions for Mercury we shall extend the field equation.

We shall set

$$R = \Lambda g^{-2} . \tag{8}$$

Because in our disposal we have an adjustable constant Λ, the same can be manipulated so that the observed amount of perihelion shift is obtained.

But equation (8) is more important from the cosmologic point of view. Because the time-dependent (and free of singularities) solution of equation (8) is

$$g = \exp[-kt] , \tag{9}$$

where k is a constant related to Λ. Reinstating the velocity of light c, the interval becomes

$$ds^2 = \exp[-2kt] \cdot \cdot (c^2\,dt^2 - (dx^1)^2 - (dx^2)^2 - (dx^3)^2) . \tag{10}$$

From (10) the radial velocity of recession comes out to be

$$v = c\ \mathrm{tgh}\ (kr/c) \simeq kr . \tag{11}$$

The last relation (11) correctly gives Hubble's expansion.

IL NUOVO CIMENTO Vol. VI, N. 6 1° Dicembre 1957

Note on the Atom Form Factor.

J. Odziemczyk and T. Tietz

Department of Theoretical Physics, University Łódz - Łódz-Poland

(ricevuto il 16 Giugno 1957)

Bragg and West [1] have for the first time calculated numerically the atom form factor $F(Z, k)$ using the Thomas-Fermi theory. In this case the atom form factor $F(Z, k)$ is [2]

$$F(Z, k) = Z\left[1 - 4\pi k\mu \int_0^\infty \sin 4\pi k\mu x \cdot \varphi(x)\,\mathrm{d}x\right], \tag{1}$$

where $\mu = 0.88534\, a_0 Z^{-\frac{1}{3}}$ is the Thomas-Fermi unit, $\varphi(x)$ is the Thomas-Fermi function and $k = (\sin\theta)/\lambda$. λ is the Broglie wavelength of the incident electron and 2θ is the scattering angle, Z is the atomic number of atoms. In this paper for the Bohr radius a_0 is adopted the value $a_0 = 0.52920 \cdot 10^{-8}$ cm. Umeda [3] using the most accurate values known hitherto for the Thomas-Fermi function $\varphi(x)$ has calculated numerically the atom form factor $F(Z, k)$ for Cs. Umeda was the first who gave an approximate analytical formula for the atom form factor $F(Z, k)$ calculated from the Thomas-Fermi model. Umeda [4] starting from equation (1) and using the Rozental [5] approximate formula for $\varphi(x)$ obtained an analytical expression for the atom form factor $F(Z, k)$. One [6] of us calculated also the atom form factor $F(Z, k)$ analytically, using his approximate formula for the Thomas-Fermi function $\varphi(x)$. The purpose of this note is to give the most accurate formula hitherto known for the atom form factor $F(Z, k)$. On account of the accuracy and the possibility of analytical integration we see that the Buchdahl [7] approximate solution for the Thomas-Fermi function $\varphi(x)$ fulfils the above mentioned requirements. The Buchdahl approximate solution for $\varphi(x)$ as known is:

$$\varphi(x) = \frac{1}{(1 + Ax)(1 + Bx)(1 + Cx)} = \frac{\alpha}{1 + Ax} + \frac{\beta}{1 + Bx} + \frac{\gamma}{1 + Cx}, \tag{2}$$

(1) W. Bragg and J. West: *Zeits. Krist. u. Min.*, **69**, 118 (1929).
(2) P. Gombás: *Die statistische Theorie des Atoms und ihre Anwendungen* (Vienna, 1949).
(3) K. Umeda: *Journ. Chem. Phys.*, **21**, 2085 (1953).
(4) K. Umeda: *Journal of the Faculty of Science, Hokkaido University*, **4**, 57 (1951).
(5) S. Rozental: *Zeits. f. Phys.*, 982, 742 (1935).
(6) T. Tietz: *Journ. Chem. Phys.*, **23**, 1565 (1955).
(7) H. A. Buchdahl: *Ann. der Phys.*, **17**, 238 (1955).

TABLE I. – *Comparison of our results for the atom form*

$(\sin\Theta)/\lambda$ Å^{-1}	0	0.1	0.2	0.3	0.4	0.5	0
BRAGG and WEST	55	50.7	43.8	37.6	32.4	28.7	2
Our results	55	50.2	43.7	37.9	31.1	29.2	2

where

$$A = 0.9288 \qquad \frac{\alpha}{A} = \frac{A}{(A-B)(A-C)},$$

$$B = 0.1536 \qquad \frac{\beta}{B} = \frac{-B}{(A-B)(B-C)},$$

$$C = 0.05727 \qquad \frac{\gamma}{C} = \frac{C}{(A-C)(B-C)},$$

Equations (1), (2) and (3) give us following analytical formula for the atom form factor $F(Z, k)$

$$(4)\qquad F(Z,k) = Z\left[1 - 4\pi k\mu\left\{\frac{\alpha}{A}\left(\cos\frac{4\pi k\mu}{A}\left(\frac{\pi}{2} - \sinh\frac{4\pi k\mu}{A}\right) + \sin\frac{4\pi k\mu}{A}\cosh\frac{4\pi k\mu}{A}\right) + \right.\right.$$

$$+ \frac{\beta}{B}\left(\cos\frac{4\pi k\mu}{B}\left(\frac{\pi}{2} - \sinh\frac{4\pi k\mu}{B}\right) + \sin\frac{4\pi k\mu}{B}\cosh\frac{4\pi k\mu}{B}\right) +$$

$$\left.\left. + \frac{\gamma}{C}\left(\cos\frac{4\pi k\mu}{C}\left(\frac{\pi}{2} - \sinh\frac{4\pi k\mu}{C}\right) + \sin\frac{4\pi k\mu}{C}\cosh\frac{4\pi k\mu}{C}\right)\right\}\right],$$

where the symbols sinh and cosh have the following meaning,

$$(5)\qquad \sinh(x) = \int_0^x \frac{\sin t}{t}\,\mathrm{d}t\,; \qquad \cosh(x) = -\int_x^\infty \frac{\cos t}{t}\,\mathrm{d}t\,;$$

For small values of k the atom form factor as given by formula (4) is quadratic in k namely:

$$(6)\qquad F(Z, k \ll 1) = Z[1 - 318.89k^2Z^{-\frac{2}{3}}]$$

and for large values of k the atom form factor $F(Z, k)$ vanishes inverse quadratically in k:

$$(7)\qquad F(Z, k \gg 1) = 0.6310\frac{Z^{\frac{5}{3}}}{k^2}.$$

The functions sinh and cosh, as known, are tabulated with seven-place accuracy. Fig. 1 gives us a comparison of the atom form factor for cosh resulting in our case with the most accurate numerical values for the atom form factor for cosh as given by UMEDA [8].

[8] See reference [3].

sh ($Z=55$) *with the numerical data given by* BRAGG *and* J. WEST.

.7	0.8	0.9	1.0	1.2	1.4	1.6	1.8	2.0
3.2	20.8	18.8	17.0	14.5	12.3	10.4	9.2	8.1
2.8	20.6	18.6	17.0	14.0	12.1	10.1	8.6	7.6

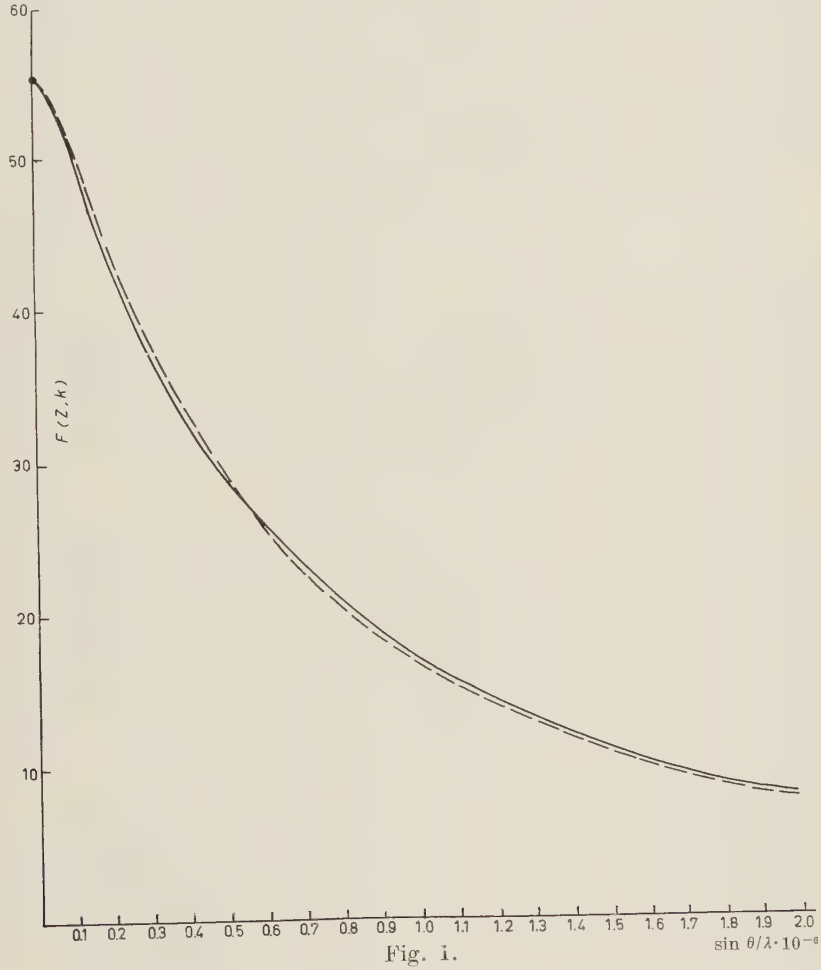

Fig. 1.

In Table I we have a comparison of our numerical data for the atom form factor for $F(Z, k)$ with the numerical data given by BRAGG and WEST ([9]).

Fig. 1 and Table I show that our results for the atom form factor $F(Z, k)$ for cosh deviate from the numerical data given by UMEDA less than 3%.

([9]) See references ([1]) and ([4]).

IL NUOVO CIMENTO Vol. VI, N. 6 1° Dicembre 1957

Widths of the Giant Resonance of Photonuclear Reaction.

M. Soga

Department of Physics, Tokyo University of Education - Tokyo

J. Fujita

Department of Physics, Faculty of Engineering, Nihon University - Tokyo

(ricevuto il 16 Luglio 1957)

Recent analyses of the experimental data concerning the widths of the giant resonance show that; 1) the widths for neutron magic nuclei are narrow and have nearly the same value independent of the mass number, and 2) the widths are wide for nuclei with neutron numbers far from magic numbers.

The theoretical attempts hitherto proposed to explain the first of the two problems are roughly divided into two classes. One of them ([1-6]) assumes that a nucleus absorbs photons first by means of excitation of collective modes, while the other ([7-9]) assumes that a nucleus absorbs photons by means of single particle excitation. These attempts, however, do not seem to settle the problem.

The second of the two problems may possibly be explained from the following viewpoints:

1) As a nucleus with open shells is generally not of spherically symmetric shape, degeneracies of energy levels with respect to spatial orientation of the angular momentum do not exist for it.

2) If nucleons in open shells absorb photons, sublevels appear near the giant peak. This makes seemingly the giant resonance be broad.

3) Level densities of compound states for closed-shell nuclei are low, at corresponding excitation energies, as compared to those for nuclei with open shells. Low density of compound levels probably makes the width of the broad peak in the gross structure narrower.

The first view was proposed by Okamoto ([10]) and Danos ([11]) independently,

([1]) U. L. Businaro and S. Gallone: *Nuovo Cimento*, **1**, 1285 (1955).

([2]) S. Fujii and S. Takagi: *Prog. Theor. Phys.*, **14**, 402, 405 (1955).

([3]) M. Soga, S. Iijima and M. Nogami: (preliminary work.

([4]) J. Fujita: *Prog. Theor. Phys.*, **16**, 112 (1956).

([5]) K. Wildermuth: *Zeits. f. Naturf.*, **10***a*, 447 (1955).

([6]) K. Wildermuth and H. Wittern: *Zeits. f. Naturf.*, **12***a*, 39 (1957).

([7]) A. Reifman: *Zeits. f. Naturf.*, **8***a*, 502 (1953).

([8]) S. Iijima: private communication.

([9]) D. H. Wilkinson: *Physica*, **22**, 1039 (1956).

([10]) K. Okamoto: to be published (private communication) and see also *Prog. Theor. Phys.*, **15**, 75 (1956).

([11]) M. Danos: *Bull. Am. Phys. Soc.*, II, **1**, 135 (1956).

who calculated the widths, using the dipole vibration model and the experimental shape parameters, and got the results which qualitatively agreed with the experimental data. The second was suggested by WILKINSON [9], who has tried to treat the nuclear photoeffect using the shell model, but his detailed calculations have not yet been published. To formulate properly the third proposal does not seem to be easy.

The aim of this short note is to point out that the Okamoto-Danos effect (O.-D. effect) is not inherent to the dipole vibration model in regard to the mechanism of photon absorption but it also exists in the case of single particle absorption in a deformed nucleus. A detailed study along this line will be able to give a clue to solve the interesting problem of studying the mechanism of photon absorption.

As an illustration we take a simple model [12], in which nucleons can move freely in a spheroidal nucleus. The shape of the nucleus may be described by:

$$(1) \qquad R(\mu) = R_0(1+\alpha_2 P_2(\mu)), \quad \mu = \cos\theta$$

R_0 being the radius of the undistorted nucleus and α_2 being related to the intrinsic quadrupole moment, Q_0, by the following equation

$$(2) \qquad \alpha_2 = \frac{\sqrt{5\pi}}{3}\frac{Q_0}{ZR_0^2}.$$

Now we consider a nucleon, which moves in a spheroidal well of infinite depth with the approximate total angular momentum j and its Z-component Ω. Energy shift ΔE of a level in the spheroidal case, relative to the spherical one, can be easily calculated by the first-oder perturbation method, if the deviation from the spherical shape is small. Namely, we have

$$(3) \qquad \Delta E_{n,l,j,\Omega} = -\frac{\hbar^2 x_{n,l}^2}{MR_0^2}\alpha_2\frac{j(j+1)-3\Omega^2}{4j(j+1)},$$

where $x_{n,l}$ is the n-th zero point of the Bessel function of the order $l+\frac{1}{2}$ and M the nucleon mass.

For simplicity we consider only the contribution from the E_1-absorptions, as it is prevalent at the giant resonance region. Since ΔE's have different values for different Ω's, each photon absorption line of the spherical nucleus is split into several lines. The split lines in each group are distributed over an energy region of extension, D:

$$(4) \qquad D = (\Delta E_{n_f,l_f,j_f,\Omega_f} - \Delta E_{n_i,l_i,j_i,\Omega_i})_{\max} - (\Delta E_{n_f,l_f,j_f,\Omega_f'} - \Delta E_{n_i,l_i,j_i,\Omega_i'})_{\min},$$

where the indices i and f indicate the initial and the final states.

Assuming that the nuclear deformation is kept unchanged during the process of photon absorption, we define the quantity, S:

$$(5) \qquad D = \frac{\sqrt{5\pi}}{3}\frac{\hbar^2}{Mr_0^4}\frac{Q_0}{ZA^{\frac{4}{3}}}S_{n_f,l_f,j_f;\,n_i,l_i,j_i},$$

where r_0 is the nuclear radius parameter, A the mass number and Z the atomic number. The numerical values for S's are tabulated in Table I, which clearly shows the tendency of D to increase rapidly with j for the same n and $Q_0/ZA^{\frac{4}{3}}$.

It may not be correct simply to assume that the calculated D's correspond to the observed widths of the giant resonance. However, in order to visualize the O.-D. effect in the case of the single particle absorption, we summarize the numerical results for D's in Table II in comparison with the observed widths and OKAMOTO's results. On deriving Table II we assumed that the excitation from core nucleon states with nodeless radial wave functions to the similar excited states gives a dominant contribution to the

[12] S. GALLONE and C. SALVETTI: *Phys. Rev.*, **84**, 1064 (1951).

TABLE I. – *The numerical results for the factor* $S_{n_f l_f j_f ; n_i l_i j_i}$ *in Eq.* (5), *which indicate the largeness of the extension of the split absorptions lines in the deformed nuclei.*

Final \ Initial	$1s_{\frac{1}{2}}$	$1p_{\frac{3}{2}}$	$1p_{\frac{1}{2}}$	$1d_{\frac{5}{2}}$	$2s_{\frac{1}{2}}$	$1d_{\frac{3}{2}}$	$1f_{\frac{7}{2}}$	$2p_{\frac{3}{2}}$	$1f_{\frac{5}{2}}$	$2p_{\frac{1}{2}}$	$1g_{\frac{9}{2}}$	$1g_{\frac{7}{2}}$
$1s_{\frac{1}{2}}$	—	—	—	—	—	—	—	—	—	—	—	—
$1p_{\frac{3}{2}}$	8.07	—	—	—	—	—	—	—	—	—	—	—
$1p_{\frac{1}{2}}$	0	—	—	—	—	—	—	—	—	—	—	—
$1d_{\frac{5}{2}}$	—	17.1	—	—	—	—	—	—	—	—	—	—
$2s_{\frac{1}{2}}$	—	8.07	0	—	—	—	—	—	—	—	—	—
$1d_{\frac{3}{2}}$	—	21.4	13.3	—	—	—	—	—	—	—	—	—
$1f_{\frac{7}{2}}$	—	—	23.3	—	—	—	—	—	—	—	—	—
$2p_{\frac{3}{2}}$	—	—	—	29.6	23.9	37.2	—	—	—	—	—	—
$1f_{\frac{5}{2}}$	—	—	—	28.1	—	25.1	—	—	—	—	—	—
$2p_{\frac{1}{2}}$	—	—	—	—	0	13.3	—	—	—	—	—	—
$1g_{\frac{9}{2}}$	—	—	—	—	—	—	28.4	—	—	—	—	—
$1g_{\frac{7}{2}}$	—	—	—	—	—	—	33.1	—	31.9	—	—	—
$2d_{\frac{5}{2}}$	—	—	—	—	—	—	42.5	42.5	45.1	—	—	—
$2d_{\frac{3}{2}}$	—	—	—	—	—	—	—	57.0	41.5	33.1	—	—
$3s_{\frac{1}{2}}$	—	—	—	—	—	—	—	23.9	—	0	—	—
$1h_{\frac{11}{2}}$	—	—	—	—	—	—	—	—	—	—	33.1	—
$1h_{\frac{9}{2}}$	—	—	—	—	—	—	—	—	—	—	37.5	37.1
$2f_{\frac{7}{2}}$	—	—	—	—	—	—	—	—	—	—	53.9	51.7
$2f_{\frac{5}{2}}$	—	—	—	—	—	—	—	—	—	—	—	55.8

Final \ Initial	$2d_{\frac{5}{2}}$	$2d_{\frac{3}{2}}$	$3s_{\frac{1}{2}}$	$1h_{\frac{11}{2}}$	$1h_{\frac{9}{2}}$	$2f_{\frac{7}{2}}$	$2f_{\frac{5}{2}}$	$3p_{\frac{3}{2}}$	$3p_{\frac{1}{2}}$	$1l_{\frac{13}{2}}$	$2g_{\frac{9}{2}}$	$3d_{\frac{5}{2}}$
$2f_{\frac{7}{2}}$	51.7	—	—	—	—	—	—	—	—	—	—	—
$2f_{\frac{5}{2}}$	65.6	55.8	—	—	—	—	—	—	—	—	—	—
$3p_{\frac{3}{2}}$	61.7	80.6	47.5	—	—	—	—	—	—	—	—	—
$3p_{\frac{1}{2}}$	—	33.1	0	—	—	—	—	—	—	—	—	—
$1i_{\frac{13}{2}}$	—	—	—	37.4	—	—	—	—	—	—	—	—
$2g_{\frac{9}{2}}$	—	—	—	64.6	58.8	58.1	—	—	—	—	—	—
$3d_{\frac{5}{2}}$	—	—	—	—	—	78.1	89.3	78.1	—	—	—	—
$1i_{\frac{11}{2}}$	—	—	—	41.7	41.7	—	—	—	—	—	—	—
$2g_{\frac{7}{2}}$	—	—	—	—	67.6	70.1	65.2	—	—	—	—	—
$4s_{\frac{1}{2}}$	—	—	—	—	—	—	—	47.5	0	—	—	—
$3d_{\frac{3}{2}}$	—	—	—	—	—	—	79.3	108.2	607.	—	—	—
$1j_{\frac{15}{2}}$	—	—	—	—	—	—	—	—	—	41.6	—	—
$2h_{\frac{11}{2}}$	—	—	—	—	—	—	—	—	—	75.3	63.5	—
$3f_{\frac{7}{2}}$	—	—	—	—	—	—	—	—	—	—	90.7	80.4
$1j_{\frac{13}{2}}$	—	—	—	—	—	—	—	—	—	46.0	—	—
$2h_{\frac{9}{2}}$	—	—	—	—	—	—	—	—	—	—	74.0	—
$3f_{\frac{5}{2}}$	—	—	—	—	—	—	—	—	—	—	—	116.4
$4p_{\frac{3}{2}}$	—	—	—	—	—	—	—	—	—	—	—	105.2

TABLE II. – *The numerical results of D for the individual nucleus, for which the deformation parameters of the ground states are known to be not so small and the widths of the giant resonance have been also measured* [10]. *We have assumed* $r_0 = 1.5^{\frac{1}{3}}$ *in accordance with Okamoto's calculation.*

Element	Proton	Neutron	e (eccentricity)	D_p	D_n	OKAMOTO (G.T.) §	OKAMOTO (S.J.J.) §	$\Gamma_{obs.}$
^{51}V	$1d_{\frac{3}{2}}^{3} \to 1f_{\frac{7}{2}}^{7}$	$1f_{\frac{7}{2}}^{7} \to 1g_{\frac{9}{2}}^{9}$	0.11 ~ 0.18	6.0 $\sim$ 9.3	6.7 ~ 10.7	5.2	6.0	5.8
^{55}Mn	»	»	0.29	8.8	10.3	6.9	8.0	8.8
^{56}Fe	»	»	0.21	10.9	12.8	6.1	7.2	6.1
^{59}Co	»	»	0.10 ~ 0.19	5.3 ~ 9.7	6.0 ~ 11.0	5.0	5.6	5.4
^{64}Zn	$1f_{\frac{7}{2}}^{7} \to 1g_{\frac{9}{2}}^{9}$	»	$\leqslant 0.19$	V 8.3	V 8.3	6.9	7.0	6.0 ~ 7.9
^{70}Ge	»	»	0.15	7.4	7.4	5.7	6.8	6.5
^{76}Ge	»	»	0.23	11.3	10.4	6.4	7.6	9.5
^{75}As	»	»	> 0.17	$>$ 9.6	$>$ 9.6	5.6	6.6	9.0
^{79}Br	»	»	0.16	11.1	11.1	5.6	6.6	6.0
^{81}Br	»	»	0.13	9.1	5.2	5.4	6.2	8.0
^{103}Rh	»	$1g_{\frac{9}{2}}^{9} \to 1h_{\frac{11}{2}}^{11}$	0.20	9.8	4.2	5.9	6.9	8.9
^{107}Ag	»	»	0.16	0.0 *	7.0	5.5	6,4	9.2
^{109}Ag	»	»	0.17	0.0 *	7.5	5.6	6.5	9.2
^{115}In	»	»	0.14	0.0 *	6.0	5.3	6.0	5.5
^{121}Sb	$1g_{\frac{9}{2}}^{9} \to 1h_{\frac{11}{2}}^{11}$	»	0.08	3.5	4.8	4.8	5.4	4.8
^{123}Sb	»	»	0.08	4.4	3.6	4.8	5.4	4.8
^{127}I	»	»	0.10	4.0	2.7	5.0	5.7	6.6 ~ 8.0
Sm (natural)	»	$1h_{\frac{11}{2}}^{11} \to 1l_{\frac{13}{2}}^{13}$	0.15	2.7	2.9	5.4	6.3	7.5
^{159}Tb	»	»	0.37	14.0	7.3	8.2	7,3	11.0
^{165}Ho	»	»	0.31	3.5 † (6.3)	6.2 † (11.3)	6.5	7.5	13.0
Er (natural)	»	»	0.29	5.9	10.6	6.7	7.7	13.5
Yb (natural)	»	»	0.27	5.4 † (8.3)	9.7 † (14.9)	6.4	7.4	10.0
^{181}Ta	»	»	0.22	0.0 *	6.8	6.0	7.0	7.0
^{197}Au	$1h_{\frac{11}{2}}^{11} \to 1i_{\frac{13}{2}}^{13}$	»	$\leqslant 0108$	$\leqslant 3.5$	$\leqslant 2.4$	4.7	5.2	5.0 ~ 6.3
^{232}Th	»	$1i_{\frac{13}{2}}^{13} \to 1j_{\frac{15}{2}}^{15}$	0.13	4.4	4.9	5.2	5,8	5.6
U	»	»	0.16	5.1	4.6	5.3	6.1	6.6

* Because of the Pauli principle only one line appears.

† ( ) is the value calculated from the Q_0 of the experimental Coulomb excitation data.

§ OKAMOTO's calculated width represents the sum of the splitting due to the nuclear deformation and the intrinsic width.

giant resonance, in accordance with Wilkinson's model. The numerical results should not be taken seriously, since several additional effects must be taken into account. For example, the second-order perturbation effect may not be negligible ([13]) in the case of $\alpha_1 > 0.15$, so that our results are generally overestimated. Moreover, if we introduce the effective mass ([9]), our numerical values will be probably increased. However, we may say qualitatively that in the case of single particle excitation an increase of the width of the giant resonance due to the nuclear deformation should depend on the special character of the shell wave function, while the O.-D. effect in the dipole vibration model is uniquely described by the geometrical shape of the nucleus and the radius R.

As an illustration, the result calculated for ^{181}Ta is shown in Fig. 1. The shape of the cross-section curve is similar to OKAMOTO's one ([10]), but the high energy part goes down abruptly in ours. If we consider contributions from many other sublevels beside the dominant levels, the slope of this part will go down more smoothly. Since D_P of ^{181}Ta is zero, as seen from Table II, the shape of its excitation function should be characterized by the two gross peaks in the neutron excitation (Fig. 1). Recent experimental data ([14]) for ^{181}Ta show that

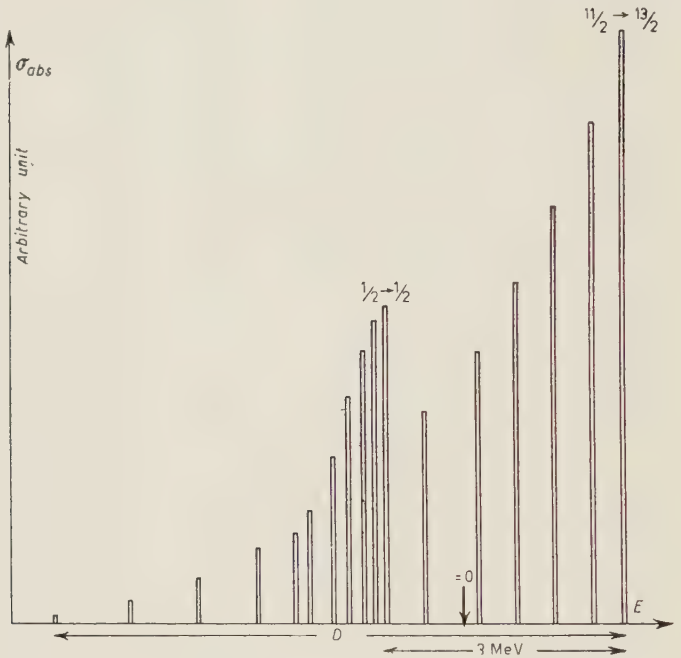

Fig. 1. - Relative transition of ^{181}Ta ($1h^{(11/2)} \rightarrow 1i^{(13/2)}$ neutron- transition)

$$\frac{\int\sigma(2\text{-nd peak})\,dE}{\int\sigma(1\text{-st peak})\,dE} \quad \begin{matrix} 616 \\ 364 + 70 \end{matrix} \sim 1.5 .$$

([13]) S. G. NILSON: *Mat. Fys. Medd. Dan. Vid.*, **29**, No. 16 (1955).

([14]) FULLER and HAYWARD: private communication from OKAMOTO.

the (γ, n) cross-section curve has two peaks, and this fact can be explained by our model as well as by OKAMOTO's one. In order to check the validity of both models one should measure more precisely the shapes of the excitation curves of ^{181}Ta, ^{107}Ag, ^{109}Ag and ^{115}In etc., for which D_p's are zero. The results of our single particle model in Table II seem to be quite similar to Okamoto's dipole vibration model, but the empirical data seem to be rather favorable to the latter model. However, as the relation between our D's and the widths of the giant resonance is not clear-cut, it may be dangerous to derive from our simple calculations a definite conclusion.

A similar effect may be also observed in the case of neutron scattering ([15]).

* * *

Authors thank Professor T. MIYAZIMA for his kind advices and Mr. K. OKAMOTO for his useful communication, having sent the preprint of his recent work.

([15]) B. MARGOLIS and E. S. TROUBETZKOY: *Phys. Rev.*, **101**, 105 (1957).

Section efficace de création dirécte de paires d'électrons par les mésons μ. Relation avec le moment magnétique.

M. Avan et L. Avan

Laboratoire de Physique Corpusculaire, Université - Caén

(ricevuto il 20 Luglio 1957)

Les expériences que nous avons effectuées dans les mines de fer de la région de Caen (France) nous ont permis de préciser pour trois profondeurs différentes: $h_1 = -300$ mètres d'eau, $h_2 = -580$ mètres d'eau; $h_3 = -1280$ mètres d'eau:

1) les lois d'intensité et de distribution angulaire de la composante pénétrante [1-3];

2) les sections efficaces d'interactions nucléaires [2] et électromagnétiques [4,5] des mésons μ;

3) les lois de variation avec la profondeur des composantes protonique, mésonique π [6] et électrophotonique [7].

La technique utilisée est celle des émulsions nucléaires Ilford G5 coulées, exposées et développées sous terre.

Il nous semble intéressant de rappeler les résultats relatifs aux sections efficaces de création directe de paires par les mésons μ, en fonction des expériences récemment effectuées à l'Université de Columbia (U.S.A.) [8].

L'influence d'un moment magnétique anormal des mésons μ se traduirait, dans la création directe de paires, par une section efficace additive:

$$\sigma_\delta = \sigma_{\text{normale}} \cdot \frac{\delta^1 E}{M_\mu c^2} \quad [9,10],$$

pour un moment magnétique total: $(1+\delta)(e\hbar/2M_\mu c)$ et une énergie E des mésons μ.

Les sections efficaces indiquées dans [4] ont été confirmées à partir d'un nombre plus important de « triplets »:

30 au niveau h_1

31 au niveau h_2

après élimination de paires créées directement par des électrons et compte tenu

(1) Congrès de l'A.F.A.S., Caén, Juillet 1955.

(2) L. Avan: *Thèse de Doctorat es Sciences*, Université de Caen, 1955; *Annales de Physique Masson*, Novembre 1956.

(3) L. et M. Avan: *Compt. Rend.*, **241**, 1122 (1955).

(4) M. et L. Avan: *Compt. Rend.*, **243**, 38 (1956).

(5) M. Avan: *Thèse de Doctorat es-Sciences*, Université de Caen (1956). En cours d'impression aux *Annales de Physique*.

(6) L. et M. Avan: *Compt. Rend.*, **244**, 589 (1957).

(7) L. et M. Avan: *Compt. Rend*, **244**, 450 (1957)

(8) R. L. Garwin, L. M. Lederman and M. Weinrich: *Phys. Rev.*, **105**, 1415 (1957).

(9) G. N. Fowler: *Nuclear Physics*, **1**, 125 (1956).

(10) C. Peaslee: *Nuovo Cimento*, **1**, 56 (1952).

de la composante électronique non résoluble par rapport aus mésons μ. Cinq exemples de pseudo-triplets ont été enregistrés, pour lesquels la distance latérale r du sommet de la paire négaton-positon à la trajectoire du primaire est d'ailleurs supérieure à 10 μm. La contribution des pseudo-triplets, résultant de la conversion d'un photon du rayonnement de freinage au voisinage de la trajectoire mésonique, et à l'intérieur des limites de résolution spatiale du microscope, est donc expérimentalement négligeable. La discontinuité observée dans la distribution en r montre qu'il s'agit bien, pour les 61 événements retenus, d'un processus de création directe dans le champ du noyau.

Les sections efficaces expérimentales correspondantes, soit:

$$\begin{cases} \sigma_{\text{exp}} = (0.67 \pm 0.12) \cdot 10^{-25} \text{ cm}^2 \\ \quad \text{par noyau d'émulsion} \\ \quad \text{à } -300 \text{ mètres d'eau} \end{cases}$$

$$\begin{cases} \sigma_{\text{exp}} = (0.86 \pm 0.16) \cdot 10^{-25} \text{ cm}^2 \\ \quad \text{par noyau d'émulsion} \\ \quad \text{à } -580 \text{ mètres d'eau} \end{cases}$$

sont directement comparables aux valeurs déduites de la section efficace différentielle de Bhabha ([11,12]) après intégration sur le spectre des mésons μ aux profondeurs envisagées ([1-3]):

$$\begin{cases} \text{au niveau } h_1\text{: } \sigma_{\text{Bh}} = 0.60 \cdot 10^{-25} \text{ cm}^2 \\ \quad \text{par noyau d'émulsion,} \end{cases}$$

$$\begin{cases} \text{au niveau } h_2\text{: } \sigma_{\text{Bh}} = 0.82 \cdot 10^{-25} \text{ cm}^2 \\ \quad \text{par noyau d'émulsion.} \end{cases}$$

Les valeurs expérimentales:

a) sont compatibles avec des sections efficaces théoriques purement normales (le méson μ étant considéré comme une particule de Dirac de spin $\frac{1}{2}$ et de moment magnétique normal: $\delta \gtrless 0$) ([13]);

b) imposent, de toute façon, comme ordre de grandeur de la limite supérieure de δ, pour les énergies moyennes des mésons μ aux profondeurs de nos expériences: $\delta \lesssim 0.1$.

Récemment, R. L. Garwin, L. M. Lederman et M. Weinrich ([8]) ont montré, en liaison avec les expériences sur la non conservation de parité proposées par T. D. Lee et C. N. Yang ([14]) que le moment magnétique du méson μ est essentiellement normal.

([11]) H. J. Bhabha: *Proc. Roy. Soc.* A **152**, 559 (1935).

([12]) M. M. Block, D. T. King and W. Wada: *Phys. Rev.*, **96**, 1627 (1954).

([13]) K. Greisen: communication privée.

([14]) T. D. Lee et C. N. Yang: *Phys. Rev.*, **104**, 254 (1956).

A Class of Exact Solutions of the Combined Gravitational and Electro-Magnetic Field Equations of General Relativity.

R. L. Brahmachary

Research and Training School, Indian Statistical Institute - Calcutta

(ricevuto il 23 Luglio 1957)

1. – In our generalization of the Reissner-Nordstrom-Jeffery solution [1], we attempted a solution of the field-equations

$$(1)\qquad \begin{cases} (a) & -8\pi T_1^1 - 8\pi t_1^1 = e^{-\lambda}\left(\frac{\nu'}{r}+\frac{1}{r^2}\right)-\frac{1}{r^2}+\Lambda \\ (b) & -8\pi T_2^2 - 8\pi t_2^2 = e^{-\lambda}\left(\frac{\nu''}{2}-\frac{\lambda'\nu'}{4}+\frac{(\nu')^2}{4}+\frac{\nu'-\lambda'}{2r}\right)+\Lambda\,. \\ (c) & T_2^2 = T_3^3 \\ (d) & -8\pi T_4^4 - \frac{C}{r^4} = -e^{-\lambda}\left(\frac{\lambda'}{r}-\frac{1}{r^2}\right)-\frac{1}{r^2}+\Lambda\,. \end{cases}$$

We will now attempt the interior solution of a space containing matter which is distributed with a spherical symmetry around a charged particle. We will later see that the charged particle should be something like an electron having a finite radius.

In the space surrounding the charged particle or sphere, we have

$$8\pi T_1^1 - 8\pi t_1^1 = 8\pi p - C/p^4\,,$$

where [2] C depends on the charge of the particle (sphere) and the density is

$$8\pi\varrho + C/r^4\,, \qquad (8\pi t_1^1 = -8\pi t_2^2 = 8\pi t_4^4 = C/r^4)\,.$$

[1] R. L. Brahmachary: *Nuovo Cimento*, **4**, 1216 (1956).
[2] A. S. Eddington: *The Mathematical Theory of Relativity* (1929), p. 185.

Following a method of TOLMAN [3], we combine the first and second equation (1) thus

$$\left\{(8\pi T_1^1 + 8\pi t_1^1) - (8\pi T_2^2 + 8\pi t_1^1)\right\}\frac{2}{r} = \frac{2}{r}\left[e^{-\lambda}\{\ldots\}\right],$$

and obtain

$$\frac{4C}{r^5} = \frac{\mathrm{d}}{\mathrm{d}r}\left\{\frac{(e^{-\lambda}-1)}{r^2}\right\} + \frac{\mathrm{d}}{\mathrm{d}r}\left(\frac{e^{-\lambda}\nu'}{2r}\right) + e^{-\lambda-\nu}\frac{\mathrm{d}}{\mathrm{d}r}\left(\frac{e^{\nu}\nu'}{2r}\right). \tag{2}$$

We thus see that it is necessary and sufficient to solve the three equations, (1*a*), (1*d*) and (2). Thus we avoid the complicated equation (1*b*).

Assumption: $\nu' = 0$, $\nu'' = 0$.

Our equations reduce to

$$\begin{cases} (a) & \dfrac{(e^{-\lambda}-1)}{r^2} = 4C\displaystyle\int\frac{\mathrm{d}r}{r^5}. \\ (b) & 8\pi p - \dfrac{C}{r^4} = \dfrac{e^{-\lambda}}{r^2} - \dfrac{1}{r^2} + \Lambda. \\ (c) & 8\pi\varrho + \dfrac{C}{r^4} = e^{-\lambda}\left(\dfrac{\lambda'}{r} - \dfrac{1}{r^2}\right) + \dfrac{1}{r^2} - \Lambda. \end{cases} \tag{3}$$

From (3*a*) we immediately obtain

$$e^{-\lambda} = 4C\alpha r^2 - C/r^2 + 1,$$

where α is a constant of integration. Putting this value in 3 (*b*) we obtain

$$8\pi p = 4C\alpha + \Lambda.$$

We further obtain from 3 (*c*)

$$8\pi\varrho = -\Lambda - 12C\alpha - 2C/r^4.$$

Discussion: We find that for $r \ll 1$, $e^{-\lambda}$ becomes negative. As $e^{-\lambda}$ must always be positive, we thus find that even outside the origin $r=0$, there is a singular domain unless we assume a shell like distribution of mass around the charged particle with a gap between the particle and the inner shell.

If however, a charged sphere of finite radius whose gravitational part of the energy tensor is negligible in comparison with its electromagnetic part (i.e. an electron) is assumed, our solution is to remain valid only outside the electron.

[3] R. C. TOLMAN: *Phys. Rev.*, **55**. 364 (1939).

At $r=r_e$, the radius of the electron, the singular region commences, or in other words we put

$$4C\alpha r_e^2 - C/r_e^2 + 1 = 0 . \tag{4}$$

Our solution is:

$$e^{\nu} = \text{const} , \qquad e^{-\lambda} = 4C\alpha r^2 - C/r^2 + 1 ,$$

$$8\pi p = 4C\alpha + \Lambda , \qquad 8\pi\varrho = -\Lambda - 12C\alpha - 2C/r^4 .$$

As p is positive and ϱ must be positive up to $r=r_e$, we have α=negative, Λ=positive

$$|\Lambda| > |4C\alpha|$$

and

$$|12C\alpha| > |\Lambda + 2C/r^4| .$$

With the help of these conditions, we can find from equation (4), the value of α. If

$$C = 10^{-10} \text{ units} \quad \text{or} \quad 10^{-38} \text{ cm} ,$$

(in relativistic units) and $r_e \sim 10^{-13}$ cm. We find $\alpha \sim -10^{64}$.

Instead of an electron we may also take a charged sphere, the solution for which has already been found [4]. Outside the sphere, the Reissner-Nordström solution would be valid (if the space were empty) with

$$T_1^1 = 0 , \qquad t_1^1 = C/r^4 .$$

Thus our equations (3) correctly represent the energy-tensor of matter-distribution having a spherical symmetry around the charged sphere.

2. – We attempted so far a solution of spherically symmetric matter-distribution around a charged sphere of finite radius. Another example of this type of solutions is now being obtained by the simple expedient of putting $p=0$, namely, considering the case of dust like particles, offering no pressure.

Assumption: $p=0$, $\nu'=0$, $\nu''=0$.

The field-equations now reduce to

$$\begin{cases} (a) & -8\pi t_1^1 = e^{-\lambda}/r^2 - 1/r^2 + \Lambda \\ (b) & -8\pi t_2^2 = e^{-\lambda}(-\lambda'/2r) + \Lambda \\ (c) & T_2^2 = T_3^3 \\ (d) & -8\pi\varrho - 8\pi t_4^4 = -e^{-\lambda}(\lambda'/r - 1/r^2) - 1/r^2 + \Lambda . \end{cases} \tag{5}$$

Outside the charged sphere,

$$8\pi t_1^1 = -8\pi t_2^2 = 8\pi t_4^4 = C/r^4 .$$

[4] R. L. BRAHMACHARY: *Nuovo Cimento*, **5**, 1520 (1957).

We therefore obtain from (5)a,

$$e^{-\lambda} = 1 - \Lambda r^2 - C/r^2 .$$

Equation (5)b is seen to be identically satisfied for this value of $e^{-\lambda}$.
We can then easily find from (5)d, the value for ϱ:

$$8\pi\varrho = 2\Lambda - 2C/r^4 .$$

As $8\pi\varrho$ and $e^{-\lambda}$ must always be positive the range of validity of our solution is restricted.

Let the lower and upper boundaries of the range of validity be r_b and r_B, respectively.

We then have

$$e^{-\lambda} = 1 - \Lambda r_b^2 - C/r_b^2 = \text{positive} ,$$

$$8\pi\varrho = 2\Lambda - 2C/r_b^4 \quad = \text{positive} .$$

If $r_b = 10^{-13}$ cm and $C = 10^{-38}$ cm, we have

$$e^{-\lambda} = 1 - \Lambda \cdot 10^{-26} - 10^{-12} = \text{positive} .$$

Thus

$$\Lambda < (10^{26} - 10^{14}) .$$

Again from the expression for $8\pi\varrho$ we have

$$8\pi\varrho = 2\Lambda - 2 \cdot 10^{14} > 0 .$$

Thus,

$$\Lambda > 10^{14} .$$

But we can now easily see that the maximum allowable value for the range of validity of the solution is $r = r_B < 10^{-7}$ that is, $e^{-\lambda}$ attains the value zero at $r_B < 10^{-7}$ if we choose the minimum (possible) value of Λ.

By taking a greater value of r_b, we can increase the range of validity. With $r_b = 2$ cm, for example, we have

$$e^{-\lambda} = 1 - 4\Lambda - C/4$$

and

$$8\pi\varrho = 2\Lambda - 2C/(2)^4 .$$

Then we have

$$\Lambda > 10^{-38}/(2)^4$$

and consequently

$$r_B^2 > 8 \cdot 10^{38}$$

if we assume the minimum possible value of Λ.

* * *

I take this opportunity for thanking Dr. T. Roy and M. Sengupta for certain discussions.

IL NUOVO CIMENTO Vol. VI. N. 6 1° Dicembre 1957

Inner Shell Structure of Nuclei.

H. Tyrén, Th. A. J. Maris and P. Hillman (*)

The Gustaf Werner Institute for Nuclear Chemistry
University of Uppsala, Sweden

(ricevuto il 31 Luglio 1956)

Most nuclear single particle states which have been studied until now differ from the ground state by a rearrangement of the particles of the highest shell. Exceptions are the giant γ-resonance in which particles of the last filled shell may also be involved [1]. and some states occurring after high energy pick-up processes [2].

States in which the inner shells are intact are comparable with atomic states leading to optical transitions. The nuclear states corresponding to X-ray states in atoms have holes in inner shells. It is the purpose of this letter to report preliminary results of a method of investigating such states.

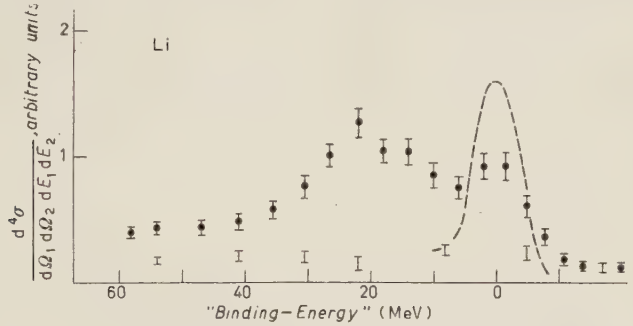

Fig. 1. – « Binding energy » spectra of protons from Li, C and Al. The plain vertical strokes indicate random coincidence rates; the dashed curves represent the results for free proton-proton scattering.

The method consists essentially of a measurement of the total energy carried away by two protons emerging simultaneously from nuclei bombarded with 185 MeV protons. To the extent to which the collision may be regarded as quasi-elastic, the difference between this total and the incident energy is the

(*) CERN (European Organisation for Nuclear Research, theoretical study division). On leave of absence from AERE, Harwell, England.

(1) D. H. Wilkinson: *Proceedings of the International Conference on Nuclear Reactions*, Amsterdam (1956), p. 1039.

(2) W. Selove: *Phys. Rev.*, **101**, 231 (1956).

« binding-energy » of the proton knocked out of the nucleus, for the moment neglecting the nuclear recoil energy.

Two identical three-scintillator range-telescopes are used to count the protons, with angular resolutions of about 10° a factor of 1.6 down to energies near 30 MeV.

Lithium is expected to have two strongly bound protons in its α-core and one outer proton bound with 10 MeV. The upper part of the spectrum is ob-

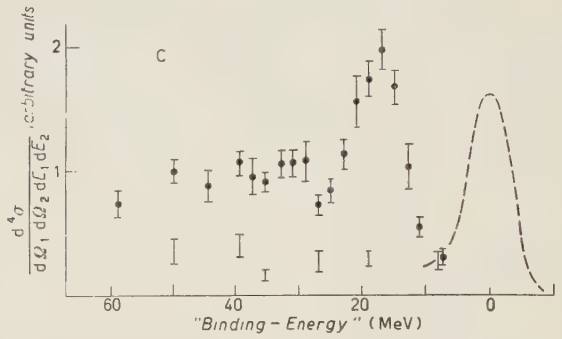

Fig. 2.

full-width. The figure shows the energy spectra in one telescope of protons emerging near 45° from lithium, carbon, and aluminium, when the angle of the other is also 45° and its energy window near 90 MeV. The abscissa is shown as the « binding-energy » of the removed proton. The random coincidences are measured

scured by the small hydrogen contamination of the lithium target. The maximum of the spectrum at 20 MeV seems to be caused by protons knocked out of the α-core. The broad energy distribution might be understood either by assuming a short lifetime for the state of ^{6}He with a hole in the α-core, or

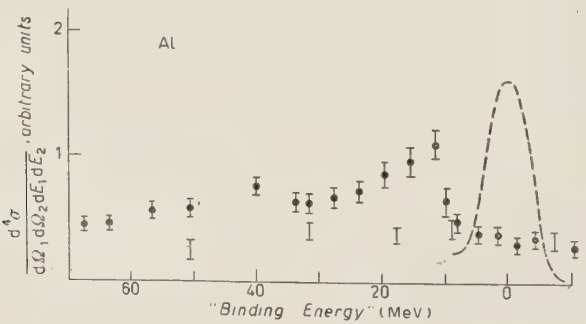

Fig. 3.

by introducing delays into one telescope with respect to the other. The free proton-proton peak shown on each diagram is measured to establish an energy-zero and to give the total energy resolution, which however becomes worse by

by remarking that the state is composed of many stationary states with energies lying in a broad spectrum, both interpretations being equivalent. At least part of the observed continuum is due to protons multiply scattered in the

nucleus, whose contribution will increase with « binding-energy » and atomic number of the target nucleus.

In carbon a clear structure is seen, apparently resulting from the fact that the protons are knocked out from different shells. The sharpness of the first peak with its maximum at 16 MeV, which is the binding energy of the least bound proton in ^{12}C, is interesting. Evidently, a knocking-out of a proton in the upper shell leads often to a ^{11}B nucleus in or nearly in its ground state. The second maximum is again broad.

The results for aluminium show a strong peak at 10 MeV, the binding energy of the least bound proton being 7 MeV. The expected second and third maxima seem to be flattened out. This may be a result of several factors, such as the deformation of the nucleus, the ncreasing absorbtion in the nucleus of protons with lower energies, and of course the increasingly bad energy resolution for these protons.

We are improving our energy resolution and intend to make a systematic investigation of the inner shell structure of several nuclei. By varying the fixed energy channel and the scattering angles we further hope to be able to check the current ideas of quasi-elastic collisions in nuclei and perhaps to observe differences in the momentum distributions of different shells.

* * *

We thank Prof. The. Svedberg for his interest. We are indebted to P. Isacsson, R. Jonsson, and P. Tove for indispensable assistance. This work was supported by the Swedish Atomic Energy Commission.

Two-Nucleon Potential from a Model of Pion-Nucleon Interaction.

F. Ferrari and L. Fonda

Istituto Nazionale di Fisica Nucleare - Sezione di Padova
Istituto Nazionale di Fisica Nucleare - Sottosezione di Trieste
Istituto di Fisica dell'Università - Padova
Istituto di Fisica dell'Università - Trieste

(ricevuto il 14 Agosto 1957)

With the development of the meson theory, several attempts have been made in order to obtain a two nucleon potential (1). It has been emphasized by Levy (2) that, if the meson is pseudoscalar, the main contribution to the nuclear forces arises from the exchange of two mesons between the nucleons. In this connection, it can be shown that, as a consequence of the impossibility of fixing the positions of the nucleons exactly, the potential has a repulsive core at small distances. However, owing to the difficulty connected with an exact evaluation of the higher order terms, it is retained that the potential is fairly well approximated outside the core region by the second and fourth order terms in the coupling constant, while the interaction at small distances is described by a phenomenological repulsive core.

On the other hand, Gartenhaus (3) has pointed out that the cut-off form of the Yukawa PS-PV theory with two adjustable parameters, i.e. the renormalized coupling constant and the cut-off energy of the virtual mesons, can reproduce with quite good accuracy all the low energy nucleon-nucleon experimental data.

The aim of this note is to show that also a quantum-mechanical potential constructed from a model in which the interaction between pions and nucleons does not occur directly, but through an intermediate boson field φ of mass μ_x (4), can account for the low energy nucleon-nucleon phenomena, and that, in addition, the insertion of an intermediate field between pions and nucleons supports a possible explanation of the fact that the core radius is different in the triplet-even and in the singlet-even state. The field φ is chosen to have the same character of covariance as the pion field π in the ordinary and in isotopic space, i.e. φ and π are isovector pseudoscalar fields. A PS-PV coupling is assumed between intermediate and nucleon fields, the coupling between the two boson fields is described by a hamiltonian invariant under Lorentz transformations, and reflections and rotations in isotopic space.

(1) H. A. Bethe and F. de Hoffmann: *Mesons and Fields* (New-York).
(2) M. Levy: *Phys. Rev.*, **88**, 725 (1952); A. Klein: *Phys. Rev.*, **90**, 1101 (1953).
(3) S. Gartenhaus: *Phys. Rev.*, **100**, 900 (1955).
(4) P. Budini: *Nuovo Cimento*, **3**, 1104 (1956).

The hamiltonian is the following:

$$H = H_0^N + H_0^\pi + H_0^\varphi + \sqrt{4\pi}\frac{g_\varphi^0}{\mu_x}\int \bar{N}\gamma_5\gamma_\mu \frac{\partial \boldsymbol{\varphi}}{\partial x_\mu}\boldsymbol{\tau} N(x)\,\mathrm{d}^3x + g_\pi^0\frac{\mu_x^3}{\mu_\pi}\int \boldsymbol{\varphi}(x)\cdot\boldsymbol{\pi}(x)\,\mathrm{d}^3x\,,$$

where H_0^N and H_0^π describe free nucleons and pions, H_0^φ is the hamiltonian for the free intermediate field φ.

We wish to point out that, after eliminating the field φ, this hamiltonian leads, in static approximation, to a classical nucleon-nucleon potential which at large distances behaves like the ordinary static PS-PV potential of the local theory. At short distances it shows in the central part a repulsive core of Levy's type; further, the high singularity of the tensor part is completely removed (5) (+).

Using the method of Brueckner and Watson (6) the construction of the quantum-mechanical potential is straightforward. One obtains:

$$V = V_\pi + V_\varphi\,, \tag{2}$$

where:

$$V_\pi = -\frac{4\pi}{(2\pi)^3}\left(\frac{g_\varphi g_\pi}{\mu_\pi}\right)^2 \boldsymbol{\tau}_1\boldsymbol{\tau}_2 \int \frac{\mathrm{d}^3k\,\exp[i\boldsymbol{k}\boldsymbol{r}]}{\omega_\pi^2}(\boldsymbol{\sigma}_1\boldsymbol{k})(\boldsymbol{\sigma}_2\boldsymbol{k})\left[\frac{\mu_x^2}{k^2+\mu_x^2}\right]^2 -$$

$$-\frac{(4\pi)^2}{(2\pi)^6}\left(\frac{g_\varphi g_\pi}{\mu_\pi}\right)^4 \int\!\!\int \frac{\mathrm{d}^3k_1\,\mathrm{d}^3k_2}{\omega_{\pi_1}^3\omega_{\pi_2}}\exp[i(\boldsymbol{k}_1+\boldsymbol{k}_2)\boldsymbol{r}]\left[\left(\frac{3}{\omega_{\pi_2}}+\frac{2\boldsymbol{\tau}_1\boldsymbol{\tau}_2}{\omega_{\pi_1}+\omega_{\pi_2}}\right)(\boldsymbol{k}_1\boldsymbol{k}_2)^2\cdot\right.$$

$$\left.\cdot V_\alpha(k_1,k_2\,|\,\mu_x\,|\,T) + (\boldsymbol{\sigma}_1\boldsymbol{k}_1\wedge\boldsymbol{k}_2)(\boldsymbol{\sigma}_2\boldsymbol{k}_1\wedge\boldsymbol{k}_2)\cdot\left(\frac{3}{\omega_{\pi_1}+\omega_{\pi_2}}+\frac{2\boldsymbol{\tau}_1\boldsymbol{\tau}_2}{\omega_{\pi_2}}\right)V_\beta(k_1,k_2\,|\,\mu_x\,|\,T)\right].$$

$$V_\varphi = -\frac{4\pi}{(2\pi)^3}\left(\frac{g\varphi}{\mu_x}\right)^2 \boldsymbol{\tau}_1\boldsymbol{\tau}_2 \int \frac{\mathrm{d}^3k\,\exp[i\boldsymbol{k}\boldsymbol{r}]}{\omega_x^2}(\boldsymbol{\sigma}_1\boldsymbol{k})(\boldsymbol{\sigma}_2\boldsymbol{k}) -$$

$$-\frac{(4\pi)^2}{(2\pi)^6}\left(\frac{g_\varphi}{\mu_x}\right)^4 \int\!\!\int \frac{\mathrm{d}^3k_1\,\mathrm{d}^3k_2}{\omega_{x_1}^3\omega_{x_2}}\exp[i(\boldsymbol{k}_1+\boldsymbol{k}_2)\boldsymbol{r}]\left[\left(\frac{3}{\omega_{x_2}}+\frac{2\boldsymbol{\tau}_1\boldsymbol{\tau}_2}{\omega_{x_1}+\omega_{x_2}}\right)\cdot\right.$$

$$\left.\cdot(\boldsymbol{k}_1\cdot\boldsymbol{k}_2)^2 + (\boldsymbol{\sigma}_1\cdot\boldsymbol{k}_1\wedge\boldsymbol{k}_2)(\boldsymbol{\sigma}_2\boldsymbol{k}_1\wedge\boldsymbol{k}_2)\left(\frac{3}{\omega_{x_1}+\omega_{x_2}}+\frac{2\boldsymbol{\tau}_1\boldsymbol{\tau}_2}{\omega_{x_2}}\right)\right].$$

$V_\alpha(k_1,k_2\,|\,\mu_x\,|\,T)$ and $V_\beta(k_1,k_2\,|\,\mu_x\,|\,T)$ are complicated functions of k_1, k_2 and μ_x (*), whereas their dependence on the total isotopic spin T is rather simple. Neglecting the T dependence and assuming $\mu_x = 5\mu_\pi$, a satisfactory approximation of the functions V_α and V_β reads as follows:

$$V_\alpha \simeq V_\beta \simeq (1.36)^2\left[\frac{\mu_x^2}{k_1^2+\mu_x^2}\right]^2\left[\frac{\mu_x^2}{k_2^2+\mu_x^2}\right]^2. \tag{3}$$

(5) P. Budini and L. Fonda: *Nuovo Cimento*, **5**, 666 (1957). A similar classical potential has been discussed by E. Clementel and C. Villi: *Nuovo Cimento*, **4**, 935 (1956), and by H. P. Noyes and S. Pandya: *Phys. Rev.*, **102**, 269 (1956).

(+) This classical potential is obviously identical with the first term of V_π.

(*) As an exemple, see formula (8') of ref. (4)

(6) K. A. Brueckner and K. M. Watson: *Phys. Rev.*, **92**, 1023 (1953).

Putting $f^2 = 1.36 g_\pi^2 g_\varphi^2$ and retaining approximation (3), the potential V_π, which arises from the compound interaction through $\varphi - \pi - \varphi$ fields, turns out to be the Gartenhaus potential [3] with the selected cut-off function:

$$v(k) = \frac{\mu_x^2}{k^2 + \mu_x^2} . \tag{4}$$

It is to be remarked that, if one does not resort to approximation (3), V_π exhibits some peculiar features which in principle seem to meet experimental requirements. In fact the form factors are found to be dependent on the total isotopic spin T: this implies that in the ordinary space the equivalent singlet and triplet core radii are different. A qualitative inspection of the correct functions $V_\alpha(k_1, k_2 | \mu_x | T)$ and $V_\beta(k_1, k_2 | \mu_x | T)$ shows that $r_{c,\,\text{singlet}} > r_{c,\,\text{triplet}}$.

On the other hand, as in BRUECKNER and WATSON, the evaluation of the potential V_φ, which describes the interaction of the nucleons through the field φ only, is rather uncertain for small distances and must be approximated by a partially phenomenological insertion of a repulsive core. However, due to the presumable smallness of the coupling constant g_φ [5] and the largeness of the denominators, V_φ is negligible compared to V_π, at least outside $r \geqslant 0.6(\hbar/\mu_\pi c)$.

With $\mu_x = 5\mu_\pi$ and $f^2 = 0.079$ satisfactory results are obtained for the low-energy properties of the two nucleon system. With this f^2 one finds $g_\varphi^2 g_\pi^2 = 0.0576$ which is very close to the value 0.0559 given by BUDINI [4] for the pion-nucleon scattering.

The possible contribution of V_φ at high energies has not been considered.

* * *

We wish to thank Prof. P. BUDINI and Prof. C. VILLI for many interesting discussions.

IL NUOVO CIMENTO Vol. VI, N. 6 1° Dicembre 1957

On the Structure of the Nucleon Core.

G. Domokos

Central Research Institute for Physics of the Hungarian Academy of Sciences
Department of Cosmic Rays - Budapest

(ricevuto il 18 Agosto 1957)

Recent investigations have shown, that present meson theories cannot account in a satisfactory manner for all properties of physical nucleons. It is well known, that, calculating the neutron-electron interaction, the calculated Foldy-term accounts for the observed interaction; the remaining term, arising from the interaction of the electron with the pion charge distribution (further called the Coulomb part of the interaction) is too large, and of the wrong sign (scil. repulsive).

A cut-off pion theory yields a fairly good value for the isovector part of the anomalous magnetic moment, while giving too large a contribution for the isoscalar one (Miyazawa [1]). Recently Sandri [2] and Vitale [3] have put forward the idea, that in calculating the anomalous moments, the contribution of heavy unstable particles should be taken into account. Vitale's paper yielded a reasonable valuè for the average number of K-mesons around the core, but the neutron-electron interaction remained unexplained.

In the present note we report the results of a simple and rough calculation, which, however, seems to indicate, that both the magnetic moment and neutron-electron interaction can be put in order by means of the K-meson contribution. (The theoretical interpretation of present e, p scattering experiments of Hofstadter *et al.* [4] is rather insensitive to the structure of the core).

We assume the following:

There is only one kind of K-meson and that is scalar.

Hyperons and nucleons are of opposite relative parities.

Hyperon-pion and nucleon-pion interactions are of similar strength.

All kinds of hyperons interact with K-mesons in the same manner.

These assumptions are in conformity with the results of Dallaporta and Ferrari [5], obtained from the theoretical analysis of hyperfragment data.

Neglecting states, containing at least

(1) H. Miyazawa: *Phys. Rev.*, **101**, 1564 (1956).
(2) G. Sandri: *Phys. Rev.*, **101**, 1516 (1956).
(3) B. Vitale: *Nuovo Cimento*, **5**, 732 (1957).
(4) R. Hofstadter: *Rev. Mod. Phys.*, **28**, 214 (1956).
(5) N. Dallaporta and F. Ferrari: *Nuovo Cimento*, **5**, 111 (1957).

two K-mesons, the following processes will be allowed:

$$N \leftrightarrow \begin{cases} \Lambda^0 + K^0 \\ \Sigma^0 + K^0 \\ \Sigma^- + K^+ \end{cases} \qquad P \leftrightarrow \begin{cases} \Lambda^0 + K^+ \\ \Sigma^0 + K^+ \\ \Sigma^+ + K^0 \end{cases}$$

Neglecting the contribution of hyperon currents to the magnetic moments, it is easily seen, that the following relation holds between the anomalous moments — μ_p^A and μ_n^A — of the proton and neutron (*): respectively

$$\mu_p^A + \mu_n^A = 2\mu_s + P_\Lambda \frac{M}{M_K} + P_\Sigma \frac{M}{M_K},$$

where μ_s is the isoscalar part of the pion contribution (cfr. MIYAZAWA, op. cit.) $\left.\begin{matrix} P_\Lambda \\ P_\Sigma \end{matrix}\right\}$ is the probability of finding the proton dissociated into $\begin{cases} \Lambda + K \\ \Sigma + K \end{cases}$; M and M_K are observed nucleon, and K-particle masses, respectively. (All quantities to be taken in nuclear magneton units).

Inserting the observed values, and

$$\mu_s \sim 0.3,$$

obtained as a reasonable estimation from a cut-off pion theory, and taking into account our last assumption, we get $P_\Lambda \sim P_\Sigma \sim 0.1$. For the total probability of finding a nucleon dissociated into a hyperon and a K-meson, we find:

$$w \sim P_\Lambda + P_\Sigma \sim 0.2.$$

In order to get some information about the distribution of K-mesons around their source, we carried out a calculation in close analogy with that of UMEZAWA *et al.* (6), i.e. we calculated different quantities in the Heisenberg picture, with a reasonable assumption about the source.

As a fixed-source calculation seemed to be a too rough approximation, we took into account energy-momentum conservation, but no other recoil effects and attributed to the bare source an extension of its Compton wavelength, obtaining in this manner a cut-off value for momenta.

The calculated density distribution of K-mesons is plotted in Fig. 1; for the average total number of them we obtain the relation

$$w \sim 0.018\, g^2,$$

which agrees with our phenomenological result, if $g^2 \sim 11$. This g^2-value does not contradict Dallaporta and Ferrari (loc. cit.), who state, that it is of the same order of magnitude as the pion-nucleon coupling constant.

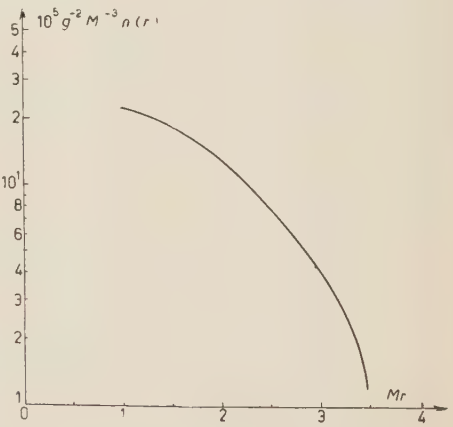

Fig. 1. – Density distribution of K-mesons. $n(r)$ is the average K-meson density/cm³, plotted in a logarithmic scale. M is the nucleon mass, g the K-nucleon coupling constant. The values of the abscissa are measured in nucleon Compton wavelength units.

With the same g^2 we find, that the average energy, contained in the K-mesonic field, is about $0.5M$.

(*) $\mu_p^A = \mathfrak{M}_p - 1 \approx 1.79$; $\mu_n^A = \mathfrak{M}_n \approx -1.91$.

(6) H. UMEZAWA, Y. TAKAHASHI and S. KAMEFUCHI: *Phys. Rev.*, **85**, 505 (1952).

If we accept (cfr. Z. KOBA [7]), that a physical nucleon contains on the average ~ 0.3 pions in its proper field (according to our previous assumption, this number is not essentially modified by the dissociation of the core), then our « dissociated » core contributes about 16 keV to the Coulomb part of a conventional neutron-electron potential, approximately compensating the contribution of the pion cloud. (We mention here, that an extended core has been *postulated* by SALZMAN [8], in order to explain n, e interaction) (*).

(7) Z. KOBA: *Prog. Theor. Phys.*, **15**, 461 (1956).

(8) G. SALZMAN: *Phys. Rev.*, **99**, 973 (1955).

(*) Actually, in our calculation, the core seems to overcompensate slightly the Coulomb contribution of the pion cloud. Note, however, that our model is a very rough one; we wanted merely to show, that a correct order of magnitude can be obtained for the core contribution.

* * *

The author is indebted to Prof. L. JÁNOSSY for valuable critical remarks and to Mr. C. NAGY for interesting discussions on the subject.

Note added in proof.

Hypotheses I-II in this paper can be modified in such a manner, that we adopt the convention, that hyperons are $\frac{1}{2}^+$ particles, then K-mesons ought to be 0^- ones, in that case in our approximation we obtain essentially the same results. The formula for magnetic moments is a Sachs-type « mirror condition », so charged hyperon-contributions are cancelled in it. Our calculation of the K-distribution corresponds to the strong coupling approximation in UMEZAWA's paper. The author is indebted to Dr. B. VITALE for a worthful discussion on the subject.

ERRATA-CORRIGE

G. ALEXANDER, R. H. W. JOHNSTON and C. O'CEALLAIGH – **The Relative Frequencies of the Decay Modes of Positive K-Mesons and the Decay Spectra of Modes $K_{\mu 3}$, τ' and K_β**; *Nuovo Cimento*, **6**, 478 (1957).

On page 494, 25-th line, the last word of the line should read « if » instead of « is ».

Statistical Fluctuations Occurring in Electron-Photon Cascades of 1000 GeV Primary Energy.

H. Fay

Max-Planck-Institut für Physik - Göttingen

(ricevuto il 28 Agosto 1957)

During the last few years there have been several publications [1-8] on high energy electron-photon cascades characterized by an initial development which deviates markedly from the mean shower development as described by cascade theory. For a given primary energy these deviations occur not only in the total number of shower particles at a given shower depth but also in their energy spectrum.

In order to find out wether these deviations are due to a failure of the theoretical cross-section for bremsstrahlung and pair production some investigations [9-11] have been completed recently, the results of which seem to indicate that the development of the cascades up to several 100 GeV primary energy is in agreement with the theoretical predictions. In special cases, however, the statistical fluctuations may be very large.

In order to obtain more information on the possible fluctuations in showers of a primary energy of about 1000 GeV the development of 15 cascades was calculated by a Monte-Carlo method. The primary particle was taken to be an electron of $E_0 = 1000$ GeV. These calculations were based on the exact cross-sections for bremsstrahlung and pair production (according to Rossi-Greisen [12]) and the energy loss by ionization was taken into account. In Table I the numbers of shower particles with energies $\geqslant E$ for $\ln(E_0/E) \leqslant 2$, 4, 6, 8,

---

(1) M. Schein, D. M. Haskin R. A. Glasser: *Phys. Rev.*, **95**, 855 (1954).

(2) A. Debenedetti, C. M. Garelli, L. Tallone and M. Vigone: *Nuovo Cimento*, **2**, 220 (1955).

(3) A. Milone: *Pisa Conference*, 1955 and private communication.

(4) M. Koshiba and M. F. Kaplon: *Phys. Rev.*, **97**, 193 (1955); **100**, 327 (1955).

(5) A. Jurak, M. Mięsowicz, O. Stanicz and W. Wolter: *Bull. Acad. Pol. Sci.*, **3**, 369 (1955).

(6) A. Debenedetti, C. M. Garelli, L. Tallone, M. Vigone and G. Wataghin: *Nuovo Cimento*, **3**, 226 (1956).

(7) L. Barbanti-Silva, C. Bonacini, C. de Pietri, J. Jori, G. Lovera, R. Perilli-Fedeli and A. Roveri: *Nuovo Cimento*, **3**, 1465 (1956).

(8) M. Mięsowicz, O. Stanicz and W. Wolter: *Nuovo Cimento*, **5**, 513 (1957).

(9) A. Debenedetti, C. M. Garelli, L. Tallone and M. Vigone: *Nuovo Cimento*, **4**, 1151 (1956).

(10) K. Pinkau: *Nuovo Cimento*, **3**, 1156, 1285 (1956).

(11) H. Fay: *Nuovo Cimento*, **5**, 293 (1957).

(12) B. Rossi and K. Greisen: *Rev. Mod., Phys.*, **13**, 240 (1941).

TABLE I. – *The integral energy spectrum of* 15 *cascades of* 1000 GeV *primary energy obtained by Monte-Carlo-calculation.*

$\ln (E_0/E) \geqslant$	10.8	$\geqslant 10$	$\geqslant 8$	$\geqslant 6$	$\geqslant 4$	$\geqslant 2$
No. of cascade	$t = 1.5$					
1	17	16	15	13	4	1
2	7	6	5	2	0	0
3	22	22	13	10	7	0
4	26	22	14	10	6	1
5	22	19	12	5	2	1
6	15	12	8	5	1	1
7	14	11	6	4	1	1
8	22	18	12	5	1	1
9	12	9	6	5	2	0
10	21	21	14	9	7	1
11	31	23	17	7	4	1
12	27	23	19	13	6	1
13	23	22	11	7	2	0
14	7	6	3	3	2	1
15	15	13	9	7	2	1
$\bar{N}$	18.7	15.5	10.9	7.0	3.1	0.67
	$t = 1.0$					
1	5	4	4	3	2	2
2	1	1	1	1	1	0
3	8	7	7	5	3	1
4	11	11	8	5	2	1
5	9	8	7	4	2	1
6	9	9	6	4	1	1
7	3	2	2	1	1	1
8	10	8	5	2	2	1
9	3	3	3	3	3	1
10	9	9	7	4	4	1
11	13	11	6	4	4	1
12	9	9	9	8	6	1
13	15	12	12	8	3	1
14	2	1	1	1	1	1
15	7	7	5	4	2	1
$\bar{N}$	7.6	6.8	5.5	3.8	2.5	1.0
	$t = 0.5$					
1	1	1	1	1	1	1
2	1	1	1	1	1	0
3	2	1	1	1	1	1
4	1	1	1	1	1	1
5	4	3	3	1	1	1
6	1	1	1	1	1	1
7	1	1	1	1	1	1
8	5	4	3	3	2	1
9	1	1	1	1	1	1
10	3	3	1	1	1	1
11	5	5	2	2	1	1
12	5	5	5	4	3	2
13	7	6	5	5	3	2
14	1	1	1	1	1	1
15	1	1	1	1	1	1
$\bar{N}$	2.6	2.33	1.86	1.66	1.33	1.07

10, 10.8, at shower depths $t=0.5$, 1.0, 1.5 are listed. The mean values together with the results of Arley's theory [13] are plotted in Fig. 1. In Fig. 2 the distribution of the 15 cascades as a function of the number of shower particles with energy $\geqslant 20$ MeV $\left(\ln (E_0/E) \leqslant \leqslant 10.8\right)$ is plotted for the three shower depths mentioned above. In addition, the distribution at $t=1.5$ is given for the case in which the energy loss of the electrons by ionization is neglected. In some cases this results in a larger number of particles due to those electrons which lose their energy by ionization and pass the 20 MeV limit but now contribute to the distribution.

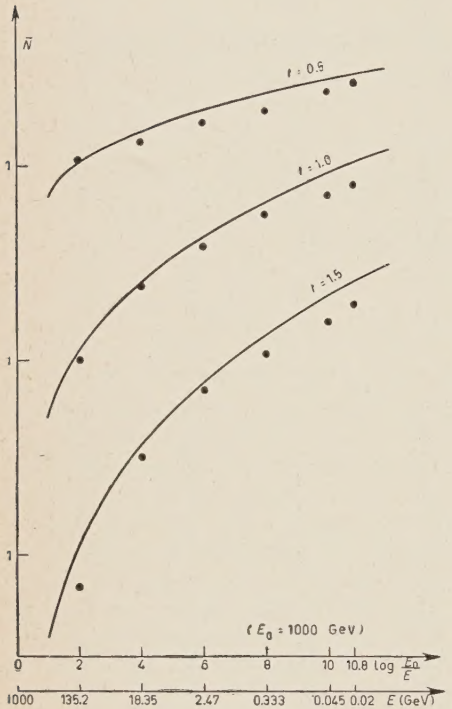

Fig. 1. – The mean number $\bar{N}$ of shower particles with energies $\geqslant E$ at various shower depths. The plotted curves are derived from Arley's theory.

It can be seen from Table I and Fig. 2 that fluctuations about the mean value $\bar{N}(\geqslant E)$ of the order of $\pm\frac{1}{2}\bar{N}(\geqslant E)$ are not rare in a sample of 15 showers. Apart from these fluctuations in the total number of particles there are also fluctuations in the integral energy spectrum of the shower particles as for instance in the cascade No. 1. Here, one finds 17 particles at $t=1.5$, 13 of which have an energy more than 2.5 GeV; the corresponding numbers as given by Arley's theory are 24.0 and 7.5. For this cascade the points of origin of the pairs and their energies are listed in Table II.

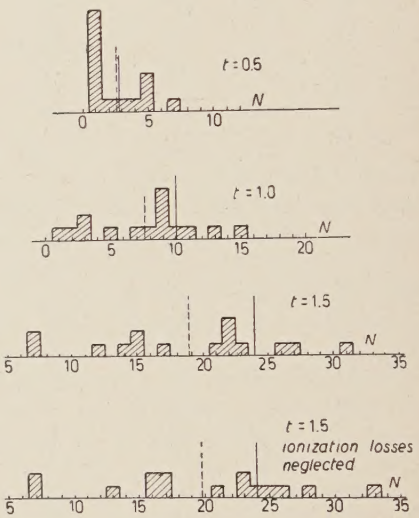

Fig. 2. – The distribution of 15 cascades obtained by the Monte-Carlo calculation as a function of the total number N of shower particles (energies $\geqslant 20$ MeV) at various shower depths. The mean values obtained from the theory of Arley are marked by heavy lines, those of the sample by broken lines.

A comparison of the cascade No. 1 with the one found experimentally by DEBENEDETTI *et al.* [2] (event No. 2) would seem to be indicated. This event might be interpreted by assuming that both electrons of the primary (high ener-

[13] N. ARLEY: *Proc. Roy. Soc.*, A **168**, 519 (1938); *Mat. Fys. Medd.*, **17**, 11 (1940).

TABLE II. – *The points of origin and the energies of cascade No. 1 obtained by the Monte-Carlo-calculation.*

First generation		Second generation	
t	E_{pair} (eV)	t	E_{pair} (eV)
0.874	$6.4 \cdot 10^{8}$	1.523	$1.22 \cdot 10^{10}$
0.91	$2.4 \cdot 10^{11}$	1.402	$5.15 \cdot 10^{9}$
1.08	$2.7 \cdot 10^{11}$		
1.24	$1.09 \cdot 10^{11}$		
1.263	$1.84 \cdot 10^{10}$		
1.414	$1.23 \cdot 10^{11}$		
1.436	$3.8 \cdot 10^{9}$		
1.564	$8.7 \cdot 10^{9}$		
1.601	$1.4 \cdot 10^{8}$		

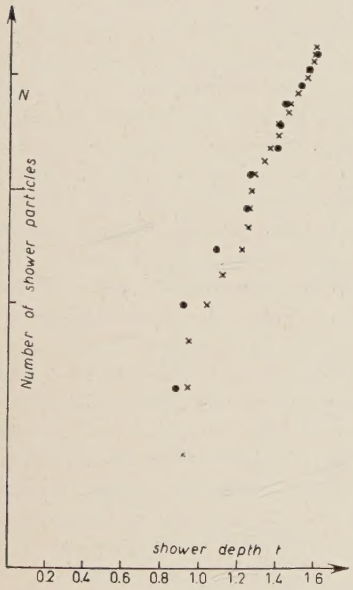

Fig. 3. – Comparison of the cascade found by DEBENEDETTI *et al.* (event No. 2) and the cascade No. 1 (●) obtained by the Monte Carlo calculation.

getic) pair produce a cascade development corresponding to our cascade No. 1 (cf. Fig. 2). Accordingly, the energy of the primary electrons should be about 1000 GeV each; the energy estimate made by DEBENEDETTI *et al.* from the opening angles is certainly much too low (see LOHRMANN [14]). The extraordinarily large relative number of highly energetic pairs is also common to both cascades.

Conclusion: In single cases, cascade developments may occur which, due to statistical fluctuations, deviate appreciably from the mean values given by cascade theory. From the consideration solely of a few strongly fluctuating cascades, therefore, one should be very careful in concluding that the cascade theory is violated.

* * *

The author is grateful to Mrs. R. MAYER for her consistent help in performing the calculations.

(14) L. LOHRMANN: *Nuovo Cimento*, **2**, 1029 (1955).

LIBRI RICEVUTI E RECENSIONI

WILHELM SPECHT – *Gruppentheorie.* Springer Verlag, Berlin, 1956, pp. 457.

Tra i molti trattati di teoria dei gruppi il presente volume si distingue anzitutto per la mole della materia che vi si trova esposta; la trattazione è fondata sulle concentrazioni più recenti della teoria ed è ricca di risultati moderni, oltre a quelli ormai classici riguardanti i gruppi astratti e le proprietà strutturali, quali sono quelle delle catene in un gruppo, dei p-gruppi e degli ampliamenti di un dato gruppo secondo un fattoriale assegnato. L'esposizione si suddivide in tre parti: la prima è dedicata alle nozioni generali sui gruppi ed alle corrispondenze di omomorfismo ed isomorfismo. In essa trovano ampia discussione le nozioni di sottogruppi invarianti, del gruppo dei commutatori, del gruppo degli automorfismi e di quello degli automorfismi interi di un gruppo dato ed infine del semigruppo costituito dagli operatori. La seconda parte riguarda la teoria dei gruppi liberi e della fattorizzazione diretta di un tale gruppo. Questo ramo moderno è, come si è potuto constatare negli ultimi anni, di fondamentale importanza nelle più svariate applicazioni pratiche; l'Autore è pertanto particolarmente meritevole per aver dato una esauriente e nello stesso tempo piuttosto elementare esposizione della difficile teoria dei gruppi liberi e, successivamente, dei gruppi, abeliani. La terza parte, di carattere più classico, viene trattata con mezzi moderni e assai generali che permettono di illuminare con assoluto rigore e semplicità la teoria delle catene culminante nel teorema di SCHREIER-ZASSENHAUS: nella trattazione di questa teoria l'Autore si basa sulle più recenti ricerche di insigni cultori viventi della teoria dei gruppi, quali ad esempio H. WIELAND, P. HALL, R. BAER e molti altri. La teoria anzidetta, per quanto ormai classica, trova così per la prima volta una formulazione del tutto moderna e concorde con le più rigorose esigenze di una trattazione generale ed astratta. Vengono esaminati con insolita diffusione i gruppi risolubili, speciali, i p-gruppi ed i sottogruppi di SYLOW con i relativi teoremi di SYLOW e molteplici loro applicazioni. Infine è esposta la teoria dell'ampliamento di un gruppo secondo il problema posto da SCHREIER: la trattazione si distingue anche qui da quelle usuali per il maggiore grado di generalità e fa uso delle nozioni di ampliamenti affini e della teoria dei caratteri. In particolare vengono esaminati gli ampliamenti di gruppi abeliani e vengono assegnati vari teoremi di immersione.

Concludendo, tra i vari pregi del presente volume sono da rilevare il vasto campo teorico ed applicativo abbracciato dagli argomenti esposti, la felice scelta della materia in relazione alle varie applicazioni in campi di ricerca non strettamente gruppali, la chiarezza dell'esposizione e l'assoluto rigore che è base di tutta la trattazione. Il volume potrà pertanto essere consultato con successo sia dagli studiosi di teoria dei gruppi che da cultori di altre materie, nelle quali la teoria dei gruppi trovi applicazione.

R. VINCIGUERRA.